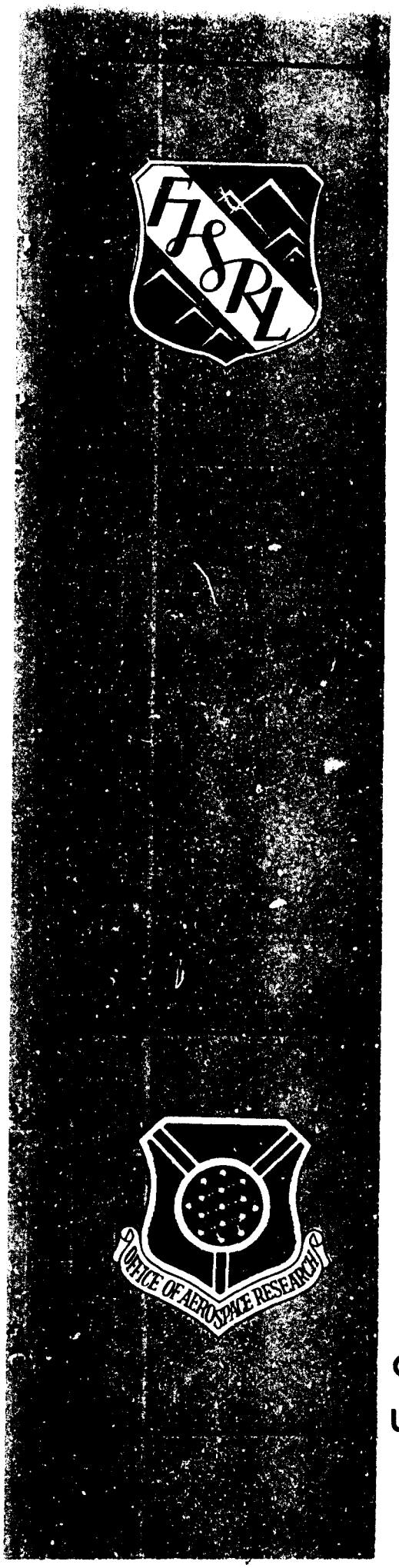

FRANK J. SEILER RESEARCH LABORATORY

SRL 69-0012

JUNE 1969

TIME-OPTIMAL ATTITUDE CONTROL OF AN AXIALLY SYMMETRIC SPINNING SPACECRAFT

CAPT DIRK H. DE DOES

PROJECT 7904

OFFICE OF AEROSPACE RESEARCH
UNITED STATES AIR FORCE

FRANK J. SEILER RESEARCH LABORATORY

SRL 69 - 0012 JUNE 1969

TIME-OPTIMAL ATTITUDE CONTROL OF AN AXIALLY SYMMETRIC SPINNING SPACECRAFT

CAPT DIRK H. DE DOES

PROJECT 7904

OFFICE OF AEROSPACE RESEARCH
UNITED STATES AIR FORCE

ABSTRACT

This report considers the problem of controlling both the attitude and angular velocities of an axially symmetric spacecraft while minimizing the maneuver duration. In particular, various combinations of thrust limited reaction jets are employed to properly orient a spinning space body with respect to specified reference directions starting from known initial conditions of the vehicle's attitude and angular rates. Five control jet configurations are considered: two gimballed systems where torques can be applied about, 1) any axis in a plane normal to the axis of symmetry, 2) two perpendicular non-rotating axis in a plane normal to the axis of symmetry; and three body-fixed configurations where the thrusters are immobile relative to the vehicle and can provide both positive and negative or only positive (negative) control torques about one or both of the vehicle's transverse axis. The control systems are realizable from a hardware standpoint and the corresponding optimal controls can be classified as: 1) a continuous function of time, 2) bang-bang, 3) on-off, and 4) a combination of (1 and 2) or (2 and 3). In addition to specifying five controller configurations the following assumptions are made: 1) the only external torques are the control torques, 2) the vehicle has a single axis of symmetry and is spinning at a constant rate about this axis, 3) motion of the vehicle's axis of symmetry is limited to small angular excursions about a nominal

direction, and 4) the maneuvers terminate with zero angular rates about the transverse axis.

The optimal control problem is formulated in terms of four state variables: two normalized angular velocities and two normalized, inertial components of angular momentum (or two dimensionless spin axis position angles). The maximum principle is used to provide a necessary (and in certain cases, a sufficient) condition for time-optimality. In taking this approach four costate variables are introduced. Thus the optimization problem is one of solving an equivalent two point boundary value problem. Exact optimal controls in terms of the initial costate and minimum final time are then determined for certain classes of state boundary conditions. In those cases where direct solutions are not available, a Newton-type iterative procedure is employed to solve the two point boundary value problem. In all cases the optimal control is ultimately expressed in terms of from one to four dimensionless physical parameters which include: vehicle geometry, spin rate, thrust magnitude, moment arms, initial state, and desired final state. In this manner families of solutions are generated with a modest expenditure of computation time.

In cases where the total angular momentum vector and the spin axis are aligned at the initiation and termination of control three modes of operation which characterize optimal steering are defined. These include the two limiting cases where, for example, the control magnitude is very large (small) compared to the angular momentum due to spin. The third mode is characterized by the transition region

between the "short" and "long" time solutions. In the latter case, the maneuver duration may be from one to ten revolutions of the spacecraft about its axis of symmetry. Finally, for certain values of the dimensionless physical parameters the response of the non-linear system is typified by that of the linear plant. Hence the results of this report are useful in determining the minimum time required for arbitrarily large reorientations of a vehicle's spin axis.

ACKNOWLEDGMENTS

The author wishes to express his gratitude to Professor R. H. Edwards for suggesting the problem considered in this report. In particular, both the guidance and consideration offered by Dr. Edwards during that period of time when the author was serving with the Office of Aerospace Research, USAF, are appreciated.

The author is also thankful to Colonel Gage H. Crocker and Lieutenant Colonel Bernard S. Morgan, Jr. for their support during his assignment at the Frank J. Seiler Research Laboratory.

For their many helpful discussions, the author wishes to thank his fellow researchers. The personnel of the computer center, FJSRL, USAF Acsdemy, are acknowledged for their support during the past years.

This report is based on a dissertation submitted in partial fulfillment of the requirements for the degree of Doctor of Philosophy at the University of Southern California, June, 1969.

TABLE OF CONTENTS

LIST OF FIGURES

LIST OF TABLES

LIST OF SYMBOLS

a	moment arm
A	control jet configuration defined in Figure 1.1
$A(t)$	n x n characteristic matrix
b	constant defined in Section 2.3
B	control jet configuration defined in Figure 1.1
c	constant
C_1, C_2, C_3	scalar coefficients
C_1', C_2', C_3'	scalar coefficients
C	control jet configuration defined in Figure 1.1
$\hat{c}$, $\hat{c}_1$	curves in the $(\hat{L}_X$-$\hat{L}_Y)$ Plane
D	control jet configuration defined in Figure 1.1
$\underline{e}_x$, $\underline{e}_y$, $\underline{e}_z$	unit vectors along the (x, y, z) Axis
$\underline{e}_{x'}$, $\underline{e}_{y'}$, $\underline{e}_{z'}$	unit vectors along the (x', y', z') Axis
E	control jet configuration defined in Figure 1.1
$\underline{f}$	n vector of functions
$\underline{\hat{f}}$	q dimensional thrust vector
$\underline{F}$	vector of functions
F	magnitude of the thrust vector
G	n x n + 1 matrix
h_j	number of zeros of S_j in (t_o, t_f)
H	Hamiltonian function
i	integer
I	moment of inertia about transverse axis
I_{sp}	specific impulse
I_x, I_y, I_z	principal moments of inertia

j	integer
$\hat{J}$	solution to Hamilton-Jacobi equation
$J(\underline{\chi}, \underline{u}, t)$	cost functional
k	iteration number
K	constant
ℓ_1, ℓ_2	integration limits
$\mathcal{L}$	continuous function used in cost functional
$\underline{L}(t)$	total angular momentum vector
$\tilde{\underline{L}}, \bar{\underline{L}}, \bar{\underline{L}}, \hat{\underline{L}}$	normalized angular momentum vectors
$\tilde{\underline{L}}, \bar{\underline{L}}, \hat{\underline{L}}$	changes in the normalized angular momentum vectors
m	integer
M	magnitude of the control vector
n	dimension of the state vector
$P_j, \hat{P}_j$	points defined by the pair $(\hat{L}_X, \hat{L}_Y)$
$\underline{P}(t)$	n dimensional adjoint vector
P_o	scalar coefficient
q	dimension of the control vector
Q_j	subsets of the $(\hat{L}_X$-$\hat{L}_Y)$ plane
r_1^1, r_1^2, r_1^3	subsets of Q_1
$\hat{R}$	Taylor series remainder term
R_n	Euclidian space
$\underline{S}(t)$	vector of switching functions
$S_x(t), S_y(t)$	switching functions defining $u_x^*(t)$ and $u_y^*(t)$
$S_{x'}(t), S_{y'}(t)$	switching functions defining $u_{x'}^*(t)$ and $u_{y'}^*(t)$
t	time
T	normalized final time
$\underline{u}(t)$	q dimensional vector of control functions
u'	scalar control function defined by Equation (4.22)
U	input space of control functions
v	normalized time
$\underline{V}$	the ordered pair $(\underline{\alpha}, T)$

$\dot{w}$	propellant flow rate
x, y, z	body fixed principal axis
x', y', z'	non-rotating body axis
X_R, Y_R, Z_R	non-rotating reference frame
X_I, Y_I, Z_I	inertial reference frame

Greek Symbols

$\alpha, \tilde{\alpha}$	normalized adjoint vector
β	angle between x and x' axis
$\tilde{\beta}_o$	defined by Equation (3.13)
β'	defined in Figure 4.3
Γ	iterative scale factor
γ	inertia parameter
ϵ	small constant
$\varepsilon_1, \varepsilon_2, \varepsilon_3$	small parameters
$\varepsilon_1', \varepsilon_2', \varepsilon_3'$	small parameters
$\underline{\zeta}$	vector defining system parameters
$\hat{\zeta}$	space of admissible parameters
η	vector in R_n
θ', φ', ψ'	Euler angles defined in Figure 2.1
θ, φ, ψ	Euler angles defined in Figure 2.2
κ_1, κ_2	defined by Equation (4.55)
$\tilde{\lambda}$	Lagrange multiplier
$\lambda_1, \lambda_2, \lambda_3$	defined in Appendix C
$\lambda^0, \lambda^1, \lambda^2$	defined in Appendix C
λ	dimensionless time
μ	nutation frequency
$\tilde{\Upsilon}$	defined by Equation C.1
Υ	defined by Equation C.1

ν	normalized time
ξ	control jet position defined by Equation (3.60)
$\tilde{\xi}$	defined by Equation (3.61)
σ	normalized time defined by Equation (4.7)
τ	normalized time defined by Equation (3.7)
Φ	n x n matrix of fundamental solutions
$\tilde{\Phi}$	n x n matrix
$\underline{\chi}$	n dimensional state vector
$\underline{\omega}$	angular velocity vector normal to spin axis
$\omega_x, \omega_y, \omega_z$	angular velocities w.r.t. Coordinate System III
$\omega_{x'}, \omega_{y'}, \omega_{z'}$	angular velocities w.r.t. Coordinate System II
Ω	space of admissible control functions
$\tilde{\underline{\omega}}(t), \bar{\underline{\omega}}(t), \hat{\underline{\omega}}(t)$	normalized angular velocity vectors

Subscripts

A	denotes Jet Configuration A
B	denotes Jet Configuration B
C	denotes Jet Configuration C
D	denotes Jet Configuration D
E	denotes Jet Configuration E
f	final condition
k	iteration number
s	component due to spin about z axis
x, y, z	component along the x, y, z axis
x', y', z'	component along the x', y', z' axis
X, Y, Z	component along the X_R, Y_R, Z_R axis
o, 0	initial condition
1, 2, 3, ...	components of a vector switching points

Superscripts

x, y	associates quantity with u_x, u_y
o	initial condition
*	optimal

CHAPTER 1

INTRODUCTION

1.1 The Problem Description

The primary objective of this research was to investigate the problem of minimum time attitude control of axially symmetric spinning spacecraft where control is provided by various combinations of thrust limited reaction jets or small rockets. Major emphasis of the study was the development of techniques for the analysis and design of flight control systems where errors in the spacecraft's attitude and angular rates must be reduced in minimum time. Specifically, both analytic and numerical procedures were employed for synthesizing optimal control systems used for properly orienting a spinning spacecraft with respect to specified reference directions starting from known initial conditions of the vehicle's attitude and transverse angular rates.

In the literature one finds that most papers on the attitude control of spinning spacecraft can be grouped into the following distinct classes: (1) discussions of the vehicle's motion and stability when some type of passive control is employed (a nutation damper), (2) designs for multi-impulse or continuous control schemes(minimization of a cost function is not considered), and (3) procedures for synthesizing both open and closed loop optimal controls (the performance criterion may be fuel, time, or power). In those papers

which deal with the problem of controlling a spinning vehicle in minimum time the major emphasis has been placed on synthesizing control laws for various idealized analytic models. Thus, it does not appear that a general theory for the time-optimal control of spinning spacecraft has been developed. An ideal general theory would: (1) illuminate the basic structure of the problem so that it can provide a foundation upon which to base the analysis and design of flight control systems, (2) provide analytic and computational procedures for synthesizing open or closed loop controls, and (3) form a foundation for synthesizing new procedures which would be useful in solving more complex problems. In the research discussed in this report emphasis has been placed on Items (1) and (2).

1.2 Discussion of the Problem

It is well known that a rigid axially symmetric body which is spinning about a principal axis of maximum or minimum moment of inertia maintains a stable orientation relative to an inertial frame when the vehicle's total angular momentum vector, the angular velocity vector, and the spin axis all coincide. However, for most mission requirements the inherent stability of a spinning vehicle must be augmented by either an active or passive control system. The type of control device employed depends, of course, on a variety of factors which includes the error that can be tolerated in the terminal conditions and the time over which a maneuver must be carried out. For example, passive dampers that dissipate energy can reduce unwanted transverse angular rates but do not, in general, provide control over

both the vehicle's attitude and nutation rate. Therefore, due to the action of disturbance torques and the resulting motion of the desired spin axis orientation or the requirement for exact reorientations of the vehicle's spin axis, it is necessary to provide an active control system. In summary, one can describe the basic functions of an active system as those of maneuvering the vehicle in a prescribed manner and stabilizing it (reducing the transverse angular rates to zero) when a desired orientation has been acquired.

Over the past years various devices have been employed for controlling the attitude of space vehicles. For example, an active control system designed for station keeping may employ magnetic torquing; however, when rapid corrections must be made in the vehicle's attitude, one would normally design the control system to include reaction jets or small rockets. Mass expulsion systems appear to be the most versatile method of altering the spin-axis direction. Such a system is self-contained and is not affected by the environment of the satellite. In addition, the control magnitudes are normally larger than those provided by other systems of comparable weight. Changes in the vehicle's attitude or transverse angular rates can be accomplished by applying either continuous or pulsed torques normal to the spin axis. Controlling the system in this manner can introduce significant transverse angular rates in the vehicle which in turn causes the spin axis to nutate following a correction. Some authors have assumed that the magnitude of the controlling torques is so small that the spin axis remains nearly aligned with the total angular momentum vector throughout the interval over which control is applied. In cases where the

important design criterion is minimum time, the control magnitude must be larger than that considered in the previous example; therefore, the transverse angular velocity and spin axis attitude must be controlled simultaneously. Thus, the time-optimal control problem becomes one of choosing from among those admissible controls which cause a specified change in state for a particular system that steering function which effects the reorientation in the least time.

In the present study we are concerned with the problem of controlling both the attitude and the transverse angular rates of an axially symmetric spacecraft by means of reaction jets. For the purpose of this analysis it is assumed that the system can be represented mathematically as a rigid body with a single axis of symmetry. Also, the vehicle is assumed to be spinning at a constant rate about its axis of symmetry and, in addition, may be nutating as a result of initial non-zero angular rates about the transverse axis. The third and final restrictive assumption is that motion of the vehicle's axis of symmetry is limited to small angular excursions about a nominal direction. This assumption is reasonable if the attitude and angular rate errors which must be corrected during an acquisition maneuver are small or if subsequent reorientations of the spin axis are through angles of approximately fifteen degrees or less.

The problem specifications must also include a statement as to the type of control device employed. For the problem considered in this report it is assumed that control is provided by various combinations of thrust limited reaction jets or small rockets; the controller configurations considered are shown in Figure 1.1. Case (A)

corresponds to a single gimballed jet which can be oriented arbitrarily in a plane normal to the vehicle's axis of symmetry. In Case (B) control is provided by four body fixed jets which produce control torques about the x and y axis. In Case (C) and (D) control is provided by two fixed jets and one fixed jet respectively. Here both positive and negative torques are produced about the y axis when control is provided by two jets-Case (C). In contrast, only a positive (negative) control moment is available about the y axis when control is provided by a single jet-Case (D). In Case (E) the basic spacecraft consists of two separate sections which are connected at the axis of symmetry by a frictionless bearing; the aft section, which houses the attitude sensors and four body fixed reaction jets, has a zero spin rate about the vehicle's axis of symmetry.

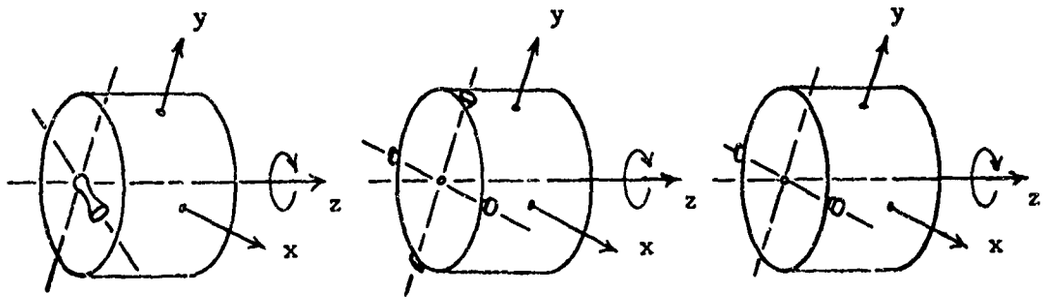

(A) Gimballed Jet (B) 4-Jets (C) 2-Jets

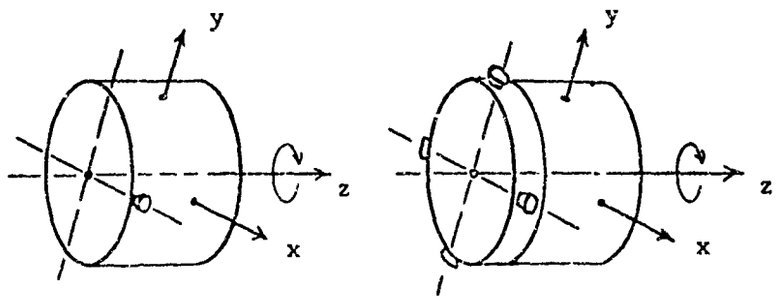

(D) 1-Jet (E) Non-Spinning Platform

Figure 1.1 Control Jet Configurations

1.3 Summary of Related Work

In the literature we find that, in general, four basic techniques have been considered for synthesizing minimum time controls. The first is to form a functional relation between the optimal control and the state. Here a necessary condition (e.g., the maximum principle) is used to determine the qualitative structure of the optimal steering functions; the exact control is then specified by the instantaneous values of the state variables. This procedure is commonly referred to as closed loop control. The major advantage offered by this method is that it allows continuous feedback control since the optimal control is known at each instant. However there are, in general, no known synthesis techniques for determining a functional relation between the optimal control and the state for both higher order linear and non-linear systems when the cost functional is time. For lower order systems it is possible to relate the position of the state point $\underline{\chi}$ to the switching surface and thus determine the sign of the control function $\underline{u}(\underline{\chi})$. This technique has been applied by Athans, et al. [1] and Gruber, et al. [2] to the problem of minimum time angular velocity control of a spinning axially symmetric spacecraft.

A second procedure which has been considered by various authors also relates the control functionally to the state and is a useful approach for feedback control systems. This method is often referred to as quasi-optimal control. Here the desirable features of closed loop control are retained, in addition, the computational task associated with synthesizing true minimum time controls is reduced. This is accomplished by approximating the true minimum time control by a

nearly time-optimal control. As could be expected, the difficulty of the synthesis problem depends upon the error that can be tolerated between the exact optimal control and the approximation. Such a procedure has been applied to a satellite attitude control problem by Friedland [3].

A third commonly used method for computing the minimum time control corresponding to specific boundary conditions is the iterative or successive approximation technique. In contrast to feedback control the iterative methods normally give the entire control law rather than an instantaneous value of $\underline{u}$. Thus one could observe the state at discrete times and solve a number of two point boundary value problems in order to determine the optimal control. In general, two types of iterative procedures have been investigated in the literature. First, those schemes which systematically adjust the control (steepest descent, second variation, etc.) until specified boundary conditions are satisfied; and second, those methods which rely on a trial and error process. An extended form of steepest descent was employed by Hales and Flugge-Lotz [4] to determine minimum fuel controls for a rigid body in orbit. The latter was used by Bass [5] in an attempt to solve the non-linear, minimum time, control problem. A drawback of iterative schemes is the length of time required to compute the optimal control. In most cases the computation time has made it impossible to employ iterative techniques to generate optimal controls in feedback systems.

Finally, there are those solutions obtained from an intuitive analysis of the attitude control problem. In many cases the model

representing the physical system has been simplified (e.g., reduced to a lower order system) or restrictions have been placed on the control system (e.g., impulsive thrusting, very low thrust, etc.) thus allowing one to solve the optimal control problem by inspection for certain initial and final values of the state variables. Studnev [6] investigated the problem of controlling both the spin axis attitude and angular rates for a number of "mixed" cost functions when the control is impulsive. Poralli and Connolly [7] used a similiar approach to obtain minimum fuel impulsive controls for a fourth order linear model of a spinning spacecraft.

In past studies of the attitude control problem where one or more of the aforementioned techniques are applied it is often the case that relatively little insight is provided as to the performance capabilities of physically realizable control systems. These analysis have not, in general, considered the inter-relation between the actual physical system, the type of controllers employed, and the initial acquisition or subsequent reorientation maneuver which must be carried out.

1.4 Summary of the Present Work

The following are the principal contributions of this study:

1. As a means of illuminating the structure of the time-optimal control problem this study provides answers to the following questions. For a given vehicle configuration what is the minimum time required to carry out a specified change in attitude? How do the system parameters affect the minimum reorientation time? What are the characteristics of the optimal control in terms of the system

parameters? For a given rate of propellant expenditure how do various control jet configurations compare with one another in terms of the minimum time required to reorient the spin axis through a given angle? Can one find analytic solutions to the optimal control problem for certain control jet configurations?

In view of these objectives exact time-optimal controls have been determined for a wide range of vehicle configurations and spin axis attitude errors when steering is provided by those control systems depicted in Figure 1.1. It is of interest to note that Controllers (D) and (E) are not usually considered in the literature. In addition, it is found that Control System (D) with unlimited control power cannot, for the class of boundary conditions considered, effect a given transition in the state point over an arbitrarily small interval of time, and that (E) is not normal. Moreover, since the jet configurations shown in Figure 1.1 are physically realizable the results of this study should be useful in the design of active control systems. For example, a comparison of performance capabilities shows that certain jet configurations are "better" than others; and, in addition, that savings in time and fuel can be obtained through an appropriate selection of both the vehicle's geometry and the thruster configuration.

2. The maximum principle approach to the optimal control problem results in the requirement for solving a two point boundary value problem. For most higher order systems it is not, in general, possible to solve directly for the optimal control in terms of the error between the actual and desired state point. For lower order

systems (control of a vehicle's angular rates) Athans, et al. [1] were able to relate the state point to the switching lines and thus obtained the optimal control in feedback form. In this study synthesis procedures are employed which involve both closed form solutions and a combination of closed form with a numerical iterative technique. In those cases where it was not possible to obtain the optimal control directly an iterative scheme similar to Newton's method was used to solve the two point boundary value problem. This algorithm was developed in view of the peculiar characteristics of the attitude control problem (the system is non-dissipative, optimal control for Jet Configuration (D) contains coast periods, and optimal steering for System (E) may be non-unique) and is described in Appendix A. Several unique features of this numerical method are:

a) In certain cases inequality constraints are placed on the magnitude of several components of the initial adjoint vector and on the magnitudes of the computed corrections to the adjoints and final time.

b) A systematic method for crossing switching surfaces is proposed which takes advantage of the apparent "smoothing" (a reduction in the magnitude of the discontinuity of the support hyperplanes at the corners) of the isochrones as the dimension of the control vector increases.

The advantage of using both analytic and numerical schemes in conjunction with a normalized state representation of the system is that families of solutions are generated and plotted as graphs with a

modest expenditure of computer time. From the graphs one can readily determine both the optimal steering law and the minimum final time. At this point it should be noted that optimal controls are only given for certain classes of error signals. Therefore, the results of this study would not, in general, be used to generate optimal controls in feedback systems. However, under "ideal" conditions numerical procedures such as the one described in this study could be employed to synthesize "usable" steering commands.

CHAPTER 2

PRELIMINARY DEVELOPMENTS

In this chapter the coordinate frames are defined; the equations of motion required in subsequent chapters are developed; and some control theory notions pertinent to the attitude control problem are presented.

2.1 Coordinate Systems

There are a number of factors that one must consider before choosing a particular coordinate geometry-among these are: (1) the effort required to determine either closed form or numerical solutions to the resulting system of equations and to easily obtain a physical interpretation of the results, and (2) mechanization requirements that constrain the manner in which various control sources must be represented. The fundamental coordinate systems required are shown in the following two figures.

Figure 2.1 defines the position of the vehicle relative to an inertially stationary (X_I, Y_I, Z_I) coordinate frame where the X_I axis forms a fixed angle with respect to the vernal equinox and the Z_I axis is normal to the orbit plane. It will be useful in the following discussions to define (X_R, Y_R, Z_R), hereafter referred to as Coordinate System I, relative to the (X_I, Y_I, Z_I) reference axis. This definition is made in terms of the angles θ', φ', and ψ' as shown in Figure 2.1.

Two additional reference frames are defined in relation to

Coordinate System I. In the analysis which follows it is assumed that the motion of the spin axis is limited to small angular excursions about the Z_R axis - a nominal direction. Thus, for this type of motion the position of the vehicle's spin axis with respect to Coordinate System I can be conveniently defined through the use of Euler angles; this would not be the case for arbitrarily large values of attitude

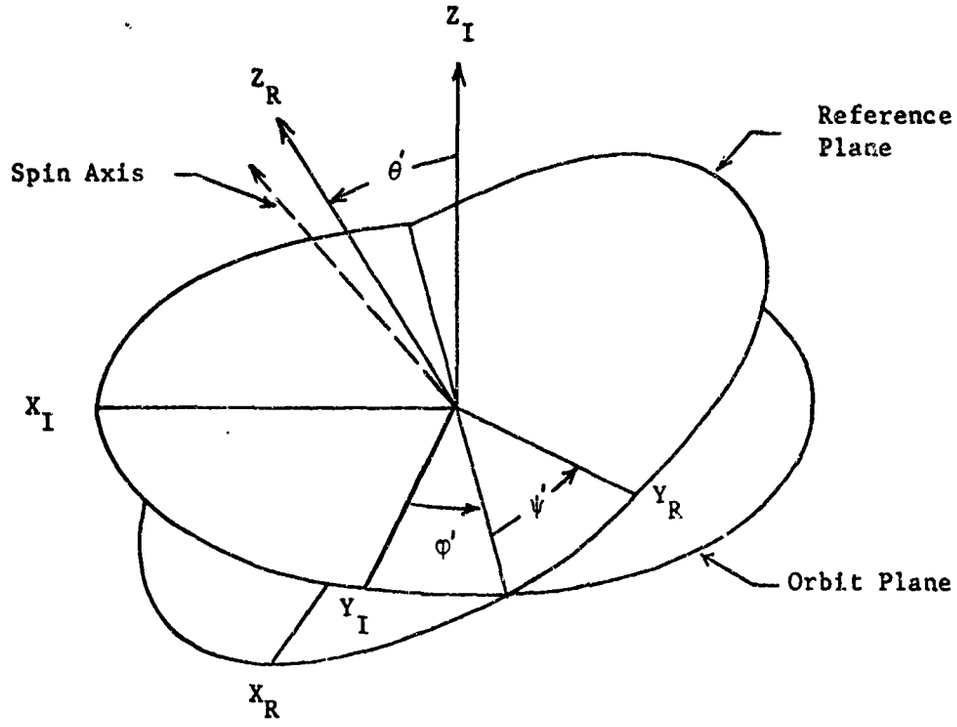

Figure 2.1. Definition of the (X_R, Y_R, Z_R) Coordinate System

error since the rate of change of one of the angles will become unbounded for certain attitudes. The orientation of the body fixed principal axis (x, y, z), hereafter referred to as Coordinate System III, is specified by the Euler angles φ, θ, and ψ as shown in Figure 2.2. The order of rotation is a precession of the line of

nodes φ about Z_R, a tilt θ of the spin axis about the line of nodes, and a rotation ψ about the z axis. The angles θ and φ that the spin axis makes with respect to Coordinate System I represents the body attitude error.

The (x', y', z') coordinate frame, hereafter referred to as Coordinate System II, is also defined in Figure 2.2. This system is the result of "de-spinning" the body fixed (x, y, z) reference frame. Thus, Coordinate System II has a zero spin rate with respect to the z axis.

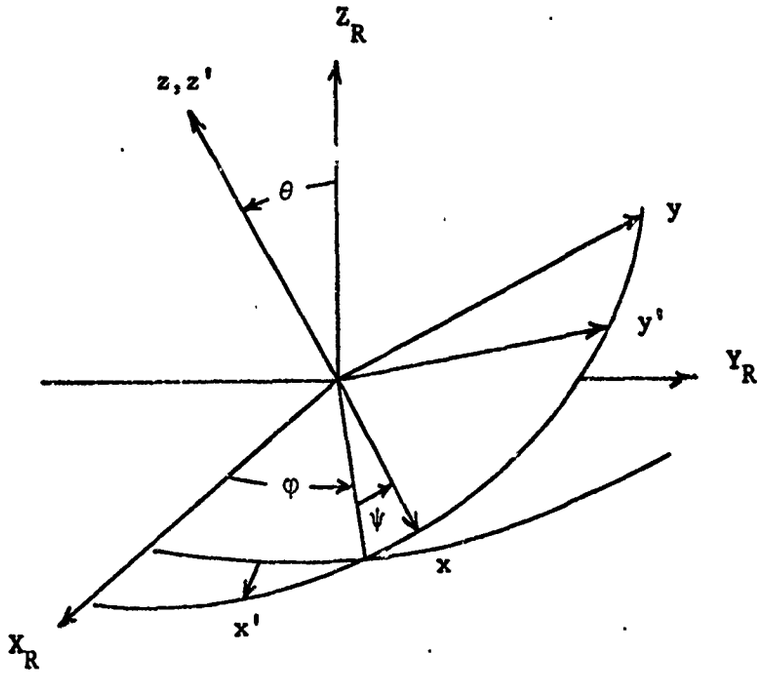

Figure 2.2. Definition of the (x,y,z) and (x',y',z') Coordinate Systems

The fundamental coordinate transformation between Reference Frames II

and III can be written as

$$\begin{bmatrix} e_{x'} \\ e_{y'} \\ e_{z'} \end{bmatrix} = \begin{bmatrix} \cos\beta & -\sin\beta & 0 \\ \sin\beta & \cos\beta & 0 \\ 0 & 0 & 1 \end{bmatrix} \begin{bmatrix} e_x \\ e_y \\ e_z \end{bmatrix} \tag{2.1}$$

where

$$\beta = \omega_z t + \beta_o .$$

2.2 Equations of Motion

It is well known that the angular motion of a rigid body may be described by the Euler equations:

$$I_x \dot{\omega}_x(t) - \omega_y(t)\omega_z(t)(I_y - I_z) = M_x(t) \tag{2.2}$$

$$I_y \dot{\omega}_y(t) - \omega_x(t)\omega_z(t)(I_z - I_x) = M_y(t) \tag{2.3}$$

$$I_z(\dot{\omega}_z(t) - \omega_y(t)\omega_x(t)(I_x - I_y) = M_z(t) \tag{2.4}$$

where the dot denotes derivative with respect to time.[1] Also, in the analysis which follows the moments of inertia are assumed to be constant throughout the interval over which control is applied. In general, a vehicle's mass changes less than 5% due to the expenditure of propellant during a nominal reorientation maneuver; therefore, this is not an unreasonable assumption.[2] If the z axis is the axis of symmetry then $I_x = I_y = I$. We can now rewrite the Euler equations as follows:

$$\dot{\omega}_x(t) = (1 - \frac{I_z}{I})\omega_z(t)\omega_y(t) + \frac{M_x(t)}{I} \tag{2.5}$$

---

[1] A derivation of the Euler equations can be found in Goldstein [8].

[2] Typical fuel requirements are presented in [9].

$$\dot{\omega}_y(t) = (1 - \frac{I_z}{I})\,\omega_z(t)\omega_x(t) + \frac{M_y(t)}{I} \qquad (2.6)$$

$$\dot{\omega}_z(t) = 0 \qquad (2.7)$$

The last of these equations results in $\omega_z(t) = \omega_s$ = constant since external moments about the z-axis are assumed absent.

For Controller Configurations (A) and (E) it is desirable to write the transverse angular velocities with respect to Coordinate System II. Applying the transformation given by (2.1) to equations (2.5) and (2.6) we find

$$\dot{\omega}_{x'}(t) = -\frac{I_z}{I}\,\omega_s\omega_{y'}(t) + \frac{M_x(t)}{I}\cos\beta - \frac{M_y(t)}{I}\sin\beta, \qquad (2.8)$$

$$\dot{\omega}_{y'}(t) = \frac{I_z}{I}\,\omega_s\omega_{x'}(t) + \frac{M_x(t)}{I}\sin\beta + \frac{M_y(t)}{I}\cos\beta\ , \qquad (2.9)$$

where

$$\omega_{x'}(t) = \omega_x(t)\cos\beta - \omega_y(t)\sin\beta, \qquad (2.10)$$

$$\omega_{y'}(t) = \omega_x(t)\sin\beta + \omega_y(t)\cos\beta\ . \qquad (2.11)$$

Using the Euler angle notation given in Figure 2.2 we can derive the following transformation that relates $\omega_{x'}$, $\omega_{y'}$, and $\omega_{z'}$ to the time rate of change of the Euler angles:

$$\omega_{x'}(t) = \dot{\phi}\sin\theta\sin\psi + \dot{\theta}\cos\psi \qquad (2.12)$$

$$\omega_{y'}(t) = \dot{\phi}\sin\theta\cos\psi - \dot{\theta}\sin\psi \qquad (2.13)$$

$$\omega_{z'} = \dot{\phi}\cos\theta + \dot{\psi} \qquad (2.14)$$

For small angular excursions about the Z_R axis $\sin\theta$ and $\cos\theta$ may be represented by the first order terms of their respective power series. Thus, $\sin\theta = \theta$, $\cos\theta = 1$ when terms of $O(\theta^2)$ are neglected. In addition, $\omega_{z'} = 0$ since Coordinate System II does not rotate about the

z' axis. Equation (2.14) is now integrated with the following result

$$\varphi(t) = -\psi(t)+c. \tag{2.15}$$

As will be shown in the following paragraphs this relation allows us to represent the spin axis attitude in terms of rotations about the x' and y' axis.

In the absence of external torques about the z axis the spin rate remains constant, and therefore the spin axis attitude can be conveniently represented by the (X_R-Y_R) components of the angular momentum vector $I_z\omega_s\underline{e}_z$ as shown in Figure 2.3.

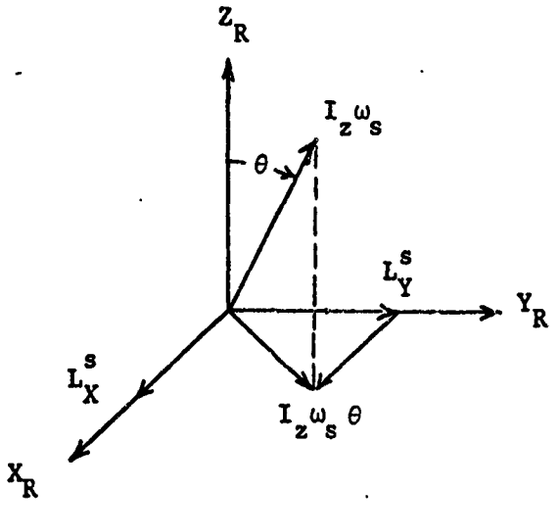

Figure 2.3. Definition of L_X^s and L_Y^s

Define the X_R and Y_R components of $I_z\omega_s\underline{e}_z$ by:

$$L_X^s(t) = I_z\omega_s\,\theta\,\sin\varphi \tag{2.16}$$

$$L_Y^s(t) = -I_z\omega_s\,\theta\,\cos\varphi. \tag{2.17}$$

Differentiating the above equations with respect to time and after combining the results with Equations (2.12) through (2.15) we find:

$$\dot{L}_X^s(t) = I_z \omega_s \omega_{y'}(t) \tag{2.18}$$

$$\dot{L}_Y^s(t) = -I_z \omega_s \omega_{x'}(t) \tag{2.19}$$

Thus L_X^s and L_Y^s are directly related to the integral of the rotation rates about y' and x' axis respectively. The equations of motion for a spinning vehicle can now be written in vector form as follows:

$$\frac{d}{dt}\begin{bmatrix} \omega_{x'}(t) \\ \omega_{y'}(t) \\ L_X^s(t) \\ L_Y^s(t) \end{bmatrix} = \begin{bmatrix} 0 & -\frac{I_z \omega_s}{I} & 0 & 0 \\ \frac{I_z \omega_s}{I} & 0 & 0 & 0 \\ 0 & I_z \omega_s & 0 & 0 \\ -I_z \omega_s & 0 & 0 & 0 \end{bmatrix} \begin{bmatrix} \omega_{x'}(t) \\ \omega_{y'}(t) \\ L_X^s(t) \\ L_Y^s(t) \end{bmatrix} + \begin{bmatrix} \frac{1}{I} & 0 \\ 0 & \frac{1}{I} \\ 0 & 0 \\ 0 & 0 \end{bmatrix} \begin{bmatrix} M_{x'}(t) \\ M_{y'}(t) \end{bmatrix} \tag{2.20}$$

The control moments which appear in (2.20) are defined by:

$$M_{x'}(t) = M_x(t)\cos\beta - M_y(t)\sin\beta \tag{2.21}$$

$$M_{y'}(t) = M_x(t)\sin\beta + M_y(t)\cos\beta \tag{2.22}$$

As will be shown, Equation (2.20) is a useful representation of the system when control is provided by Thruster Configuration(A). In addition, integration of (2.20), providing $M_x(t)$ and $M_y(t)$ are known, gives the instantaneous position of the spin axis which is required if minimum time trajectories are to be plotted in the $(X_R\text{-}Y_R)$ plane.

For the remaining controller configurations, Cases (B) through (E), it is convenient to describe the spin axis attitude in terms of the total angular momentum of the system. This approach is desirable from a computational standpoint since the equations representing angular velocity are uncoupled from those representing angular momentum. The spin axis attitude can be readily determined if one expresses the

systems total angular momentum with respect to Coordinate System I. Components of the total angular momentum about the X_R and Y_R axis are the result of two contributions: a projection of the angular momentum vector $I_z \omega_s \underline{e}_z$ onto the $(X_R\text{-}Y_R)$ plane and the $X_R\text{-}Y_R$ components of the transverse angular momentum $I\omega_x$ and $I\omega_y$. Thus, the X_R and Y_R components of angular momentum, when the spin axis is restricted to small angular excursions about the Z_R-axis, are given by the following expressions:

$$L_X(t) = I\omega_{x'}(t) + I_z\omega_s\,\theta \sin\varphi \qquad (2.23)$$

$$L_Y(t) = I\omega_{y'}(t) - I_z\omega_s\,\theta \cos\varphi \qquad (2.24)$$

A geometric interpretation of L_X and L_Y is presented in Figure 2.4.

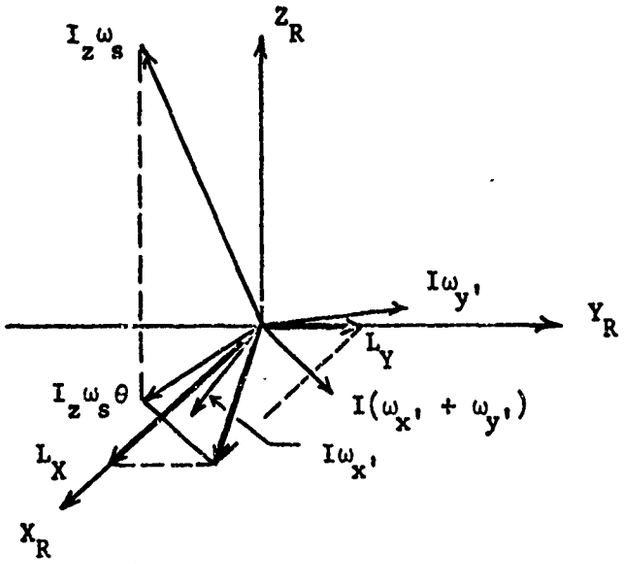

Figure 2.4. Definition of L_X and L_Y

Differentiating (2.23) and (2.24) with respect to time and combining the result with (2.8) and (2.9) we find:

$$\dot{L}_X(t) = M_{x'}(t) \qquad (2.25)$$

$$\dot{L}_Y(t) = M_{y'}(t) \qquad (2.26)$$

When control is provided by Thruster Configurations (B) through (D), it is convenient to represent the spin axis attitude by Equations (2.25) and (2.26) and to use the Euler equations, (2.5) and (2.6), to describe the transverse angular velocities with respect to the body fixed reference frame. Thus, the controlled equation becomes:

$$\frac{d}{dt}\begin{bmatrix}\omega_x(t)\\ \omega_y(t)\\ L_X(t)\\ L_Y(t)\end{bmatrix} = \begin{bmatrix}0 & \gamma\omega_s & 0 & 0\\ -\gamma\omega_s & 0 & 0 & 0\\ 0 & 0 & 0 & 0\\ 0 & 0 & 0 & 0\end{bmatrix}\begin{bmatrix}\omega_x(t)\\ \omega_y(t)\\ L_X(t)\\ L_Y(t)\end{bmatrix} + \begin{bmatrix}\frac{1}{I} & 0\\ 0 & \frac{1}{I}\\ \cos\beta & -\sin\beta\\ \sin\beta & \cos\beta\end{bmatrix}\begin{bmatrix}M_x(t)\\ M_y(t)\end{bmatrix} \quad (2.27)$$

The controller depicted in Figure 1.1.E employs a non-spinning platform which is mounted to the vehicle by a frictionless bearing; therefore, the thrusters are stationary with respect to Coordinate System II. For this control system it is convenient to use Equations (2.25) and (2.26) to describe the spin axis attitude and the transformed Euler equations, (2.8) and (2.9), to represent the vehicle's transverse angular velocities. Hence, the controlled equation is:

$$\frac{d}{dt}\begin{bmatrix}\omega_{x'}(t)\\ \omega_{y'}(t)\\ L_X(t)\\ L_Y(t)\end{bmatrix} = \begin{bmatrix}0 & -\frac{I_z\omega_s}{I} & 0 & 0\\ \frac{I_z\omega_s}{I} & 0 & 0 & 0\\ 0 & 0 & 0 & 0\\ 0 & 0 & 0 & 0\end{bmatrix}\begin{bmatrix}\omega_{x'}(t)\\ \omega_{y'}(t)\\ L_X(t)\\ L_Y(t)\end{bmatrix} + \begin{bmatrix}\frac{1}{I} & 0\\ 0 & \frac{1}{I}\\ 1 & 0\\ 0 & 1\end{bmatrix}\begin{bmatrix}M_{x'}(t)\\ M_{y'}(t)\end{bmatrix} \quad (2.28)$$

In order to complete the mathematical formulation of the problem we must specify the control vector which appears in Equations (2.20),

(2.27), and (2-28) in accordance with the physical limitations of each control jet configuration. This process is carried out in Chapters 3 through 5 where the problem of synthesizing optimal control laws for each of the five jet configurations is investigated in detail. Specifically, the mathematical problem to be considered is one of selecting a control vector $\underline{M}(t)=M_x(t)\underline{e}_x+M_y(t)\underline{e}_y$ from among the admissible controls which will take each of the fourth order systems from a specified initial state to a desired terminal state in less time than any other admissible control.

2.3 Some Pertinent Control Theory Concepts

The purpose of this section is to formally define some control theory notions which are pertinent to the attitude control problem (controllability, normality, etc.).

Definition 2.1 (The Optimal Control Problem)

Let $U([t_o,t_f];\Omega)$ be the input space of a given dynamical system. Let $(\underline{x}(t),\underline{u}(t),t)$ a continuous function from $R_n \times R_q \times [t_o,t_f]$ into R_1 and define

$$J(\underline{x}_o,t_o;\underline{u}(t)) = \int_{t_o}^{t_f} (\underline{x}(t),\underline{u}(t),t)dt \qquad (2.29)$$

to be a performance functional mapping $R_n \times R_1 \times U$ into R_1. Then the optimal control problem is defined as: find the control sequence $\underline{u}(t)$, $t\epsilon[t_o,t_f]$, which drives the state from $\underline{x}_o$ at time t_o to the desired final state $\underline{x}_f$ at time t_f (t_f not necessarily given) such that $J(\underline{x}_o,t_o,\underline{u})$ is minimized (maximized).

In this study the vector $\underline{x}(t)$ represents the vehicle's attitude angles and rotation rates and must satisfy a linear differential

equation of the following form

$$\dot{\underline{x}}(t) = A\underline{x}(t) + B(t)\underline{u}(t) = \underline{f}(\underline{x}(t),\underline{u}(t),t) \tag{2.30}$$

where $\underline{x}_o, t_o, \underline{x}_f$ are given and the allowable control sets corresponding to Jet Configurations (A) thru (E) are:

Scheme A

$$\underline{u}_A(t) \in \Omega_A \quad \Omega_A = \{ \underline{u}(t): \sqrt{u_{x'}^2(t)+u_{y'}^2(t)} \leq 1\} \tag{2.31}$$

Scheme B

$$\underline{u}_B(t) \in \Omega_B \quad \Omega_B = \{ \underline{u}(t): |u_x(t)| \leq 1, \ |u_y(t)| \leq 1\} \tag{2.32}$$

Scheme C

$$\underline{u}_C(t) \in \Omega_C \quad \Omega_C = \{ \underline{u}(t): u_x(t) = 0, |u_y(t)| \leq 1\} \tag{2.33}$$

Scheme D

$$\underline{u}_D(t) \in \Omega_D \quad \Omega_D = \{ \underline{u}(t): u_x(t) = 0, \ 0 \leq u_y(t) \leq 1\} \tag{2.34}$$

Scheme E

$$\underline{u}_E(t) \in \Omega_E \quad \Omega_E = \{ \underline{u}(t): |u_{x'}(t)| \leq 1, |u_{y'}(t)| \leq 1\} \tag{2.35}$$

The controls $\underline{u}_A(t)$ through $\underline{u}_E(t)$ are defined in terms of both the maximum thrust produced by the gas jets and the moment arms in Sections 3.1, 4.1, and 5.1. Note that the bounds on the components of the control vectors were determined under the assumption that the maximum rate of fuel flow is the same in each of the five control schemes. This appears to be a fair way of comparing performance capabilities.

Definition 2.2 (Complete Controllability)

Assume that in the definition of control sets Ω_A thru Ω_E, $||\underline{u}(t)||$

is unbounded. Then System (2.30) is said to be completely controllable on a finite interval $[t_o,t_f]$ if for every state $\underline{X}_o \epsilon R_n$ at time t_o and any desired final state $\underline{X}_f$ at $t_f, \underline{X}_f \epsilon R_n$, there exists a control $\underline{u}(t)$ defined on $[t_o,t_f]$ such that $\underline{X}(t_f)=\underline{X}_f$.

Under certain conditions it may be required to carry out a given change in the state point when the interval $[t_o,t_f]$ is arbitrarily small. This naturally leads to the question as to whether a system can be driven from some initial state $\underline{X}_o$ at t_o to a desired final state $\underline{X}_f$ at t_f' when $[t_o,t_f']$ is a subinterval of $[t_o,t_f]$.

Definition 2.3 (Total Controllability)

System (2.30) is said to be totally controllable on an interval $[t_o,t_f]$ if it is completely controllable on every subinterval of $[t_o,t_f]$.

If $\Phi(t,t_o)$ is the transition matrix for (2.30) and $\tilde{\Phi}(t,t_o) = \Phi(t,t_o)B(t)$ then the necessary and sufficient conditions for complete and total controllability can be summarized as follows:

Theorem 2.1

System (2.30) is completely controllable on an interval $[t_o,t_f]$ if and only if the rows of $\tilde{\Phi}(t,t_o)$ are linearly independent functions of t on $[t_o, t_f]$.

Theorem 2.2

System (2.30) is totally controllable on the interval $[t_o,t_f]$ if and only if the rows of $\Phi(t,t_o)$ are linearly independent functions of t on every subinterval of $[t_o,t_f]$.

Note that Theorems (2.1) and (2.2) only provide necessary conditions for complete and total controllability when restrictions are

placed on the admissible control. From the necessary and sufficient conditions for complete controllability we find:

1. For System (2.20)

$$\tilde{\Phi}(t) = \frac{1}{I}\begin{bmatrix} \cos\frac{I_z\omega_s t}{I} & \sin\frac{I_z\omega_s t}{I} \\ -\sin\frac{I_z\omega_s t}{I} & \cos\frac{I_z\omega_s t}{I} \\ 1 & 0 \\ 0 & 1 \end{bmatrix} \tag{2.36}$$

2. For System (2.27)

a) 4 - Jets

$$\tilde{\Phi}(t) = \begin{bmatrix} \frac{1}{I}\cos(\gamma\omega_s t) & -\frac{1}{I}\sin(\gamma\omega_s t) \\ \frac{1}{I}\sin(\gamma\omega_s t) & \frac{1}{I}\cos(\gamma\omega_s t) \\ \cos\beta & -\sin\beta \\ \sin\beta & \cos\beta \end{bmatrix} \tag{2.37}$$

b) 2 - Jets and 1 - Jet

$$\tilde{\Phi}(t) = \begin{bmatrix} -\frac{1}{I}\sin(\gamma\omega_s t) \\ \frac{1}{I}\cos(\gamma\omega_s t) \\ -\sin\beta \\ \cos\beta \end{bmatrix} \tag{2.38}$$

3. For System (2.28)

$$\tilde{\Phi}(t)=\begin{bmatrix} \frac{1}{I}\cos\left(\frac{I_z}{I}\omega_s t\right) & \frac{1}{I}\sin\left(\frac{I_z}{I}\omega_s t\right) \\ -\frac{1}{I}\sin\left(\frac{I_z}{I}\omega_s t\right) & \frac{1}{I}\cos\left(\frac{I_z}{I}\omega_s t\right) \\ 1 & 0 \\ 0 & 1 \end{bmatrix} \tag{2.39}$$

Note that in the above equations we have assumed that $t_o = 0$. Thus, in the three systems considered the control can influence each component of the state vector for all $t\in[t_o,t_f]$. Hence, in the absence of restrictions which may be placed on the admissible control sets, the systems are both completely and totally controllable. However, we note that Control System (D) can be defined as: $0 \leq u_y \leq b_y$, $B(t) \neq 0$; $-b_y \leq u_y < 0$, $B(t) = 0$. If b_y is unbounded then Ω_D becomes the line $(-\infty,\infty)$. Moreover, if $u_y < 0$ then $B(t) = 0$ and the system is neither completely or totally controllable.

Definition 2.4 (Maximum Region of Recoverability)

An element of R_n is a recoverable state in $[t_o,t]$ with respect to $\underline{X}_f$ if there exists an admissible control which will drive the system from this state at t_o to state $\underline{X}_f$ at time t. The maximum region of recoverability with respect to $\underline{X}_f$ in $[t_o,t]$ is the set of all recoverable states in $[t_o,t]$ with respect to $\underline{X}_f$. The definition of a maximum region of reachability with respect to $\underline{X}_o$ follows directly.

From Theorem 2.1 we found that the concept of controllability is basically concerned with the type of coupling that exists between the input and state of a system. However, when the input vector is constrained to belong to a compact, convex subset (Ω) of its vector space

the question of recoverable (reachable) states becomes important. That is, if we wish to synthesize optimal controls for a wide range of boundary conditions (flooding) then it is desirable to know a priori if all states which conform to the small angle approximation are recoverable (reachable) when control is provided by the thruster configurations depicted in Figure 1.1.

Following the work of LeMay [10] and others we find that when certain conditions are satisfied, namely:

1. System (2.30) is completely controllable for a general time t_o.
2. The matrices A and B(t) are piecewise continuous in t, $t_o < t < \infty$.
3. The input is admissible ($\underline{u}(t)$ is measurable and $\underline{u}(t) \epsilon \Omega$).

then a necessary and sufficient condition for the entire state space to be recoverable is given by the following theorem.

Theorem 2.3

The entire state space is recoverable in (t_o, ∞) if and only if

$$\int_{t_o}^{\infty} \|(\Phi(t_o,t)B(t))\ \underline{\eta}\| dt = \infty, \text{ all } \underline{\eta} \neq 0, \underline{\eta} \in R_n \qquad (2.40)$$

where for convenience the vector norm $\| \quad \|$ is defined by $\|\underline{x}\| = \sum_{i=1}^{n} |x_i|$.[3]

It is readily shown that the necessary and sufficient condition provided by Theorem (2.3) is satisfied by Systems (2.20), (2.27), and (2.28); therefore, all states which conform to the small angle restriction are recoverable when control is provided by the five jet

---

[3] LaSalle [11] defines systems which satisfy this condition as "asymptotically proper".

configurations depicted in Figure 1.1. However, in the flooding process we are also concerned with reachable sets since in most cases optimal trajectories are computed between a fixed initial state (the origin) and a selected number of different terminal states. The problem was formulated in this manner since it is somewhat easier to show symmetry properties of the optimal control when the initial state lies at the origin. The control problem considered here can be easily transformed into regulator form since the real parts of the eigenvalues for Systems (2.20), (2.27), and (2.28) are zero; therefore, if the entire state space is recoverable with respect to the origin then it is also reachable with respect to the origin.

Comment 2.1 (Some Properties of the Maximum Reachable Set)

Providing the assumptions listed in [10] are satisfied (the system is totally controllable, the control set is compact and convex, etc.) one can show that the maximum recoverable set (in this case also the maximum reachable set) is compact and convex and is symmetric if Ω is symmetric. Furthermore, for $t > t_o$, the recoverable set has dimension n, grows continuously and strictly monotonically with t in the interval $t_o < t < \infty$, and contains the origin as an interior point.

Definition 2.5 (Minimum Time Isochrone)

The minimum time isochrone is defined by the relation

$$\underline{X}(t) = \{\underline{X}(t): \quad t_f^* (\underline{X}_f) = t; \; t > t_o \}. \tag{2.41}$$

Since the boundary of the maximum recoverable set in (t_o, t_f^*) is the minimum time isochrone and in view of Comment (2.1) we find that the surfaces defined by t_f^* = constant have certain symmetry properties when control is provided by Jet Configurations (A), (B), (C), and (E).

However, control set Ω_D is not symmetric and, in addition, does not contain the origin as an interior point. Therefore, the maximum recoverable (reachable) sets may not grow continuously in all directions with time. Consequently, System (2.27) may not be controllable over an arbitrarily small interval of time even if unlimited power is available to the control system.

2.4 The Maximum Principle

The Maximum Principle of Pontryagin is one of the most useful theorems available for the solution of optimal control problems. The proof of the theorem is discussed in detail in [12] and [13]. The necessary condition for optimality provided by this principle, as it applies to the attitude control problem, is stated here without proof.

Theorem 2.4

Let $\underline{f}(\underline{x},\underline{u}(t),t)$, $\underline{f}_{\underline{x}}(\underline{x},\underline{u},t)$, $\underline{f}_t(\underline{x},\underline{u},t)$, $\mathcal{L}(\underline{x},\underline{u},t)$, $\mathcal{L}_{\underline{x}}(\underline{x},\underline{u},t)$, $\mathcal{L}_t(\underline{x},\underline{u},t)$ be continuous on $R_n \times R_1 \times \Omega$. Define a continuous function from $R_n \times R_q \times R_n \times R_1$ into R_1 as the Hamiltonian by

$$H(\underline{x}(t),\underline{u}(t),P(t),P_o,t) = P_o\mathcal{L}(\underline{x}(t),\underline{u}(t),t) + \langle \underline{P}(t), \underline{f}(\underline{x}(t),\underline{u}(t),t)\rangle. \tag{2.42}$$

If $\underline{u}^*(t)$, $t\in[t_o,t_f^*]$, is an optimal control sequence in $U([t_o,t_f^*];\Omega)$ then there necessarily exists a constant P_o^* and an n-vector $\underline{P}^*(t)$ such that

$$H(\underline{x}^*(t),\underline{u}^*(t), \underline{P}^*(t), P_o^*,t) \geq H(\underline{x}^*(t), \underline{u}(t), P^*(t),P_o^*,t) \quad \underline{u}(t) \in \Omega \tag{2.43}$$

where:

1. $P_o^* \leq 0$

2. $\begin{bmatrix} P_o^* \\ \underline{P}^*(t) \end{bmatrix} \neq 0$

3. $\dot{\underline{P}}^*(t) = - H_{\underline{X}}(\underline{X}^*(t), \underline{u}^*(t), \underline{P}^*(t), P_o^*, t)$

4. $\dot{\underline{X}}^*(t) = H_{\underline{P}}(\underline{X}^*(t), \underline{u}^*(t), \underline{P}^*(t), P_o^*, t)$

5. $\underline{X}^*(t_o) = \underline{X}_o, \ \underline{X}^*(t_f^*) = \underline{X}_f$

If the plant is autonomous and t_f is "free" then

$$H(\underline{X}^*(t), \underline{u}^*(t), \underline{P}^*(t), P_o^*) = 0.$$

An application of the maximum principle transforms the optimal control problem to a two point boundary value problem. To solve the latter we must determine the optimal control (i.e., solve for both the n-vector $\underline{P}^*(t)$ and the final time t_f^*) that takes the system from a specified initial state to a desired final state. For the attitude control problem considered in this study we have assumed that the initial and final states are known; thus, the problem becomes one of selecting the ordered pair $(P^*(t_o), t_f^*)$ such that the state is driven from $\underline{X}_o$ to $\underline{X}_f$ in minimum time.

2.5 Uniqueness of the Bang-Bang Control Law

In the previous section we stated a necessary condition for the optimal control. Perhaps the most useful result of Theorem 2.4 is that it serves to limit the search for $\underline{u}^*(t)$ to a specific class of controls, e.g., the class of bang-bang controls. However, even though a control is found which satisfies the necessary condition there is still the question as to whether the control is globally optimal. This dilemma can be resolved when the allowable control set is of the form $- b_1 \leq u_i \leq b_2$, $b_1 \geq 0$, $b_2 > 0$, $i = 1, 2, \ldots q$, through the concept of

normality.

Definition 2.6 (Normal Control System)

System (2.30) is said to be normal if for each j = 1, 2,...q the functions $\tilde{\Phi}_1^j(t,t_o),\ldots\ldots \tilde{\Phi}_n^j(t,t_o)$ are linearly independent on each interval of positive length ($\tilde{\Phi}^j(t,t_o)$ is the $j^{\underline{th}}$ column vector of $\tilde{\Phi}(t,t_o)$). This is equivalent to saying that the system is controllable with respect to each component of $\underline{u}(t)$.

Theorem 2.5

If the linear system $\dot{\underline{X}}(t) = A(t)\underline{X}(t) + B(t)\underline{u}(t)$ is normal then the time-optimal control is unique (if it exists).

For non-normal systems which are controllable the most that can be said is that there is a bang-bang steering function that is optimal. However, there may be other control laws which cause a specified change in the state of the system in the same minimum time. In view of the definition of normality we find that System (2.27) is normal when control is provided by Jet Configuration (B) thru (D); therefore, the optimal steering functions are unique and, in addition, must operate in a bang-bang (in the case of $\underline{u}_D^*(t)$ an "on-off") mode.

Control System (2.28) is not normal since the elements of each column vector of (2.39) are not linearly independent - consequently, there may be an infinity of optimal steering functions. However, this system is, according to LaSalle, "proper"; from Reference [11] we find that in proper control systems optimal steering has the property that at any given time some component of $\underline{u}^*[t]$ assumes an extreme value. The implications of normality and properness will become evident in Chapter 5 where the optimal steering law for [2.28] is derived. For

Jet Configuration(A) we find that the optimal control is a continuous function of time; therefore, the Hamilton-Jacobi equation provides a sufficient condition for optimality.

2.6 The Hamilton-Jacobi Equation

In cases where the cost functional is sufficiently smooth the Hamilton-Jacobi equation provides both necessary and sufficient conditions for optimality.

Theorem 2.6

Let $H(\underline{\chi},\underline{P},P_o,\underline{u},t)$ be the Hamiltonian of our problem. Let $\hat{\underline{u}}(t)$ and $\tilde{\underline{u}}(t)$ be admissible controls such that

1. The function $H(\underline{\chi},\underline{P},P_o,\underline{u},t)$ has a unique absolute maximum with repect to all $\underline{u}(t)\epsilon\ \Omega$ at $\underline{u}(t) = \tilde{u}(t)$ for each point $(\underline{\chi},t)$ in $(R_n \times R_o)$.
2. $\hat{\underline{u}}(t)$ transfers $(\underline{\chi}_o,t_o)$ to $(\underline{\chi}_f,t_f)$.
3. If $\hat{\underline{\chi}}(t)$ is the trajectory corresponding to $\hat{\underline{u}}(t)$ then $(\hat{\underline{\chi}}(t),t)\epsilon$ $R_n \times R_1$ for t in $[t_o,t_f]$.
4. There is a solution $\hat{J}(\underline{\chi},t)$ of the Hamilton-Jacobi equation

$$-\frac{\partial\hat{J}(\underline{\chi},t)}{\partial t} + H\left[\underline{\chi},\ \frac{\partial\hat{J}(\underline{\chi},t)}{\partial\underline{\chi}}\ ,\ \hat{u}(\underline{\chi},\ \frac{\partial\hat{J}(\underline{\chi},t)}{\partial\underline{\chi}}\ ,t\right] = 0$$

such that

$$\hat{\underline{u}}(t) = \underline{u}(\hat{\underline{\chi}}(t),\ \frac{\partial\hat{J}}{\partial\underline{\chi}}\ (\hat{\underline{\chi}}(t),t),t)$$

for t in $[t_o,t_f]$.

Then $\hat{\underline{u}}(t)$ is an optimal control and $\hat{\underline{\chi}}(t)$ is optimal trajectory in R_n.

CHAPTER 3

REALIZATION OF OPTIMAL STEERING FOR THE GIMBALLED JET

In this chapter we consider the problem of controlling in an optimal manner both the attitude and the transverse components of angular velocity of an axially symmetric spinning spacecraft when control is provided by a reaction jet or small rocket. Specifically, a technique is proposed for synthesizing time-optimal steering commands for the control jet configuration depicted in Figure 3.1. A summary of the work presented in this chapter can be found in Reference [14].

3.1 The Equations of Motion

The gimballed jet corresponds to a control moment of limited magnitude which can be oriented arbitrarily in a plane normal to the vehicle's axis of symmetry. Assume that the single jet delivers a thrust $\hat{f}(t)$. The controller is gimballed; therefore, the thrust vector $\underline{\hat{f}}(t)$ can be decomposed into two components $\hat{f}_{x'}(t)$ and $\hat{f}_{y'}(t)$ as shown in Figure 3.1. The thrust components $\hat{f}_{x'}(t)$ and $\hat{f}_{y'}(t)$ cause torques $a.\hat{f}_{x'}(t)$ and $a.\hat{f}_{y'}(t)$ about the x' and y' axis respectively. If the thrust vector $\underline{\hat{f}}(t)$ is bounded in magnitude by F then

$$\|\underline{\hat{f}}(t)\| \leq F. \tag{3.1}$$

The components of thrust are related by

$$\|\underline{\hat{f}}(t)\| = \sqrt{\hat{f}_{x'}^2(t) + \hat{f}_{y'}^2(t)} \tag{3.2}$$

hence

$$\hat{f}_{x'}^2(t) + \hat{f}_{y'}^2(t) \leq F^2. \tag{3.3}$$

Define the vector $\underline{u}_A(t)$ by

$$\underline{u}_A(t) = \frac{\hat{f}(t)}{F}. \tag{3.4}$$

The components of $\underline{u}_A(t)$, denoted by $u_{x'}(t)$ and $u_{y'}(t)$, are restricted by

$$u_{x'}^2(t) + u_{y'}^2(t) \leq 1. \tag{3.5}$$

Thus, the admissible control space Ω_A is a circle of unit radius in R_2. The torque components $M_{x'}(t)$ and $M_{y'}(t)$ can now be expressed as:

$$\begin{aligned} M_{x'}(t) &= M \cdot u_{x'}(t) \\ M_{y'}(t) &= M \cdot u_{y'}(t) \end{aligned} \tag{3.6}$$

where

$$M = a \cdot F.$$

Combining (3.6) with (2.20) allows us to rewrite the equations of motion as follows:

$$\frac{d}{d\tau}\begin{bmatrix} \tilde{\omega}_{x'}(\tau) \\ \tilde{\omega}_{y'}(\tau) \\ \tilde{L}_X(\tau) \\ \tilde{L}_Y(\tau) \end{bmatrix} = \begin{bmatrix} 0 & -1 & 0 & 0 \\ 1 & 0 & 0 & 0 \\ 0 & 1 & 0 & 0 \\ -1 & 0 & 0 & 0 \end{bmatrix} \begin{bmatrix} \tilde{\omega}_{x'}(\tau) \\ \tilde{\omega}_{y'}(\tau) \\ \tilde{L}_X(\tau) \\ \tilde{L}_Y(\tau) \end{bmatrix} + \begin{bmatrix} 1 & 0 \\ 0 & 1 \\ 0 & 0 \\ 0 & 0 \end{bmatrix} \begin{bmatrix} u_{x'}(\tau) \\ u_{y'}(\tau) \end{bmatrix} \tag{3.7}$$

where

$$\tilde{\omega}_{x'}(\tau) = \frac{I_z \omega_s \omega_{x'}(t)}{M}, \qquad \tilde{\omega}_{y'}(\tau) = \frac{I_z \omega_s \omega_{y'}(t)}{M}$$

$$\tilde{L}_X(\tau) = \frac{I_z \omega_s L_X^s(t)}{IM}, \qquad \tilde{L}_Y(\tau) = \frac{I_z \omega_s L_Y^s(t)}{IM}$$

$$\tau = \frac{I_z \omega_s}{I} t .$$

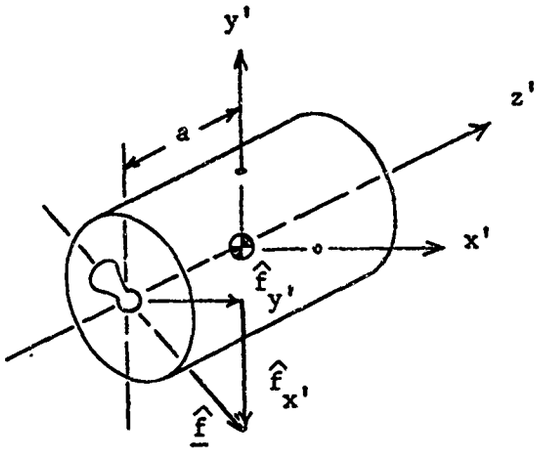

Figure 3.1 Schematic of the Gimballed Jet

The initial and final values of the normalized state variables were chosen to be as realistic as possible and yet be of that form which allows us to solve directly for the optimal control $(\underline{u}^*, T_A^*)$ without resorting to an iterative scheme which requires a digital computer. The boundary conditions considered are:

$$\begin{aligned}
&\tilde{\omega}_{x'}(0) = \tilde{\omega}_{x'}(T_A) = 0 \\
&\tilde{\omega}_{y'}(0) = \tilde{\omega}_{y'}(T_A) = 0 \\
&\tilde{L}_X(0) = \tilde{L}_X(T_A) = 0 \\
&\tilde{L}_Y(0) = 0, \ \tilde{L}_Y(T_A) = \tilde{L}_{Y_f} = -\frac{I_z^2 \omega_s^2 \theta_f}{IM}
\end{aligned} \tag{3.8}$$

Solving (3.7) for $\tilde{\omega}_{x'}(T_A)$, $\tilde{\omega}_{y'}(T_A)$, $\tilde{L}_X(T_A)$, $\tilde{L}_Y(T_A)$ subject to (3.8) and after straightforward mathematical manipulation we can write the following set of governing equations which must be satisfied by the optimal control:

$$\int_0^{T_A} [u_{x'}(\tau)\cos\tau + u_{y'}(\tau)\sin\tau]d\tau = 0 \tag{3.9}$$

$$\int_0^{T_A} [u_{x'}(\tau)\sin\tau - u_{y'}(\tau)\cos\tau]d\tau = 0 \tag{3.10}$$

$$\int_0^{T_A} [u_{x'}(\tau)]d\tau = 0 \tag{3.11}$$

$$\int_0^{T_A} [u_{y'}(\tau)]d\tau = -\tilde{L}_Y \tag{3.12}$$

Thus, for boundary conditions as given by (3.8) the optimal control $(\underline{u}_A^*, T_A^*)$ is only a function of the dimensionless parameter $\tilde{L}_Y$.

At this point it should be noted that the control which satisfies (3.9) through (3.12) can be used to drive the system when $L_X(t_f) = 0$ if the de-spun reference frame is pre-rotated in a counter clockwise direction through the angle $\bar{\beta}_o$ where

$$\bar{\beta}_o = \tan^{-1}\left[\frac{L_X(t_f)}{L_Y(t_f)}\right] \tag{3.13}$$

Also note that the control which is defined by Equation (3.8) can be applied when the boundary conditions are specified in regulator form $(\tilde{L}_Y(0) = I_z^2\omega_s^2\theta_o/IM,\ \tilde{L}_Y(T_A) = 0)$. Moreover, it is found that such cases arise whenever the initial or final orientation corresponds to $\theta = 0$; the problem is essentially independent of θ (the whole problem is

invariant under rotation about the Z_R axis).

3.2 A Necessary Condition for Time-Optimality

The maximum principle is used to determine necessary conditions for the optimal steering functions. Forming the Hamiltonian

$$H = P_1(\tau)[-\tilde{\omega}_y'(\tau) + u_x'(\tau)] + P_2(\tau)[\tilde{\omega}_x'(\tau) + u_y'(\tau)] + P_3(\tau)\tilde{\omega}_y'(\tau) - P_4(\tau)\tilde{\omega}_x'(\tau). \tag{3.14}$$

Maximization of the Hamiltonian with respect to $u_x'(\tau)$ and $u_y'(\tau)$ subject to the constraints given by (3.5) occurs when

$$u_x'(\tau) = \frac{P_1(\tau)}{\sqrt{P_1^2(\tau) + P_2^2(\tau)}} \tag{3.15}$$

$$u_y'(\tau) = \frac{P_2(\tau)}{\sqrt{P_1^2(\tau) + P_2^2(\tau)}} \tag{3.16}$$

which implies $\|\underline{u}_A(\tau)\| = 1$. The variables $P_1(\tau)$ through $P_4(\tau)$, called the adjoints, are solutions of the differential equations

$$\frac{dP_1(\tau)}{d\tau} = -\frac{\partial H}{\partial \tilde{\omega}_x'}, \quad \frac{dP_2(\tau)}{d\tau} = -\frac{\partial H}{\partial \tilde{\omega}_y'}, \quad \frac{dP_3(\tau)}{d\tau} = -\frac{\partial H}{\partial \tilde{L}_X}, \quad \frac{dP_4(\tau)}{d\tau} = -\frac{\partial H}{\partial \tilde{L}_Y} \tag{3.17}$$

which may be written in vector form as

$$\frac{d}{d\tau}\begin{bmatrix} P_1(\tau) \\ P_2(\tau) \\ P_3(\tau) \\ P_4(\tau) \end{bmatrix} = \begin{bmatrix} 0 & -1 & 0 & 1 \\ 1 & 0 & -1 & 0 \\ 0 & 0 & 0 & 0 \\ 0 & 0 & 0 & 0 \end{bmatrix}\begin{bmatrix} P_1(\tau) \\ P_2(\tau) \\ P_3(\tau) \\ P_4(\tau) \end{bmatrix}. \tag{3.18}$$

The solution to this equation is

$$\begin{bmatrix} P_1(\tau) \\ P_2(\tau) \\ P_3(\tau) \\ P_4(\tau) \end{bmatrix} = \begin{bmatrix} \cos\tau & -\sin\tau & 1 & 0 \\ \sin\tau & \cos\tau & 0 & 1 \\ 0 & 0 & 1 & 0 \\ 0 & 0 & 0 & 1 \end{bmatrix} \begin{bmatrix} P_1^o \\ P_2^o \\ P_3^o \\ P_4^o \end{bmatrix} \tag{3.19}$$

where P_1^o through P_4^o are constants of integration. We can now rewrite (3.19 in the following equivalent form:

$$P_1(\tau) = \alpha_1 \cos(\tau + \alpha_2) + \alpha_3 \tag{3.20}$$

$$P_2(\tau) = \alpha_1 \sin(\tau + \alpha_2) + \alpha_4 \tag{3.21}$$

$$P_3(\tau) = \alpha_3 \tag{3.22}$$

$$P_4(\tau) = \alpha_4 \tag{3.23}$$

3.3 Normalization of the Adjoint Vector

As given by the maximum principle the necessary condition for optimality requires that the Hamiltonian be a maximum along an optimal trajectory. When the cost criterion is time we find that $\max_{\underline{u}} H(\underline{\chi}, \underline{u}, \underline{P}, P_o, \tau)$ is independent of $\|\underline{P}(\tau)\|$. Therefore, the adjoint vector can be normalized with respect to one component or a combination of several components of $\underline{\alpha}$.[1] The objective of such a procedure is to reduce the number of independent parameters which quantitatively define the optimal control. In this case normalization also significantly simplifies the optimal steering functions. If the normalizing

[1] Normalization of the adjoint vector is discussed in greater detail in Appendix A.

Note that β_o is the only physical parameter which appears in the first order terms of (4.40) and (4.41) and, therefore, represents the strongest influence on the location of the switching points within the interval $(0, T_B)$. If u^o is positive then σ_1^y and σ_2^y are shifted toward zero when β_o is montone increasing and $0 \leq \beta_o < \pi/4$. It is readily shown that ε_2 is negative when $0 \leq \beta_o < \pi/4$; consequently, the switch point σ_1^y is lost from the left end of the interval $(0, T_B)$ when β_o reaches a value which is slightly less than $\pi/4$. The exact value of β_o at which this occurs depends, of course, on both the system description and the reorientation angle and is denoted by β_o' (see Figure 4.3). Thus when $\beta_o \geq \beta_o'$ the optimal steering functions are no longer described qualitatively by Switching Sequence (2-a). To determine an explicit relation between β_o' and the physical parameters we must consider both Switching Sequence (2-a) and (2-b).

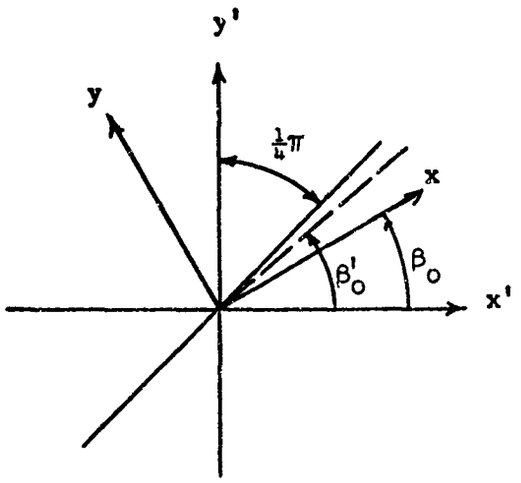

Figure 4.3. Definition of β_o'

results gives

$$(\tilde{P}_1 - \cos\tilde{\alpha}_3)^2 + (\tilde{P}_2 - \sin\tilde{\alpha}_3)^2 = \tilde{\alpha}_1^2 . \qquad (3.31)$$

The trajectory of (3.31), plotted in the $(\tilde{P}_1\text{-}\tilde{P}_2)$ plane, is a circle with center at $(\cos\tilde{\alpha}_3, \sin\tilde{\alpha}_3)$ and radius of $\tilde{\alpha}_1$. Thus, the optimal control can be interpreted geometrically as shown in Figure 3.2.

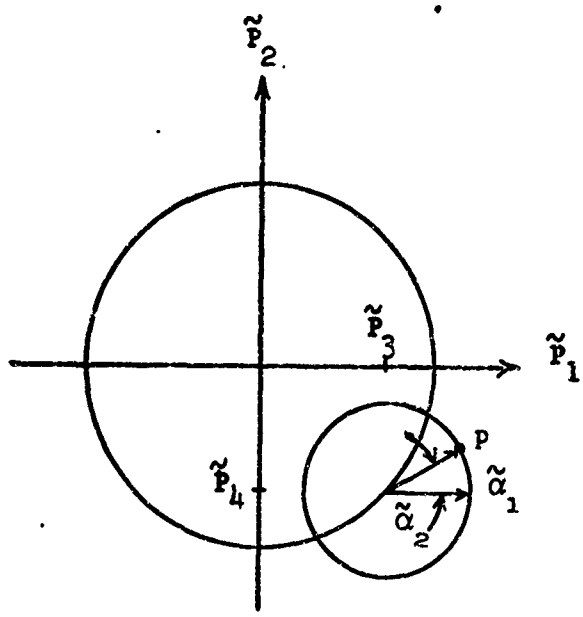

Figure 3.2 A Geometric Interpretation of Equations (3.25) and (3.26)

Here, $u_{x'}^*(\tau)$ and $u_{y'}^*(\tau)$ change with time as p traces out the circle defined by (3.31) in a counterclockwise direction; the position of p at $\tau = 0$ is determined by $\tilde{\alpha}_2$. Thus, the minimum time steering functions are defined quantitatively by the location of the center of the circle, its radius, and the reference angle $\tau + \tilde{\alpha}_2$. As will be shown presently this interpretation of the steering functions provides significant insight as to the exact nature of the optimal steering functions which satisfy boundary conditions of the form given by (3.8).

3.5 Synthesis of the Time-Optimal Control

The optimal control which effects the change in state described by (3.8) must satisfy Equations (3.9) through (3.12). Substituting (3.29) and (3.30) into the governing equations we find that the only terms not fixed by the system description are $\underline{\alpha}$ and T_A^*. Thus, (3.9) through (3.12) can be written in vector form as

$$\underline{\chi}(T_A^*) = \underline{F}(\underline{\alpha}, T_A^*) \tag{3.32}$$

where

$$\underline{\chi}(T_A^*) = \begin{bmatrix} 0 \\ 0 \\ 0 \\ -\tilde{L}_Y \end{bmatrix}$$

The mathematical problem is now one of solving (3.32) for the pair $(\underline{\alpha}, T_A^*)$ as functions of the normalized angular momentum $\tilde{L}_Y$. Thus, the problem of determining a minimum time control is equivalent to that of computing an inverse to (3.32). In general, it is impossible to determine this inverse directly. However, as will be shown, the geometric interpretation of the optimal control, as discussed in Section 3.4, provides the insight required to solve for $(\underline{\alpha}, T_A^*)$.

The task of evaluating $(\underline{\alpha}, T_A^*)$ in terms of $\tilde{L}_Y$ is carried out in two parts. First, based on both the response characteristics of the system when $T_A^* \ll 1$ and when $T_A^* \gg 1$, and in view of the boundary conditions which must be satisfied, we can make certain observations as to the structure of the optimal control. Then, through the geometric interpretation of the steering functions, specific expressions for $\tilde{\alpha}_2$

and $\tilde{\alpha}_3$ can be judiciously chosen which quantify $u^*_{x'}(\tau)$ and $u^*_{y'}(\tau)$ to the point where Equations (3.9) and (3.11) are satisfied. The remaining task is then to solve (3.10) and (3.12) simultaneously for $\tilde{\alpha}_1$ and T^*_A.

3.5.1 Optimal Steering When the Final Time is Small Compared to the Spin Rate

A control which appears to satisfy the boundary conditions when $T^*_A \ll 1$ and, in addition, can be synthesized, at least qualitatively, from (3.29) and (3.30) is depicted in Figure 3.3.

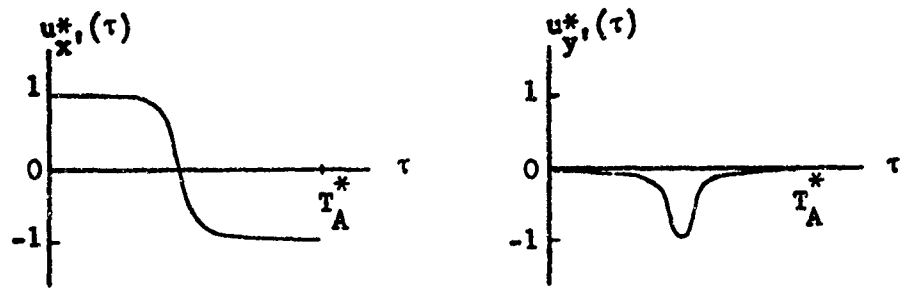

Figure 3.3 A Candidate for Optimal Steering when $T^*_A \ll 1$

Here, a large percentage of the control effort is about the x' axis; during the first part of the interval $[0,T^*_A]$ a positive moment is applied to start the spin axis moving in the proper direction; the control jet must then apply a braking moment in order to reduce the transverse component of angular velocity which has been excited. The controller must also provide a negative moment about the y' axis since the total angular momentum vector must be rotated through the angle θ_f.

Since the ultimate objective is to specify $\underline{\tilde{\alpha}}$ and T^*_A in terms of $\tilde{L}_Y$, the above qualitative description must be translated into appropriate quantitative terms. Let us now reconsider the geometric interpretation of (3.29) and (3.30). From Figure 3.2 we find that the center

of the circle traced out by the point p must lie on a circle of unit radius with center located at the origin. Thus, it appears that control of the form depicted in Figure 3.3 will result when the center of the circle defined by (3.31) lies at approximately (0,-1) and when $\tilde{\alpha}_1$ is slightly less than unity. This ensures that $u_{y'}^*(\tau)$ is negative and that the magnitude of $u_{x'}^*(\tau)$ is considerably larger than the magnitude of $u_{y'}^*(\tau)$, except when $\tau \approx T_A^*/2$. Further, let us postulate that the center of the circle defined by (3.31) lies at exactly (0,-1); therefore, $\tilde{\alpha}_3 = 3\pi/2$. If this is the case then the arc defined by p in Figure 3.2 must be symmetric about the $\tilde{P}_2$ axis if $u_{x'}^*(\tau)$ is to satisfy (3.11); hence, $\tilde{\alpha}_2 = \frac{1}{2}(\pi - T_A^*)$.

In the following sections expressions are derived for $\tilde{\alpha}_2$ and $\tilde{\alpha}_3$ when $T_A^* = m\pi$, $m = 2,4,6,\ldots$, and when $T_A^* \ll 1$. The objective is then to compare all results in an effort to determine expressions for $\tilde{\alpha}_2$ and $\tilde{\alpha}_3$ which are valid for all T_A^*, $0 < T_A^* < \infty$. At this point it should be noted that the "short time" control problem ($T_A^* \ll 1$) is discussed further in Sections 3.5.4 and 3.7.

3.5.2 Optimal Steering When the Final Time is an Even Multiple of π

Confidence in the above choice for $\tilde{\alpha}_3$ is further strengthened if we consider those terminal states for which $T_A^* = m\pi$, $m = 2,4,6,\ldots$. In this case Equations (3.9) through (3.12) are satisfied when $u_{x'}^*(\tau) = 0$ and $u_{y'}^*(\tau) = -1$ for $\tau \in [0, T_A^*]$. Control of this form is given by (3.29) and (3.30) when $\tilde{\alpha}_1 = 0$, $0 \leq \tilde{\alpha}_2 \leq 2\pi$, and $\tilde{\alpha}_3 = 3\pi/2$.

3.5.3 The Case When Optimal Steering is Nearly a Constant Moment

Additional insight as to both the response of the system and the quantitative behavior of the optimal control can be gained if we

examine the case when $\underline{u}^*(\tau)$ is nearly a steadily applied moment about the y' axis. Specifically, let us consider a steering function of the following form: $u^*_{y'}(\tau) = -1$ and $u^*_{x'}(\tau)$ is oscillatory with a period of 2π and amplitude of ϵ where $\epsilon \ll 1$. The optimal steering functions as given by (3.29) and (3.30) will be of this form if $\tilde{\alpha}_1 = \epsilon$ and $\tilde{\alpha}_3 \cong \frac{3\pi}{2}$. Thus the circle defined by (3.31) has a very small radius and center located at approximately (0,-1). If we assume that the optimal control is a constant moment plus a perturbation of $O(\tilde{\alpha}_1)$ then the optimal steering functions become:

$$u^*_{x'}(\tau) = [\tilde{\alpha}_1 \cos(\tau+\tilde{\alpha}_2) + \cos\tilde{\alpha}_3][1-\tilde{\alpha}_1\cos(\tau+\tilde{\alpha}_2-\tilde{\alpha}_3) + o(\tilde{\alpha}_1)] \tag{3.33}$$

$$u^*_{y'}(\tau) = [\tilde{\alpha}_1 \sin(\tau+\tilde{\alpha}_2) + \sin\tilde{\alpha}_3][1-\tilde{\alpha}_1\cos(\tau+\tilde{\alpha}_2-\tilde{\alpha}_3) + o(\tilde{\alpha}_1)] \tag{3.34}$$

Substituting this control into (3.9) through (3.12) and after performing the required integration we find:

$$\frac{\tilde{\alpha}_1}{2} T^*_A \cos\tilde{\alpha}_2 + \sin(T^*_A-\tilde{\alpha}_3) + \sin\tilde{\alpha}_3 + \frac{\tilde{\alpha}_1\cos\tilde{\alpha}_2}{4}\left[\sin 2(\tilde{\alpha}_3 - T^*_A) - \sin 2\tilde{\alpha}_3\right] + o(\tilde{\alpha}_1)T^*_A = 0 \tag{3.35}$$

$$\frac{\tilde{\alpha}_1}{2} T^*_A \sin\tilde{\alpha}_2 + \cos(T^*_A-\tilde{\alpha}_3) - \cos\tilde{\alpha}_3 + \frac{\tilde{\alpha}_1\cos\tilde{\alpha}_2}{2}\left[\sin^2(\tilde{\alpha}_3-T^*_A) - \sin^2\tilde{\alpha}_3\right] + \frac{\tilde{\alpha}_1\sin\tilde{\alpha}_2}{4}\left[\sin 2\tilde{\alpha}_3 + \sin 2(T^*_A-\tilde{\alpha}_3)\right] + o(\tilde{\alpha}_1)T^*_A = 0 \tag{3.36}$$

$$\tilde{\alpha}_1\left[\sin(T^*_A+\tilde{\alpha}_2) - \cos\tilde{\alpha}_3\sin(T^*_A+\tilde{\alpha}_2-\tilde{\alpha}_3) + \cos\tilde{\alpha}_3\sin(\tilde{\alpha}_2-\tilde{\alpha}_3) - \sin\tilde{\alpha}_2\right] + T^*_A\cos\tilde{\alpha}_3 + o(\tilde{\alpha}_1)T^*_A = 0 \tag{3.37}$$

$$\tilde{\alpha}_1 \left[\cos \tilde{\alpha}_2 - \cos (T_A^* + \tilde{\alpha}_2) - \sin \tilde{\alpha}_3 \sin (T_A^* + \tilde{\alpha}_2 - \tilde{\alpha}_3) + \sin \tilde{\alpha}_3 \sin (\tilde{\alpha}_2 - \tilde{\alpha}_3)\right] + T_A^* \sin \tilde{\alpha}_3 + o(\tilde{\alpha}_1)\, T_A^* = -\tilde{L}_Y \qquad (3.38)$$

Assuming that $\tilde{\alpha}_1 = O(1/T_A^*)$ where $T_A^* \gg 1$ (this appears to be a reasonable approach if one considers the response of a spinning body when the term $I_z^2\omega_s^2\theta/IM$ is much greater than unity) and if terms of $O(1/T_A^*)$ are neglected, then the solution to (3.35) through (3.38) is written as follows:

$$\alpha_1 \cong \frac{4}{\tilde{L}_Y} \sin \frac{1}{2}\tilde{L}_Y \qquad (3.39)$$

$$\alpha_2 \cong \sin^{-1}(\cos \tfrac{1}{2}\tilde{L}_Y) \qquad (3.40)$$

$$\alpha_3 \cong \tfrac{3\pi}{4} \qquad (3.41)$$

$$T_A^* \cong \tilde{L}_Y \qquad (3.42)$$

Let us now consider a geometric interpretation of the above results. From (3.39) it is evident that the radius of the circle defined by (3.31) approaches zero as $\tilde{L}_Y \to \infty$; therefore, in the limit, optimal control which satisfies boundary conditions of the form given by (3.8) is a constant moment about the y' axis. Note that the optimal control corresponding to those state boundary conditions defined in Section 3.5.2 is also a steadily applied moment about the y' axis. Examining the control defined by (3.39) through (3.42) in greater detail one observes certain characteristics in common with those described in Section 3.5.1. First, the center of the circle lies at approximately (0, -1) in both cases. In addition, from (3.40) we find

that $\tilde{\alpha}_2 \cong \frac{1}{2}(\pi - T_A^*)$. Thus, the trajectory of (3.31) is nearly symmetric about the $\tilde{P}_2$ axis. In view of the correlation observed to this point it appears reasonable to make the following conjectures as to the exact structure of the optimal control:

1. The parameter $\tilde{\alpha}_3$ is independent of $\tilde{L}_Y$ (the center of the circle remains at (0, -1); hence,

$$\tilde{\alpha}_3 = \frac{3\pi}{2} \tag{3.43}$$

2. The phase angle α_2 is given by

$$\tilde{\alpha}_2 = \tfrac{1}{2}(\pi - T_A^*) \tag{3.44}$$

for all values of $\tilde{L}_Y$.

3.5.4 Optimal Steering: The General Case

When $\tilde{\alpha}_2 = \frac{1}{2}(\pi - T_A^*)$ and $\tilde{\alpha}_3 = \frac{3\pi}{2}$ the optimal steering functions, Equations (3.29) and (3.30), become:

$$u_x^*,(\tau) = \frac{-\tilde{\alpha}_1 \sin\left(\tau - \frac{T_A^*}{2}\right)}{\sqrt{\tilde{\alpha}_1^2 + 1 - \tilde{2}\alpha_1 \cos\left(\tau - \frac{T_A^*}{2}\right)}} \tag{3.45}$$

$$u_y^*,(\tau) = \frac{\tilde{\alpha}_1 \cos\left(\tau - \frac{T_A^*}{2}\right) - 1}{\sqrt{\tilde{\alpha}_1^2 + 1 - 2\tilde{\alpha}_1 \cos\left(\tau - \frac{T_A^*}{2}\right)}} \tag{3.46}$$

Rewriting (3.9) and (3.10) in complex form and multiplying the results $e^{\frac{1}{2}iT_A^*}$ gives

$$\int_0^{T_A^*} e^{i\left(\frac{1}{2}T_A^* - \tau\right)} [u_x^*,(\tau) + iu_y^*,(\tau)]\, d\tau = 0 \tag{3.47}$$

Substituting (3.45) and (3.46) into (3.47), (3.11), and (3.12) we find:

$$\int_{\ell_1}^{\ell_2} \frac{\sin \tau'}{\sqrt{\tilde{\alpha}_1^2 + 1 - 2\tilde{\alpha}_1 \cos \tau'}}\, d\tau' = 0 \tag{3.48}$$

$$(\tilde{\alpha}_1 + 1)\int_{\ell_1}^{\ell_2} \sqrt{1 - K^2 \cos^2 \tfrac{1}{2}\tau'}\, d\tau' + (\tilde{\alpha}_1 - 1)\int_{\ell_1}^{\ell_2} \frac{d\tau'}{\sqrt{1 - K^2 \cos^2 \tfrac{1}{2}\tau'}} = 0 \tag{3.49}$$

$$\int_{\ell_1}^{\ell_2} \frac{\tilde{\alpha}_1 \sin \tau'}{\sqrt{\tilde{\alpha}_1^2 + 1 - 2\tilde{\alpha}_1 \cos \tau'}}\, d\tau' = 0 \tag{3.50}$$

$$(\tilde{\alpha}_1 + 1)\int_{\ell_1}^{\ell_2} \sqrt{1 - K^2 \cos^2 \tfrac{1}{2}\tau'}\, d\tau' + (1 - \tilde{\alpha}_1)\int_{\ell_1}^{\ell_2} \frac{d\tau'}{\sqrt{1 - K^2 \cos^2 \tfrac{1}{2}\tau'}} = 2\tilde{L}_Y \tag{3.51}$$

where

$$\ell_1 = -\tfrac{1}{2}T_A^* \,, \quad \ell_2 = \tfrac{1}{2}T_A^* \,, \quad \tau' = \tau + \tfrac{1}{2}T_A^* \,, \quad K^2 = \frac{4\tilde{\alpha}_1}{(\tilde{\alpha}_1 + 1)^2} \,.$$

Note that the integrands of (3.48) and (3.50) are odd functions of τ' ; therefore, these equations are satisfied for all values of $\tilde{\alpha}_1$ and T_A^*. Thus it appears that the expressions for $\tilde{\alpha}_2$ and $\tilde{\alpha}_3$ as given by (3.43) and (3.44) are correct.

The remaining task is one of expressing $\tilde{\alpha}_1$ and T_A^* in terms of $\tilde{L}_Y$. Such a solution is readily obtained if we introduce the new independent variable

$$v = \tfrac{1}{2}(\tau' + \pi) \,. \tag{3.52}$$

Thus, (3.49) and (3.51) can be rewritten as follows:

$$(\tilde{\alpha}_1 + 1)\int_{\tilde{\ell}_1}^{\tilde{\ell}_2} \sqrt{1 - K^2\sin^2 v}\, dv + (\tilde{\alpha}_1 - 1)\int_{\tilde{\ell}_1}^{\tilde{\ell}_2} \frac{dv}{\sqrt{1 - K^2\sin^2 v}} = 0 \qquad (3.53)$$

$$(\tilde{\alpha}_1 + 1)\int_{\tilde{\ell}_1}^{\tilde{\ell}_2} \sqrt{1 - K^2\sin^2 v}\, dv + (1 - \tilde{\alpha}_1)\int_{\tilde{\ell}_1}^{\tilde{\ell}_2} \frac{dv}{\sqrt{1 - K^2\sin^2 v}} = \tilde{L}_Y \qquad (3.54)$$

Note that the terms of the above expressions are elliptic integrals of the first and second kinds and, therefore, can be evaluated directly from their respective tables once $\tilde{\alpha}_1$ and T_A^* are known.

To solve for $\tilde{\alpha}_1$ and T_A^* in terms of $\tilde{L}_Y$ the following iterative procedure was employed: First, appropriate values were assigned to T_A^* and $\tilde{\alpha}_1$ was then adjusted until the two terms of (3.53) became equal in magnitude. This procedure was then repeated for each T_A^*. The results are presented in Figure 3.4. Since (3.53) is identical to (3.54) if the sign of the second term in the former is reversed, the solution for T_A^* in terms of $\tilde{L}_Y$ is direct. The results of this computation are shown in Figure 3.5. By cross plotting between Figures 3.4 and 3.5 we are able to evaluate $\tilde{\alpha}_1$ in terms of $\tilde{L}_Y$; these results are presented in Figure 3.6.

It should be pointed out that the aforementioned procedure for computing $\tilde{\alpha}_1$ and T_A^* cannot be employed when $\tilde{L}_Y \ll 1$. This is due to the fact that accurate interpolation from a table of elliptic integrals becomes difficult when both $K^2 \to 1$ and $\tilde{\ell}_1, \tilde{\ell}_2 \to \pi/2$ (an elliptic integral of the first kind is not defined for $K^2 = 1$ when the amplitude becomes $\pi/2$). Therefore, in order to determine the behavior of both $\tilde{\alpha}_1$ and T_A^* when $\tilde{L}_Y \ll 1$, the integration of (3.53) and (3.54) was carried out on a

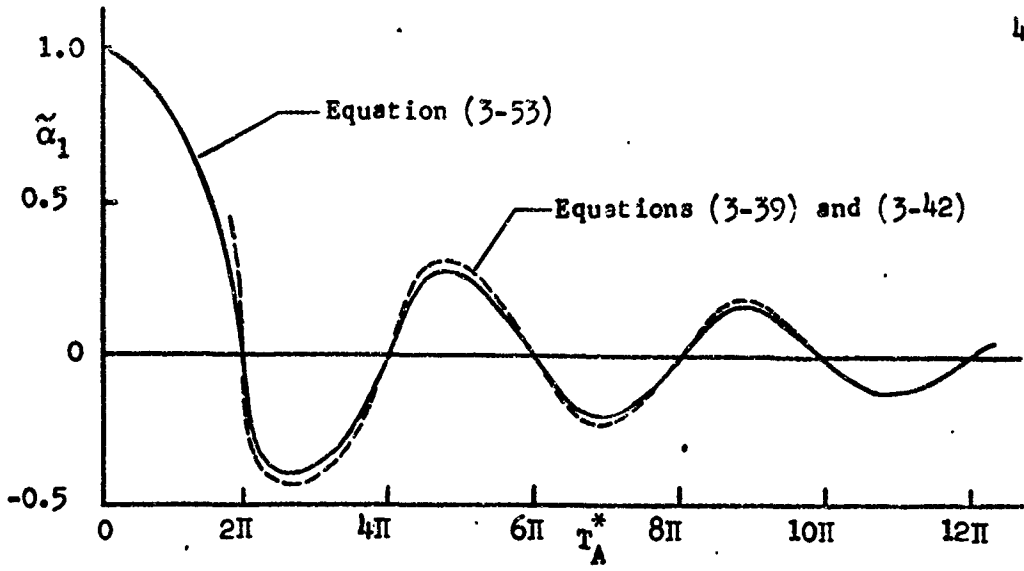

Figure 3-4. Solution for $\tilde{\alpha}_1$ in Terms of T_A^*

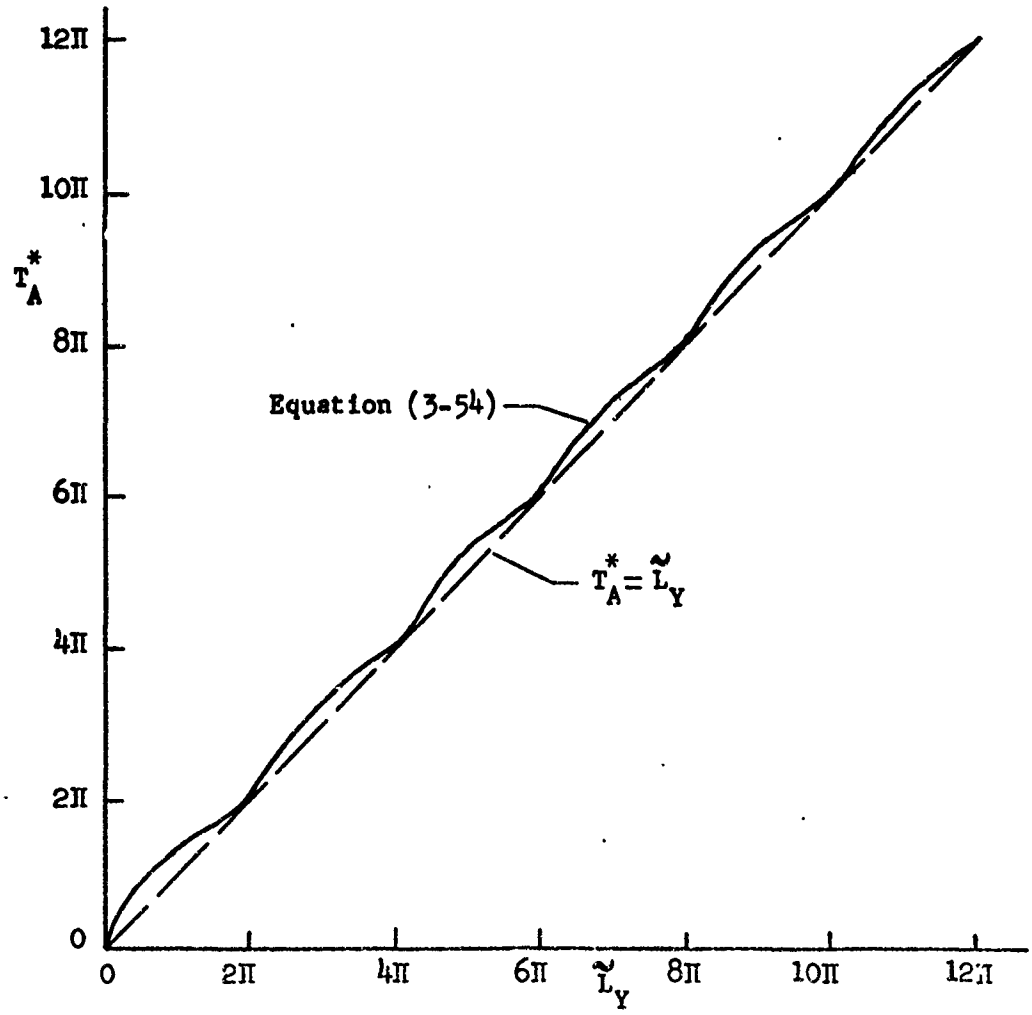

Figure 3-5. Solution for T_A^* in Terms of $\tilde{L}_Y$

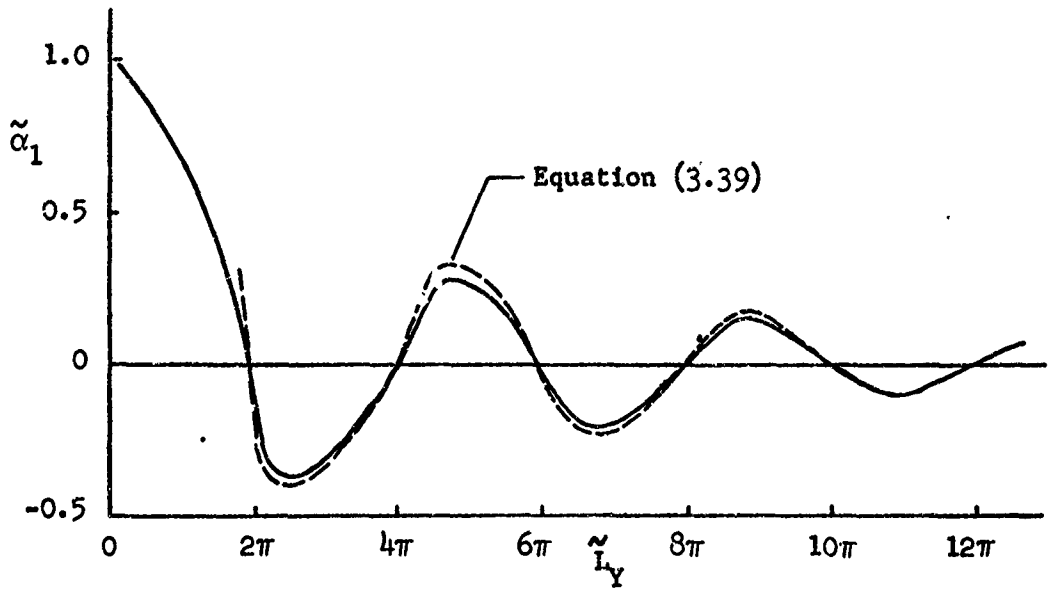

Figure 3.6 Solution for $\tilde{\alpha}_1$ in Terms of $\tilde{L}_Y$

digital computer using a sixth order Runge-Kutta procedure. The computational technique was again one of iteratively adjusting $\tilde{\alpha}_1$ for a given T_A^* until (3.53) was satisfied; the corresponding value of $\tilde{L}_Y$ was then determined from (3.54). The results are presented in Figure 3.7. As could be expected an elliptic integral of the first kind, evaluated on the interval $[\tilde{\ell}_1, \tilde{\ell}_2]$ when $T_A^* \ll 1$, is very sensitive to changes in $\tilde{\alpha}_1$ as $K^2 \to 1$. In contrast an elliptic integral of the second kind is relatively insensitive to changes in $\tilde{\alpha}_1$ for $0.99 \leq \tilde{\alpha}_1 < 1$; therefore, a good approximation for T_A^* can be obtained from Equation (3.54) which becomes

$$\int_0^{\frac{1}{2}T_A^*} \sqrt{1 - \cos^2 \tfrac{1}{2}\tau'}\, d\tau = \tfrac{1}{4}\tilde{L}_Y \qquad (3.55)$$

when $\tilde{\alpha}_1 = 1$. If one neglects terms of $O(\tau'^3)$ in the power series representation of $\sin \frac{1}{2}\tau'$ then (3.55) can be rewritten as

$$T_A^* = 2\sqrt{\tilde{L}_Y} \quad . \tag{3.56}$$

To demonstrate the accuracy of this approximation (3.56) is plotted against the numerical solution in Figure 3.7.

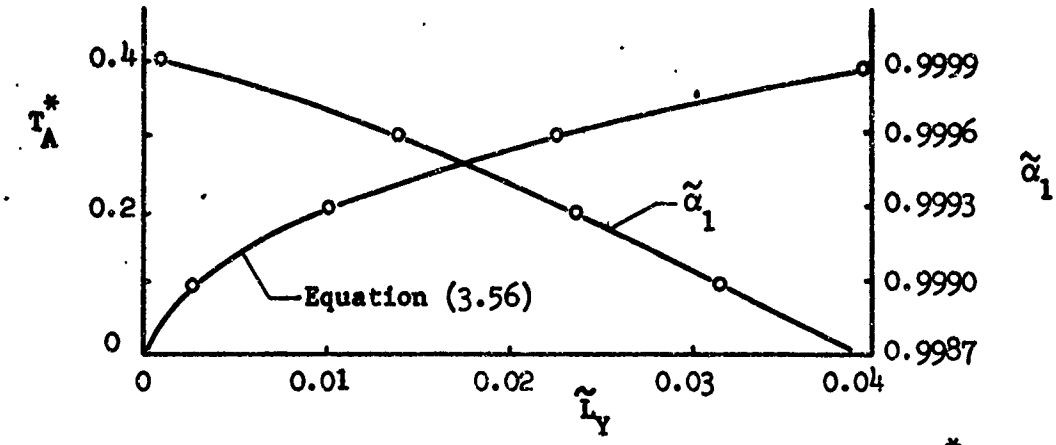

Figure 3.7 Results of the Computer Solution for $\tilde{\alpha}_1$ and T_A^*

3.6 A Sufficient Condition for Time-Optimal Control

In the previous sections we derived a control law which satisfies the necessary condition provided by the maximum principle. In addition, from a physical interpretation this control "appears" to be optimal. We shall now strengthen our claim as to the optimality of the control through the concept of the Hamilton-Jacobi equation.

First, we find that for each point $(\underline{\chi}, \tau)$ in $R_4 \times [0, T_A]$ the Hamiltonian, Equation (3.14), has a unique absolute minimum when $\underline{u}^*(\tau)$ is given by Equations (3.15) and (3.16). In addition, this control is a continuous function of $\tau, \tau \in [0, T_A^*]$. Thus, both the trajectory and the cost functional corresponding to a given pair $(\underline{P}(0), T_A)$ are sufficiently smooth to allow the Hamilton-Jacobi equation to be applied globally.

We note that for many problems the Hamilton-Jacobi equation, being a partial differential equation, is often difficult if not impossible to solve. In cases where a complete global solution cannot be found it may still be possible to use this equation to check the optimality of a control derived from the maximum principle along particular trajectories. This is the approach we must resort to since it is not, in general, possible to write the steering law, Equations (3.29) and (3.30), in terms of a continuous error signal. In the sequel we show that solutions to the Hamilton-Jacobi equation can be found along trajectories between certain pairs of those initial and final states described by Equation (3.8). While this approach does not show that a global sufficiency condition is satisfied it, nevertheless, serves to strengthen our confidence that the control given by Equation (3.29) and (3.30) is indeed optimal.

For our minimum time control problem the Hamilton-Jacobi equation is

$$(-\tilde{\omega}_{y'} + u_{x'}) \frac{\partial J}{\partial \tilde{\omega}_{x'}} + (\tilde{\omega}_{x'} + u_{y'}) \frac{\partial J}{\partial \tilde{\omega}_{y'}} + \tilde{\omega}_{y'} \frac{\partial J}{\partial \tilde{L}_X} - \tilde{\omega}_{x'} \frac{\partial J}{\partial \tilde{L}_Y} = 1 . \tag{3.57}$$

In cases where $u_{x'}(\tau) = 0$ and $u_{y'}(\tau) = -1$ for all $\tau \in [0, T_A]$ (i.e., for trajectories connecting the state points (0, 0, 0, 0) and (0, 0, 0, $-m\pi$, $m = 2,4,6,\ldots$)) the above equation becomes

$$-\tilde{\omega}_{y'} \frac{\partial J}{\partial \tilde{\omega}_{x'}} + (\tilde{\omega}_{x'} - 1) \frac{\partial J}{\partial \tilde{\omega}_{y'}} + \tilde{\omega}_{y'} \frac{\partial J}{\partial \tilde{L}_X} - \tilde{\omega}_{x'} \frac{\partial J}{\partial \tilde{L}_Y} = 1. \tag{3.58}$$

A solution to (3.58) with boundary conditions $J = 0$ at $\tilde{\omega}_{x'} = \tilde{\omega}_{y'} = \tilde{L}_X = \tilde{L}_Y = 0$ is

$$J = -\tilde{\omega}_{y'} - \tilde{L}_Y \cdot \tag{3.59}$$

This is the exact expression we obtain by solving (3.7) for $\tilde{\omega}_{x'}$, $\tilde{\omega}_{y'}$, $\tilde{L}_X$, and $\tilde{L}_Y$ when $u_{x'}(\tau) = 0$, $u_{y'}(\tau) = -1$, and then solving the resulting expressions for τ in terms of the normalized state variables, i.e., $J = T_A^*$. Moreover, we find that $\frac{\partial J}{\partial \underline{\chi}} = \underline{P}^*(\tau)$. Hence, (3.45) and (3.46) satisfy both the necessary and sufficient conditions for optimality when $\tilde{\alpha}_1 = 0$.

This result agrees with the solution one would obtain from a direct inspection of the control problem for those boundary conditions described previously. That is, the entire control moment is applied as co-linear as possible with the desired angular momentum change $I_z \omega_s \theta_f$. Moreover, the characteristics of the steering functions, as observed up to this point, coincide with those predicted by a heuristic approach to the control problem; therefore, in the absence of a rigorous proof we will consider the control given by (3.45) and (3.46) to be optimal.

3.7 Summary of the Controller Characteristics

It is convenient to consider the characteristics of the time-optimal control in terms of $\tilde{L}_Y$. Thus the results may be logically separated into three sections. The first corresponds to values of $\tilde{L}_Y$ less than 2π where control is effected over a "short period of time" or in terms of τ less than one revolution of the vehicle about the spin axis when $I_z/I = 1$. The second group corresponds to values of $\tilde{L}_Y$ greater than 2π. In this range the local maximum of $\tilde{\alpha}_1$ decreases as $\tilde{L}_Y$ becomes large. For $\tilde{L}_Y$ greater than approximately 16π the optimal control is nearly a steadily applied moment. The third group is

comprised of discrete values of $\tilde{L}_Y$. When $\tilde{L}_Y = m\pi$, $m = 2,4,6,\ldots$, $\tilde{\alpha}_1$ is identically zero; therefore, the optimal control is a constant moment about the y' axis.

3.7.1 Optimal Control When $\tilde{L}_Y \leq 2\pi$

Control in this region is bounded by two different modes of operation: a constant moment about the y' axis when $\tilde{L}_Y = 2\pi$, and the "race-brake" type of control as $\tilde{L}_Y \to 0$. The latter is obviously a limiting case if one considers either the geometric interpretation of the control or the position of the gimballed thruster with respect to τ as $T_A^* \to 0$.

First, let us summarize the characteristics of the optimal steering functions when $\tilde{L}_Y \ll 1$. In the previous analysis we found that the arc defined by the point p in Figure 3.2 is symmetric with respect to the $\tilde{P}_2$ axis and has length $\alpha_1 T_A^*$. From Figure 3.4 we find that $\tilde{\alpha}_1 \to 1$ as $\tilde{L}_Y \to 0$; therefore, $u_{y'}^*(\tau)/u_{x'}^*(\tau) \to 0$ as the arc defined by (3.31) decreases in length and is shifted toward the origin. Hence, in the limit the control operates in a "race-brake" mode.

Additional insight as to the behavior of the optimal control when $\tilde{L}_Y \ll 1$ can be gained if we consider the position of the control jet with respect to τ. Define the angle between the thruster and the x' axis by ξ as shown in Figure 3.8. Expressing ξ in terms of the control components we find

$$\xi = \pi - \tilde{\xi}, \quad \xi_0 = \xi(0), \tag{3.60}$$

$$\tilde{\xi} = \tan^{-1}\left[\frac{u_{x'}^*(\tau)}{u_{y'}^*(\tau)}\right], \quad -\tfrac{1}{2}\pi \leq \xi \leq \tfrac{1}{2}\pi. \tag{3.61}$$

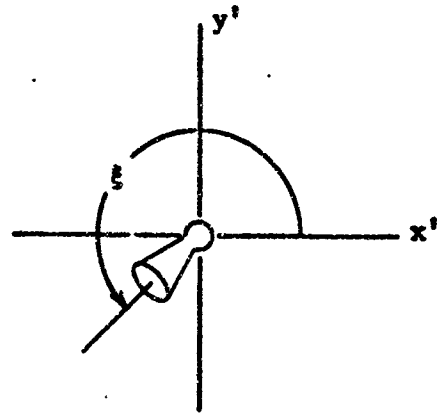

Figure 3.8 Definition of Thruster Position

From Equations (3.45) and (3.46) plots of ξ vs τ for specific values of T_A^* can be constructed. The results of such computation for typical values of T_A^* are presented in Figure 3.9.

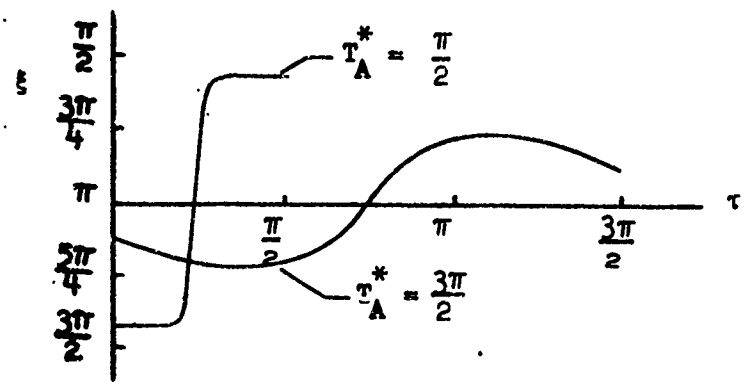

Figure 3.9 Plots of Thruster Position vs τ

When curves similiar to those in Figure 3.9 are plotted for yet smaller values of T_A^* ($T_A^* < \frac{1}{2}\pi$) it becomes apparent that $\xi_o \to \frac{1}{2}\pi$ when $\tilde{L}_Y \to 0$ (see Figure 3.10) and the control approaches the "race-brake" mode of operation. This characteristic of the control law is illustrated by trajectories plotted in the $(\tilde{L}_X\text{-}\tilde{L}_Y)$ plane (see Figures 3.11 and 3.12). From these plots we note that the ratio of $\tilde{L}_X$ to $\tilde{L}_Y$

decreases as $\tilde{L}_Y$ is reduced and therefore there is less out of plane motion due to precession of the spin axis.

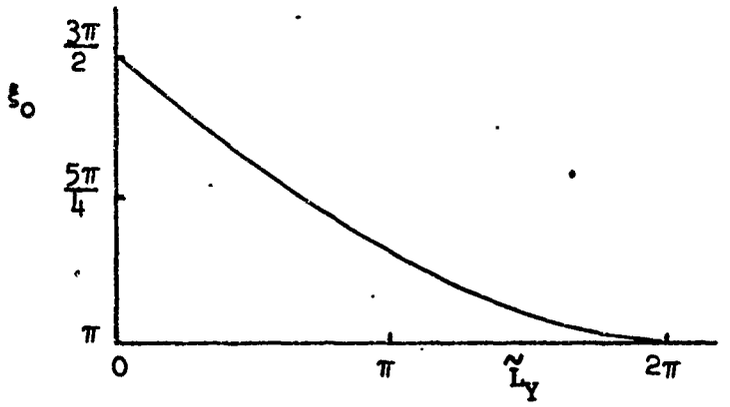

Figure 3.10 Initial Thruster Position vs $\tilde{L}_Y$

3.7.2 Optimal Control When $\tilde{L}_Y > 2\pi$

In this case the local maximum of $\tilde{\alpha}_1$ decreases as $\tilde{L}_Y$ increases, and the control approaches a steadily applied moment about the y' axis.

The closed form solution for $\tilde{\alpha}_1$ and T_A^*, as given by (3.39) and (3.42), is represented by the dashed curves in Figures 3.5 and 3.6 (note that these relations were obtained under the assumption that $\tilde{\alpha}_1 = O(1/T_A^*)$, $T_A^* \gg 1$). Moreover, we also note that the terms of $O(1/T_A^*)$ which were neglected in Equation (3.35) are identically zero when $\tilde{L}_Y = m\pi$, $m = 2,4,6,\ldots$; consequently, (3.39) is a good representation of $\tilde{\alpha}_1$ when $\tilde{L}_Y = m\pi$.

As illustrated by Figure 3.6 the solution to (3.54) approaches the predicted linear relation as $\tilde{L}_Y$ increases. An empirical approximation to the exact solution is given by

$$T_A^* = \tilde{L}_Y + \frac{2|\sin \tilde{L}_Y|}{(\tilde{L}_Y)^{0.7\pi}} \quad . \tag{3.62}$$

For large values of $\tilde{L}_Y$ the control approaches a steadily applied moment; consequently, we expect trajectories in the $(\tilde{\omega}_{x'}, -\tilde{\omega}_{y'})$ plane to be nearly circular in shape. This situation is illustrated by Figure 3.18.

3.7.3 Optimal Control When $\tilde{L}_Y = m\pi$, $m = 2,4,6,\ldots$

For these ordered values of $\tilde{L}_Y$ the optimal control is a constant moment about the y' axis ($u^*_{x'}(\tau) = 0$, $u^*_{y'}(\tau) = -1$) and is, therefore, nearly aligned during the entire interval $[0, T^*_A]$ with the desired angular momentum change $\underline{I_z \omega_s \theta_f}$. The response of the system when this type of control is applied is illustrated by Figures 3.13, 3.15, and 3.17 where trajectories in the $(\tilde{\omega}_{x'}, -\tilde{\omega}_{y'})$ plane are circles defined by

$$(\tilde{\omega}_{x'}(\tau) - 1)^2 + \tilde{\omega}_{y'}(\tau) = 1 \qquad (3.63)$$

When $\tilde{\alpha}_1 = 0$ the terminal time in seconds is given by

$$t^*_f = \frac{m\pi}{\mu}$$

where μ is the nutation frequency.

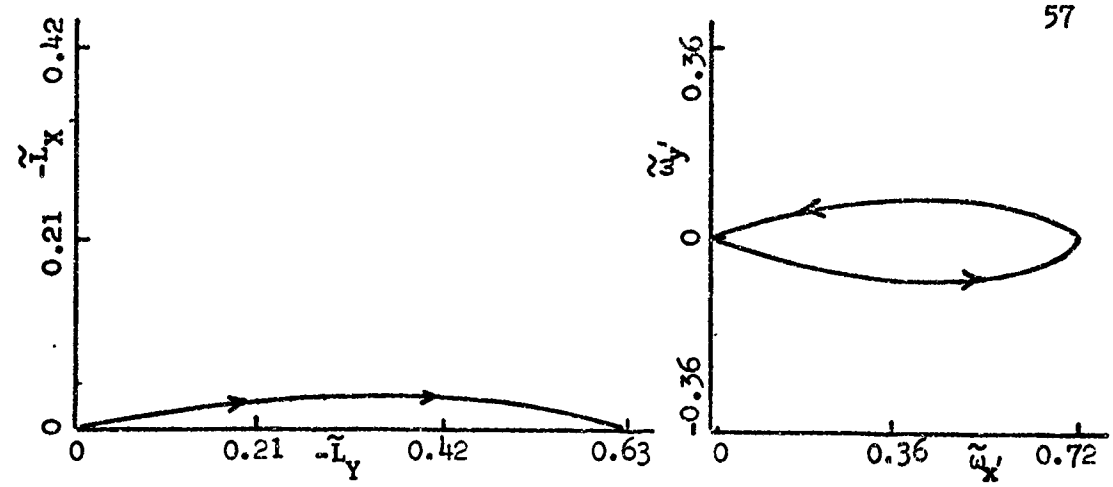

Figure 3.11 Optimal Trajectories in the $(\tilde{\omega}_{x'}\text{-}\tilde{\omega}_{y'})$ and $(\tilde{L}_X\text{-}\tilde{L}_Y)$ Planes for $\tilde{L}_Y = 0.63$, $T_A^* = \Pi/2$.

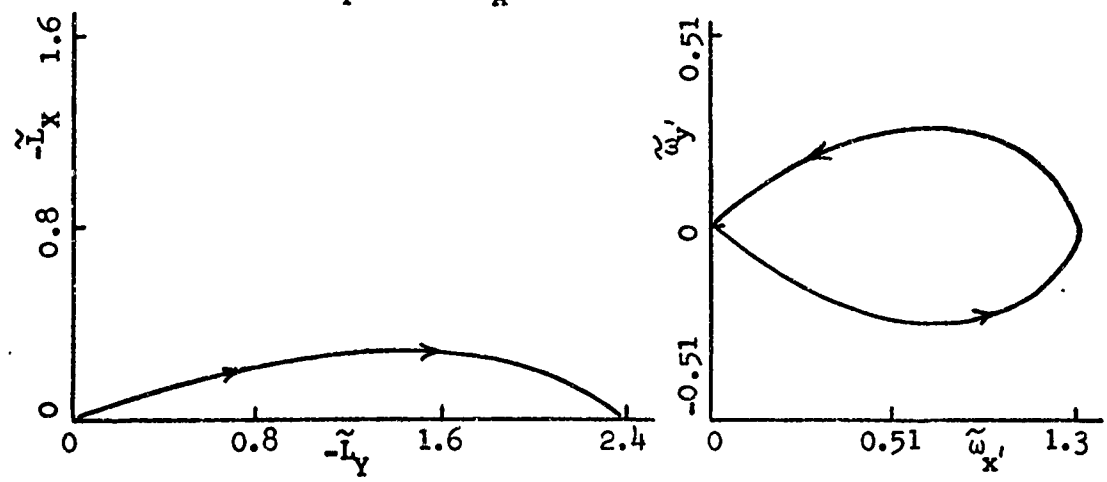

Figure 3.12 Optimal Trajectories in the $(\tilde{\omega}_{x'}\text{-}\tilde{\omega}_{y'})$ and $(\tilde{L}_X\text{-}\tilde{L}_Y)$ Planes for $\tilde{L}_Y = 2.4$, $T_A^* = \Pi$

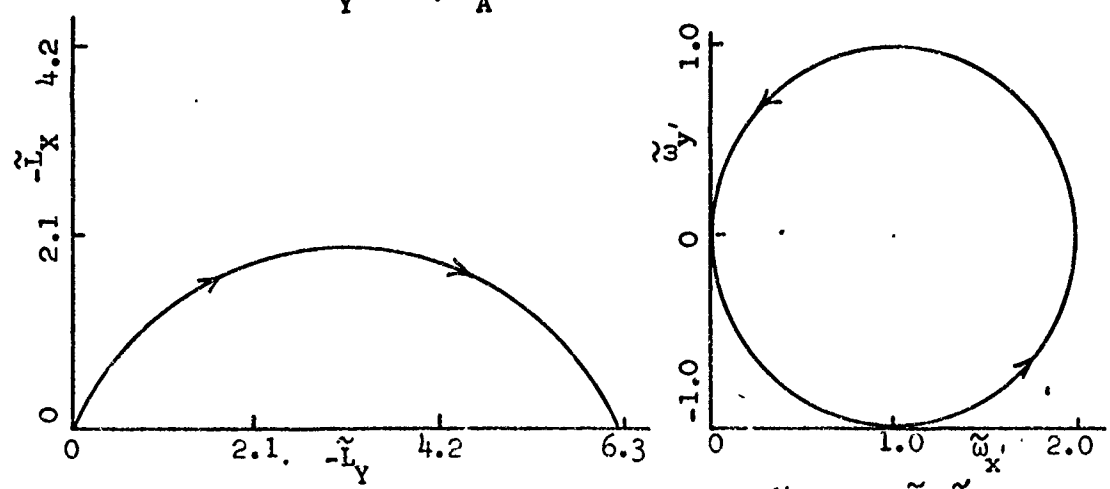

Figure 3.13 Optimal Trajectories in the $(\tilde{\omega}_{x'}\text{-}\tilde{\omega}_{y'})$ and $(\tilde{L}_X\text{-}\tilde{L}_Y)$ Planes for $\tilde{L}_Y = 2\Pi$, $T_A^* = 2\Pi$

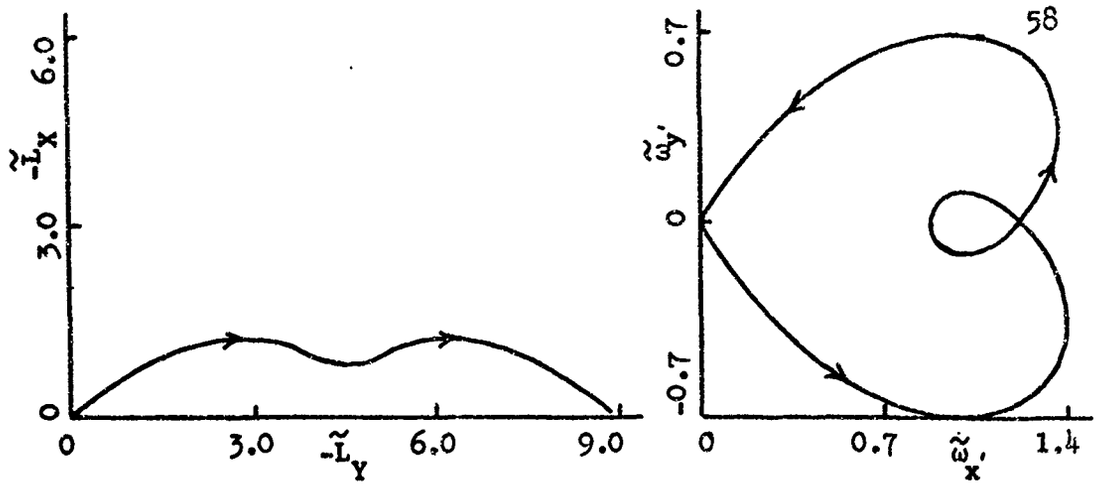

Figure 3-14. Optimal Trajectories in the $(\tilde{\omega}_{x'}\text{-}\tilde{\omega}_{y'})$ and $(\tilde{L}_X\text{-}\tilde{L}_Y)$ Planes for $\tilde{L}_Y = 9.0$, $T_A^* = 9.42$

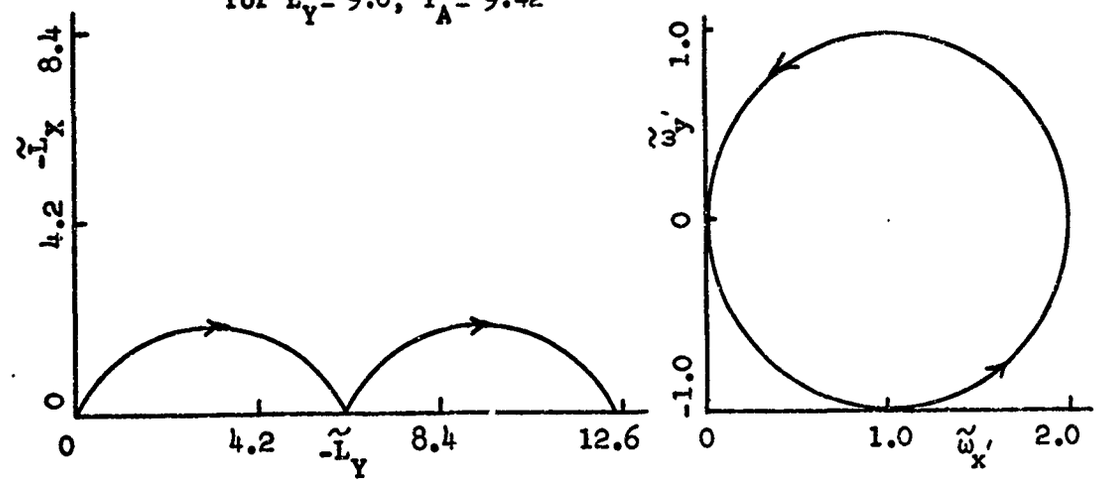

Figure 3-15. Optimal Trajectories in the $(\tilde{\omega}_{x'}\text{-}\tilde{\omega}_{y'})$ and $(\tilde{L}_X\text{-}\tilde{L}_Y)$ Planes for $\tilde{L}_Y = 4\pi$, $T_A^* = 4\pi$

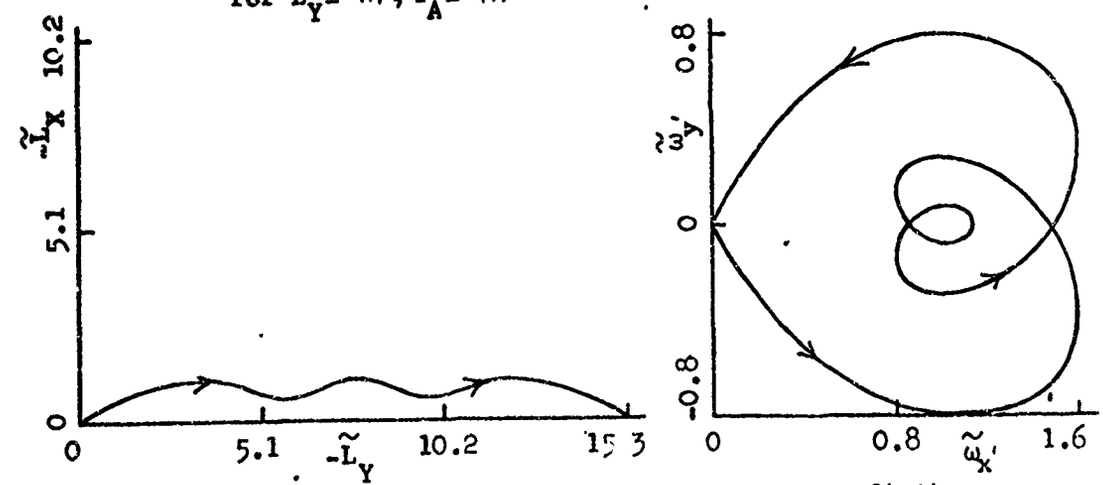

Figure 3-16. Optimal Trajectories in the $(\tilde{\omega}_{x'}\text{-}\tilde{\omega}_{y'})$ and $(\tilde{L}_X\text{-}\tilde{L}_Y)$ Planes for $\tilde{L}_Y = 15.3$, $T_A^* = 15.7$

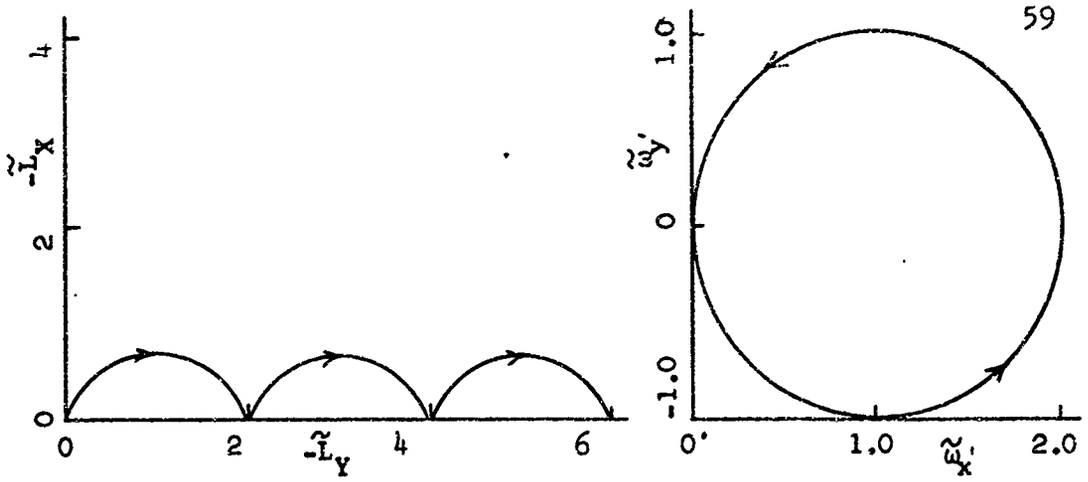

Figure 3-17. Optimal Trajectories in the $(\tilde{\omega}_{x'} - \tilde{\omega}_{y'})$ and $(\tilde{L}_X - \tilde{L}_Y)$ Planes for $\tilde{L}_Y = 6\pi$ $T_A^* = 6\pi$

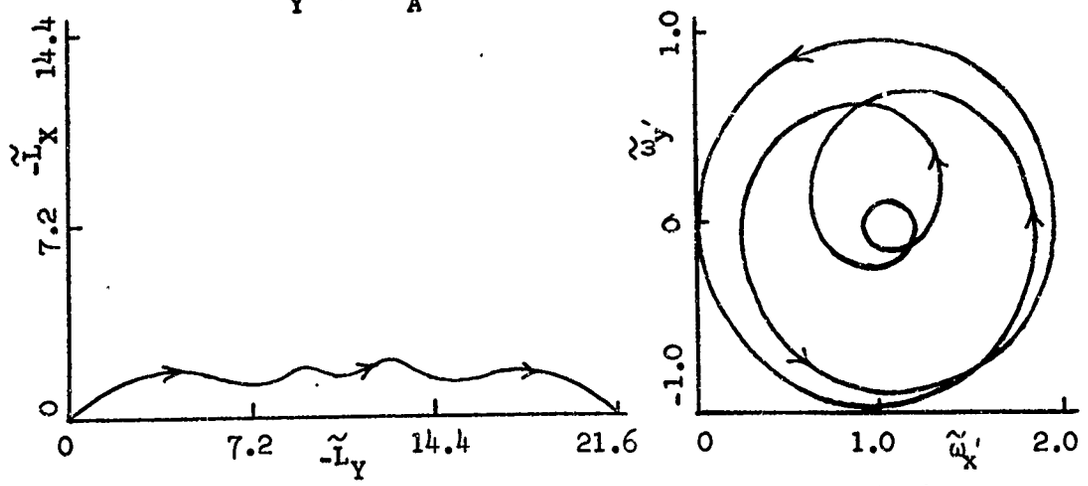

Figure 3-18. Optimal Trajectories in the $(\tilde{\omega}_{x'} - \tilde{\omega}_{y'})$ and $(\tilde{L}_X - \tilde{L}_Y)$ Planes for $\tilde{L}_Y = 21.6$, $T_A^* = 22.0$

CHAPTER 4

TIME-OPTIMAL STEERING WHEN CONTROL IS PROVIDED BY BODY-FIXED REACTION JETS

The problem considered in this chapter is one of synthesizing minimum time controls for the jet configurations depicted in Figure 1.1, Cases (B) through (D). The maximum principle is used to provide a necessary condition for time-optimality. A solution to the resulting two point boundary value problem is obtained through an analytic technique when the final time is small compared to the spin rate or, in the general case, by an iterative procedure which requires the use of a digital computer. Since the steering functions obtained in this manner are not expressed in terms of a continuous error signal they would not, in general, be used to generate optimal controls in feedback systems. However, true, time-optimal control laws have been determined for a wide range of vehicle configurations and reorientation angles; the steering functions are presented graphically in terms of a set of dimensionless parameters - as in the previous chapter.

Therefore, the results should be useful in the design of active control systems.

4.1 Equations of Motion

In this section the dynamical equations for a spinning vehicle are developed when control is provided by Jet Configurations (B) through (D). In the discussions which follow, except where noted, the

three controller configurations are considered simultaneously since Controllers (C) and (D) are special cases of (B).

Assume that one pair of jets delivers a thrust $\hat{f}_x(t)$ and the second pair $\hat{f}_y(t)$ as shown in Figure 4.1.

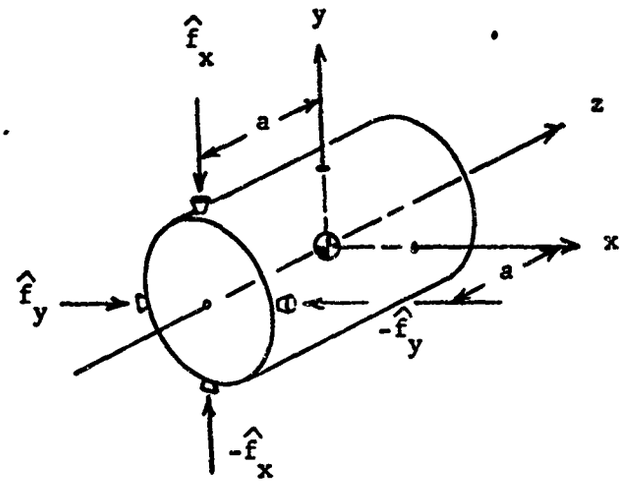

Figure 4.1. Schematic of the Body-Fixed Control Jets

Thus, the control moments which appear in equation (2.27) can be expressed as

$$M_x(t) = a \cdot \hat{f}_x(t) \tag{4.1}$$

$$M_y(t) = a \cdot \hat{f}_y(t) \tag{4.2}$$

where (a) is the moment arm. If the thrust of each jet is bounded by F then $|\hat{f}_x(t)| \leq F$ and $|\hat{f}_y(t)| \leq F$. Define the new control variables $u_x(t)$ and $u_y(t)$ by

$$u_x(t) = \frac{\hat{f}_x(t)}{F} \tag{4.3}$$

$$u_y(t) = \frac{\hat{f}_y(t)}{F} \tag{4.4}$$

thus $|u_x(t)| \leq 1$ and $|u_y(t)| \leq 1$. We can now write the control as follows:

$$M_x(t) = M \cdot u_x(t) \tag{4.5}$$

$$M_y(t) = M \cdot u_y(t) \tag{4.6}$$

where $M = a \cdot F$. After substituting (4.5) and (4.6) into (2.27) we find that the controlled equation becomes:

$$\frac{d}{d\sigma}\begin{bmatrix} \bar{\omega}_x(\sigma) \\ \bar{\omega}_y(\sigma) \\ \bar{L}_X(\sigma) \\ \bar{L}_Y(\sigma) \end{bmatrix} = \begin{bmatrix} 0 & \gamma & 0 & 0 \\ -\gamma & 0 & 0 & 0 \\ 0 & 0 & 0 & 0 \\ 0 & 0 & 0 & 0 \end{bmatrix}\begin{bmatrix} \bar{\omega}_x(\sigma) \\ \bar{\omega}_y(\sigma) \\ \bar{L}_X(\sigma) \\ \bar{L}_Y(\sigma) \end{bmatrix} + \begin{bmatrix} 1 & 0 \\ 0 & 1 \\ \cos(\sigma+\beta_o) & -\sin(\sigma+\beta_o) \\ \sin(\sigma+\beta_o) & \cos(\sigma+\beta_o) \end{bmatrix}\begin{bmatrix} u_x(\sigma) \\ u_y(\sigma) \end{bmatrix} \tag{4.7}$$

where the dimensionless angular velocities and momentum components are:

$$\bar{\omega}_x(\sigma) = \frac{I\omega_s\omega_x(t)}{M}, \quad \bar{\omega}_y(\sigma) = \frac{I\omega_s\omega_y(t)}{M}, \quad \bar{L}_X(\sigma) = \frac{\omega_s L_X(t)}{M}, \quad \bar{L}_Y(\sigma) = \frac{\omega_s L_y(t)}{M}$$

and

$$\sigma = \omega_s t.$$

From a computational standpoint it is very convenient to describe the system dynamics in the above form. However, if we are interested in the instantaneous position of the spin axis then a representation similar to Equations (2.18) and (2.19) must be employed. For the present case we can define the spin axis position in terms of rotations about the x' and y' axis as follows:

$$\bar{L}_X(\sigma) = \frac{I_z}{I}\int_o^\sigma [\bar{\omega}_x(\nu)\sin(\nu+\beta_o) + \bar{\omega}_y(\nu)\cos(\nu+\beta_o)]d\nu \tag{4.8}$$

$$\bar{L}_Y(\sigma) = \frac{I_z}{I}\int_o^\sigma [\bar{\omega}_y(\nu)\sin(\nu+\beta_o) - \bar{\omega}_x(\nu)\cos(\nu+\beta_o)]d\nu \tag{4.9}$$

When control is provided by four jets, Case (B), the vector $\underline{u}_B(\sigma)$ has two components; therefore, the space of admissible controls Ω_B is a square in R_2. The dynamical systems corresponding to Cases (C) and (D) can be obtained from (4.7) by setting $u_x(\sigma) \equiv 0$ for all $\sigma \epsilon [0, T]$ and restricting the remaining component in the following manner: (1) for Case (C) $u_y(\sigma) \epsilon [-1, 1]$, and (2) for Case (D) $u_y(\sigma) \epsilon [0, 1]$.

The boundary conditions considered in conjunction with (4.7) are as follows:

$$\bar{\omega}_x(0) = \bar{\omega}_x^o , \quad \bar{\omega}_x(T) = 0$$

$$\omega_y(0) = \bar{\omega}_y^o , \quad \bar{\omega}_y(T) = 0$$

$$\bar{\bar{L}}_X(0) = \bar{\omega}_x^o \cos \beta_o - \bar{\omega}_y^o \sin \beta_o + \frac{I_z \omega_s^2 \theta_o \sin \varphi_o}{M}, \bar{\bar{L}}_X(T) = 0 \tag{4.10}$$

$$\bar{\bar{L}}_Y(0) = \bar{\omega}_x^o \sin \beta_o + \bar{\omega}_y^o \cos \beta_o - \frac{I_z \omega_s^2 \theta_o \cos \varphi_o}{M}, \bar{\bar{L}}_Y(T) = - \bar{\bar{L}}_Y = \frac{-I_z \omega_s^2 \theta_f}{M}$$

In cases where $\bar{\omega}_x^o = \bar{\omega}_y^o = 0$ the origin is considered to be the initial state of the system ($\theta_o = 0$).

It should be noted that $\bar{\omega}_x^o$ and $\bar{\omega}_y^o$ need not be zero as was the case in Chapter 3. In general, optimal controls for Jet Configurations (B) through (D) must be determined by numerical means; therefore, a non-zero initial nutation rate presents no additional computational difficulties. Also, it is of no apparent advantage to specify the boundary conditions in regulator form since the angular velocity and momentum equations are not coupled; therefore, setting all the final states equal to zero does not simplify the control problem.

Solving (4.7) for $\bar{\omega}_x(T)$, $\bar{\omega}_y(T)$, $\bar{\bar{L}}_X(T)$, and $\bar{\bar{L}}_Y(T)$ subject to (4.10) results in the following set of governing equations which must

be satisfied by the admissible steering functions $u_x(\sigma)$ and $u_y(\sigma)$:

$$\int_0^T [u_x(\sigma) \cos \gamma\sigma - u_y(\sigma) \sin \gamma\sigma]d\sigma + \bar{\omega}_x(0) = 0 \qquad (4.11)$$

$$\int_0^T [u_x(\sigma) \sin \gamma\sigma + u_y(\sigma) \cos \gamma\sigma]d\sigma + \bar{\omega}_y(0) = 0 \qquad (4.12)$$

$$\int_0^T [u_x(\sigma) \cos (\sigma + \beta_o) - u_y(\sigma) \sin (\sigma+\beta_o)]d\sigma + \bar{\bar{L}}_X(0) = 0 \qquad (4.13)$$

$$\int_0^T [u_x(\sigma) \sin (\sigma+\beta_o) + u_y(\sigma) \cos (\sigma+\beta_\sigma)]d\sigma + \bar{\bar{L}}_Y(0) = -\bar{\bar{L}}_Y \qquad (4.14)$$

Thus the control (the pair $(\underline{u}(\sigma),T)$ which satisfies (4.11) through (4.14)) is a function of the dimensionless physical parameters $\bar{\omega}_x^o$, $\bar{\omega}_y^o$, γ, β_o and $\bar{\bar{L}}_Y$ when $\theta_o = 0$ or by a similiar set when $\theta_f = 0$. At this point it should be noted that control laws which are expressed in terms of these parameters can be applied when $\bar{\bar{L}}_X(T) \neq 0$ if coordinate System II is pre-rotated through the angle $\bar{\beta}_o$ (see Equation (3.13)). However, unlike the case considered in the previous chapter where the control jet could be oriented arbitrarily in the (x-y) plane, we must account for the change in β_o as coordinate system II is rotated about the Z_R axis. Also, note that if $\bar{\omega}_x^o = \bar{\omega}_y^o = 0$ then the control which satisfies (4.11) through (4.14) can be applied when the boundary conditions are specified in regulator form $\bar{\bar{L}}_Y(0) = \frac{I_z \omega^2 s \theta_o}{M}$, $\bar{\bar{L}}_Y(T) = 0$.

4.2 Some Symmetry Properties of the Control

In many of the cases which are investigated in subsequent sections it is assumed that $\bar{\omega}_x^o = \bar{\omega}_y^o = 0$. Under such conditions we can show that the controls which satisfy (4.11) through (4.14), whether they are admissible or not, have certain symmetry properties when referenced to the despun coordinate system.

To demonstrate this symmetry let us first consider the case when

control is provided by Jet Configuration (B). If the pair $(\tilde{\underline{u}}(\sigma), \tilde{T})$ satisfies (4.11) through (4.14) when $0 \leq \tilde{\beta}_o < \pi/2$ then the steering functions $u_x(\sigma)$ and $u_y(\sigma)$ and the final time T corresponding to $\pi/2 \leq \beta_o < 2\pi$) can be determined as follows:

1. For $\pi/2 \leq \beta_o < \pi$

$$u_x(\sigma) = \tilde{u}_y(\sigma),\ u_y(\sigma) = -\tilde{u}_x(\sigma)\ ,\ T = \tilde{T}. \tag{4.15}$$

2. For $\pi \leq \beta_o < 3\pi/2$

$$u_x(\sigma) = -\tilde{u}_x(\sigma),\ u_y(\sigma) = -\tilde{u}_y(\sigma)\ ,\ T = \tilde{T} \tag{4.16}$$

3. For $3\pi/2 \leq \beta_o < 2\pi$

$$u_x(\sigma) = -\tilde{u}_y(\sigma)\ ,\ u_y(\sigma) = \tilde{u}_x(\sigma)\ ,\ T = \tilde{T} \tag{4.17}$$

To show that the above controls satisfy the requirement that $\bar{\omega}_x(0) = \bar{\omega}_y(0) = \bar{\omega}_x(T) = \bar{\omega}_y(T) = 0$ we substitute (4.15) through (4.17), in sequence, into (4.11) and (4.12); the resulting equations have the same form as (4.11) and (4.12). Substituting the following expressions

$$\beta_o = \tilde{\beta}_o + \frac{\pi}{2}\ ,\ \beta_o = \tilde{\beta}_o + \pi,\ \beta_o = \tilde{\beta}_o + \frac{3\pi}{2} \tag{4.18}$$

in addition to (4.15) through (4.17), in sequence, into (4.13) and (4.14) we find that the resulting pair of equations is identical to (4.13) and (4.14) in each case. Thus, control laws corresponding to $\pi/2 \leq \beta_o < 2\pi$ can be readily determined from those corresponding to $0 \leq \tilde{\beta}_o < \pi/2$ when γ and $\bar{L}_y$ remain constant.

Performing a similar analysis in the case when control is provided by two jets we can readily show that if $(\tilde{u}_y(\sigma), \tilde{T})$ satisfies the governing equations for $0 \leq \tilde{\beta}_o < \pi$ then the control law for $\pi \leq \beta_o < 2\pi$ is given by

$$u_y(\sigma) = -\tilde{u}_y(\sigma) \ , \ T = \tilde{T} \tag{4.19}$$

for $\beta_o = \tilde{\beta}_o + \pi$. When control is provided by a single thruster only a positive (negative) control torque is available; therefore, we must solve equations (4.11) through (4.14) for the pair $(u_y(\sigma), T)$ for each set of values of the physical parameters γ, β_o and $\bar{L}_Y$ (in terms of β_o, there is no simple relation between the control laws as was found in the previous cases).

4.3 A Necessary and Sufficient Condition for Optimality

In Section 2.2 we showed that Control Systems (B) through (D) are normal. Hence, the maximum principle provides both a necessary and sufficient condition for optimality. Forming the Hamiltonian

$$\begin{aligned} H = {} & P_1(\sigma)[\gamma\tilde{\omega}_y(\sigma) + u_x(\sigma)] + P_2(\sigma)[-\gamma\omega_x(\sigma) + u_y(\sigma)] + P_3(\sigma)[u_x(\sigma) \\ & \cos(\sigma+\beta_o) - u_y(\sigma)\sin(\sigma+\beta_o)] + P_4(\sigma)[u_x(\sigma)\sin(\sigma+\beta_o) \\ & + u_y(\sigma)\cos(\sigma+\beta_o)]. \end{aligned} \tag{4.20}$$

Maximization of the Hamiltonian subject to the constraints given by Equations (4.3) and (4.4) occurs when

$$u_x^*(\sigma) = \begin{bmatrix} \text{SGN}[S_x(\sigma)]: & \text{Controller (B)} \\ 0: & \text{Controllers (C) and (D)} \end{bmatrix} \tag{4.21}$$

$$u_y^*(\sigma) = \begin{bmatrix} \text{SGN}[S_y(\sigma)]: & \text{Controllers (B) and (C)} \\ u'[S_y(\sigma)]: & \text{Controller (D)} \end{bmatrix} \tag{4.22}$$

where

$$u'[S_y(\sigma)] = \begin{bmatrix} 1, & S_y(\sigma) > 0 \\ 0, & S_y(\sigma) \leq 0 \end{bmatrix}$$

$$S_x(\sigma) = P_1(\sigma) + P_3(\sigma)\cos(\sigma+\beta_o) + P_4(\sigma)\sin(\sigma+\beta_o) \quad (4.23)$$

$$S_y(\sigma) = P_2(\sigma) - P_3(\sigma)\sin(\sigma+\beta_o) + P_4(\sigma)\cos(\sigma+\beta_o). \quad (4.24)$$

The adjoint variables, $P_1(\sigma)$ through $P_4(\sigma)$, which satisfy the canonical equations

$$\frac{dP_1}{d\sigma} = -\frac{\partial H}{\partial \bar{\omega}_x}, \quad \frac{dP_2}{d\sigma} = -\frac{\partial H}{\partial \bar{\omega}_y}, \quad \frac{dP_3}{d\sigma} = -\frac{\partial H}{\partial \bar{L}_x}, \quad \frac{dP_4}{d\sigma} = -\frac{\partial H}{\partial \bar{L}_y}$$

can be written in vector form as follows

$$\begin{bmatrix} P_1(\sigma) \\ P_2(\sigma) \\ P_3(\sigma) \\ P_4(\sigma) \end{bmatrix} = \begin{bmatrix} \cos\gamma\sigma & \sin\gamma\sigma & 0 & 0 \\ -\sin\gamma\sigma & \cos\gamma\sigma & 0 & 0 \\ 0 & 0 & 1 & 0 \\ 0 & 0 & 0 & 1 \end{bmatrix} \begin{bmatrix} P_1^o \\ P_2^o \\ P_3^o \\ P_4^o \end{bmatrix} \quad (4.25)$$

where P_1^o through P_4^o are constants of integration. In view of (4.25) the switching functions become:

$$S_x(\sigma) = \alpha_1 \sin(\gamma\sigma + \alpha_2) + \alpha_4 \sin(\sigma+\alpha_3) \quad (4.26)$$

$$S_y(\sigma) = \alpha_1 \cos(\gamma\sigma + \alpha_2) + \alpha_4 \cos(\sigma+\alpha_3) \quad (4.27)$$

Since the steering functions are bang-bang the optimal control is independent of $\underline{P}(\sigma)$; therefore, only three components of the initial adjoint vector are essential. Thus, we can set either $\alpha_1 = 1$ or $\alpha_4 = 1$ without loss of generality.[1]

Upon substitution of the optimal steering functions (4.21) and (4.22) into (4.11) through (4.14) we find that the only terms not fixed by the system description are $\underline{\alpha}$ and T^*. Hence, the governing equations can be written in vector form as

$$\underline{X}(T^*) = \underline{X}(0) + \underline{F}(\underline{\alpha}, T^*). \quad (4.28)$$

[1] The normalization procedure, that is, the choice of an appropriate α_i as the unit element, is discussed in Appendix A.

Equation (4.28) represents a mapping between the pair $(\underline{\alpha}, T^*)$ and $\underline{\chi}(T^*)$ for a given $\underline{\chi}(0)$. Thus, the problem of determining a minimum time control is equivalent to that of finding an inverse to (4.28).

The remainder of this chapter is devoted to the problem of synthesizing exact optimal controls for specified ranges of values of the physical parameters ω_x^o, ω_y^o, γ, β_o and $\bar{L}_Y$. First, the characteristics of the optimal controls are investigated when $T^* \ll 1$. To include a more general class of boundary conditions and system parameters we then discuss the development and application of a numerical procedure for solving a number of two point boundary value problems.

4.4 Optimal Steering When the Dimensionless Final Time is Small Compared to Unity

In this section we consider the optimal control problem when $T^* \ll 1$. As in the previous chapter, control of both the vehicle's attitude and transverse components of angular velocity over the interval $[0, T^*]$ when $T^* \ll 1$ is referred to as the "short-time" control problem. The motivation for studying the characteristics of the optimal control law when the final time is small has been discussed in Chapter 1.

4.4.1 The Case When Control is Provided by Four Jets

For $\sigma \in [0, T_B]$, $T_B \ll 1$, Equations (4.11) through (4.14) become:

$$\int_0^{T_B} [u_x(\sigma)\left(1 - \frac{\gamma^2\sigma^2}{2}\right) - u_y(\sigma)\ (\gamma\sigma)]\ d\sigma + o(T_B) = 0 \qquad (4.29)$$

$$\int_0^{T_B} [u_x(\sigma)\ (\gamma\sigma) + u_y(\sigma)\left(1 - \frac{\gamma^2\sigma^2}{2}\right)]\ d\sigma + o(T_B) = 0 \qquad (4.30)$$

$$\int_0^{T_B} [u_x(\sigma)\left\{K_1(1 - \frac{\sigma^2}{2}) - K_2\sigma\right\} - u_y(\sigma)\left\{K_2(1 - \frac{\sigma^2}{2}) + K_1\sigma\right\}]\ d\sigma + o(T_B) = 0 \qquad (4.31)$$

$$\int_0^{T_B} [u_x(\sigma)\left\{K_1\sigma + K_2\left(1 - \frac{\sigma^2}{2}\right)\right\} + u_y(\sigma)\left\{K_1\left(1 - \frac{\sigma^2}{2}\right) - K_2\sigma\right\}]d\sigma + o(T_B) = -\bar{L}_Y \quad (4.32)$$

when $\bar{\omega}_x^o = \bar{\omega}_y^o = 0$ and $K_1 = \cos\beta_o$, $K_2 = \sin\beta_o$. The mathematical problem is now one of determining an optimal control in terms of the dimensionless parameters γ, β_o and $\bar{L}_Y$ such that (4.29) through (4.32) are satisfied. From the necessary condition provided by the maximum principle we found that the optimal steering functions are bang-bang. Consequently, it is possible to completely describe the optimal control in terms of the switching times, the initial value of the steering functions, and the final time. If the control is given in this form then it is unnecessary to compute the initial adjoint $\underline{\alpha}$ as is usually done; to add completeness we show in Appendix C that there exists a corresponding $\underline{\alpha}$. Instead, a method is presented whereby the number of times each component of $\underline{u}^*(\sigma)$ changes sign can be determined from the switching functions. Once the optimal switching sequence has been established, the actual switch times, the initial value of the control, and the time at which control is terminated are determined from a simultaneous solution to Equations (4.29) through (4.32).

The first step in this procedure is to establish upper limits on the number of times $u_x^*(\sigma)$ and $u_y^*(\sigma)$ change sign in the interval $(0, T_B')$. Since the steering functions are uniquely defined by $S_x(\sigma)$ and $S_y(\sigma)$ we can determine the maximum number of switchings in $(0, T_B')$, $T_B^* \leq T_B'$, by examining the roots of the following equations:

$$S_x(\sigma_i) = \alpha_1 \sin(\gamma\sigma_i + \alpha_2) + \sin(\sigma_i + \alpha_3) = 0 \quad (4.33)$$

where $i = 1, 2, 3, \ldots\ldots h_x$, $\sigma_j \epsilon (0, T_B')$

$$S_y(\sigma_j) = \alpha_1 \cos(\gamma\sigma_j + \alpha_2) + \cos(\sigma_j + \alpha_3) = 0 \qquad (4.34)$$

where

$$j = 1, 2, 3, \ldots\ldots h_y, \quad \sigma_j \epsilon (0, T_B')$$

For the above switching functions it is possible to show that $(h_x)_{max} = 3$ and $(h_y)_{max} = 3$ when $T_B' < \frac{1}{2}\pi$.[2] Furthermore, by examining the roots of (4.33) and (4.34) simultaneously, we find that the switching sequence given in Table 4.1 represent the maximum number of times both $u_x^*(\sigma)$ and $u_y^*(\sigma)$ change in the interval $(0, T_s')$; that is, the sum $h_x + h_y$ is a maximum.[3] Thus, from the maximum principle, we find that if $\underline{u}(\sigma)$ is optimal for $\sigma \epsilon [0, T_B']$ then $h_x + h_y \leq 3$ and, in addition, both $u_x^*(\sigma)$ and $u_y^*(\sigma)$ must operate at their extreme values. Control laws which require the sum $h_x + h_y$ to be less than three can be eliminated as candidates for optimal steering if we assume that the initial (final) state does not lie on a switching surface which contains time-optimal trajectories. In view of this assumption the task of determining an optimal control which satisfies (4.29) through (4.32) becomes one of choosing an appropriate switching sequence from Table 4.1 and then solving for the exact switch times, $\underline{u}^*(0)$, and the final time.

CASE	h_x	h_y
1-a	3	0
1-b	0	3
2-a	1	2
2-b	2	1

Table 4.1. Maximum Number of Switchings when $T_B < T_B'$

[2] Consult Appendix C for a detailed discussion of this topic.

[3] For example, if $h_x = 3$ then $\underline{u}(\sigma)$ will not be optimal if $h_y \geq 1$.

Let us first consider Cases (1-a) and (1-b). If the steering functions which appear in Equations (4.29) through (4.32) operate in a bang-bang mode and switch according to (1-a) or (1-b) then we find, by comparing terms which appear on the left sides of the resulting equations on an order of magnitude basis, that both $u_x^*(\sigma)$ and $u_y^*(\sigma)$ must at least one switch point in the interval $(0,T_B')$. Therefore, cases (1-a) and (1-b) can be elminated as candidates since this type of switching cannot satisfy the boundary conditions specified by (4.10). At this point the problem becomes one of determining whether Switching Sequence (2-a) or (2-b) is to be applied in a particular situation. To complete the task we must then compute the exact switch times, the final time, and the initial value of the steering functions.

Let us proceed according to the following schedule: First, bang-bang control which switches according to the logic given by Cases (2-a) and (2-b) is substituted into (3.29) through (3.32); the resulting sets of equations are then solved simultaneously for the three switch times and the final time. From these results we can then determine $\underline{u}^*(0)$ and, in addition, specify on the basis of the system description the correct switching sequence.

Bang-bang control which is governed by Switching Logic (2-a) can be represented geometrically as shown in Figure 4.2.

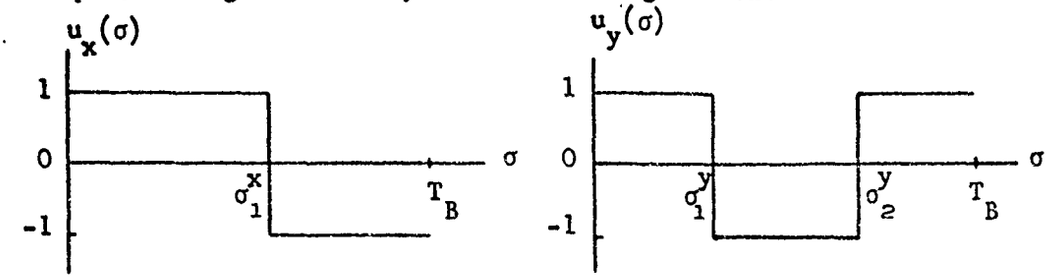

Figure 4.2. A Geometric Representation of Switching Sequence (2-a)

Upon substitution of this control into Equations (4.29) through (4.32) and after straightforward mathematical manipulation we find:

$$2\sigma_1^x - T_B + \gamma^2[\frac{1}{6}T_B^3 - \frac{1}{3}(\sigma_1^x)^3] - u^o\gamma[(\sigma_1^y)^2 - (\sigma_2^y)^2 + \frac{T_B^2}{2}] = 0 \qquad (4.35)$$

$$\gamma[(\sigma_1^x)^2 - \frac{T_B^2}{2}] + u^o[2\sigma_1^y - 2\sigma_2^y + T_B] - u^o\gamma^2[\frac{1}{3}(\sigma_2^y)^3 - \frac{1}{3}(\sigma_2^y)^3 + \frac{T_B^3}{6}] = 0 \qquad (4.36)$$

$$\kappa_1[2\sigma_1^x - T_B] - \kappa_1[\frac{1}{3}(\sigma_1^x)^3 - \frac{T_B^3}{6}] - \kappa_2[\sigma_1^x)^2 - \frac{T_B^2}{2}]$$
$$-\kappa_2u^o[2\sigma_1^y - 2\sigma_2^y + T_B] + \kappa_2u^o[\frac{1}{3}(\sigma_1^y)^3 - \frac{1}{3}(\sigma_2^y)^3 + \frac{T_B^3}{6}] \qquad (4.37)$$
$$-\kappa_1u^o[(\sigma_1^y)^2 - (\sigma_2^y)^2 + \frac{T_B^2}{2}] = 0$$

$$\kappa_1[(\sigma_1^x)^2 - \frac{T_B^2}{2}] + \kappa_2[2\sigma_1^x - T_B] - \kappa_2[\frac{1}{3}(\sigma_1^x)^3 - \frac{T_B^3}{6}] + \kappa_1u^o[2\sigma_1^x - 2\sigma_2^x + T_B]$$
$$-\kappa_1u^o[\frac{1}{3}(\sigma_1^y)^3 - \frac{1}{3}(\sigma_2^y)^3 + \frac{T_B^3}{6}] + \kappa_2u^o[(\sigma_1^y)^2 - (\sigma_2^y)^2 + \frac{T_B^2}{2}] = -\frac{L_y}{u_x(0)} \qquad (4.38)$$

when terms of $O(T_B^4)$ are neglected and $u^o = \frac{u_y(0)}{u_x(0)}$.

The switching times can be written as combinations of linear and higher order terms as follows:

$$\sigma_1^x = C_1T_B + \varepsilon_1 \qquad (4.39)$$

$$\sigma_1^y = C_2T_B + \varepsilon_2 \qquad (4.40)$$

$$\sigma_2^y = C_3T_B + \varepsilon_3 \qquad (4.41)$$

Substituting the above expressions into (4.35) through (4.37) and solving the resulting equations simultaneously for the required parameters gives:

$$C_1 = \frac{1}{2}\,,\quad C_2 = \frac{1}{4}(1 - \frac{\tan\beta_o}{u^o})\,,\quad C_3 = \frac{1}{4}(3 - \frac{\tan\beta_o}{u^o})$$

$$\varepsilon_1 = \frac{\gamma T_B^2 \tan \beta_o}{8} + O(T_B^3)$$

$$\varepsilon_2 = [(\frac{\gamma}{2} - 1)u^o - \frac{3\gamma+1}{4} \tan \beta_o - u^o \tan^2 \beta_o + \frac{\gamma+1}{4} \tan^3 \beta_o] \frac{T_B^2}{8} + O(T_B^3)$$

$$\varepsilon_3 = [-(\frac{\gamma}{2} + 1)u^o - \frac{3\gamma+1}{4} \tan \beta_o - u^o \tan^2 \beta_o + \frac{\gamma+1}{4} \tan^3 \beta_o] \frac{T_B^2}{8} + O(T_B^3)$$

With the switching times known it is now possible to solve (4.38) for the dimensionless final time

$$T_B^* = 2\sqrt{\frac{-\bar{L}_Y \cos \beta_o}{u_x(0)(\gamma-1)}}. \qquad (4.42)$$

Note that terms of $O(T_B^3)$ have been neglected in this solution. Also note that the switching times and the final time are functions of $\underline{u}(0)$ as well as of the physical parameters γ, β_o and $\bar{L}_Y$. To determine $u(0)$ we must refer to both Equation (4.42) and the necessary condition for time optimality. First, $u_x(0)$ is chosen such that the radicand in (4.42) is positive. Since $(\gamma-1) < 0$ for $-1 < \gamma < 1$ and if $0 \leq \beta_o < \pi/2$ then $u_x(0) = 1$ when $\bar{L}_Y > 0$ and $u_x(0) = -1$ when $\bar{L}_Y < 0$. Unfortunately, $u_y(0)$ cannot be determined in a similar manner since it only appears in terms of $O(T_B^3)$ in Equation (4.38). However, when both the switching sequence and the initial value of one component of $\underline{u}(0)$ are known then the initial value of the second component is given by the necessary condition for time optimality. Thus, when $\bar{L}_Y > 0$ and $\beta_o = 0$ we find that $S_y(0) > 0$ and therefore $u_y(0) = 1$.

To determine those values of the physical parameters for which the optimal steering functions are given qualitatively by Switching Sequence (2-a), $u_x(0) = 1$, $u_y(0) = 1$, we must investigate the behavior of the switching points as changes are made in β_o, starting at $\beta_o = 0$.

Note that β_o is the only physical parameter which appears in the first order terms of (4.40) and (4.41) and, therefore, represents the strongest influence on the location of the switching points within the interval $(0, T_B)$. If u^o is positive then σ_1^y and σ_2^y are shifted toward zero when β_o is montone increasing and $0 \leq \beta_o < \pi/4$. It is readily shown that ε_2 is negative when $0 \leq \beta_o < \pi/4$; consequently, the switch point σ_1^y is lost from the left end of the interval $(0, T_B)$ when β_o reaches a value which is slightly less than $\pi/4$. The exact value of β_o at which this occurs depends, of course, on both the system description and the reorientation angle and is denoted by β_o' (see Figure 4.3). Thus when $\beta_o \geq \beta_o'$ the optimal steering functions are no longer described qualitatively by Switching Sequence (2-a). To determine an explicit relation between β_o' and the physical parameters we must consider both Switching Sequence (2-a) and (2-b).

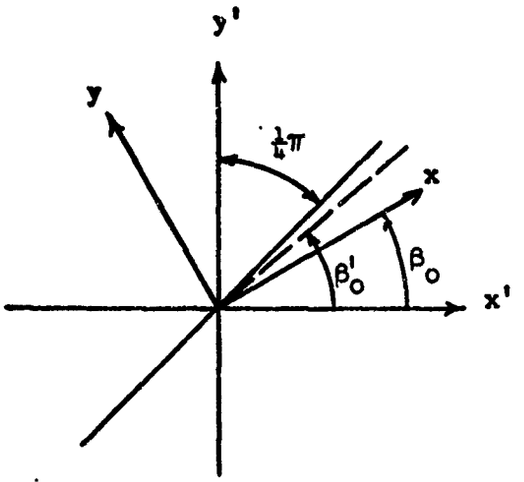

Figure 4.3. Definition of β_o'

When the switching logic is given by case (2-b) the optimal control can be represented geometrically as shown in Figure 4.4.

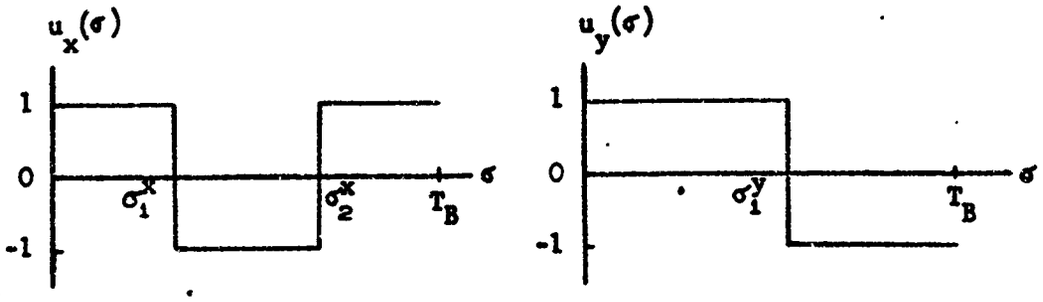

Figure 4.4. A Geometric Representation of Switching Sequence (2-b)

Substituting this control into Equations (4.29) through (4.32) and after straightforward mathematical manipulation we find:

$$2\sigma_1^x - 2\sigma_2^x + T_B - \gamma^2[\tfrac{1}{3}(\sigma_1^x)^3 - \tfrac{1}{3}(\sigma_2^x)^3 + \tfrac{1}{6}T_B^3] - \gamma u^o[(\sigma_1^y)^2 - \tfrac{1}{2}T_B^2] = 0 \quad (4.43)$$

$$\gamma[(\sigma_1^x)^2 - (\sigma_2^x)^2 + \tfrac{1}{2}T_B^2] + u^o[2\sigma_1^y - T] - 2u^o[\tfrac{1}{3}(\sigma_1^y)^3 - \tfrac{1}{6}T_B^3] = 0 \quad (4.44)$$

$$\kappa_1[2\sigma_1^x - 2\sigma_2^x + T_B] - \kappa_1[\tfrac{1}{3}(\sigma_1^x)^3 - \tfrac{1}{3}(\sigma_2^x)^3 + \tfrac{1}{6}T_B^3] - \kappa_2[(\sigma_1^x)^2 - (\sigma_2^x)^2 + \tfrac{1}{2}T_B^2]$$
$$-\kappa_2 u^o[2\sigma_1^y - T_B] + \kappa_2 u^o[\tfrac{1}{3}(\sigma_1^y)^3 - \tfrac{1}{6}T_B^3] - \kappa_1 u^o[(\sigma_1^y)^2 - \tfrac{1}{2}T_B^2] = 0 \quad (4.45)$$

$$\kappa_1[(\sigma_1^x)^2 - (\sigma_2^x)^2 + \tfrac{1}{2}T_B^2 + u^o \quad 2\sigma_1^y - T_B - \tfrac{1}{3}(\sigma_1^y)^3 + \tfrac{1}{6}T_B^3 \quad]$$
$$+ \kappa_2[2\sigma_1^x - 2\sigma_2^x + T_B - \tfrac{1}{3}(\sigma_1^x)^3 + \tfrac{1}{3}(\sigma_2^x)^3 - \tfrac{1}{6}T_B^3 + u^o\ (\sigma_1^y)^2 - \tfrac{1}{2}T_B^2\ ] = \frac{-\Gamma_Y}{u_x(0)} \quad (4.46)$$

when terms of $O(T_B^4)$ are neglected.

Following the procedure outlined in the previous paragraph we write the switching times as combinations of linear and higher order terms:

$$\sigma_1^x = C_1'\ T_B + \varepsilon_1' \quad (4.47)$$

$$\sigma_2^x = C_2' T_B + \varepsilon_2' \tag{4.48}$$

$$\sigma_1^y = C_3' T_B + \varepsilon_3' \tag{4.49}$$

In this case:

$$C_1' = \frac{1}{4}(1 - u^o \cot \beta_o) \; ; \; C_2' = \frac{1}{4}(3 - u^o \cot \beta_o) \; ; \; C_3' = \frac{1}{2}$$

$$\varepsilon_1' = [(1 - \frac{\gamma}{2})u^o + \frac{3\gamma+1}{4} \cot \beta_o + u^o \cot^2\beta_o - \frac{\gamma+1}{4} \cot^3\beta_o]\frac{T_B^2}{8} + O(T_B^3)$$

$$\varepsilon_2' = [(1 + \frac{\gamma}{2})u^o + \frac{3\gamma+1}{4} \cot \beta_o + u^o \cot^2\beta_o - \frac{\gamma+1}{4} \cot^3\beta_o]\frac{T_B^2}{8} + O(T_B^3)$$

$$\varepsilon_3' = -\frac{\gamma T_B^2 \cot \beta_o}{8} + O(T_B^3)$$

Solving Equation (4.46) for the dimensionless final time when terms of $O(T_B^3)$ are neglected gives

$$T_B^* = 2\sqrt{\frac{\bar{L}_Y \sin \beta_o}{u_o(0)(\gamma-1)}}. \tag{4.50}$$

The initial value of the steering functions are determined through a procedure similar to that employed in Case (2-a). First, the radicand in (4.50) will be positive when $0 \leq \beta_o < \pi$, $\bar{L}_Y > 0$, if $u_y(0) = -1$. Second, from the necessary condition for optimality we find that when the switching sequence is given by (2-b) and $S_y(0) < 0$ then $S_x(0) > 0$ therefore $u_x(0) = 1$.

By observing the behavior of the switching times as changes are made in β_o, $\beta_o' < \beta_o < \pi/2$, we can determine those values of the physical parameters for which the optimal steering is specified qualitatively by Switching Sequence (2-b). If u^o is negative then σ_1^x and σ_2^x are shifted toward the right end of the interval $(0, T_B)$ when β_o is monotone decreasing and $\beta_o' < \beta_o < \pi/2$. As $\beta_o \to \beta_o'$ we find that $\sigma_2^x \to T_B^*$ and at the

critical value, $\beta_o = \beta_o'$, $\sigma_2^x = T_B^*$. When this situation occurs there are only two switching points in the interval $(0,T_B)$ and therefore Switching Sequence (2-b) no longer represents optimal steering since we have assumed that $(h_x + h_y) = 3$. Thus, the problem of determining β_o' is equivalent to that of computing a value of β_o for which $\sigma_1^y = 0$ and $\sigma_2^x = T_B^*$. Using Equations (4.40) and (4.48) it is readily shown that

$$\beta_o' = \frac{1}{2}\left(\frac{\pi}{2} - T_B^*\right). \tag{4.51}$$

In summary, we find that the optimal control which satisfies Equations (4.29) through (4.32) has the following characteristics:

1. When $0 \leq \beta_o < \beta_o'$ the optimal switching logic is given by (2-a). Hence, $u_x^*(\sigma)$ operates in a "race-brake" mode with the switch time located at nearly $T_B^*/2$. The second steering function, $u_y^*(\sigma)$, switches twice in the interval $(0,T_B^*)$, and the switching points are shifted toward zero when β_o is monotone increasing, $0 \leq \beta_o < \beta_o'$.
2. When $\beta_o' < \beta_o < \pi/2$ the optimal switching logic is given by (2-b). Here, $u_y^*(\sigma)$ operates in a race-brake mode. The remaining steering function, $u_x^*(\sigma)$, switches twice in the interval $(0,T_B^*)$, and the switching times are shifted toward zero when β_o is monotone increasing, $\beta_o' < \beta_o < \pi/2$.
3. The optimal control corresponding to $\beta_o \epsilon (\pi/2, 2\pi)$ can be readily determined from the symmetry properties of the reachable set as outlined by Equations (4.15) through (4.17).

4.4.2 The Case When Control is Provided by Two Jets

The controller configuration considered in this section is de-

picted in Figure 1.1.C. Since the two-jet controller is a special case of the four-jet configuration the optimal steering function is given by Equation (4.22). Our objective is to obtain an explicit expression for the optimal control in terms of the physical parameters such that Equations (4.11) through (4.14) are satisfied when $u_x(\sigma) \equiv 0$ and $T_C \ll 1$.

Following both the assumptions made and the method of analysis employed in Section 4.4.1 we find that $(h_y)_{max} = (h_y)_{min} = 3$. Therefore, the mathematical problem becomes one of solving for the switching times σ_1^y, σ_2^y, σ_3^y; the initial value of the steering function $u_y^*(0)$; and the dimensionless final time T_C.

When $T_C \ll 1$ Equations (4.11) through (4.14) become:

$$\int_0^{T_C} u_y(\sigma)[\gamma\sigma - \frac{\gamma^3\sigma^3}{6} + O(\sigma^5)]d\sigma = 0 \qquad (4.52)$$

$$\int_0^{T_C} u_y(\sigma)\,[1 - \frac{\gamma^2\sigma^2}{2} + O(\sigma^4)]d\sigma = 0 \qquad (4.53)$$

$$\int_0^{T_C} u_y(\sigma)\,\kappa_1(\sigma - \frac{\sigma^3}{6}) + \kappa_2(1 - \frac{\sigma^2}{2}) + O(\sigma^4)]d\sigma = 0 \qquad (4.54)$$

$$\int_0^{T_C} u_y(\sigma)[\kappa_1(1 - \frac{\sigma^2}{2}) + \kappa_2(\sigma - \frac{\sigma^3}{6}) + O(\sigma^4)]d\sigma = -\bar{L}_Y \qquad (4.55)$$

for $\bar{\omega}_x^o = \bar{\omega}_y^o = 0$ and $\kappa_1 = \cos\beta_o$, $\kappa_2 = \sin\beta_o$. Note that in the above equations cubic terms have been retained in the power series representation of both sin $\gamma\sigma$ and sin σ; it is readily shown that the left side of (4.55) is identically zero if $u_y(\sigma)$ satisfies (4.52) through (4.54) and providing the remainder terms of the previously mentioned power series are of $O(\sigma^3)$. Since this order of accuracy must be maintained in order to ensure that the left side of (4.55) is not identically zero, it is worthwhile to determine the order of magnitude of T_C in

terms of $\bar{L}_Y$ before an attempt is made to solve (4.52) through (4.55) for the switching times and the final time.

Consider the case when $\kappa_1 = 1$ and $\kappa_2 = 0$. Combining equations (4.53) and (4.55) we find

$$\int_0^{T_C} [(\frac{1-\gamma^2}{2})\sigma^2 + O(\sigma^4)]u_y(\sigma)d\sigma = \bar{L}_Y \tag{4.56}$$

therefore

$$\bar{L}_Y < \frac{1-\gamma^2}{2} O(T_C^3). \tag{4.57}$$

However, if $\kappa_1 = 0$ and $\kappa_2 = 1$ it follows that

$$\int_0^{T_C} [(\frac{1-\gamma^2}{6})\sigma^3 + O(\sigma^5)]u_y(\sigma)d\sigma = \bar{L}_Y \tag{4.58}$$

hence

$$\bar{L}_Y < \frac{\gamma^2-1}{6} O(T_C^4). \tag{4.59}$$

In view of (4.57) and (4.59) it is evident that the reorientation time depends very strongly on the initial position of the thrusters. That is, the form of the functional relation between T_C^* and $\bar{L}_Y$ depends upon β_o. In contrast, when control is provided by four jets β_o only influences the radicand in (4.42) and (4.50).

In view of the above discussion it does not appear worthwhile to employ the method of solution described in the previous section to determine the optimal control for the two-jet controller. However, since the system is totally controllable there exists a pair $(\underline{\alpha}, T_C^*)$ which satisfies (4.11) through (4.14), $u_x(\sigma) \equiv 0$, when $T_C^* \ll 1$. Such controls have been computed numerically and are described in Section 4.5.2.

4.5 A Numerical Procedure for Computing Time-Optimal Controls

In general, it is not possible to solve directly for the optimal control when steering is provided by Thruster Configurations (B) through (D). Therefore, some type of numerical procedure must be used to solve the two point boundary value problem. In this section an iterative technique for solving the two point boundary value problem is discussed, and optimal controls are computed for two classes of boundary conditions. As a result of this flooding we are able to deduce both the qualitative and quantitative structure of the optimal control.

4.5.1 A Systematic Variation of the Physical Parameters

The equations which must be satisfied by the optimal control can be written in vector form as

$$\underline{X}(T^*) = \underline{X}(0) + \underline{F}(\gamma, \varepsilon_o, \underline{\alpha}, T^*). \tag{4.60}$$

The control problem now becomes one of solving (4.60) for the pair $(\underline{\alpha}, T^*)$ or, equivalently, that of determining an inverse to $\underline{F}$. It is impossible, in general, to evaluate this inverse analytically; therefore, an iterative procedure is suggested. Unfortunately, in the latter method the parameters $\underline{X}(T^*)$, $\underline{X}(0)$, γ, and ε_o must be specified prior to any numerical computation. Therefore, if we are to synthesize optimal control laws for a wide range of vehicle configurations and reorientation angles, then the iterative procedure must be applied repeatedly as appropriate changes are made in the physical parameters.

In the following paragraphs a method is presented whereby exact time-optimal controls based on the dimensionless physical parameters

$\bar{\omega}_x^o$, $\bar{\omega}_y^o$, $\bar{T}_y$, γ and β_o are computed with a modest expenditure of computer time. Specifically, this method involves computing optimal trajectories between selected sets of points in the normalized state space X(i.e., flooding). Since the resulting control laws are specified in terms of the physical parameters, the affect of changes in these dimensionless quantities on the optimal control is readily observed. Thus the necessity of condensing the system parameters into a reduced number of dimensionless parameters becomes apparent. If this technique is not used then: (1) the number of cases which must be considered increases significantly, and in turn the computation time becomes excessive, and (2) the global characteristics of the optimal control cannot be readily determined.

To establish guidelines for a flooding process the following questions concerning the design of an active control system are considered:

1. For a specific vehicle configuration (i.e., given geometry, spin rate, and thruster configuration) what is the minimum control moment required to reorient the spacecraft through a specified angle in a given amount of time?
2. What is the affect of initial non-zero transverse components of angular velocity on the minimum time required to control a spacecraft to a given terminal attitude?
3. How do changes in the spacecraft's geometry, mass and spin rate influence the minimum time for reorientation?
4. For a given rate of propellant expenditure how do the various controller configurations compare with one another in terms of the

minimum time required to reorient the spin axis through a given angle?

By systematically perturbing the physical parameters as indicated in the following outline and solving the resulting two point boundary value problem at each step we are able to provide answers to the above questions and, in addition, illuminate the basic structure of the minimum time control problem:

1. For a given geometry and mass (i.e., γ = constant) the characteristics of the optimal control in terms of spin rate, reorientation angle, and control magnitude are a determined by varying $\bar{\bar{L}}_Y$ when $\bar{\omega}_x^o = \bar{\omega}_y^o = 0$ and β_o = constant.
2. The influence of the spacecraft's geometry and mass on the optimal control is investigated by systematically varying γ in Item 1.
3. In Items 1 and 2 above it is assumed that $\bar{\bar{L}}_X(T) = 0$. In Section 4.1 we found the optimal control corresponding to boundary conditions of the form given by (4.10) can be applied when $\bar{\bar{L}}_X(T) \neq 0$ if Coordinate System II is prerotated through the angle $\bar{\beta}_o$. Therefore, the influence of both $\bar{\bar{L}}_X(T) \neq 0$ and the initial orientation of the thruster(s) on the optimal control are determined by systematically varying β_o for fixed values of $\bar{\omega}_x^o$, $\bar{\omega}_y^o$, $\bar{\bar{L}}_Y$ and γ.
4. The affect of $\bar{\omega}_x^o \neq 0$ or $\bar{\omega}_y^o \neq 0$ on the optimal control is determined by systematically varying these quantities while holding $\bar{\bar{L}}_Y$, β_o and γ constant.

To implement the flooding procedure described above an algorithm was developed for solving the required number of two point boundary value problems with a modest expenditure of computer time. Specifi-

cally, a method similar to that proposed by Knudsen [15] was employed (see Appendix A). Knudsen's algorithm like those of Neustadt's [16], [17], Eaton's [18], and Plant's [19] relies on the connection between the system's adjoint equations and the time-optimal control. In order to initiate the computational process a "guess" is made for the pair $(\underline{\alpha}, T^*)$. The iterative procedure is then used to systematically correct the control and the final time until Equations (4.11) through (4.14) are satisfied. In this procedure, like those proposed by other authors, the number of iterations required to converge on the optimal control depends upon how close the nominal control is to the optimal control. The major advantage of a Newton type iterative procedure (both Knudsen's and Plant's techniques make use of the basic Newton recursive relation) is that it converges rapidly when this error is small.

An efficient algorithm was designed around Knudsen's iterative procedure by taking advantage of the fact that exact analytic solutions to the two point boundary value problem have been found for certain values of the parameters $\bar{\omega}_x^o$, $\bar{\omega}_y^o$, $\bar{L}_Y$, β_o and γ. Thus, in general, the error between the computed and actual control laws is small if small variations are made in the physical parameters starting from those values for which the control law is known. For example, in Item 1, page 82, small changes were made in $\bar{L}_Y$, $(\bar{L}_Y)_{i+1} = (\bar{L}_Y) + \Delta \bar{L}_Y$, starting at $\bar{L}_Y = (\bar{L}_Y)_1$; in this case the control corresponding to $(\bar{L}_Y)_1$ was determined by analytic methods (see Section 4.5.2).

In certain situations physical parameters were chosen as starting points in the flooding process for which the control could not be

determined by straightforward analytic methods. Under such circumstances a guess was made for the pair $(\underline{\alpha},T^*)$; the iterative procedure was then used to compute the required control. Once a "starting" control had been determined the flooding process was carried out as outlined previously.

4.5.2 Analytic Solutions to the Control Problem

In this section our primary objective is to provide exact time-optimal controls which can be used as starting points for the flooding process when $\bar{\omega}_x^o = \bar{\omega}_y^o = 0$. For convenience we can rewrite the governing equations which must be satisfied by the optimal control as follows:

$$\int_0^T [u_x(\sigma) \cos \gamma\sigma - u_y(\sigma) \sin \gamma\sigma]d\sigma = 0 \qquad (4.61)$$

$$\int_0^T [u_x(\sigma) \sin \gamma\sigma + u_y(\sigma) \cos \gamma\sigma]d\sigma = 0 \qquad (4.62)$$

$$\int_0^T [u_x(\sigma) \cos (\sigma + \beta_o) - u_y(\sigma) \sin (\sigma + \beta_o)]d\sigma = 0 \qquad (4.63)$$

$$\int_0^T [u_x(\sigma) \sin (\sigma+\beta_o) + u_y(\sigma) \cos (\sigma + \beta_o)]d\sigma = -\bar{L}_Y \qquad (4.64)$$

In addition, if the control is optimal then the steering functions must have the following form:

$$u_x^*(\sigma) = \text{SGN}[\alpha_1 \sin (\gamma\sigma+\alpha_2) + \sin (\sigma + \alpha_3)] \qquad (4.65)$$

$$u_y^*(\sigma) = \text{SGN}[\alpha_1 \cos (\gamma\sigma+\alpha_2) + \cos (\sigma + \alpha_3)] \qquad (4.66)$$

In Chapter 3 we found that the control which generates optimal trajectories between certain initial and final state points is a constant moment about y' axis; a similar situation occurs when control is provided by Thruster Configurations (B) through (D). However, in the latter

cases the control jets are rigidly attached to the spacecraft; hence, the most efficient mode of operation occurs when the control moments are applied either in phase or π radians out of phase with the coefficients of $u_x(\sigma)$ and $u_y(\sigma)$ in (4.64). The optimal steering functions (4.65) and (4.66) will be of this form when $\alpha_1 = 0$ and $\alpha_3 = \beta_o + \pi$. It is readily shown that Equations (4.63) and (4.64) are satisfied if the control is given by

$$u_x^*(\sigma) = \begin{bmatrix} \text{SGN}[-\sin(\sigma+\beta_o)]: & \text{Controller (B)} \\ 0: & \text{Controllers (C) and (D)} \end{bmatrix} \quad (4.67)$$

$$u_y^*(\sigma) = \begin{bmatrix} \text{SGN}[-\cos(\sigma+\beta_o)]: & \text{Controllers (B) and (C)} \\ u'[-\cos(\sigma+\beta_o)]: & \text{Controller (D)} \end{bmatrix} \quad (4.68)$$

$$T^* = m\pi, \; m = 2, 4, 6, 8, \ldots\ldots \quad (4.69)$$

when the normalized angular momentum $\bar{L}_Y$ assumes those values in Table 4.2.

	4-Jets	2-Jets	1-Jet
$\bar{L}_Y$	4m	2m	m

Table 4.2. Maximum Values for $\bar{L}_Y$ when T^* is Given by Equation (4.69)

However, it is evident that (4.61) and (4.62) are not satisfied for all values of T^* as given by (4.69) when $\underline{u}^*$ is defined by (4.67) and (4.68). Therefore we must judiciously select appropriate values for m from among those given by (4.69). This can be accomplished through a physical interpretation of the integrands which appear in (4.61) and (4.62). First, the control moments change sign at a frequency which is directly proportional to the spin rate. Second, the coefficients of $u_x(\sigma)$ and

$u_y(\sigma)$ oscillate at a frequency which is proportional to the difference between the spin and nutation rates (i.e., $\gamma\sigma = (1 - I_z/I)\omega_s t$). It can be readily shown that the integral over $[0,m\pi]$ of the product of such functions is zero when the spin and nutation rates are related by

$$\omega_s \left(1 - \frac{m_2}{m_1}\right) = \frac{I_z \omega_s}{I} \tag{4.70}$$

where m_1 and m_2 are integers. Thus one value of m for which Equations (4.61) through (4.64) are satisfied is given by

$$m = 2m_1 = \frac{2m_2}{\gamma} . \tag{4.71}$$

Note that in deriving (4.70) and (4.71) we have assumed that γ is a rational number; for engineering purposes this is not restrictive since there exists a rational number which is arbitrarily close to any given number in R_1.

Let us now demonstrate the validity of Equation (4.71) when control is provided by Jet Configurations (B) and (C). Specifically, we wish to show that each term in (4.61) and (4.62) is identically zero when $u_x^*(\sigma)$, $u_y^*(\sigma)$ and T^* are given by Equations (4.67), (4.68), and (4.69) respectively. Actually, we need only consider terms of the form

$$\bar{\omega}_x^1 = \int_0^T \mathrm{SGN}[\sin(\sigma + \alpha_3)]\cos\gamma\sigma \, d\sigma \tag{4.72}$$

$$\bar{\omega}_y^1 = \int_0^T \mathrm{SGN}[\sin(\sigma + \alpha_3)]\sin\gamma\sigma \, d\sigma \tag{4.73}$$

since the control which appears in the remaining terms changes sign at the same frequency but is shifted by $\pi/2$ (it will be shown that $\bar{\omega}_x^1 = \bar{\omega}_y^1 = 0$ for all values of α_3). Define a new independent variable σ' by $\sigma' = \sigma - \frac{T}{2}$. Thus (4.72) and (4.73) become

$$\bar{\omega}_x^1 = \int_{-\frac{1}{2}T}^{\frac{1}{2}T} \mathrm{SGN}[\pm \sin(\sigma' + \alpha_3)]\cos\gamma\sigma'\, d\sigma' \tag{4.74}$$

$$\bar{\omega}_y^1 = \int_{-\frac{1}{2}T}^{\frac{1}{2}T} \mathrm{SGN}[\pm \sin(\sigma' + \alpha_3)]\sin\gamma\sigma'\, d\sigma' \tag{4.75}$$

where $T = 2\pi m_1$.

If $\alpha_3 = 0, \pi$ then $\bar{\omega}_x^1 = 0$ since the integrand of (4.74) is an odd function of σ'. In general, integration of (4.74) yields

$$\bar{\omega}_x^1 = \frac{2}{\gamma} \sum_{j=1}^{2m_1} (-1)^j \sin\gamma[\alpha_3 + (m_1 - j)\pi]. \tag{4.76}$$

After straightforward mathematical manipulation this equation becomes

$$\bar{\omega}_x^1 = \frac{2}{\gamma}\left([\sum_{j=1}^{m_1} (-1)^j \cos\gamma j\pi + \sum_{j=m_1+1}^{2m_1} (-1)^j \cos\gamma j\pi]\sin\gamma\alpha_3 - [\sum_{j=1}^{m_1} (-1)^j \sin\gamma j\pi + \sum_{j=m_1+1}^{2m_1} (-1)^j \sin\gamma j\pi \cos\gamma\alpha_3]\right). \tag{4.77}$$

If m_1 (m_2) is an even integer and m_2 (m_1) is odd then the first m_1 terms exactly cancel the second m_1 terms; a similar situation occurs in the coefficient of $\cos\gamma\alpha_3$. However, when m_1 and m_2 are both odd we find:

$$\sum_{j=1}^{m_1} (-1)^j \cos\gamma j\pi = 0\,, \qquad \sum_{j=m_1+1}^{2m_1} (-1)^j \cos\gamma j\pi = 0$$

$$\sum_{j=1}^{m_1} (-1)^j \sin\gamma j\pi = 0\,, \qquad \sum_{j=m_1+1}^{2m_1} (-1)^j \sin\gamma j\pi = 0$$

Hence, if $T = 2\pi m_1 = 2\pi m_2/\gamma$ then $\bar{\omega}_x' = 0$ irrespective of the value of α_3. By following a similar procedure we can readily show that $\bar{\omega}_y' = 0$. Therefore, Equations (4.61) through (4.64) are satisfied when $\alpha_1 = 0$, $\alpha_3 = \beta_o + \pi$, $T = 2\pi m_1$, for those values $\bar{L}_y$ given in Table 4.2 when

control is provided by Jet Configurations (B) and (C).

If the system is controlled by a single jet then the above procedure for selecting a "starting" control cannot be applied directly. This is due to the fact that the minimum time control has coast periods. If the final time is to be indeed a minimum then the control must terminate with a thrust period; this fact must be considered when choosing the pair $(\underline{\alpha}, T)$. Also, the final time associated with those values of $\bar{L}_Y$ given in Table 4.2 may no longer be independent of β_o as is the case when control is provided by Thruster Configurations (B) and (C).

When $\pi/2 < \beta_o < 3\pi/2$ the primary criterion for choosing a control is that of maximizing $\bar{L}_Y$ for a given T_D. Thus, $u_y^*(\sigma)$ must operate either in phase $(\bar{L}_Y(T) > 0)$ or π radians out of phase $(\bar{L}_Y(T) < 0)$ with $\cos(\sigma + \beta_o)$. In order to satisfy the requirement that the control terminates with a thrust period we can set $T_D^* = 2\pi m_1$. It is readily shown that the pair $(u_y^*(\sigma), T_D^*)$, which is now completely specified, satisfies Equations (4.61) and (4.64) for those values of $\bar{L}_Y$ given by Table 4.2. To complete the solution we must demonstrate that the transverse components of angular velocity are zero when $\sigma = T_D^*$. Substituting (4.68) and (4.69) into (4.61) and (4.62) gives:

$$\bar{\omega}_x^2 = \int_0^{2m_1\pi} u'[-\cos(\sigma + \beta_o)]\sin\gamma\sigma \, d\sigma \tag{4.78}$$

$$\bar{\omega}_y^2 = \int_0^{2m_1\pi} u'[-\cos(\sigma + \beta_o)]\cos\gamma\sigma \, d\sigma \tag{4.79}$$

In view of the definition of control set Ω_D the function $u'[\ ]$ is

$$u'[-\cos(\sigma+\beta_o)] = \begin{cases} +1 & ;[-\cos(\sigma+\beta_o)] > 0 \\ 0 & ;[-\cos(\sigma+\beta_o)] \leq 0 \end{cases}.$$

Thus, after straightforward mathematical manipulation (4.78) becomes

$$\bar{\omega}_x^2 = [\sum_{j=1}^{m_1}(-1)^j \cos \gamma\pi(\tfrac{1}{2}+j) + \cos m_2\pi \sum_{j=1}^{m_1}(-1)^{j+m_1}\cos \gamma\pi(\tfrac{1}{2}+j)]\cos \gamma \beta_o$$

$$+ [\sum_{j=1}^{m_1}(-1)^j \sin \gamma\pi(\tfrac{1}{2}+j) + \cos m_2\pi \sum_{j=1}^{m_1}(-1) \sin \gamma\pi(\tfrac{1}{2}+j)]\sin \gamma \beta_o. \tag{4.80}$$

If m_1 (m_2) is an even integer and m_2 (m_1) is odd then:

$$\sum_{j=1}^{m_1}(-1)^j \cos \gamma\pi(\tfrac{1}{2}+j) = -\cos m_2\pi \sum_{j=1}^{m_1}(-1)^{j+m_1}\cos \gamma\pi(\tfrac{1}{2}+j)$$

$$\sum_{j=1}^{m_1}(-1)^j \sin \gamma\pi(\tfrac{1}{2}+j) = -\cos m_2\pi \sum_{j=1}^{m_1}(-1)^{j+m_1}\sin \gamma\pi(\tfrac{1}{2}+j)$$

However, if both m_1 and m_2 are odd integers then:

$$\sum_{j=1}^{m_1}(-1)^j \cos \gamma\pi(\tfrac{1}{2}+j) = 0 \; ; \; \sum_{j=1}^{m_1}(-1)^{j+m_1}\cos \gamma\pi(\tfrac{1}{2}+j) = 0$$

$$\sum_{j=1}^{m_1}(-1)^j \sin \gamma\pi(\tfrac{1}{2}+j) = 0 \; ; \; \sum_{j=1}^{m_1}(-1)^{j+m_1}\sin \gamma\pi(\tfrac{1}{2}+j) = 0$$

Therefore, $\bar{\omega}_x^2 = 0$ irrespective of the value of β_o. By a similar procedure we can show that $\bar{\omega}_y^2 = 0$.

Now, let us consider the case when $3\pi/2 < \beta_o \leq 5\pi/2$. For values of β_o within this range the control will not terminate with a thrust period if, as in the previous cases, the initial co-state is selected so as to maximize $\bar{L}_Y$ for a specified final time-namely $T = 2\pi m_1$. That is, the choice for $\underline{\alpha}$ cannot be based on the assumption that $u_y^*(\sigma)$ must operate directly in phase ($\bar{L}_Y < 0$) or π radians out of phase ($\bar{L}_Y > 0$) with $\cos(\sigma + \beta_o)$. However, as will be shown presently the proper choice for the initial co-state is that $\underline{\alpha}$ which nearly maximizes $\bar{L}_Y$ for a

given T (i.e., $\alpha_1 \approx 0$, $\alpha_3 \approx \beta_o + \pi$).

First, let us consider possible choices for T_D. If $T_D < 2\pi m_1$ then (4.64) is not satisfied for those values of $\bar{L}_Y$ given in Table 4.1. Therefore $T_D > 2\pi m_1$. When $\alpha_1 = 0$ and $\alpha_3 = \beta_o + \pi$ the control will terminate with a thrust period if the normalized final time is defined by

$$T_D > 2\pi m_1 + \frac{\pi}{2} - \beta_o \ , \ 0 \leq \beta_o \leq \frac{\pi}{2} \tag{4.81}$$

$$T_D > 2\pi m_1 + \frac{5\pi}{2} - \beta_o, \ \frac{3\pi}{2} < \beta_o < 2\pi \tag{4.82}$$

If T_D is given by either (4.81) or (4.82) it is readily shown that (4.63) is not satisfied; in addition, $\bar{L}_Y$ will be larger than the desired value.

In previous work we showed that $\bar{\omega}_x(T) = \bar{\omega}_y(T) = 0$ when $\alpha_1 = 0$ $\alpha_3 = \pi + \beta_o$ and $T = 2\pi m_1$. Changing the normalized final time from this value to

$$T_D = 2\pi m_1 + \frac{\pi}{2} - \beta_o + \epsilon \ , \ 0 \leq \beta_o \leq \frac{\pi}{2} \tag{4.83}$$

$$T_D = 2\pi m_1 + \frac{5\pi}{2} - \beta_o + \epsilon \ , \ \frac{3\pi}{2} < \beta_o < 2\pi \tag{4.84}$$

where $\epsilon \ll 1$ introduces an additional coast period plus a thrust period of duration ϵ. Thus $\bar{\omega}_x(T)$ and $\bar{\omega}_y(T)$ will be very nearly zero. A detailed examination of (4.64) shows that if T_D is given by (4.83) or (4.84) and $\alpha_3 \gtrless \pi + \beta_o$, then the actual value of $\bar{L}_Y$ is less than the desired value. In addition, (4.63) is not satisfied. Actually, the difference between $(\bar{L}_Y)_{\text{actual}}$ and $(\bar{L}_Y)_{\text{required}}$ increases as α_3 is made less than or greater than $\beta_o + \pi$; in order to reduce this error T_D must

be made larger than that specified by (4.83) or (4.84). Therefore, there can be but one conclusion - $\alpha_1 \neq 0$. In view of the previous discussion the following appear to be reasonable starting values for the iterative procedure: $\alpha_1 = 0(\epsilon)$, $\alpha_3 \approx \pi + \beta^o$, T_D given by Equation (4.83) or (4.84). Note that the normalized final time is no longer independent of β_o as was the case when $\pi/2 < \beta_o \leq 3\pi/2$.

4.6 Simulation Results for Control System B

The flooding procedure outlined in Section 4.5.1, which utilizes the iterative method described in Appendix A, was programmed for a Burroughs B5500 digital computer. Optimal controls were then computed for a number of different vehicle configurations and boundary conditions. The objective was to provide sufficient quantitative results to allow a discussion of the characteristics of the optimal controls in view of those questions posed in Section 4.5.1. In the present section, as well as in those that follow, results of this numerical approach are summarized and a number of comments concerning the structure of the optimal controls are presented.

Optimal controls defined quantitatively by $(\underline{\alpha}, T_B^*)$, corresponding to boundary conditions defined by (3-10), are summarized in Figures 4.6 through 4.16. For discussion purposes, and in view of the goals outlined in 4.5.1, it is convenient to separate these results into three parts. First, from Figures 4.6 through 4.13 we can make certain observations as to the characteristics of the optimal control in terms of the vehicles shape and mass, its spin rate, the control magnitude, and the maneuvering angle θ_f when $\bar{\omega}_x^o = \bar{\omega}_y^o = 0$. Second, to demonstrate

the influence of β_o on T_B^* optimal controls have been computed in terms of the pair $(\beta_o, \bar{L}_Y)$. These solutions allow us to make certain conjectures as to the geometry of the minimum time isochrones when: (1) $\gamma = C$, and (2) $\bar{\omega}_x^o = \bar{\omega}_y^o = 0$. Finally, Figures 4.14 through 4.16 show the influence of an initial non-zero transverse component of angular velocity on the optimal control.

4.6.1 Characteristics of the Optimal Control in Terms of the Vehicle's Moments of Inertia and Normalized Angular Momentum

The pair $(\underline{\alpha}, T_B^*)$ is plotted in terms of $(\gamma, \bar{L}_Y)$ for $\bar{\omega}_x^o = \bar{\omega}_y^o = 0$, $\beta_o = 0$, in Figures 4.6 through 4.13. From these solutions we find that the optimal controls for Jet Configurations (A) and (B) have certain distinguishing traits in common. First, the local maximum of α_1 decreases as $\bar{L}_Y$ increases; therefore, in the limit, when $\bar{L}_Y \to \infty$ both $u_x^*(\sigma)$ and $u_y^*(\sigma)$ operate either directly in phase $(\bar{L}_Y < 0)$ or π radians out of phase $(\bar{L}_Y > 0)$ with $\sin(\sigma + \beta_o)$ and $\cos(\sigma + \beta_o)$ respectively in (4.14). In this case the dimensionless final time is given by

$$T_B^* = \frac{\pi}{4} |\bar{L}_Y| . \qquad (4.85)$$

For specific values of $\bar{L}_Y$, as shown in Figures 4.6 and 4.10, α_1 is identically zero; hence, the control operates either directly in phase or π radians out of phase with $\sin(\sigma + \beta_o)$ and $\cos(\sigma + \beta_o)$. Such points represent the most efficient mode of operation since they correspond to local minima of the dimensionless final time curves with respect to the limiting linear relation given by (4.85).

For small values of $\bar{L}_Y$ $(M \gg I_z \omega_s^2 \theta_f)$ the dimensionless final time and switch times are given by (4.39) through (4.50). Note that one

component of $\underline{u}^*(\sigma)$, depending upon the relation between β_o and β_o', operates in a "race-brake" mode. In this respect the control is quite similar to that for the gimballed jet. It is of interest to compare the time required (in seconds) for the 4-jet controller to that for the gimballed jet to reorient a given spacecraft through a specified angle when $T_B^* \ll 1$ ($T_A^* \ll 1$). From (3.56), (4.42), and (4.50) we find:

$$(t_f^*)_A = 2\sqrt{\frac{I\,\theta_f\,g}{a\,\dot{w}\,I_{sp}}} \qquad \text{(Gimballed Jet)} \qquad (4.86)$$

$$\left.\begin{aligned} (t_f^*)_B &= 2\sqrt{\frac{2I\theta_f \cos\beta_o}{a\,\dot{w}\,I_{sp}}}\,,\ 0 \le \beta_o < \beta_o' \qquad (4.87)\\ (t_f^*)_B &= 2\sqrt{\frac{2I\theta_f \sin\beta_o}{a\,\dot{w}\,I_{sp}}}\,,\ \beta_o' < \beta_o < \frac{\pi}{2} \qquad (4.88)\end{aligned}\right\} \text{(4-Jets)}$$

where $\dot{w}$ is the maximum total rate of propellant flow to the control jet(s). Thus, when a comparison is based on a given $\dot{w}$, and when both $\tilde{L}_Y$ and $\bar{L}_Y$ are "small" we find that the 4-jet configuration requires at most $\sqrt{2}(t_f^*)_A$ seconds to reorient a spinning vehicle.

Consider now the behavior of T_B^* in terms of the pair $(\gamma, \bar{L}_Y)$ for values of $\bar{L}_Y$ excluded by the "short time" solutions. Figure 4.6 shows that when $\gamma > 0$ and $\bar{L}_Y < 10$ increasing γ(decreasing I_z/I) always reflects in an increase in T_B^* for a given $\bar{L}_Y$. Note the sizeable reduction in T_B^* when γ is reduced from 0.8 to 0.6 compared to changes in T_B^* corresponding to similar reductions in γ when $\gamma < 0.6$. Also note that for $\gamma = 0.01$, 0.2, and 0.4 the dimesnsionless final time is nearly that given by (4.85) which is represented by the dashed line.

In contrast, when $\gamma < 0$ the minimum time curves, in general, lie very close to the straight line defined by (4.85). A noteable deviation occurs when $\bar{L}_Y \lesssim 4$; however, the dispersion is not as great as when $\gamma > 0$. This behavior can be attributed to changes in the vehicle's mass distribution as γ increases from -0.8 to + 0.8. Such changes tend to reduce the sensitivity of the system to control inputs. This fact is clearly illustrated in Figures 4.17, 4.18, 4.21, and 4.22 where optimal trajectories are plotted in terms of γ for fixed values of $\bar{L}_Y$ within the range of interest (i.e., $\bar{L}_Y \lesssim 10$). Note that the motion of the spin axis tends to assume the characteristics of that of a non-spinning body as $\gamma \to 1$. That is, the ratio of $\bar{L}_X(\sigma)$ to $\bar{L}_Y(\sigma)$ decreases as γ increases. This is due to the fact that the nutation rate is proportional to I_z/I.[4] In this respect the "short time" solution resembles that for the single axis control of a non-spinning body. Thus a decrease in the nutation rate coupled with an increase in the transverse moment of inertia results in an increase in T_B^*. However, as indicated by the progressively larger values of T_B^* as γ changes from 0.4 to 0.8 for a given $\bar{L}_Y$, the dimensionless final time is not directly proportional to γ. This can be attributed to the rapid change in the vehicle's mass distribution as $\gamma \to 1$. That is, for a given change in γ the transverse moment of inertia must increase according to the following relation

$$\Delta I = \frac{I_z \Delta\gamma}{(1-\gamma-\Delta\gamma)(1-\gamma)} \tag{4.89}$$

[4] Results of the "short time" analysis, Equations (4.42) and (4.[illegible]), show that I is the only system parameter which influences T_B^*).

when I_z remains constant. In contrast, the geometry of a symmetrical body approaches that of an infinitely thin disk as $\gamma \to -1$.

Figures 4.10 through 4.13 show that when $\bar{L}_Y > 10$ the minimum time control is one which nearly maximizes the change in angular momentum $I_z \omega_s \theta_f$ over a given interval of time. That is, $u_x^*(\sigma)$ and $u_y^*(\sigma)$ operate nearly π radians out of phase with $\sin(\sigma + \beta_o)$ and $\cos(\sigma + \beta_o)$ respectively. This behavior is also observed in the optimal control when $\gamma > 0$. However, comparing Figures 4.6 and 4.10 we find that, in general, $|\alpha_1|_{\gamma<0} < |\alpha_1|_{\gamma>0}$ and, in addition, that $\alpha_1|_{\gamma<0}$ damps out more rapidly than $\alpha_1|_{\gamma>0}$. Therefore, the minimum time curves shown in Figure 4.13 approach the linear relation given by (4.87) for smaller values of $\bar{L}_Y$ then when $\gamma > 0$, Figure 4.9. This is further illustrated by Figures 4.22 through 4.24 where optimal trajectories of the spin axis are plotted for specific values of the parameters $(\gamma, \bar{L}_Y)$. Note that when α_1 is "small" (i.e., $|\alpha_1| < 0.2$) the optimal trajectories are characterized by a sequence of "half loops"; in view of the trajectories shown in Figures 3.13, 3.15, and 3.17 this response is similar to that of System (A) when the optimal steering law is a steadily applied moment about the y' axis.

4.6.2 Influence of Initial Thruster Position on the Optimal Control

In section 4.2 it was shown that the optimal control possesses certain symmetry properties when $\bar{\omega}_x^o = \bar{\omega}_y^o = 0$. Specifically, it was noted that if the control which satisfies (4.11) through (4.14) is known for $0 \le \beta_o < \pi/2$ then it is also known for $\pi/2 \le \beta_o < 2\pi$. In addition, when the control is expressed in terms of both β_o and $\bar{L}_Y$ we

are able to transform boundary conditions where $L_X(T) \neq 0$ to the form of (4.10) by a prerotation of Coordinate System II through the angle $\bar{\varepsilon}_o$. Therefore, once controls have been computed in terms of the pair $(\beta_o, \bar{L}_Y)$, $0 \leq \beta_o < \pi/2$, then it is possible to plot minimum time isochrones in the $(\bar{L}_X - \bar{L}_Y)$ plane.

Through successive applications of the iterative technique described in Appendix A optimal controls corresponding to specific values of the pair $(\beta_o, \bar{L}_Y)$ have been determined for $\gamma = -0.2$ and $\gamma = 0.6$. Results of this numerical computation indicate that for engineering purposes T_B^* is independent of β_o when $\bar{L}_Y \geq 1.0$. Upon further investigation of the problem it was noted that the value of $\bar{L}_Y$ at which β_o begins to influence T_B^* depends upon γ. From the numerical results for $\gamma = -0.2, 0.6$ and in view of Figures 4.6 and 4.13 it appears reasonable to make the following conjecture as to the relation between T_B^* and the pair (γ, β_o). In general, T_B^* remains sensitive to changes in β_o for increasingly larger values of $\bar{L}_Y$ as $\gamma \to 1$. Hence, the greater the deviation between the actual value of T_B^* and the limiting linear relation (Figures 4.6 and 4.13) the more sensitive T_B^* becomes to changes in β_o. Since the minimum time isochrones for $\gamma = -0.2, 0.6$ when $\bar{L}_Y > 1.0$ are nearly circular, we find that the time required to reach a terminal state point in the $(\bar{L}_X - \bar{L}_Y)$ plane is very close to that given by Figures 4.6 and 4.13; therefore, the numerical results for $\beta_o \neq 0$ are not presented.[5]

---

[5]Note that the minimum time isochrones for Controller (A) are circles for all values of $\bar{L}_Y$.

4.6.3. Influence of an Initial Non-Zero Transverse Component of Angular Velocity on the Optimal Control

In this section we consider the optimal control problem when the total angular momentum vector is not aligned with the spin axis at $\sigma = 0$. As for the cases considered in previous sections, the iterative procedure was employed to compute optimal trajectories between certain pairs of initial and final state points which are of engineering interest. From these quantitative results we are then able to conjecture as to the general nature of the optimal control.

The initial and final states considered are typified by those shown in Figure 4.5. Hence, we consider situations where the change in total angular momentum is zero, Case 1; and where the angular momentum addition $\Delta\bar{\underline{L}}$ results in the total angular momentum vector being aligned with the spin axis at $\sigma = T^*$, Case 2.

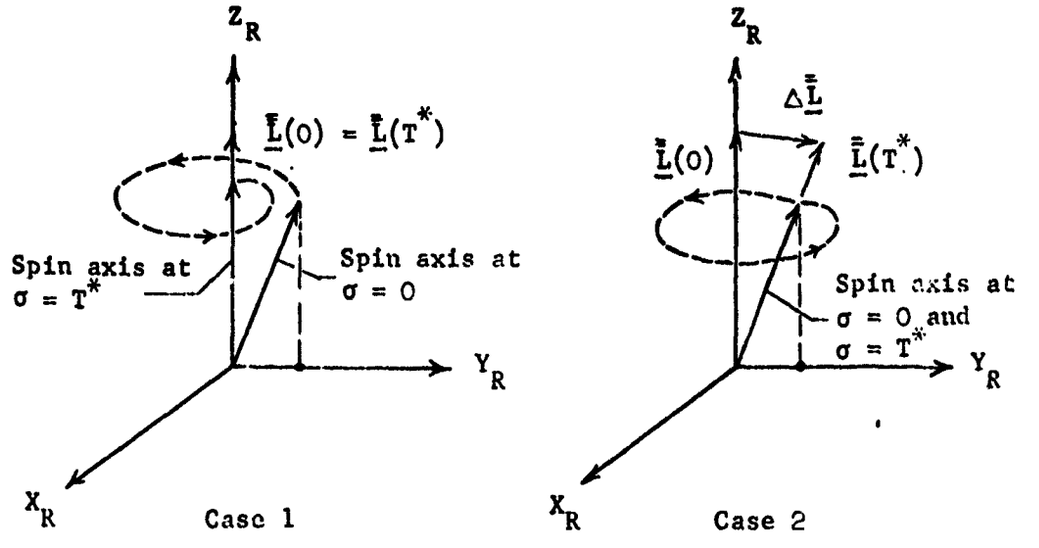

Figure 4.5. Typical Initial and Final Spin Axis Positions when $\omega_y^o \neq 0$

Case 1

A quantitative description of the optimal control, which satisfies boundary conditions of the form defined by Case 1, is presented in Figures 4.14 and 4.15. These results, though not as complete as in previous sections, are sufficient to give some indication as to the characteristics of the optimal control in terms of both the system parameters and the boundary conditions.

The essential features of optimal steering for two different vehicle configurations, $\gamma = \pm 0.8$, are shown in Figure 4.14. Note that in all cases when $\bar{\underline{\omega}}(0) \neq 0$, $\underline{P}(\sigma)$ has been normalized with respect to α_1. Thus α_4 determines the relative weighting between the high and low frequency terms in Equations (4.26) and (4.27).

At this point it is interesting to compare the characteristics of the optimal controls when $\bar{\underline{\omega}}(0) \neq 0$ and when $\bar{\underline{\omega}}(0) = 0$. In the latter case we found that when $\bar{\underline{L}}_Y \to \infty$ the higher frequency terms of the switching functions become dominant. In contrast, when $\bar{\omega}_y^o \to \infty$, $\Delta\bar{\underline{L}} = 0$, the lower frequency terms dominate; therefore, the optimal control depends only on the transverse component of angular velocity. That is, in the limit, $u_x^*(\sigma) = \text{sgn}[-\omega_x(\sigma)]$ and $u_y^*(\sigma) = \text{sgn}[-\omega_y(\sigma)]$. Hence the attitude control problem can be described by a two dimensional plant involving $\omega_x(\sigma)$ and $\omega_y(\sigma)$. Optimal controls for such a two dimensional model are well known and have been found in terms of the system's state by Athans, et al. [1]. If the admissible control set is a circle, as in Controller Configuration (A), then in the limit optimal steering is given by:

$$u_x^*(t) = \frac{-\omega_x'(t)}{\|\underline{\omega}(t)\|} \quad , \quad u_y^*(t) = \frac{-\omega_y'(t)}{\|\underline{\omega}(t)\|} \qquad (4.2?)$$

Let us now examine the characteristics of $\underline{u}^*(\sigma)$ in terms of γ. Figure 4.14 shows that the rate at which α_4 damps out depends directly on the vehicle's shape and mass. The reason for this behavior becomes evident if one considers the unforced motion of the system when $\bar{\omega}_y^o \neq 0$. From the theory we find that the rate at which $\underline{\omega}$ precesses about the Z_R axis is directly proportional to I_z/I. Hence, when I_z/I is "large" and if the controls switch sign at the nutation frequency then

$$\frac{1}{T_B}\int_0^{T_B} u_{x'}(\sigma)d\sigma \approx 0 \ , \ \frac{1}{T_B}\int_0^{T_B} u_{y'}(\sigma)d\sigma \approx 0 \qquad (4.91)$$

which is required if $\Delta\bar{\underline{L}} \approx 0$. However, if I_z/I is "small" and T_B is not "large" then the average control will not be small and $\Delta\bar{\underline{L}} \neq 0$. Thus the higher frequency terms in (4.26) and (4.27) cannot be neglected.

Case 2

Under certain conditions it may be desirable to drive the spin axis to a position in the $(Y_R - Z_R)$ plane other than that defined by $\theta_f = 0$. To qualitatively define the optimal control corresponding to boundary conditions of this type the iterative procedure was employed to determine optimal controls for certain initial and final states typified by Case 2. Results for two different vehicle configurations ($\gamma = \pm 0.8$) are presented in Figure (4.16). Also, the dimensionless final time T_B^* required for controlling spacecraft defined by $\gamma = 0.2$, -0.4, when the initial and final states are of the form given by Cases 1 and 2 is shown in Figure 4.15.

When the change in state is defined by Case 2 it is of interest to note that the two terms in Equations (4.26) and (4.27) are weighed

nearly the same (i.e., $\alpha_4 \approx 1$) for those values of $\bar{\omega}_y^o$ shown in Figure 4.16 (this is undoubtedly true for values of $|\bar{\omega}_y^o| \gtrsim 40$. Extending these results allows one to at least qualitatively define the behavior of α_3 and α_4 in terms of $\bar{\underline{\omega}}(0)$ and $\bar{L}_Y$.

Typical optimal trajectories in the $(\bar{L}_X - \bar{L}_Y)$ and $(\bar{\omega}_x - \bar{\omega}_y)$ planes are plotted for both Cases 1 and 2, $\gamma = 0.2, -0.4$, in Figures 4.25 through 4.29.

4.7 Simulation Results for Control System C

In the previous section we discussed the salient characteristics of the optimal control for the 4-jet configuration in terms of the parameters $\bar{\omega}_y^o$, $\bar{\omega}_x^o$, $\bar{L}_Y$, γ, and β_o. Noting that the two and four jet control systems are similar (i.e., the jets are rigidly attached to and spin with the vehicle; in addition, Ω_B and Ω_C are symmetrical with respect to the u_x and/or u_y axis) and in view of the numerical results presented in Figures 4.6 through 4.13 and 4.30 through 4.33 it is evident that the control laws have certain characterisitcs in common. Therefore, in this section the influence of the governing parameters on the optimal control is not discussed in detail; instead, a comparison is made of the "degree of control" provided by the two control systems.

4.7.1 Characteristics of the Optimal Control in Terms of the Vehicle's Moments of Inertia and Normalized Angular Momentum

A comparison of the dimensionless final time curves in Figures 4.9, 4.13, and 4.33 shows certain similarities (and differences) in the performance of the 4 and 2-jet controllers. First, the minimum time required for spin axis reorientation is nearly the same when both $(\bar{L}_Y)_B$

and $(\bar{L}_Y)_C$ are large - independent of the value of γ. Results of the numerical solutions, as summarized in Figure 4.33, indicate that a good approximation for the dimensionless final time T_C^* is given by

$$T_C^* \approx \frac{\pi}{4} \bar{L}_Y \tag{4.92}$$

when $\bar{L}_Y \geq 40$. Hence,

$$(t_f^*)_C \approx \frac{\pi I_z \omega_s \theta_f}{2aw I_{sp}} \tag{4.93}$$

and in the limit when $\bar{L}_Y \to \infty$

$$(t_f^*)_C = \frac{\pi I_z \omega_s \theta_f}{2aw I_{sp}} . \tag{4.94}$$

For values of $\bar{L}_Y \leq 40$ the performance capabilities of the two systems begin to differ; moreover, the relative loss in performance by the 2-jet system becomes very evident when $\bar{L}_Y$ is small. In this region T_C^* is influenced to a greater degree by the vehicle's moments of inertia than is T_B^*. Also, the characteristics of the "short time" solution differ remarkably when the number of control jets is reduced from four to two.

Comparing Figures 4.9 and 4.33 we find that, in general, the performance of the two systems are similar from $\gamma > 0$ and $(\bar{L}_Y)_B \geq 2$, $(\bar{L}_Y)_C \gtrsim 1$. The fact that the terminal time is relatively independent of the controller configuration when $\gamma > 0$ can be attributed to two factors. First, we know that a "pencil shaped" vehicle responds relatively "slowly" to control inputs when compared to configurations where $\gamma < 0$. The influence of coupling between ω_x and ω_y on the system response can be observed if one applies, for example, a unit step func-

tion; when $\gamma < 0$ the spin axis undergoes rapid excursions as the result of this input. Therefore, when $\gamma > 0$ there is sufficient time to apply both positive and negative control torques about the x' and y' axis before the spin axis has precessed to an unfavorable position.

The second contributing factor is undoubtedly the control magnitude; that is, $M_C = 2M_B$. Thus, it appears that the increase in control magnitude nearly compensates for the loss of two jets when $(\bar{L}_Y)_C \gtrsim 1$ and $\gamma > 0$. In contrast, from both the numerical solution and the results of the "short time" analysis of Section 4.4.2 we find that the "degree of control" provided by each system begins to differ when $(\bar{L}_Y)_C \lesssim 15$, $\gamma < 0$. In the "short time" case the relative loss in performance is attributed to the geometry of control set Ω_C. Restricting the control set to the real line [-1, 1] prevents the simultaneous and proper application of both a "race-brake" moment and a moment which produces the required change in angular momentum $\underline{I_z \omega_s \theta_f}$.

As mentioned previously, the greastest difference in performance of the two systems occurs when $\gamma < 0$. A comparison of Figures 4.9 and 4.33 shows that for a fixed value of $\bar{L}_Y$ there is an increase in T_C^* as $\gamma \to -1$. In contrast, the minimum time curves for the 4-jet controller be very close to limiting curve, defined by (4.87), when $-1 < \gamma < 0$. Thus, unlike the case when $\gamma > 0$, control set geometry (Ω_B vs Ω_C) becomes important when the nutation rate is larger than the spin rate.

A comparison of the minimum time trajectories when control is provided by both 4-jets and 2-jets shows the similarity in response when $\gamma > 0$; Figures 4.17 through 4.19, 4.35 through 4.37 and the difference when $\gamma < 0$; Figures 4.21 through 4.24, 4.38 through 4.40. Note

the excessive excursions of the spin axis in Figures 4.38 and 4.39 compared to the optimal motion in Figures 4.22 and 4.23. In the latter cases the 2-jet system does not provide the "fineness" or "degree" of control to prevent the spin axis from "looping" and thus traveling in a direction opposite to that desired.

4.7.2 Influence of Initial Thruster Position on the Optimal Control

Through a procedure similar to that described in Section 4.6.2 minimum time controls have been computed in terms of the pair $(\beta_o, \bar{L}_Y)$. Results for $\gamma = -0.2$ are summarized in Figure 4.34. Due to the increased computation time (for the 2-jet system optimal controls must be computed for $0 \leq \beta_o < \pi$) only the disk shaped vehicle, $\gamma = -0.2$, was considered.

Although optimal controls have been computed for only a single value of γ we can, nevertheless, based upon the results obtained to this point, deduce the behavior of T_B^* in terms of $\bar{L}_Y$, γ, and β_o. Let us begin by reconsidering the results of Section 4.6.2. Here, we determined that the "degree of control" provided by the 4-jet system is such that the minimum time isochrones are nearly circular except when $\bar{L}_Y \lesssim 1$ ($\gamma \lesssim 0.6$). In contrast, Figure 4.34 shows that the loss of two jets has significant influence on the sensitivity of T_C^* to change in β_o when $\bar{L}_Y \leq 10$. In fact, results of the numerical solutions show that the minimum time isochrones do not become circular until $\bar{L}_Y \gtrsim 30$ for $\gamma = -0.2$. After examining Figure 4.33 we find that, in general, the difference between the actual value of T_C^* and that predicted by (4.99) increases as $|\gamma|$ increases. Therefore based on the behavior of T_C^* in

in terms of γ we would expect T_C^* to be sensitive to changes in β_o when $\bar{L}_Y > 30$ for $|\gamma| > 0.2$.

4.8 Simulation Results for Control System D

From a construction standpoint the single jet design is appealing because of its simplicity and minimum hardware requirements. Hence, this controller would be useful in situations where the weight or space which is allocated to a control system must be minimized. Also, it may be desirable to apply the optimal control law for a single jet in the event of a failure of one or more of the jets in Control Systems (B) or (C).

Optimal steering for the single jet was developed in Section 4.3 and is given qualitatively by Equation (4.22). As in previous cases exact optimal controls (i.e., the pairs $(\underline{\alpha}, T_D^*)$) corresponding to selected sets of values of the dimensionless parameters $\bar{\underline{\omega}}(0)$, $\bar{L}_Y$, γ, and β_o were determined by solving a number of two point boundary value problems. From the results of this flooding process, which are presented in Figures 4.41 through 4.53, we find that optimal steering for the single jet bears little resemblance to that for the gimballed, four, or two-jet controllers. This is due to the fact that control set Ω_D is not symmetric with respect to the origin of the $(u_x - u_y)$ reference system. Actually, certain dissimilarities were observed when the switching functions were derived in Section 4.3. The necessary condition for optimality requires that the optimal control contain coast periods, and in this respect the minimum time system resembles a minimum fuel system. An additional characteristic which is peculiar to

the single jet is observed in Figures 4.44 and 4.45. Here we note that the dimensionless final time is not a continuous function of $\bar{L}_Y$. This means that the maximum recoverable (reachable) sets do not expand continuously in all directions with increasing time.

For the purpose of the following discussion it is convenient to consider the optimal control in terms of $\bar{L}_Y$. First, we find that the dimensionless final time (Figures 4.44 and 4.45) does not approach zero in a continuous fashion as $\bar{L}_Y \to 0$. This is in direct contrast to the behavior of T^* in Control Systems (A) through (C). The lower limit of $\bar{L}_Y$ (i.e., $\bar{L}_Y = 0$) will occur, for example, when the control magnitude becomes unbounded (i.e., $M \to \infty$). Thus Ω_D expands in the positive direction and in the limit becomes the real line $[0, \infty)$. However, unlike Ω_A, Ω_B, and Ω_C which expand symmetrically, Ω_D remains unsymmetrical; and for this reason the system is not completely controllable over an arbitrarily small interval of time. Note that the lower limit of T_D^*, that is, the smallest subinterval of $[0, T_D]$ over which the system is completely controllable, depends upon both γ and β_o.

Under certain conditions the influence of γ on the system's response is quite different from that in Cases (A) through (C). Figures 4.44 and 4.45 show that the time required by the single jet to effect a given change in the state of the system increases as $\gamma \to 0$ for "small" values of $\bar{L}_Y$. This is in direct contrast to the behavior of the optimal control for Systems (A) through (C) where T^* decreases when $\gamma \to 0$. Such behavior can be attributed to the degree of coupling which exists between $\bar{\omega}_x$ and $\bar{\omega}_y$. This coupling becomes weaker as $\gamma \to 0$ and is non-existent when $\gamma = 0$ (the system is not controllable when $\gamma = 0$).

Since a single jet can provide only positive (negative) control moments there must be coast periods of sufficient duration to allow $\bar{\omega}_y$ to become negative at least once during the interval $(0, T_D^*)$; this is necessary since control must terminate with a thrust period which causes $\bar{\omega}_y$ to increase. In the absence of control $\bar{\omega}_y$ oscillates with frequency $\gamma\omega_s$; therefore, the time required for $\bar{\omega}_y$ to change from $+\bar{\omega}_y^o$ to $-\bar{\omega}_y^o$ is proportional to π/γ. Thus the coast periods must increase in length as $\gamma \to 0$. This requirement is reflected in the switching function, Equation (4.22), since the low frequency term dominates when both $\bar{L}_Y$ and γ are small (i.e., $|\alpha_1| > 1$, see Figure 4.41).

To illustrate the behavior of the controlled system when $\bar{L}_Y$ is small and, in addition, to attempt to justify the limiting value of T_D^*, as given in Figures 4.44 and 4.45, optimal trajectories of the spin axis are plotted in the $(\bar{L}_X - \bar{L}_Y)$ plane (see Figures 4.46 through 4.49). Note that in all cases represented there are no initial coast periods; that is, the jet is turned on at $\sigma = 0$ even though the spin axis is initially driven away from the desired terminal position. These figures also clearly illustrate both the forced response and the force free motion of a spinning body - a norm invariant system. Note the rapid excursions of the spin axis in Figure 4.49 compared to the system response illustrated in Figure 4.46 (the final times are the same in both cases). In Figures 4.50 through 4.53 we have attempted to demonstrate the characteristics of minimum time trajectories for vehicle configurations of practical interest to the engineer (e.g., $\gamma = 0.03$, $\gamma = +0.2$). Values of $\bar{L}_Y$ used in the computation of the corresponding controls were selected to be similar to those in previous sections.

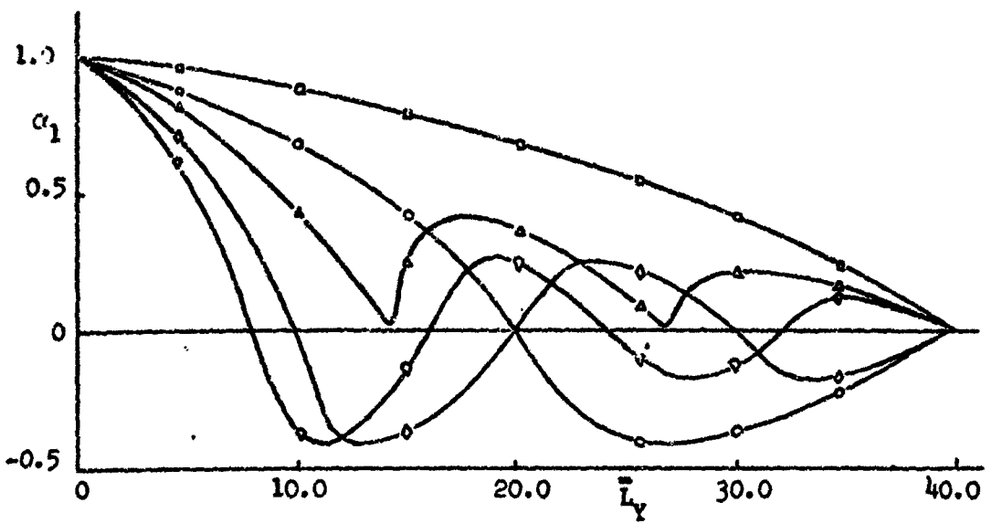

Figure 4.6 Solution for α_1 in terms of $\bar{L}_Y$, $\beta_0=0$, $\gamma>0$, 4-jets

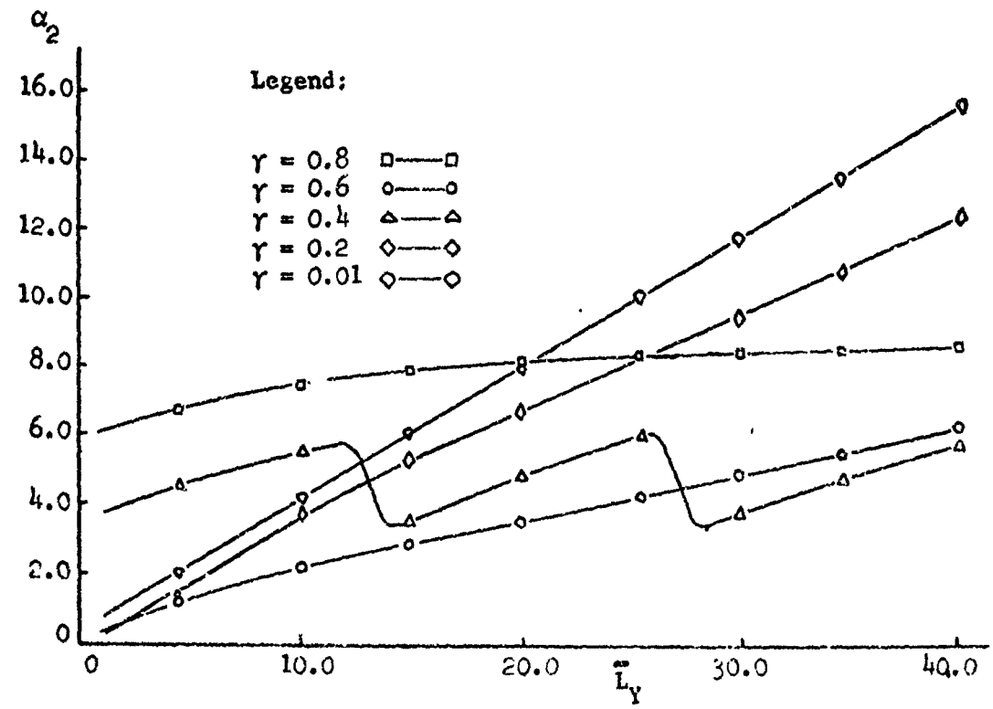

Figure 4.7 Solution for α_2 in terms of $\bar{L}_Y$, $\beta_0=0$, $\gamma>0$, 4-jets

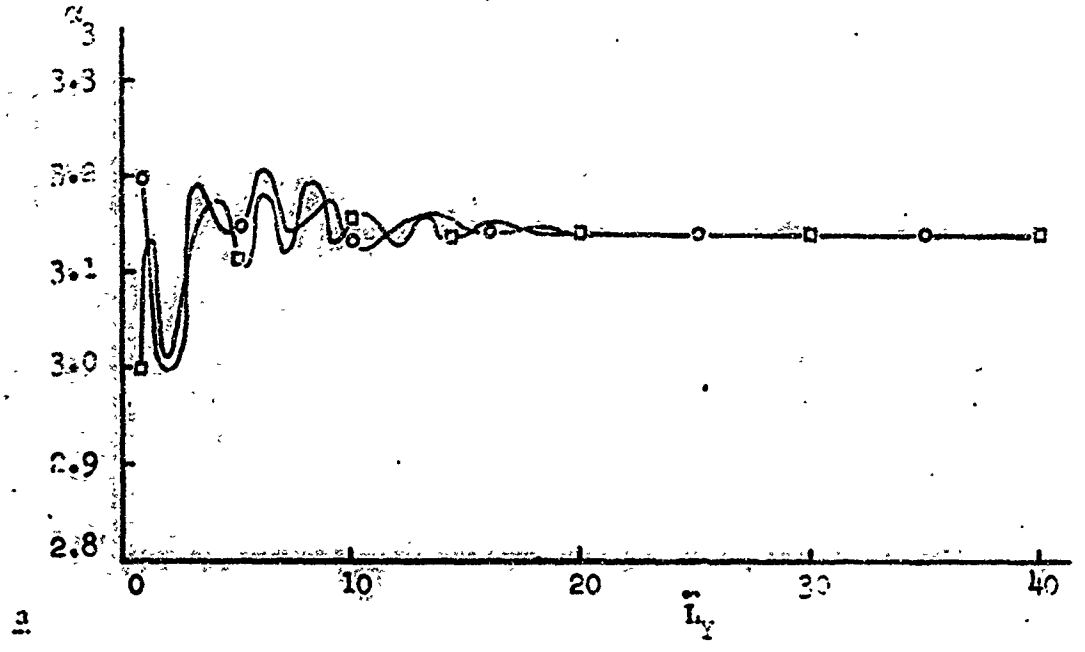

a

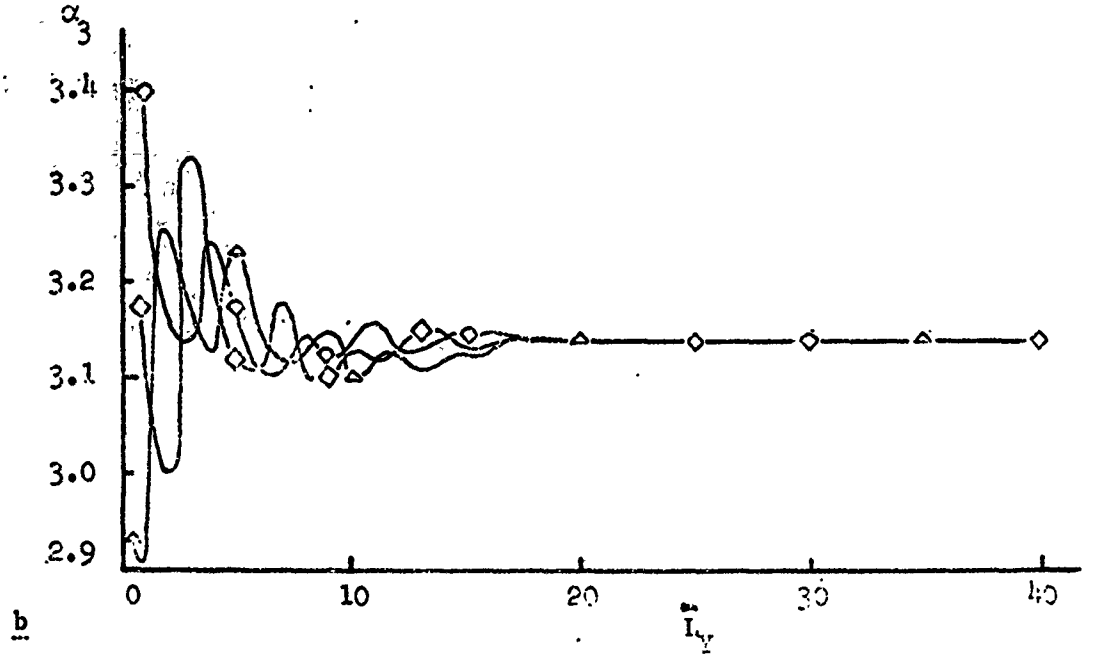

b

Figure 4.8 Solution for α_3 in terms of $\bar{I}_Y$, $\beta_o = 0$, $\gamma > 0$, 4-jets

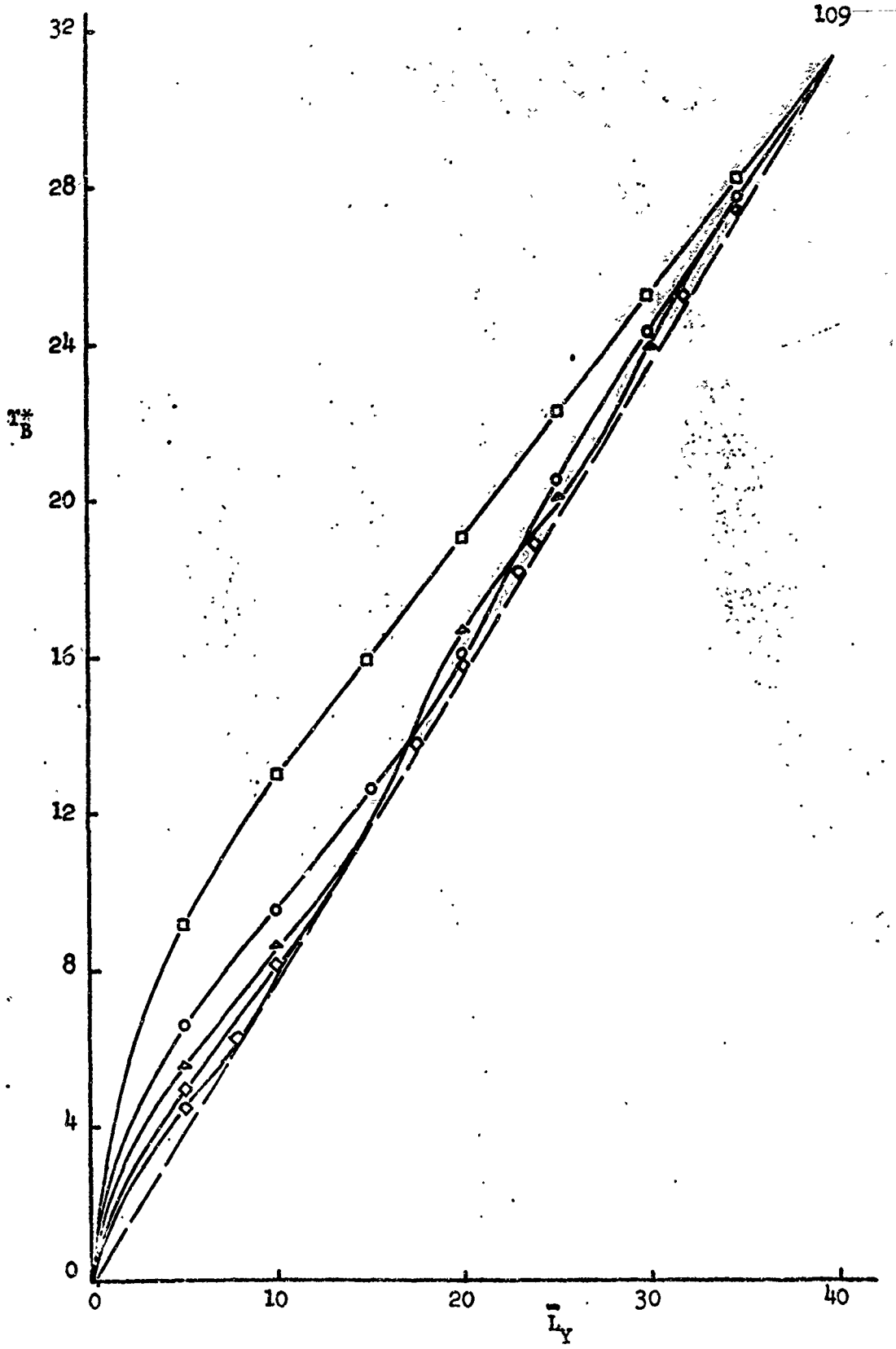

Figure 4.9 Solution for T_B^* in terms of $\bar{L}_Y$, $\beta_o = 0$, $\gamma > 0$, 4-jets

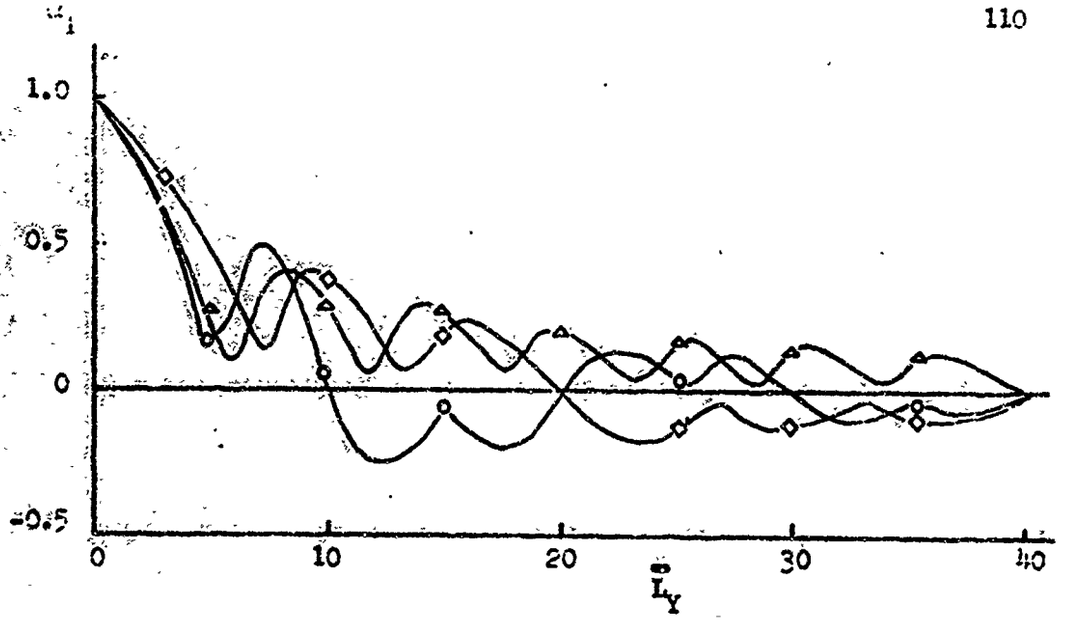

Figure 4.10 Solution for α_1 in terms of $\bar{L}_Y$, $\beta_0=0$, $\gamma<0$, 4-jets

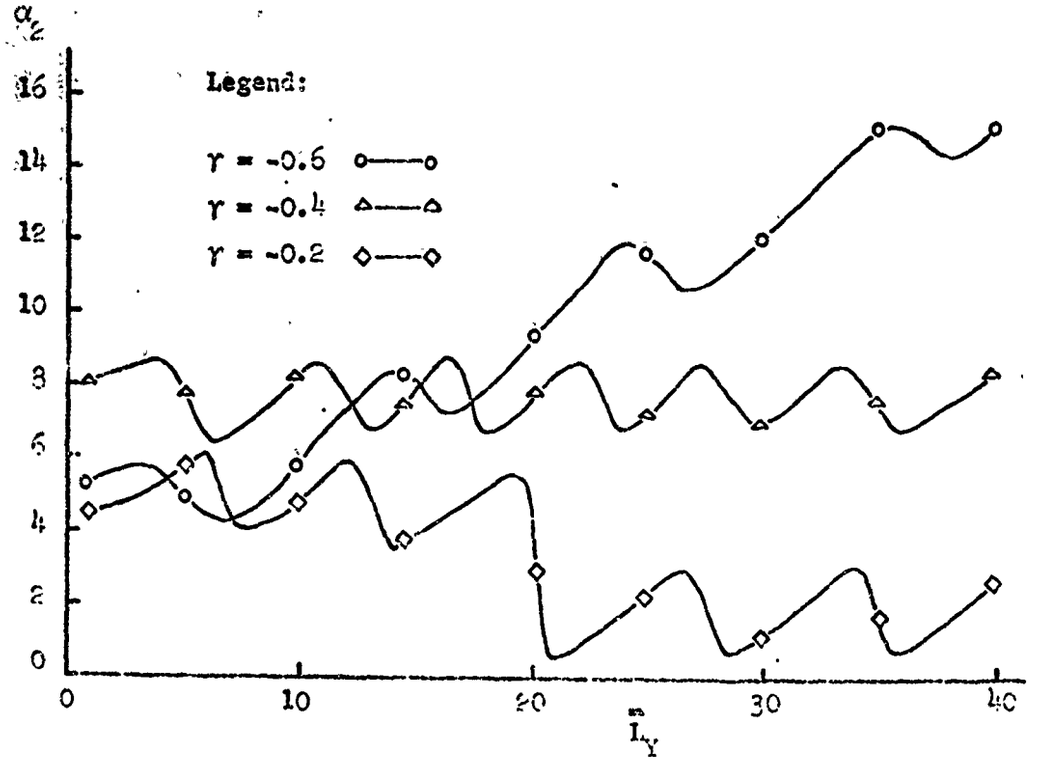

Figure 4.11 Solution for α_2 in terms of $\bar{L}_Y$, $\beta_0=0$, $\gamma<0$, 4-jets

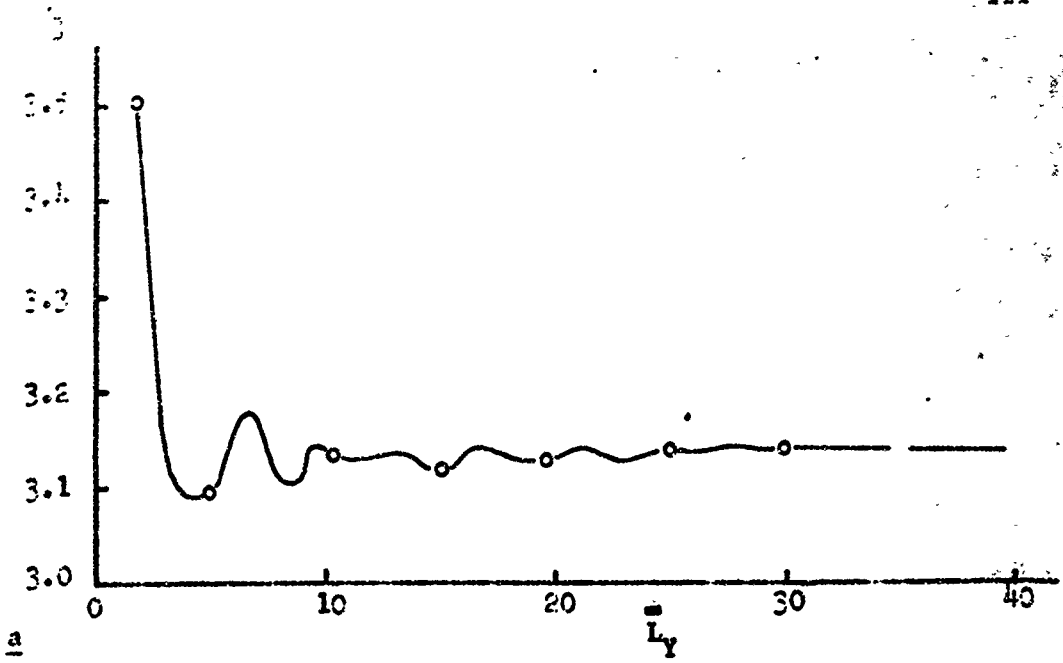

a

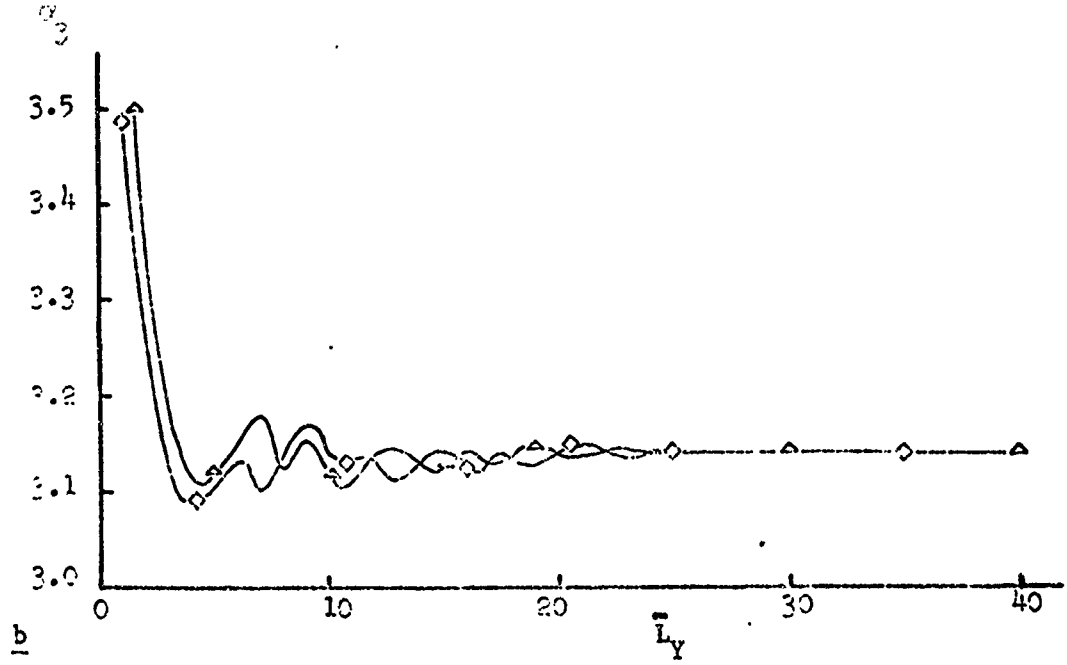

b

Figure 4.12 Solution for α_3 in terms of $\bar{L}_Y$, $\beta_c = 0$, $\gamma < 0$, 4-jets

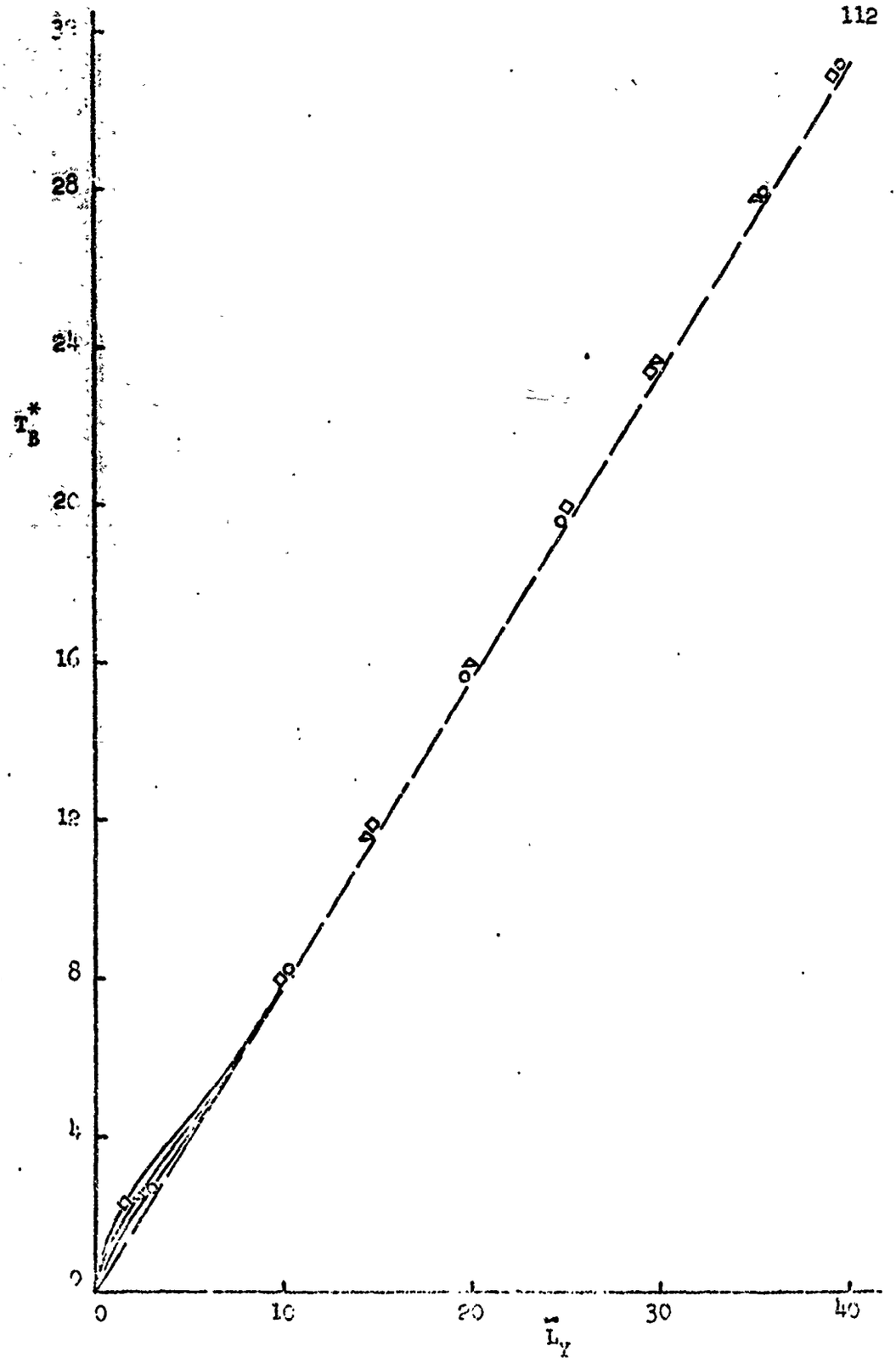

Figure 4.13 Solution for T_B^* in terms of $\bar{L}_y$, $\beta_c=0$, $\gamma<0$, L_{inj}

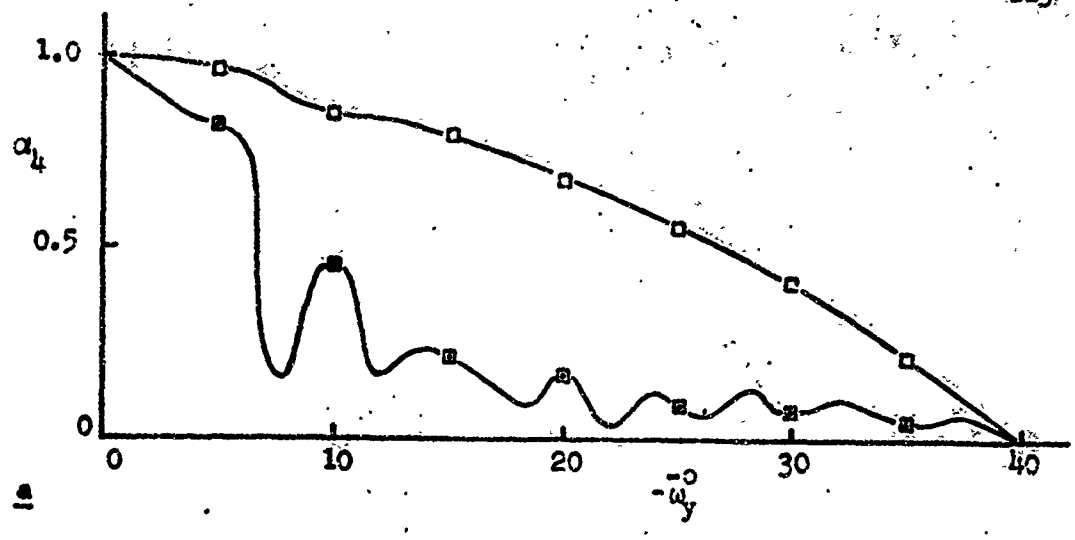

a

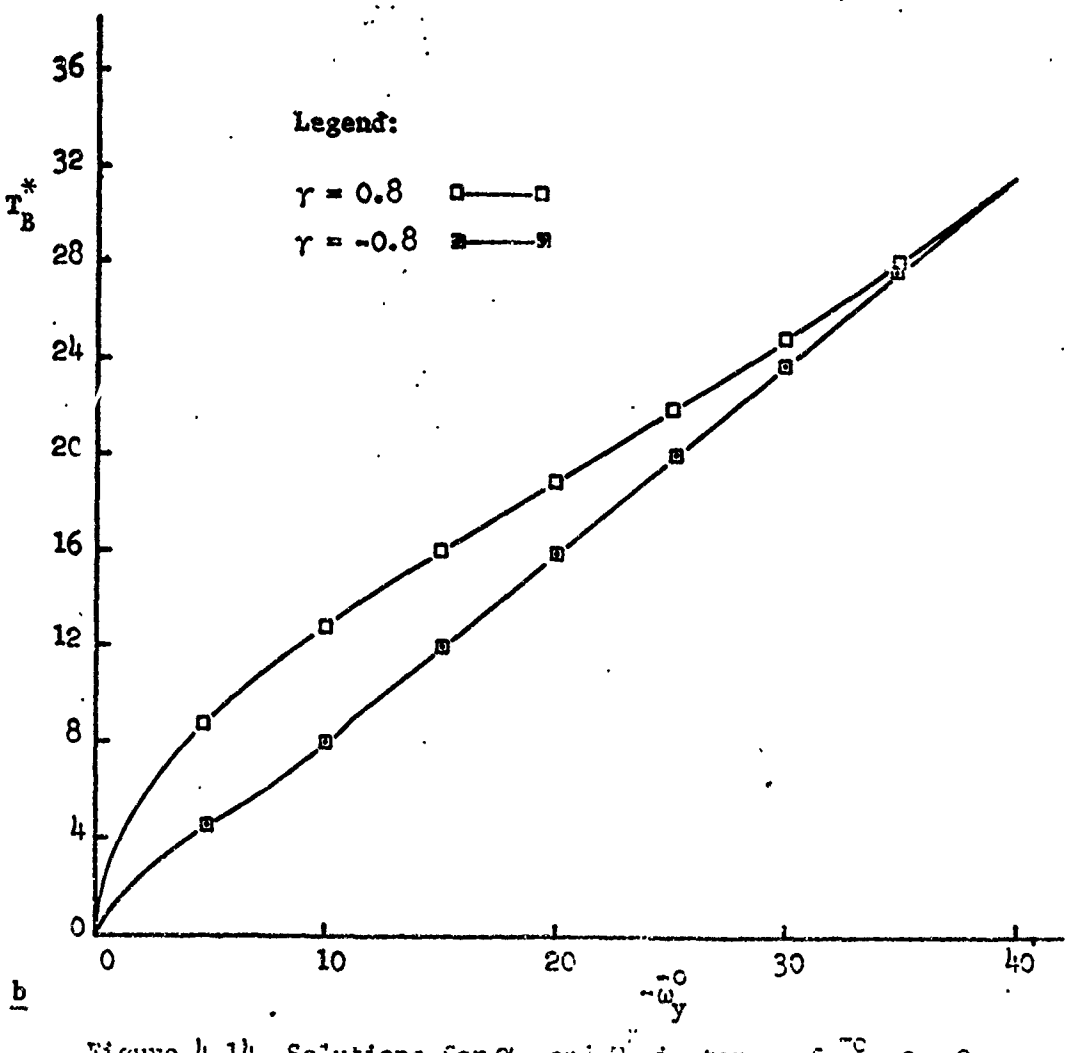

b

Figure 4.14 Solutions for α_4 and T_B^* in terms of $\bar{\omega}_y^o$, $\beta_o = 0$, Case 1, 4-jets

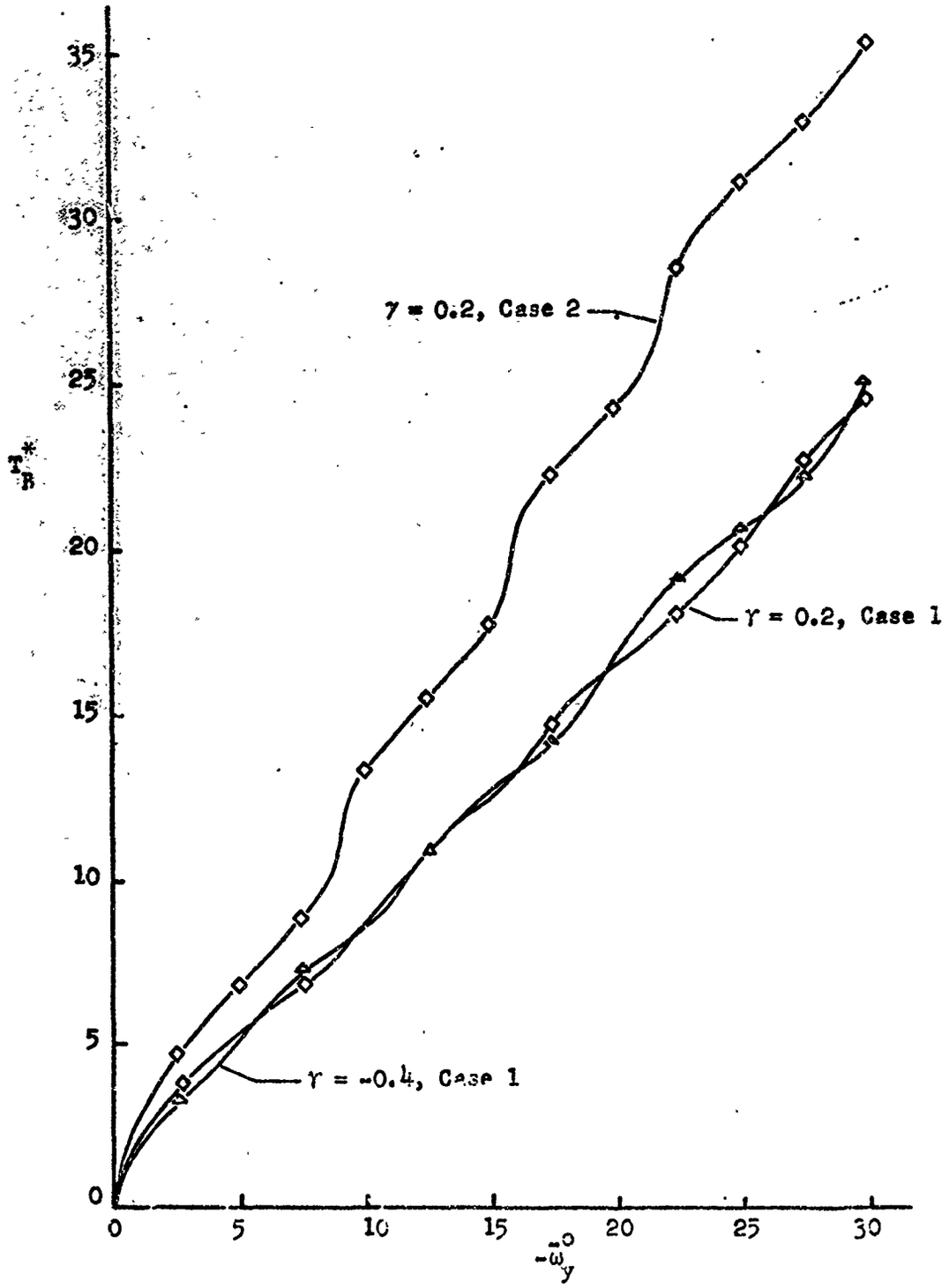

Figure 4.15 Solution for T_B^* in terms of $\bar{\omega}_y^o$, $\beta_o = 0$, 4-jets

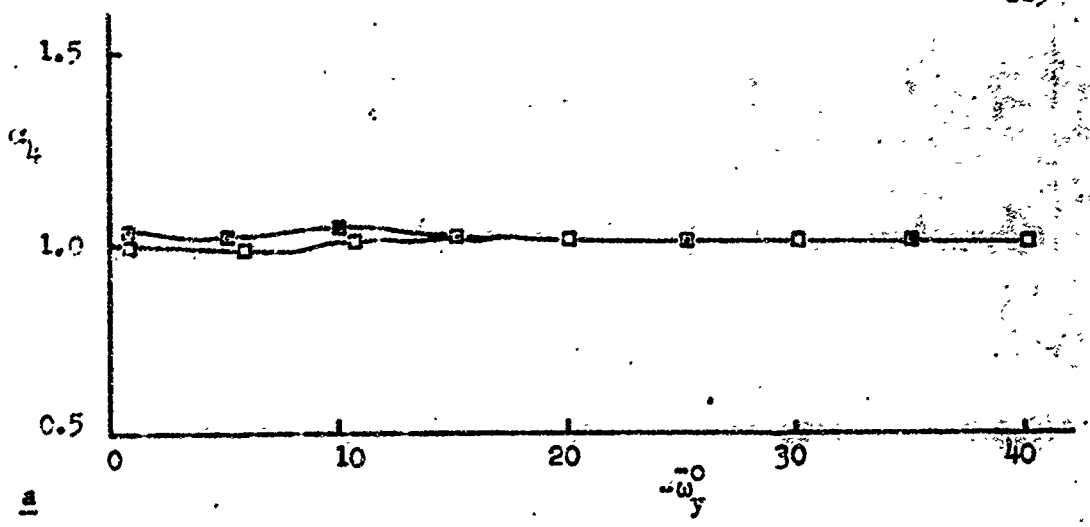

a

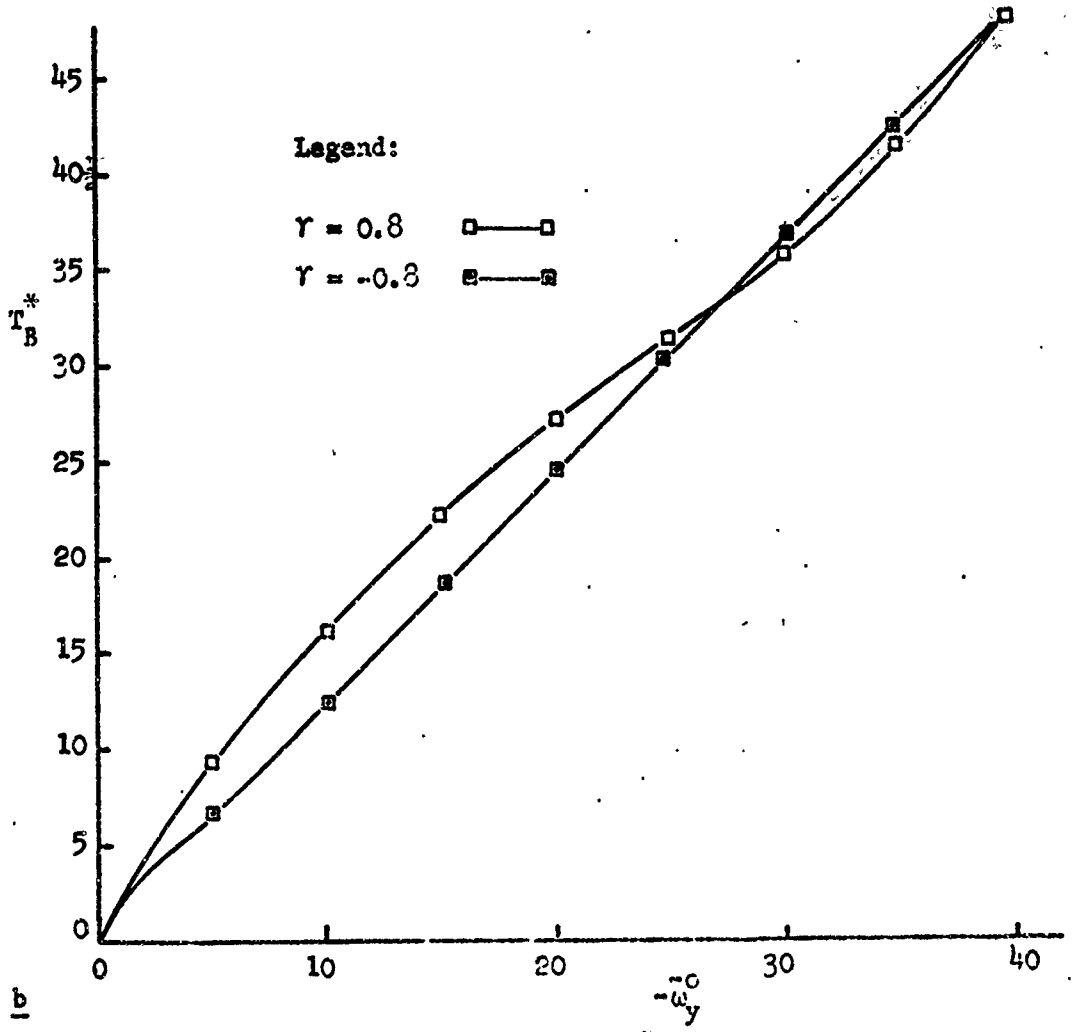

b

Figure 4.16 Solutions for α_4 and T_B^* in terms of $\bar{\omega}_y^o$, $\beta_c = 0$, Case 2, 4-jets

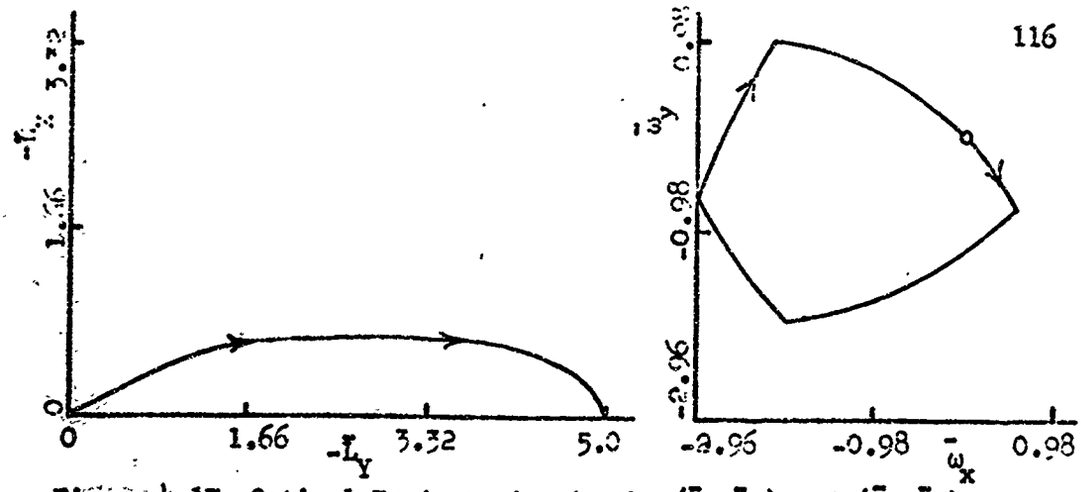

Figure 4.17 Optimal Trajectories in the $(\bar{L}_X-\bar{L}_Y)$ and $(\bar{\omega}_x-\bar{\omega}_y)$ Planes for $\bar{L}_Y=5, \beta_o=0, \gamma=0.4$, 4-jets

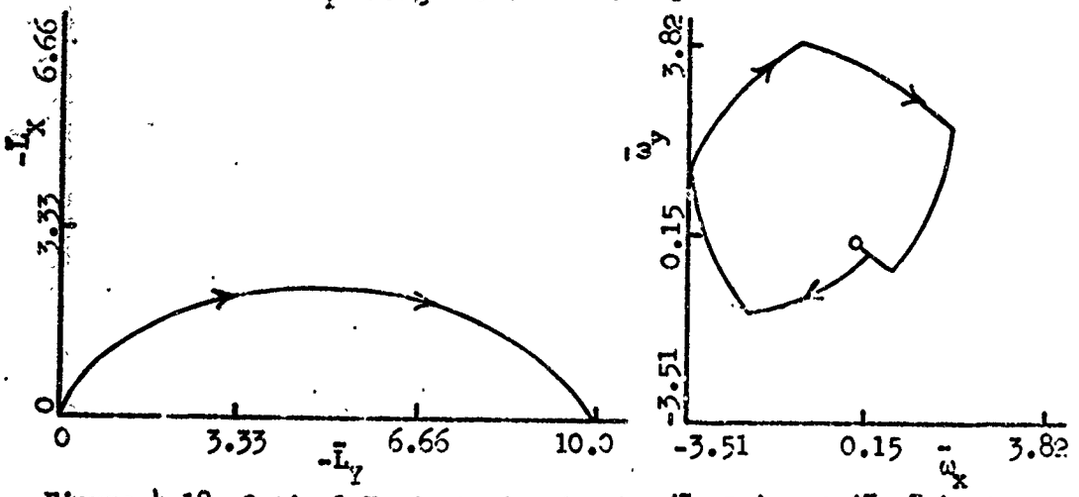

Figure 4.18 Optimal Trajectories in the $(\bar{L}_X-\bar{L}_Y)$ and $(\bar{\omega}_x-\bar{\omega}_y)$ Planes for $\bar{L}_Y=10, \beta_o=0, \gamma=0.4$, 4-jets

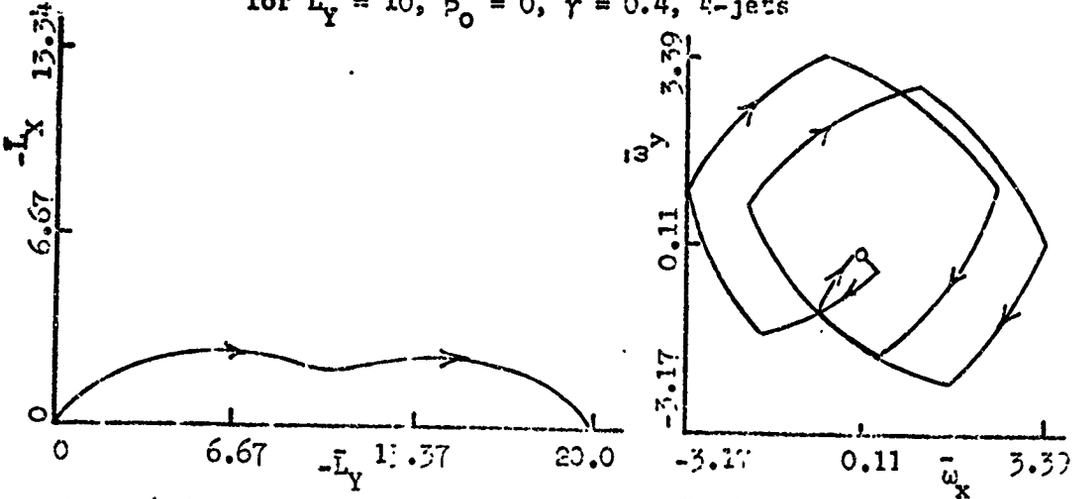

Figure 4.19 Optimal Trajectories in the $(\bar{L}_X-\bar{L}_Y)$ and $(\bar{\omega}_x-\bar{\omega}_y)$ Planes for $\bar{L}_Y=20, \beta_o=0, \gamma=0.4$, 4-jets

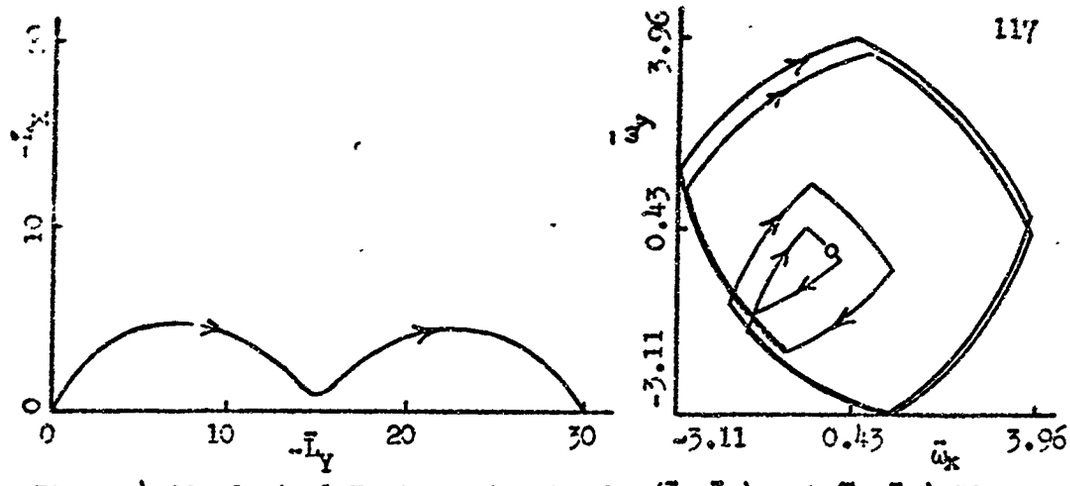

Figure 4.20 Optimal Trajectories in the $(\bar{L}_X\text{-}\bar{L}_Y)$ and $(\bar{\omega}_x\text{-}\bar{\omega}_y)$ Planes for $\bar{L}_Y = 30$, $\beta_o = 0$, $\gamma = 0.4$, 4-jets

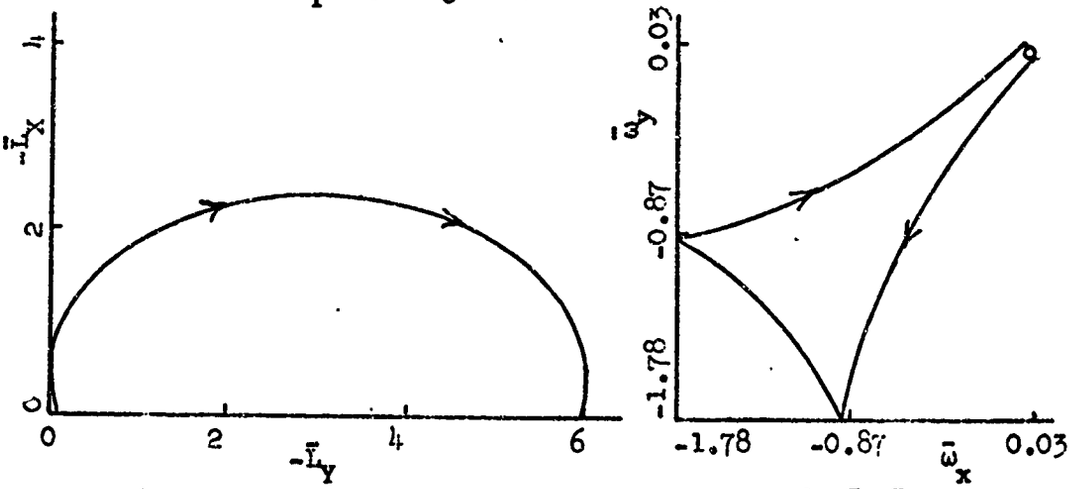

Figure 4.21 Optimal Trajectories in the $(\bar{L}_X\text{-}\bar{L}_Y)$ and $(\bar{\omega}_x\text{-}\bar{\omega}_y)$ Planes for $\bar{L}_Y = 6$, $\beta_o = 0$, $\gamma = -0.4$, 4-jets

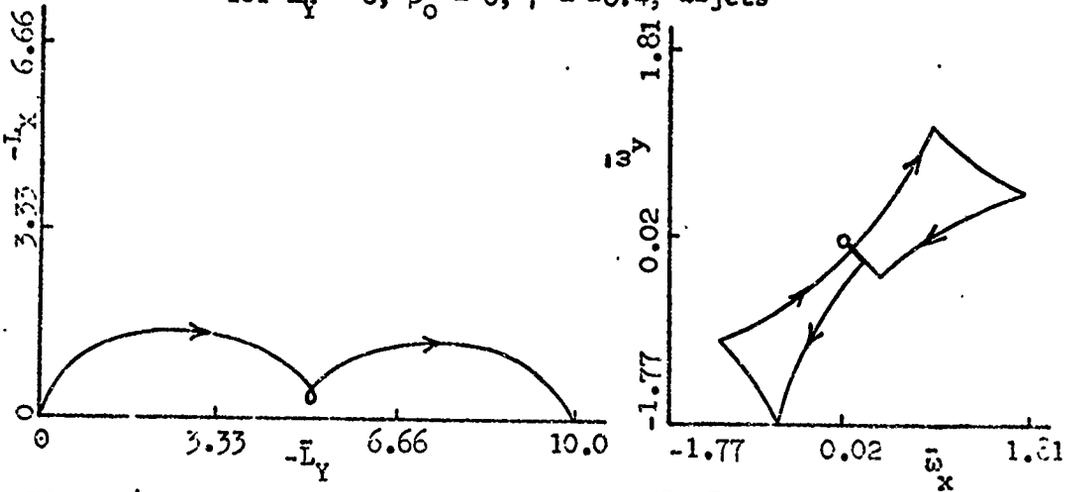

Figure 4.22 Optimal Trajectories in the $(\bar{L}_X\text{-}\bar{L}_Y)$ and $(\bar{\omega}_x\text{-}\bar{\omega}_y)$ Planes for $\bar{L}_Y = 10$, $\beta_o = 0$, $\gamma = -0.4$, 4-jets

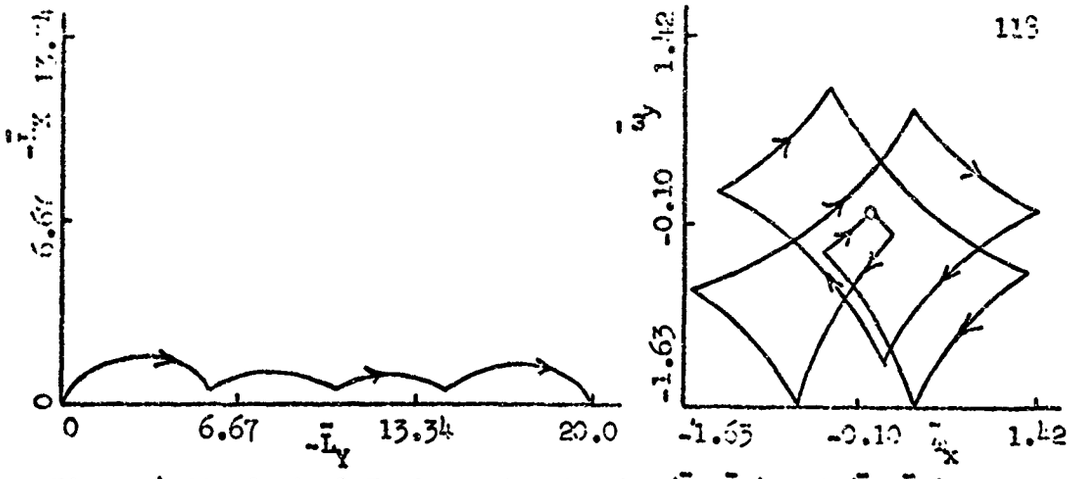

Figure 4.23 Optimal Trajectories in the $(\bar{L}_X-\bar{L}_Y)$ and $(\bar{\omega}_x-\bar{\omega}_y)$ Planes for $\bar{L}_Y = 20$, $\beta_o = 0$, $\gamma = -0.4$, 4-jets

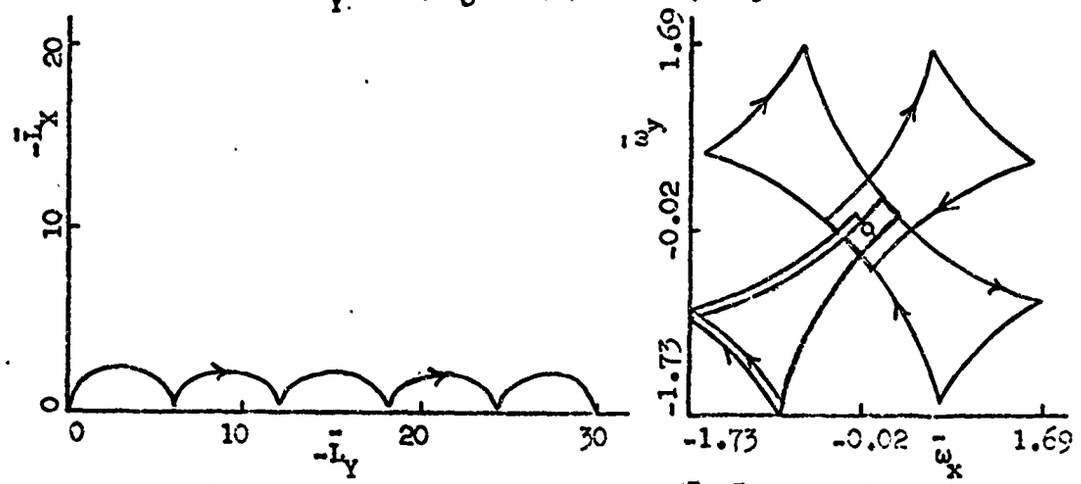

Figure 4.24 Optimal Trajectories in the $(\bar{L}_X-\bar{L}_Y)$ and $(\bar{\omega}_x-\bar{\omega}_y)$ Planes for $\bar{L}_Y = 30$, $\beta_o = 0$, $\gamma = -0.4$, 4-jets

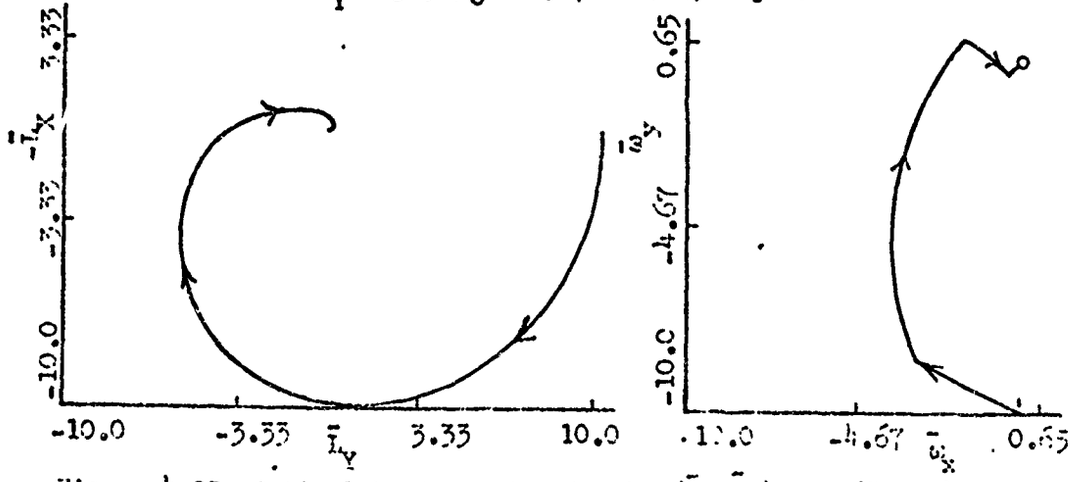

Figure 4.25 Optimal Trajectories in the $(\bar{L}_X-\bar{L}_Y)$ and $(\bar{\omega}_x-\bar{\omega}_y)$ Planes for $\bar{\omega}_x^o = 0$, $\bar{\omega}_y^o = -10$, $\beta_o = 0$, $\gamma = -0.4$, Case 1, 4-jets

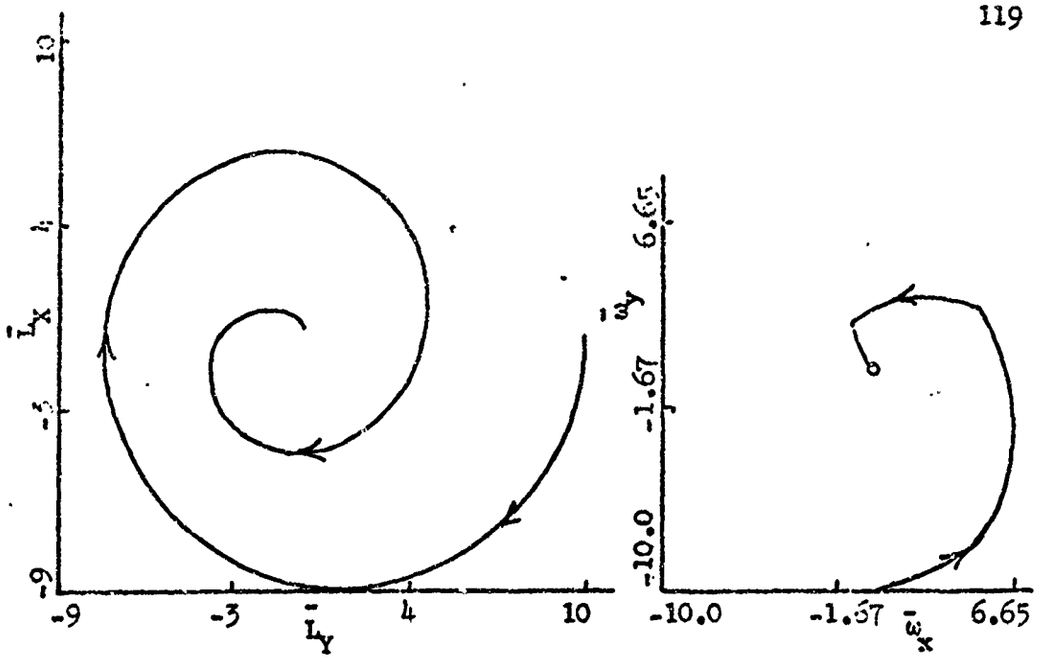

Figure 4.26 Optimal Trajectories in the $(\bar{L}_X\text{-}\bar{L}_Y)$ and $(\bar{\omega}_x\text{-}\bar{\omega}_y)$ Planes for $\bar{\omega}_x^o = 0$, $\bar{\omega}_y^o = -10$, $\beta_o = 0$, $\gamma = -0.4$, Case 1, 4-jets

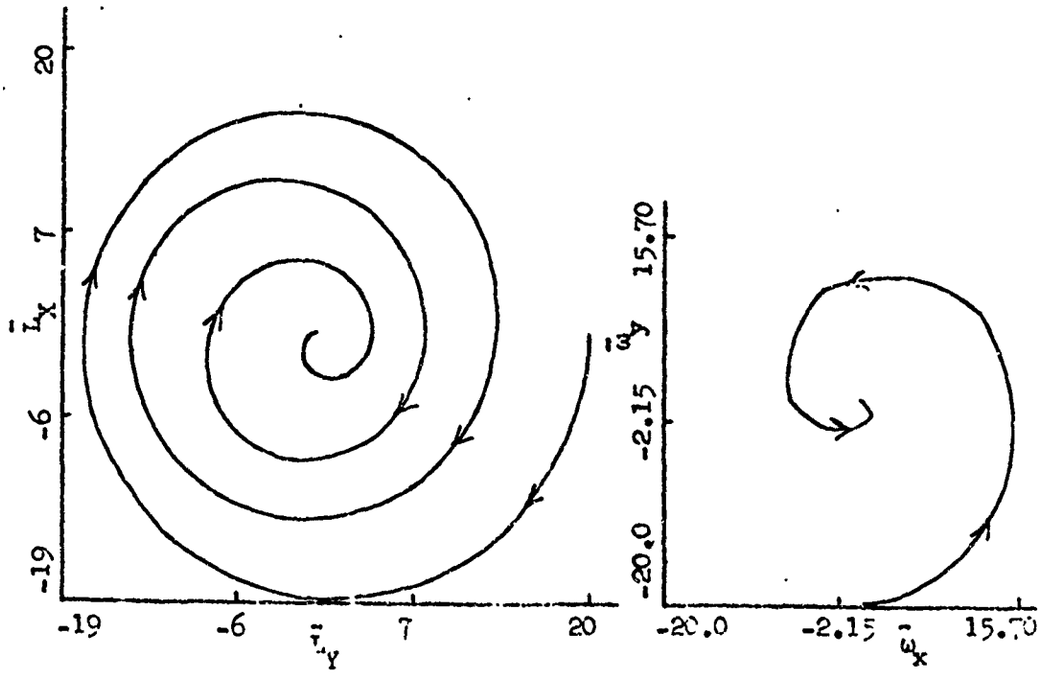

Figure 4.27 Optimal Trajectories in the $(\bar{L}_X\text{-}\bar{L}_Y)$ and $(\bar{\omega}_x\text{-}\bar{\omega}_y)$ Planes for $\bar{\omega}_x^o = 0$, $\bar{\omega}_y^o = -20$, $\beta_o = 0$, $\gamma = -0.4$, Case 1, 4-jets

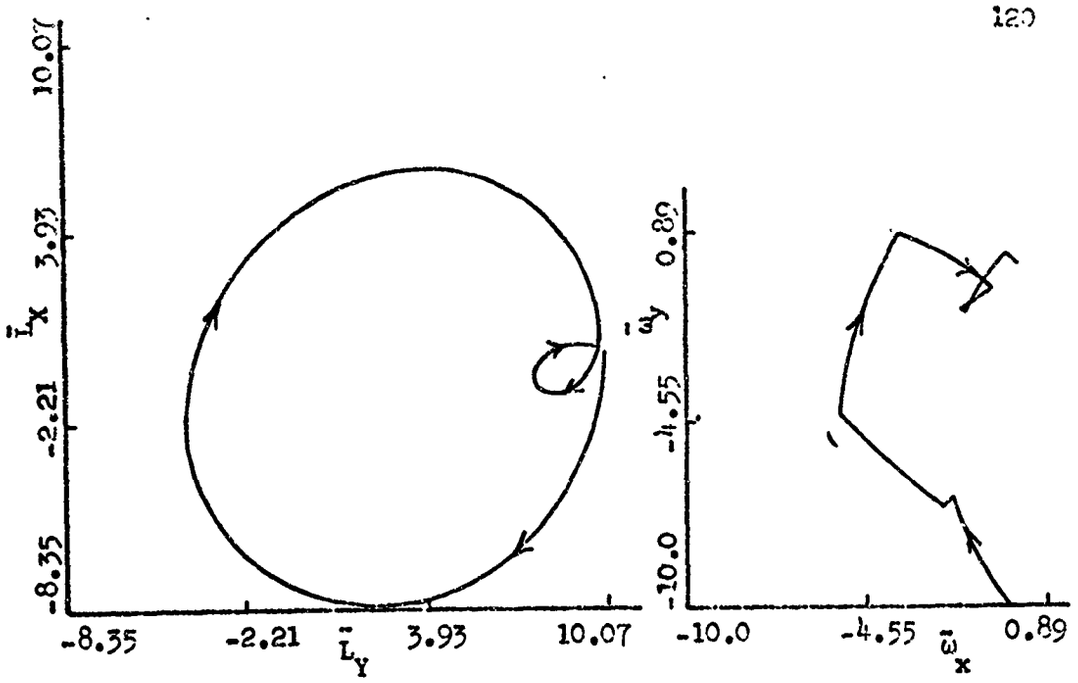

Figure 4.28 Optimal Trajectories in the $(\bar{L}_X\text{-}\bar{L}_Y)$ and $(\bar{\omega}_x\text{-}\bar{\omega}_y)$ Planes for $\bar{\omega}_x^o = 0$, $\bar{\omega}_y^o = -10$, $\beta_o = 0$, $\gamma = 0.2$, Case 2, 4-jets

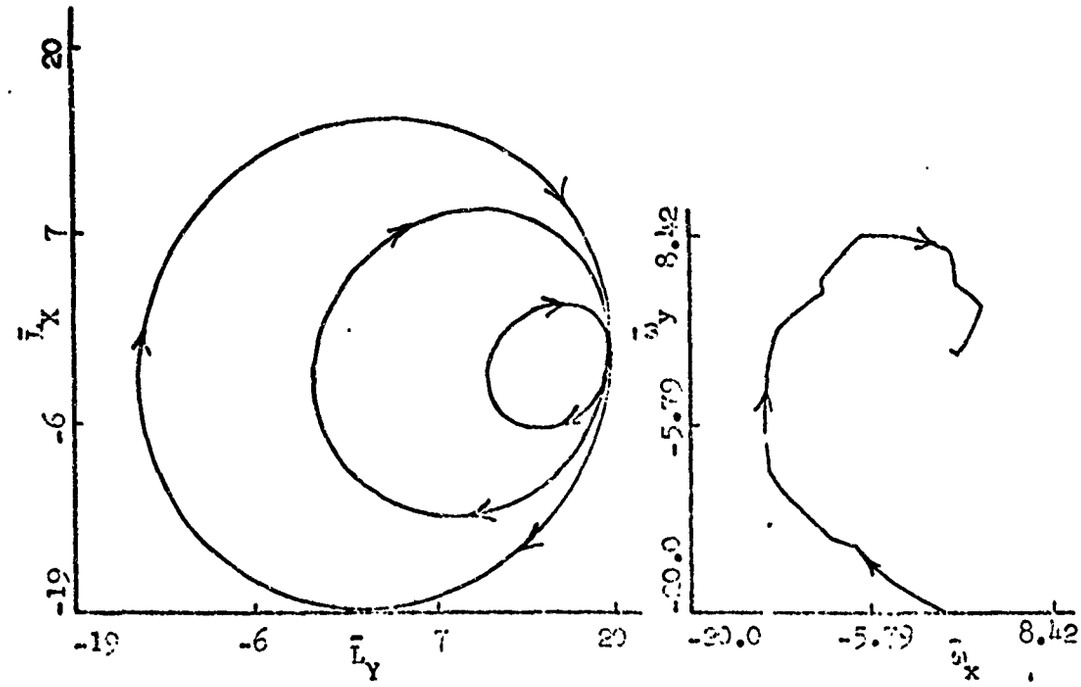

Figure 4.29 Optimal Trajectories in the $(\bar{L}_X\text{-}\bar{L}_Y)$ and $(\bar{\omega}_x\text{-}\bar{\omega}_y)$ Planes for $\bar{\omega}_x^o = 0$, $\bar{\omega}_y^o = -20$, $\beta_o = 0$, $\gamma = 0.2$, Case 2, 4-jets

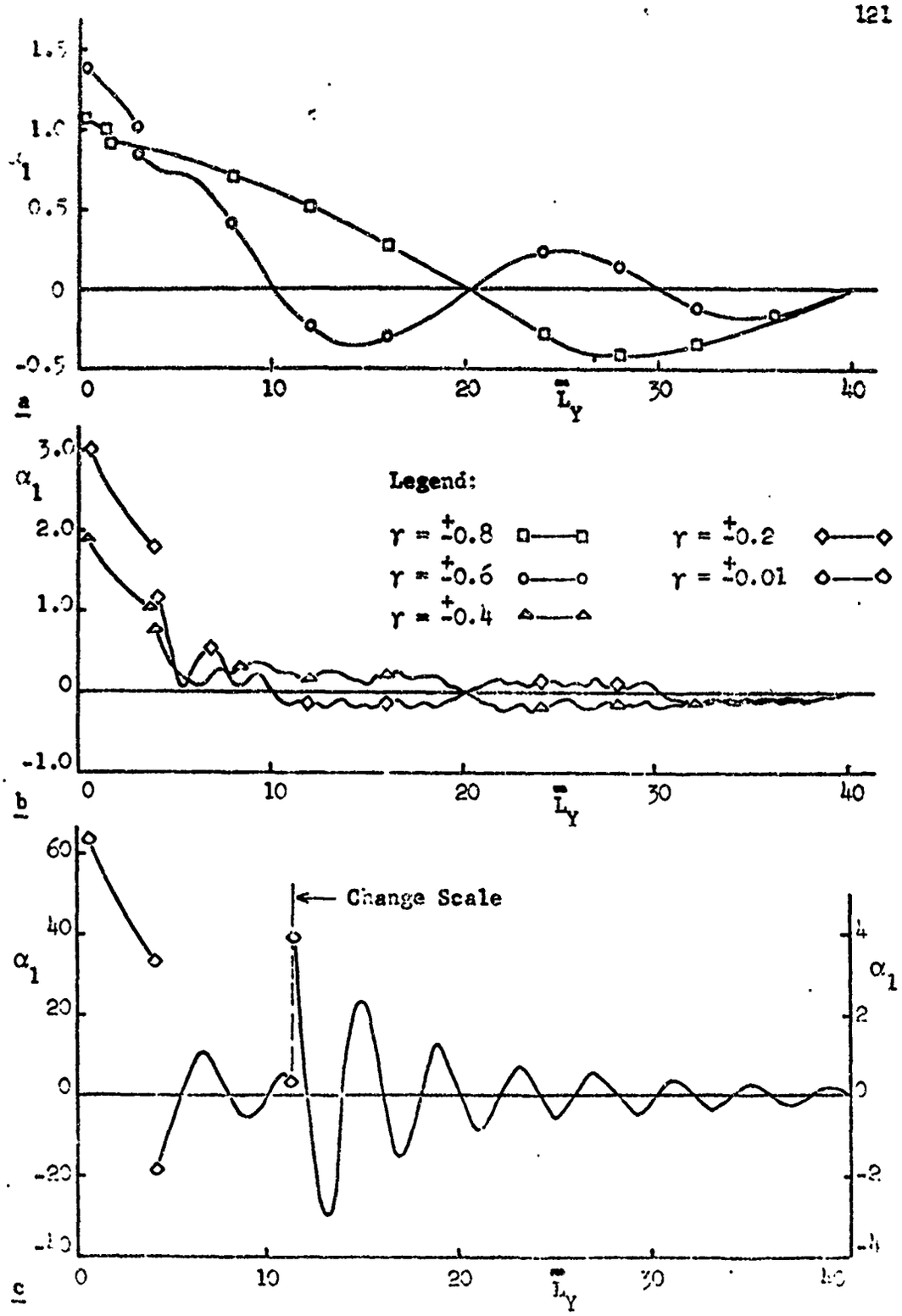

Figure 4.30 Solution for α_1 in terms of $\bar{L}_Y$, $\beta_0 = 0$, 2-jets

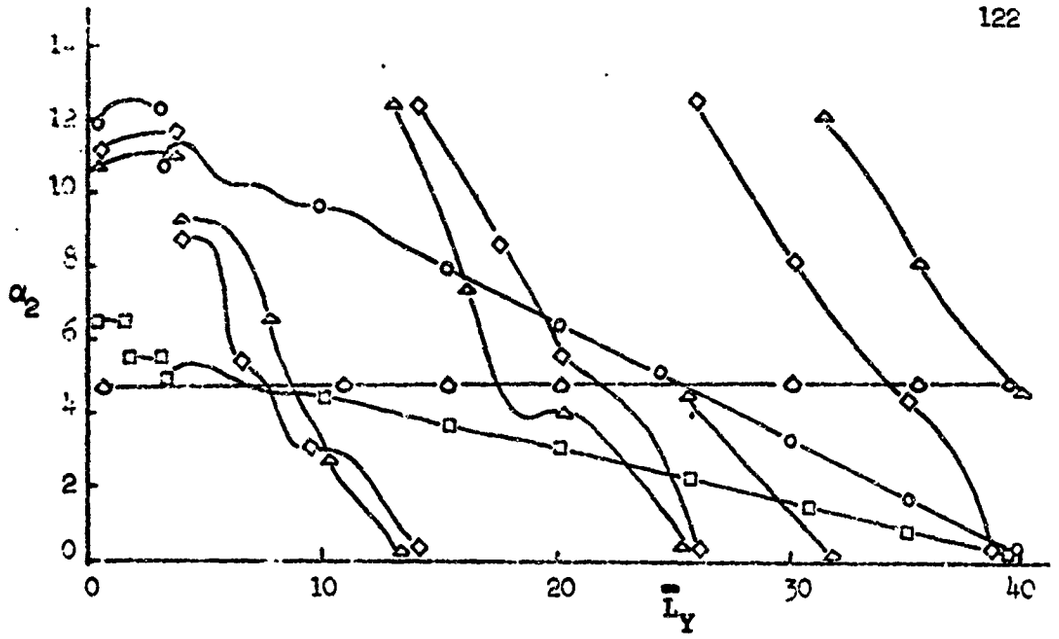

Figure 4.31 Solution for α_2 in terms of L_Y, $\beta_o = 0$, 2-jets

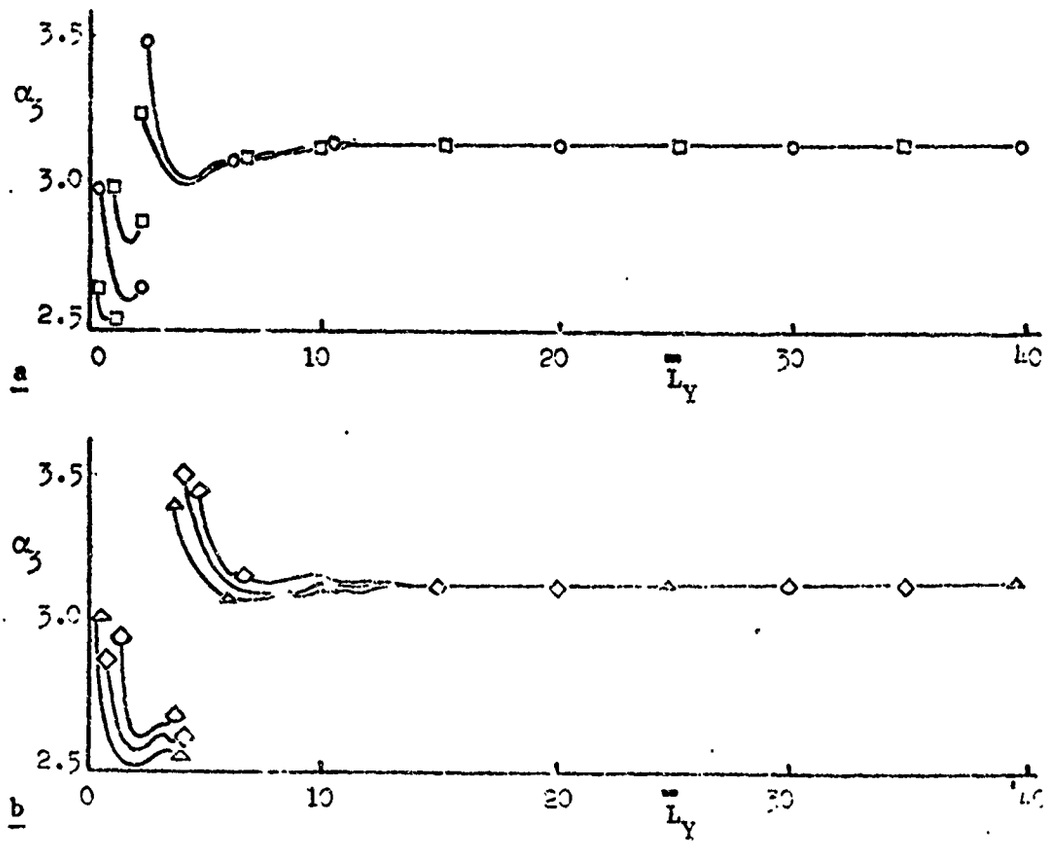

Figure 4.32 Solution for α_3 in terms of $\bar{L}_Y$, $\beta_o = 0$, 2-jets

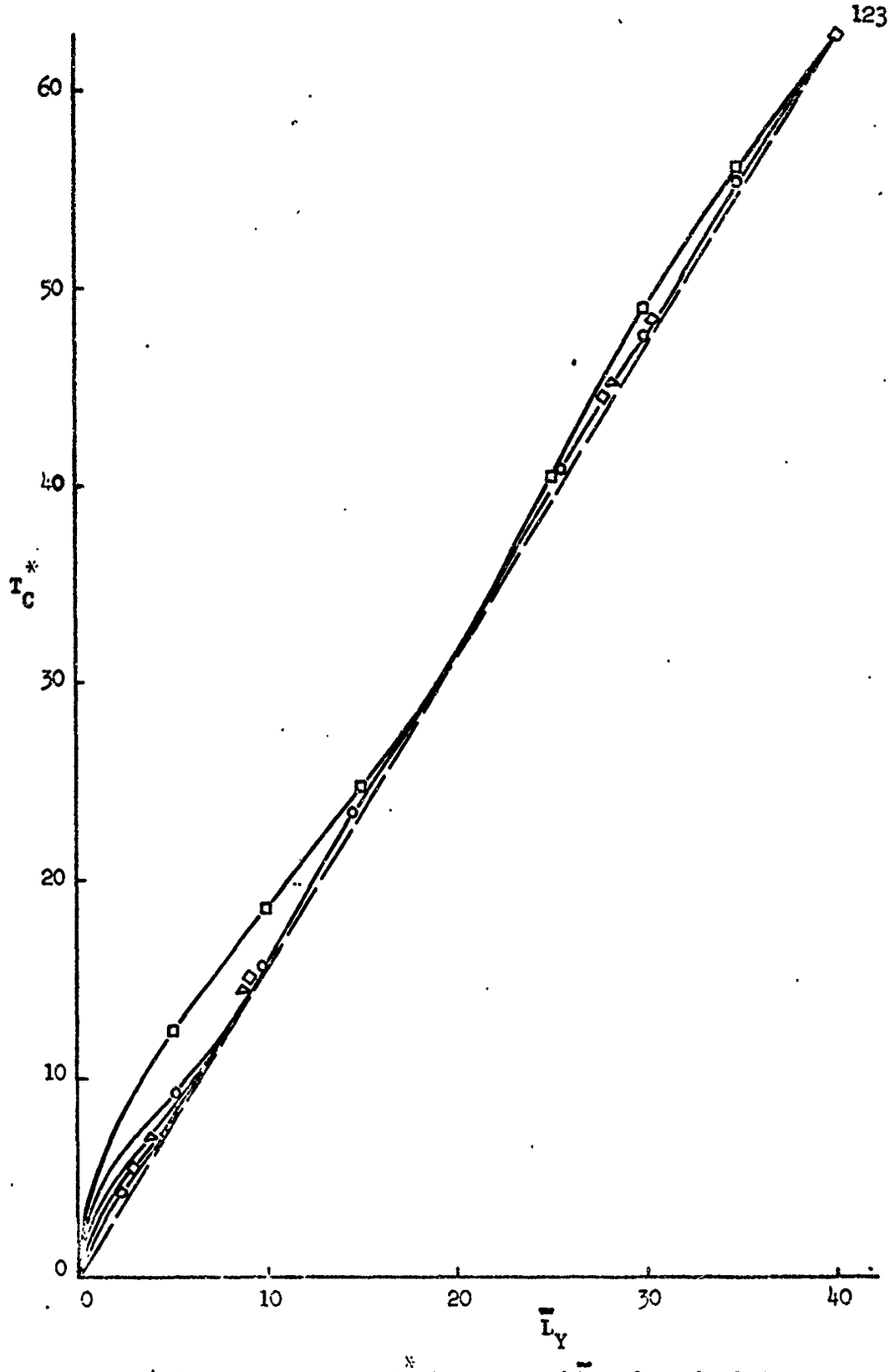

Figure 4.33 Solution for T_c^* in terms of $\bar{L}_Y$, $\theta_0 = 0$, 2-jets

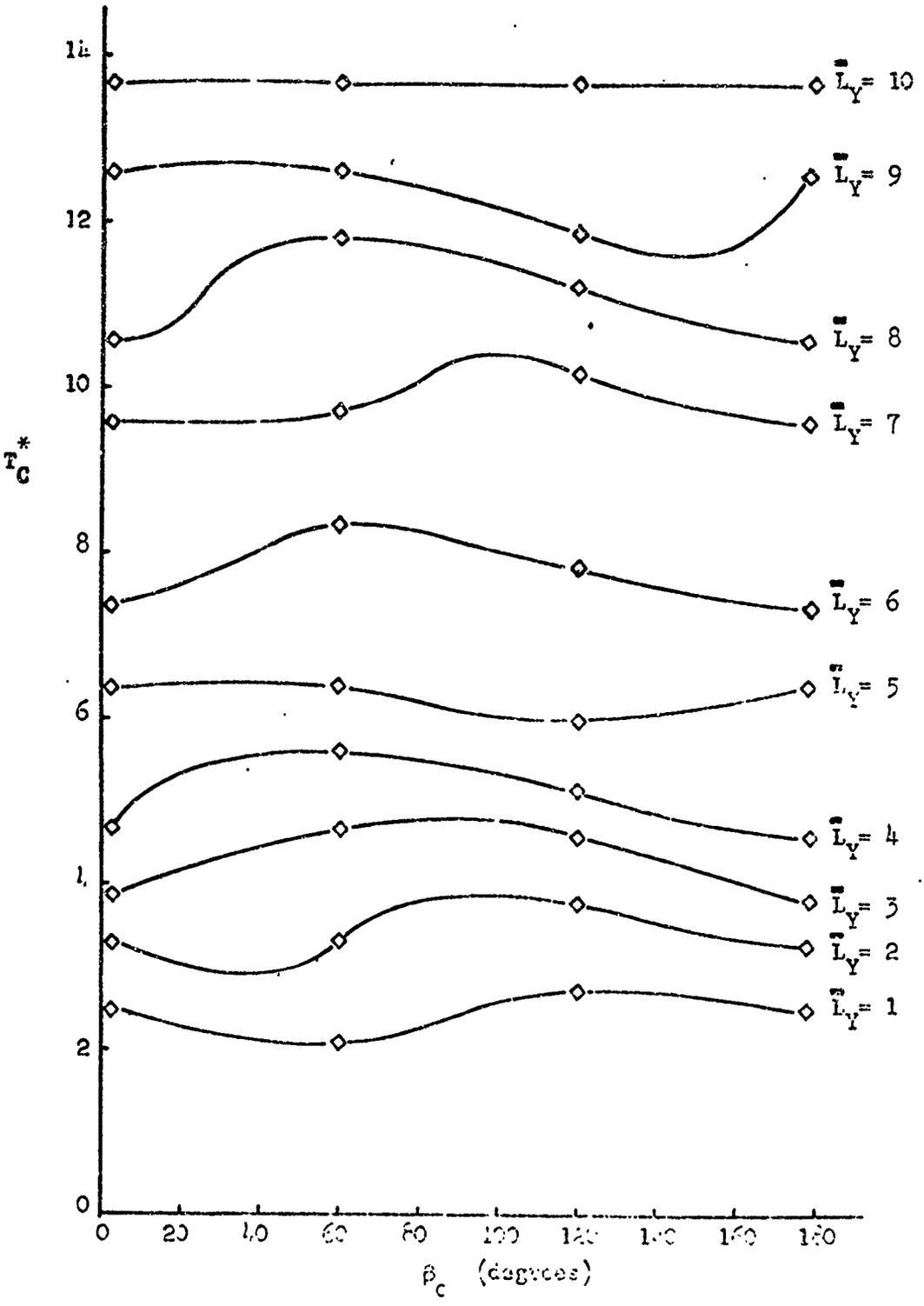

Figure 4.34 Solution for T_C^* in terms of β_c and $\bar{L}_Y$, 2-jets

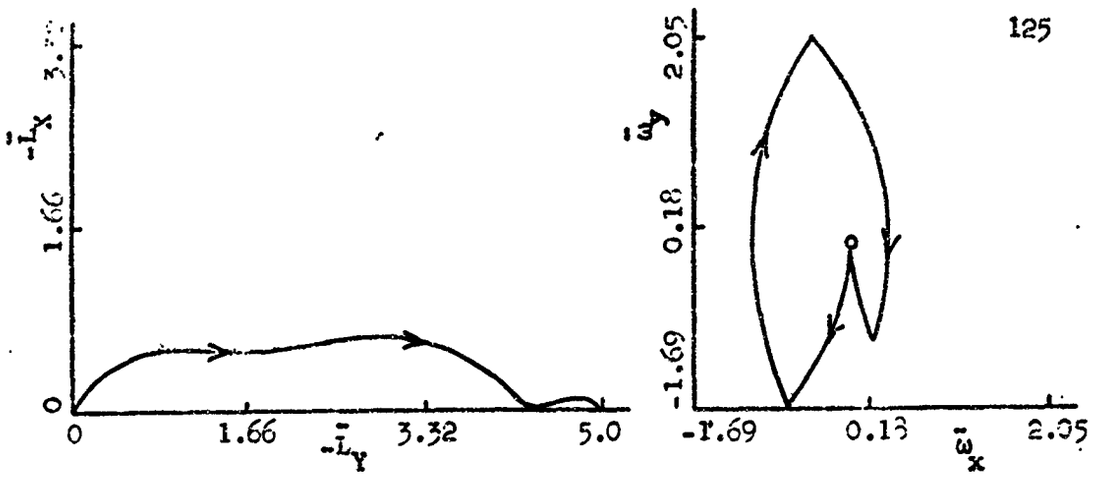

Figure 4.35 Optimal Trajectories in the $(\bar{L}_X\text{-}\bar{L}_Y)$ and $(\bar{\omega}_x\text{-}\bar{\omega}_y)$ Planes for $\bar{L}_Y = 5$, $\beta_o = 0$, $\gamma = 0.4$, 2-jets

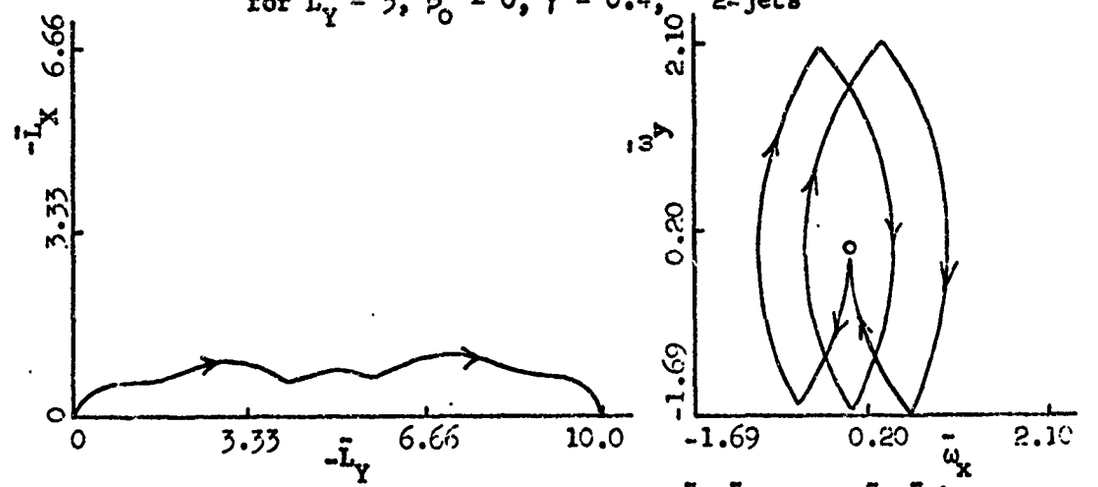

Figure 4.36 Optimal Trajectories in the $(\bar{L}_X\text{-}\bar{L}_Y)$ and $(\bar{\omega}_x\text{-}\bar{\omega}_y)$ Planes for $\bar{L}_Y = 10$, $\beta_o = 0$, $\gamma = 0.4$, 2-jets

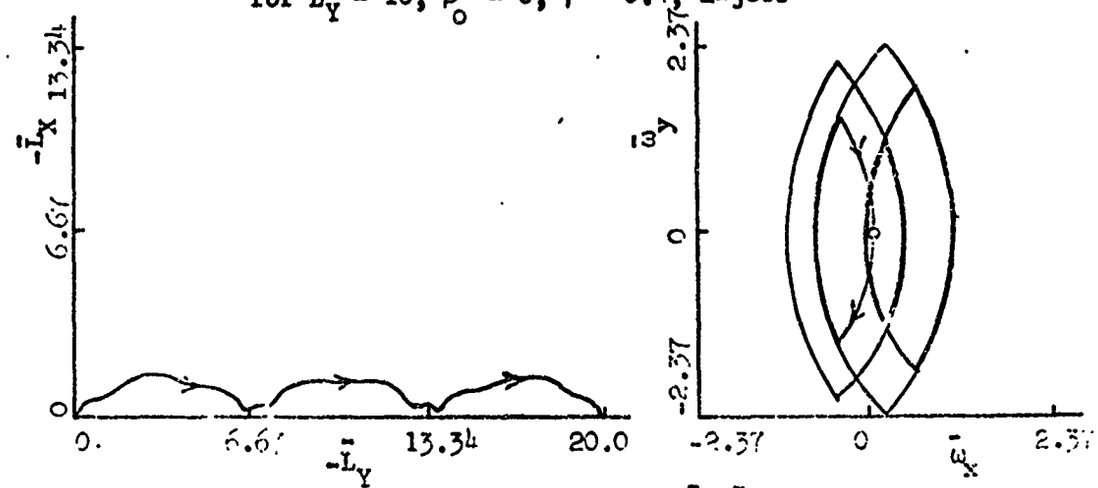

Figure 4.37 Optimal Trajectories in the $(\bar{L}_X\text{-}\bar{L}_Y)$ and $(\bar{\omega}_x\text{-}\bar{\omega}_y)$ Planes for $\bar{L}_Y = 20$, $\beta_o = 0$, $\gamma = 0.4$, 2-jets

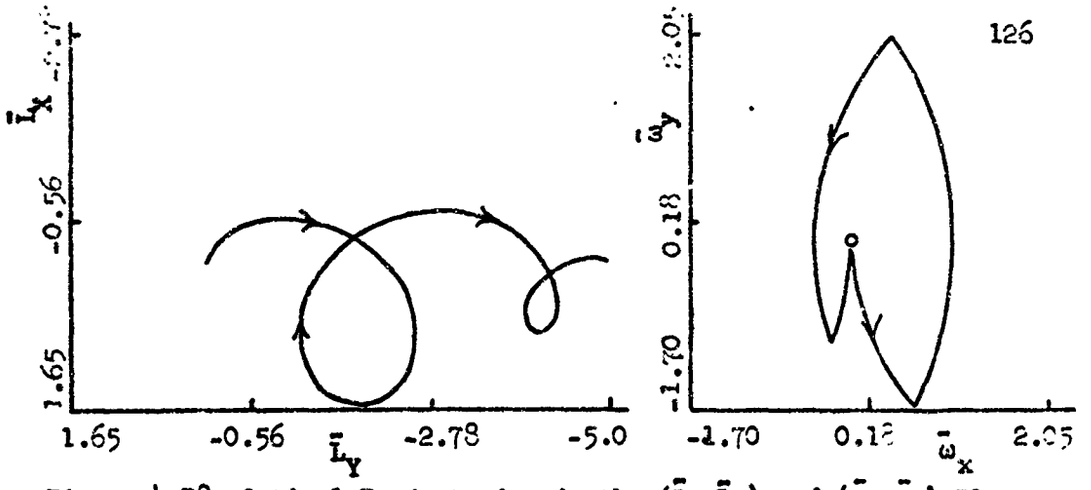

Figure 4.38 Optimal Trajectories in the $(\bar{L}_X\text{-}\bar{L}_Y)$ and $(\bar{\omega}_x\text{-}\bar{\omega}_y)$ Planes for $\bar{L}_Y = 5$, $\beta_o = 0$, $\gamma = -0.4$, 2-jets

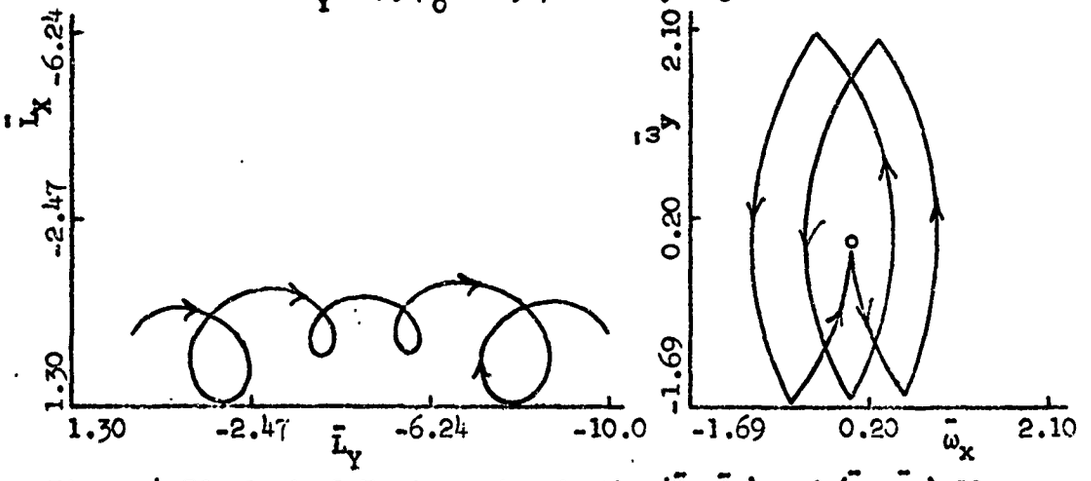

Figure 4.39 Optimal Trajectories in the $(\bar{L}_X\text{-}\bar{L}_Y)$ and $(\bar{\omega}_x\text{-}\bar{\omega}_y)$ Planes for $\bar{L}_Y = 10$, $\beta_o = 0$, $\gamma = -0.4$, 2-jets

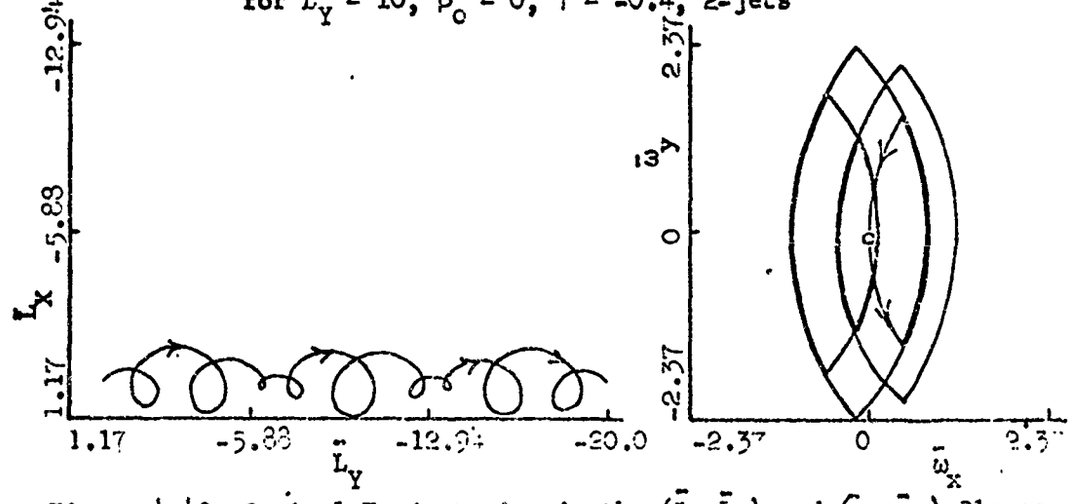

Figure 4.40 Optimal Trajectories in the $(\bar{L}_X\text{-}\bar{L}_Y)$ and $(\bar{\omega}_x\text{-}\bar{\omega}_y)$ Planes for $\bar{L}_Y = 20$, $\beta_o = 0$, $\gamma = -0.4$, 2-jets

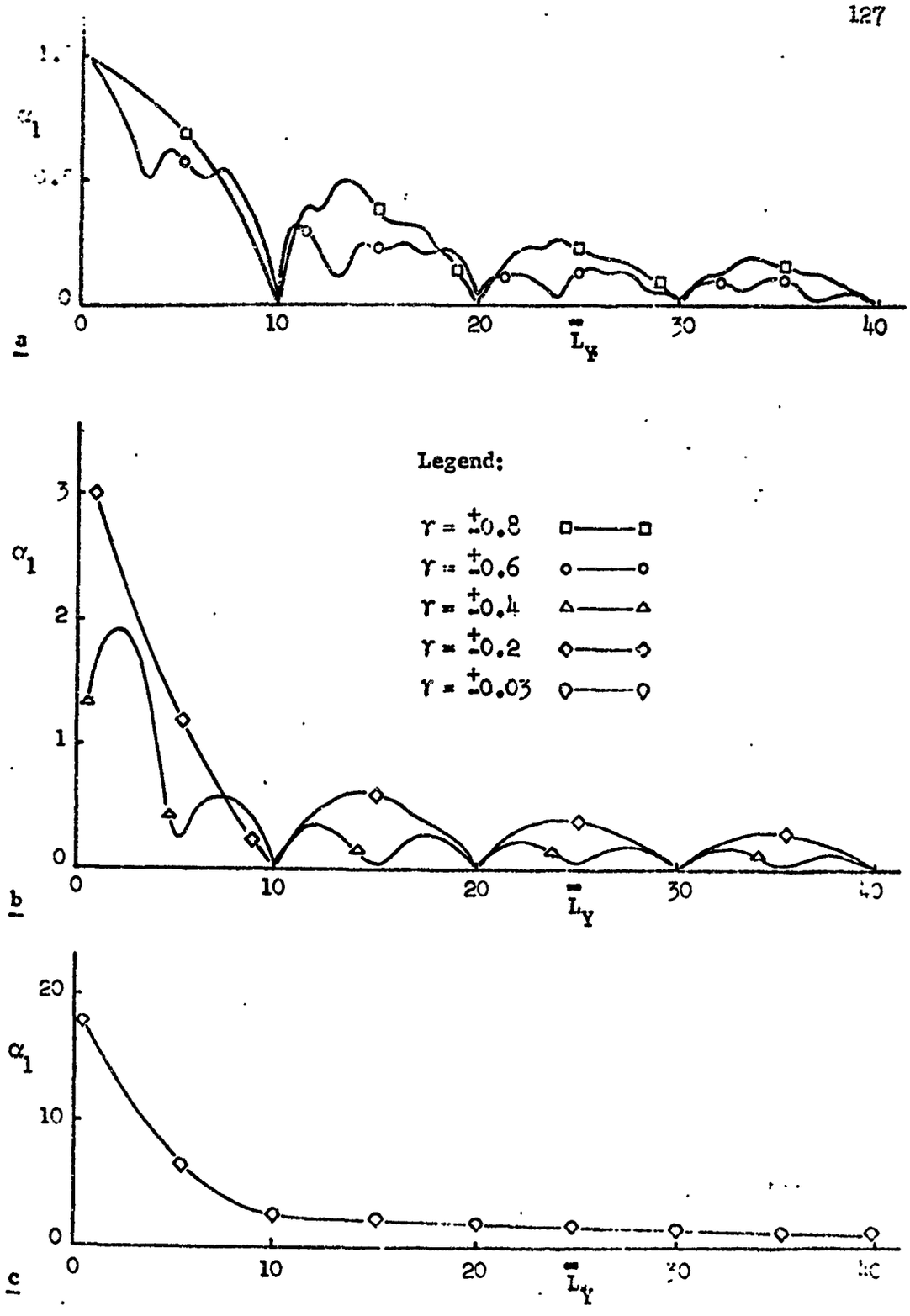

Figure 4.41 Solution for α_1 in terms of $\bar{L}_Y$, $\beta_c = 0$, 1-jet

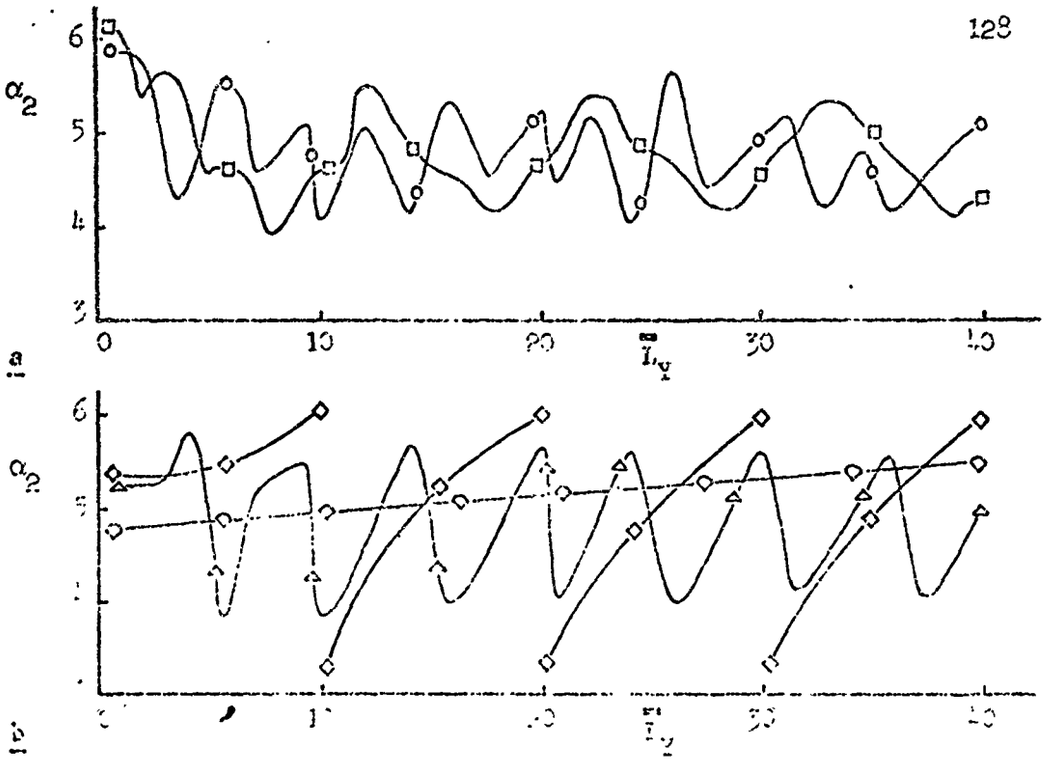

Figure 4.4-2 Solution for α_2 in terms of $\bar{L}_y$, $\beta_0 = 0$, 1-jet

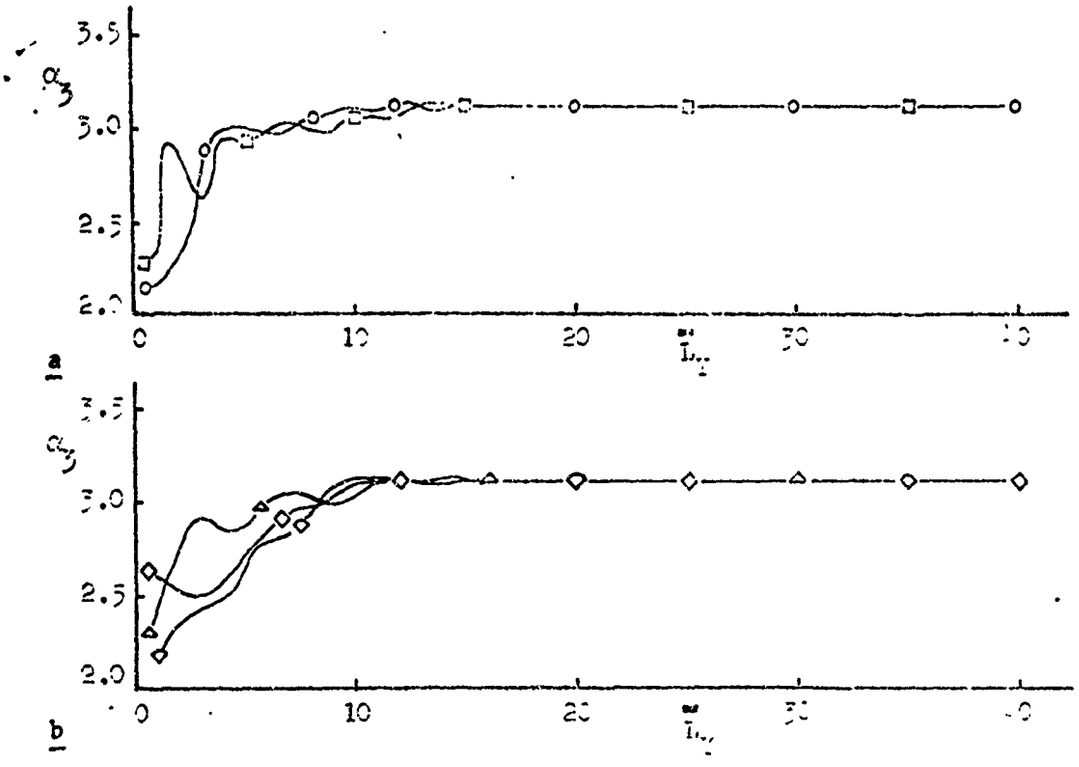

Figure 4.4-3 Solution for α_3 in terms of $\bar{L}_y$, $\beta_0 = 0$, 1-jet

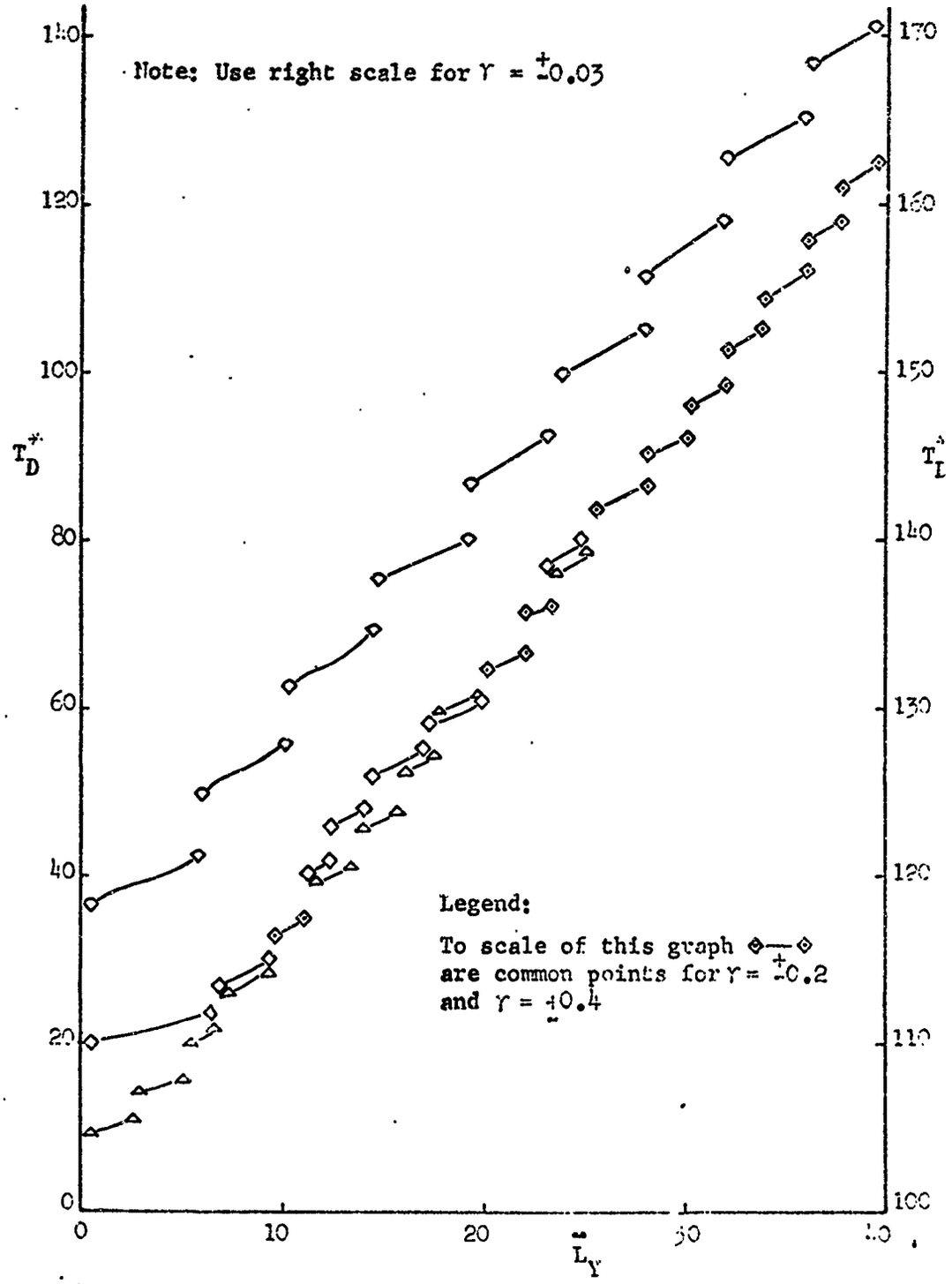

Figure 4.44 Solution for T_D^* in terms of $\bar{L}_Y$, $\Upsilon_0 = 0$, 1-jet

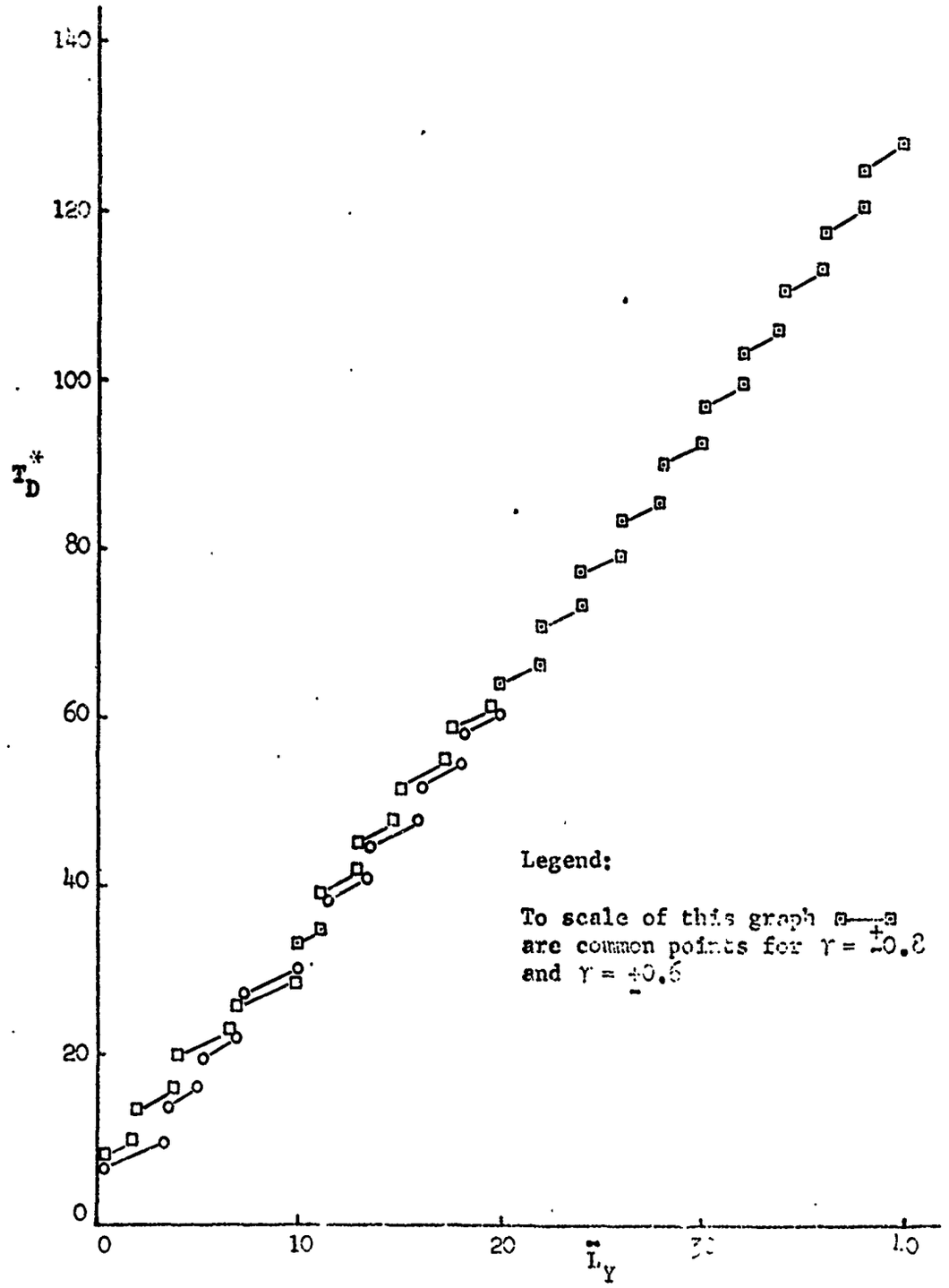

Figure 4.45 Solution for T_D^* in terms of $\tilde{L}_Y$, $\beta_c = 0$, 1-jet

Note: Heavy lines indicate that the control jet is "on"

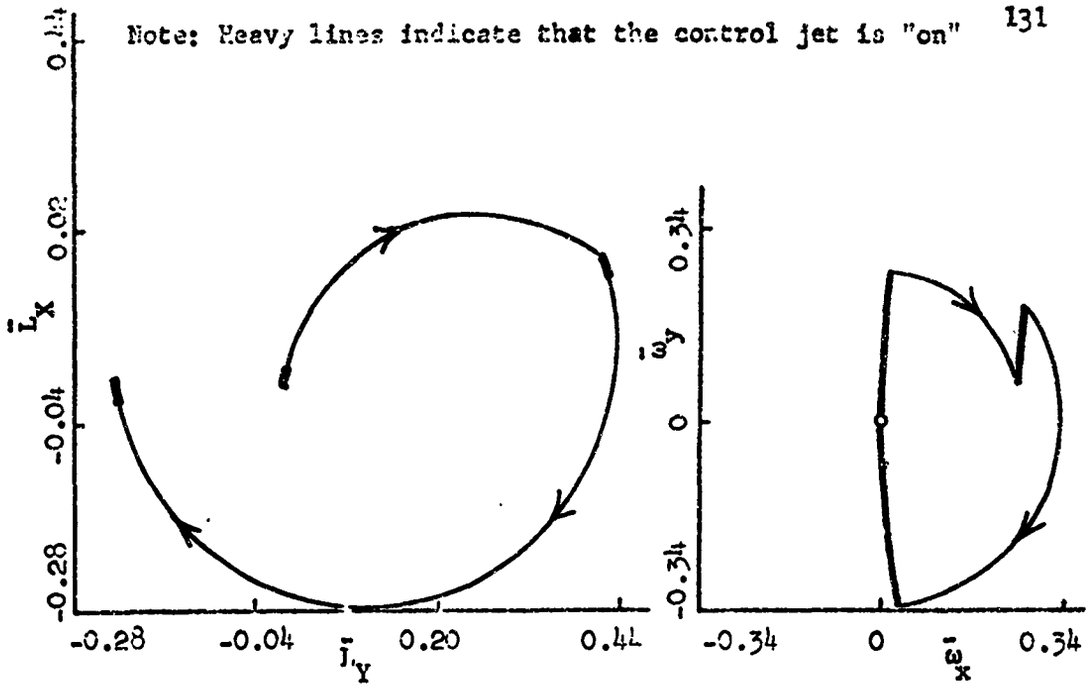

Figure 4.46 Optimal Trajectories in the $(\bar{L}_X\text{-}\bar{L}_Y)$ and $(\bar{\omega}_x\text{-}\bar{\omega}_y)$ Planes for $\bar{L}_Y = 0.2$, $\beta_o = 0$, $\gamma = 0.4$, 1-jet

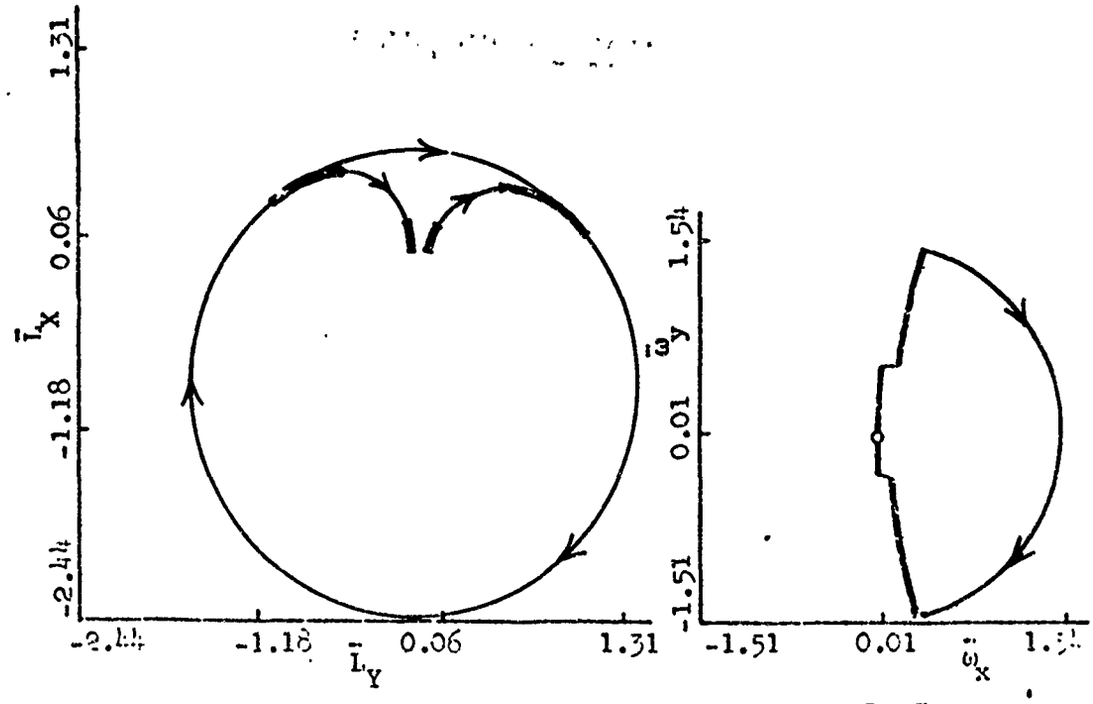

Figure 4.47 Optimal Trajectories in the $(\bar{L}_X\text{-}\bar{L}_Y)$ and $(\bar{\omega}_x\text{-}\bar{\omega}_y)$ Planes for $\bar{L}_Y = 0.2$, $\beta_o = 0$, $\gamma = 0.2$, 1-jet

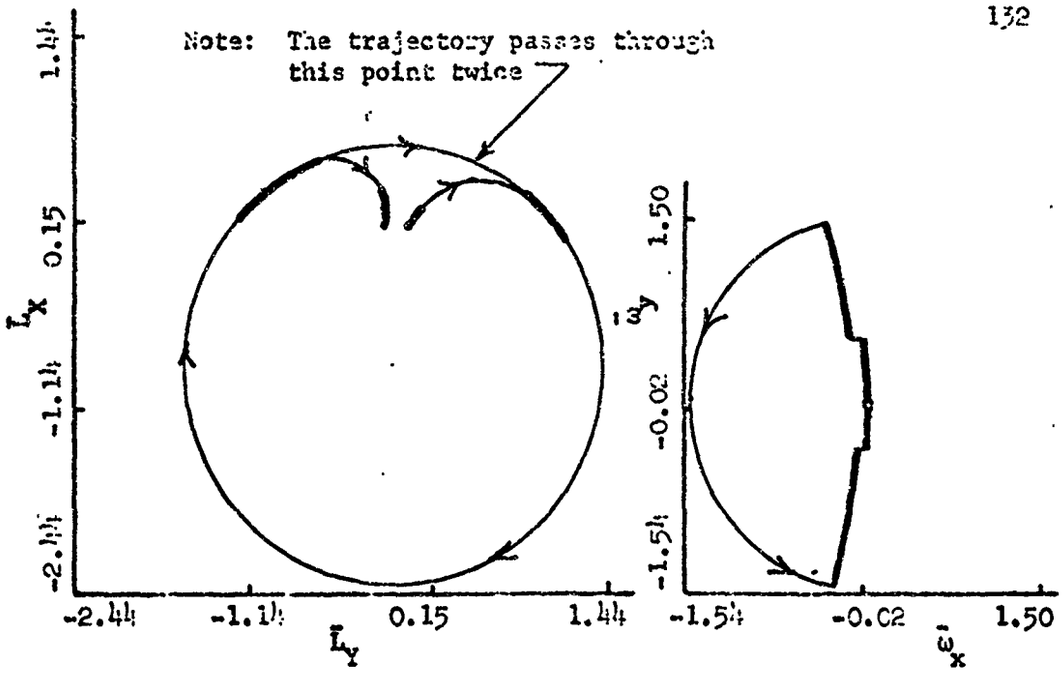

Figure 4.48 Optimal Trajectories in the $(\bar{L}_x-\bar{L}_y)$ and $(\bar{\omega}_x-\bar{\omega}_y)$ Planes for $\bar{L}_y = 0.0, \beta_0 = 0, \gamma = -0.2$, 1-jet

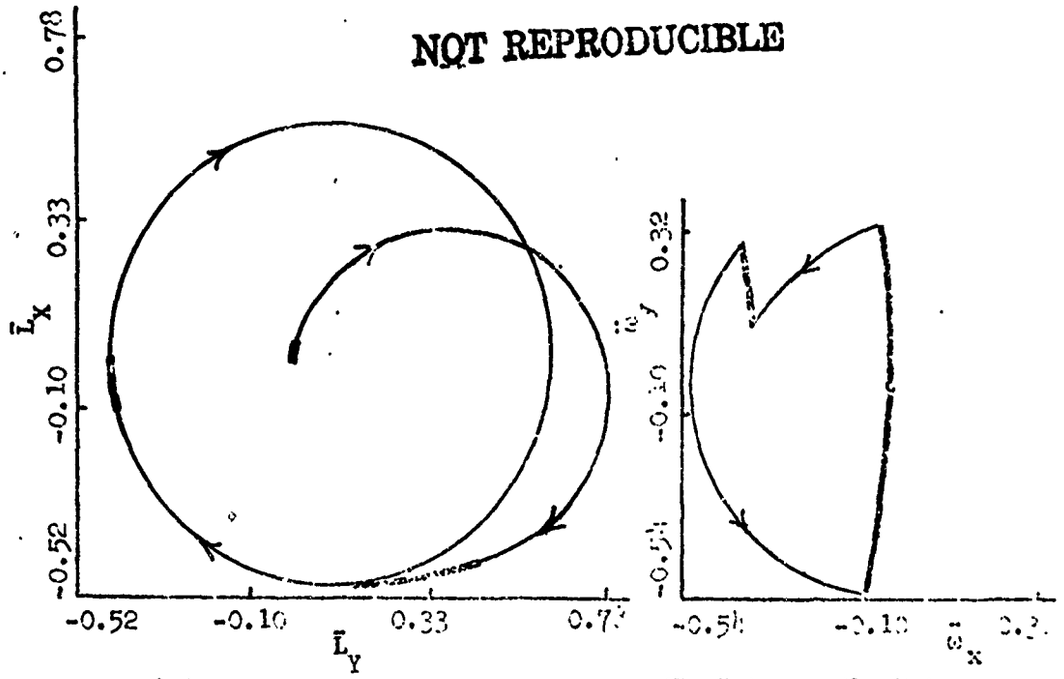

Figure 4.49 Optimal Trajectories in the $(\bar{L}_x-\bar{L}_y)$ and $(\bar{\omega}_x-\bar{\omega}_y)$ Planes for $\bar{L}_y = 0.0, \beta_0 = 0, \gamma = -0.2$, 1-jet

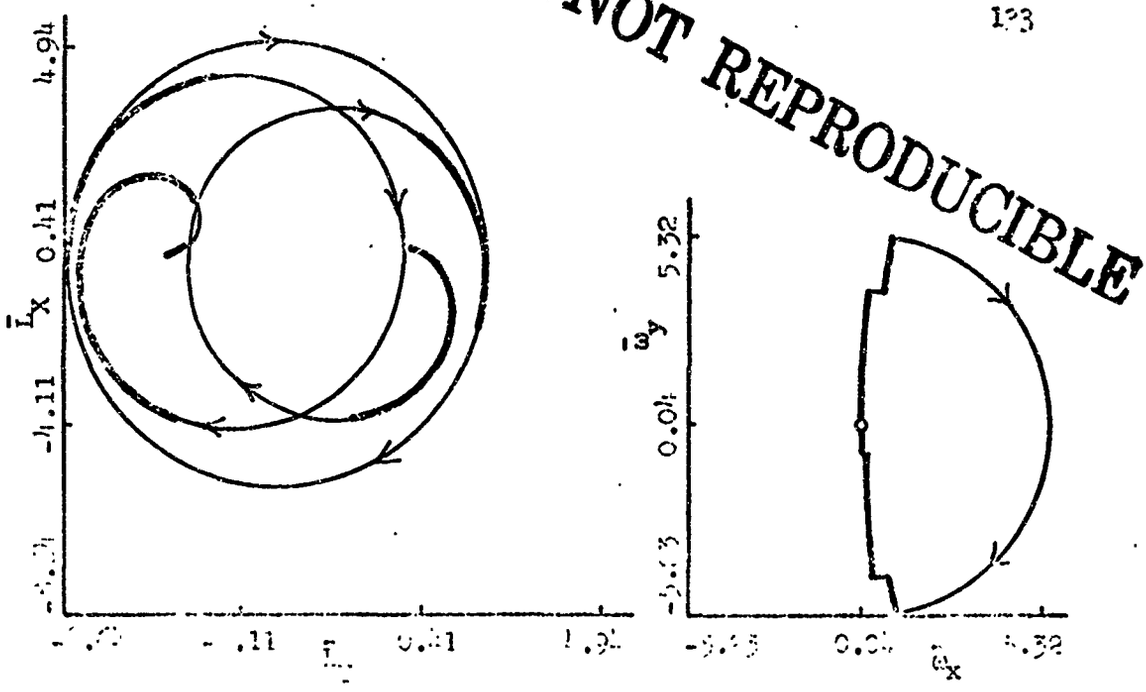

Figure 4.50 Optimal Trajectories in the $(\bar{L}_x\text{-}\bar{L}_y)$ and $(\bar{\omega}_x\text{-}\bar{\omega}_y)$ Planes for $\bar{L}_y = 6$, $\beta_o = 0$, $\gamma = 0.03$, 1-jet

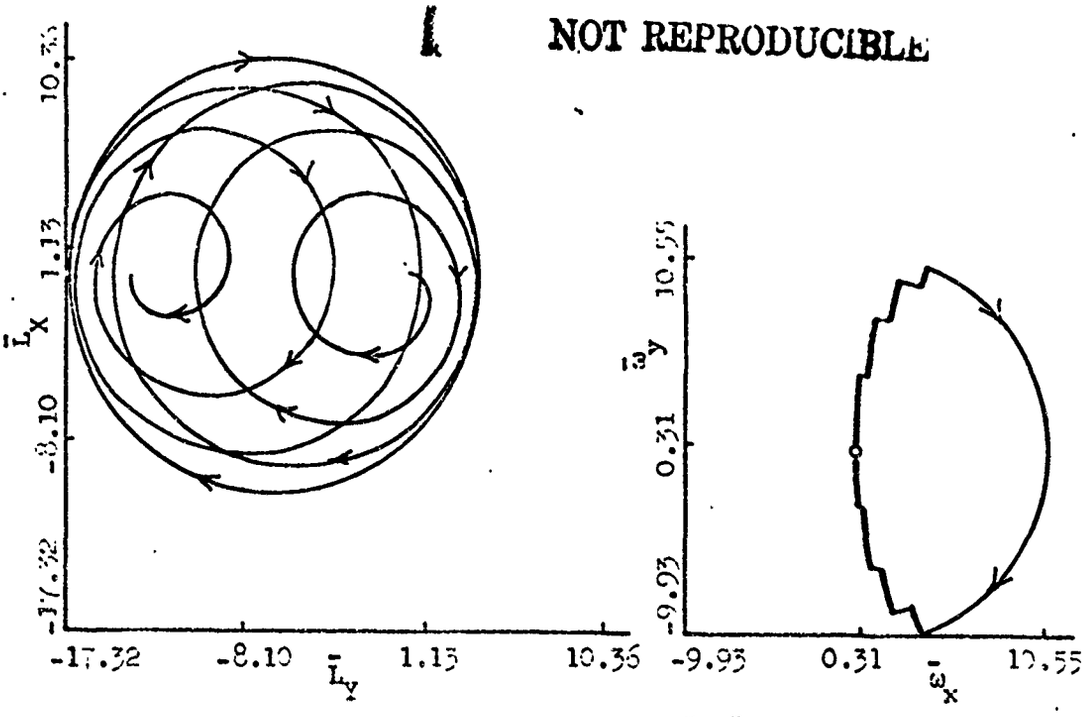

Figure 4.51 Optimal Trajectories in the $(\bar{L}_x\text{-}\bar{L}_y)$ and $(\bar{\omega}_x\text{-}\bar{\omega}_y)$ Planes for $\bar{L}_y = 14$, $\beta_o = 0$, $\gamma = 0.03$, 1-jet

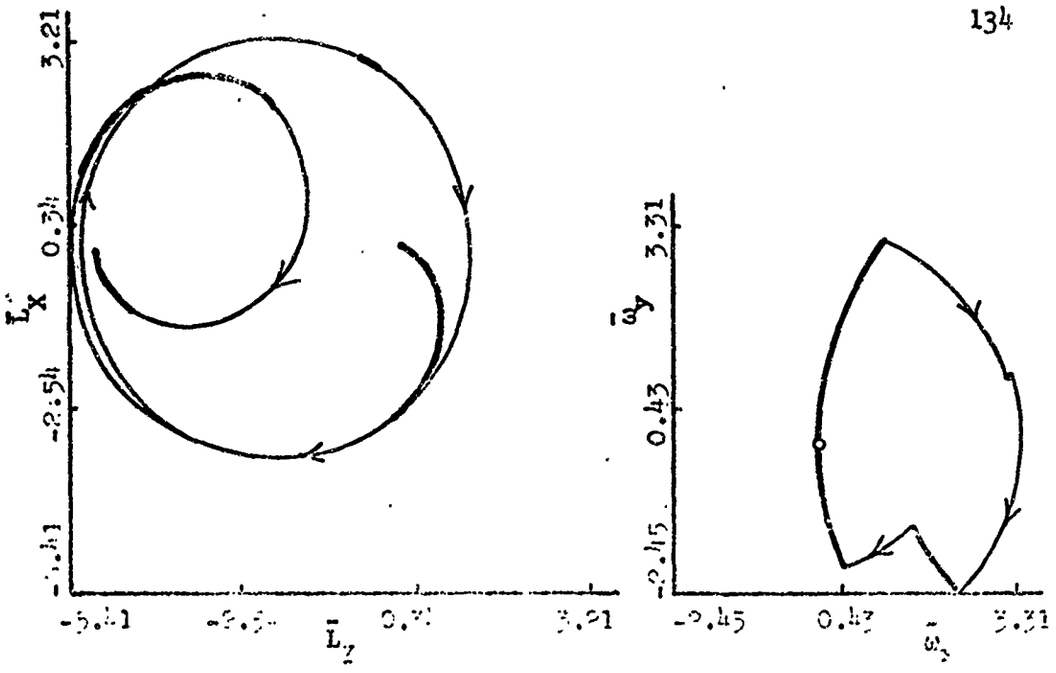

Figure 4.52 Optimal Trajectories in the $(\bar{L}_x\text{-}\bar{L}_y)$ and $(\bar{\omega}_x\text{-}\bar{\omega}_y)$ Planes for $\bar{L}_y = 5$, $\beta_o = 0$, $\gamma = 0.2$, 4-jet

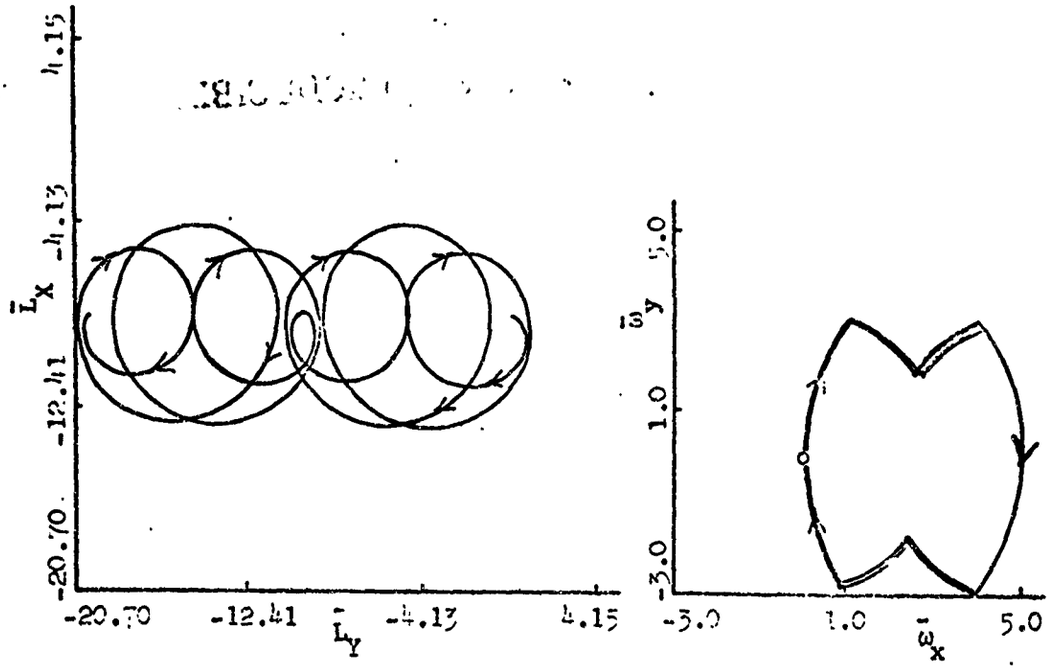

Figure 4.53 Optimal Trajectories in the $(\bar{L}_x\text{-}\bar{L}_y)$ and $(\bar{\omega}_x\text{-}\bar{\omega}_y)$ Planes for $\bar{L}_y = 10$, $\beta_o = 0$, $\gamma = 0.2$, 4-jet

CHAPTER 5

OPTIMAL CONTROL FOR JETS FIXED TO A NON-SPINNING PLATFORM

The controller configuration considered in this chapter is depicted in Figures 1.1.E and 5.1. As shown, the basic spacecraft consists of two separate sections which are connected at the axis of symmetry by an ideal (frictionless) bearing. The front section has been spun up to provide stability. The aft section which houses the required sensors and four fixed reaction jets has a zero spin rate with respect to the vehicle's axis of symmetry. The control problem is again one of properly orienting the spacecraft with respect to Coordinate System I starting from known initial conditions of the vehicle's attitude and transverse components of angular velocity.

A control system mounted on a non-spinning platform offers several advantages when control is required in inertial space. For example, the de-spun segment of the spacecraft, shown in Figure 5.1, is fixed with respect to Coordinate System II and, therefore, only experiences small changes in attitude with respect to the non-rotating reference frame. Hence, this section of the spacecraft is ideally suited as a platform for mounting attitude sensors. In addition, the optimal control law for the non-spinning jets should be less complex to mechanize than those for the fixed jet controller configurations. If the control jets are attached directly to the spinning vehicle, as in Configurations (B) through (D), then the jet

"on-off" times are explicit functions of the spacecraft's roll rate. In such cases delays in the control loop could conceivably cause considerable error between the desired and actual terminal state of the system.

5.1 Equations of Motion

In this section the dynamical equations for a spinning vehicle are developed when control is provided by four reaction jets mounted on a non-spinning platform. The specific control system considered is shown in relation to Coordinate Systems II and III in Figure 5.1.

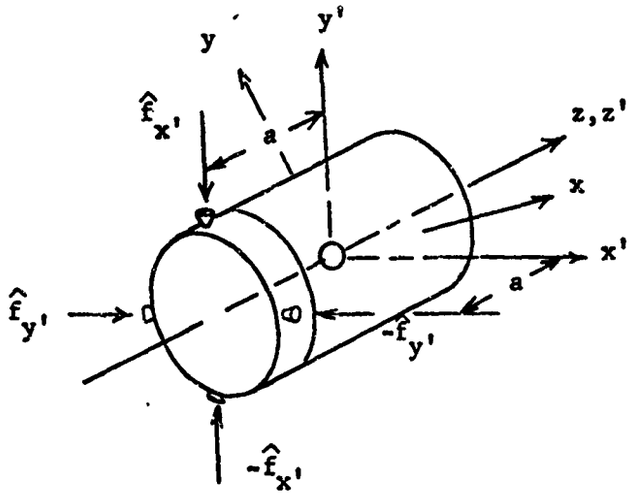

Figure 5.1. Schematic of the Control Jets Fixed to a Non-Spinning Platform

Assume that one pair of jets delivers a thrust $\hat{f}_{x'}(t)$ and the second pair $\hat{f}_{y'}(t)$. Thus, the control moments which appear in equation (2.28) can be expressed as

$$M_{x'}(t) = a \cdot \hat{f}_{x'}(t) \tag{5.1}$$

$$M_{y'}(t) = a \cdot \hat{f}_{y'}(t) \tag{5.2}$$

where (a) is the moment arm. If the thrust of each jet is bounded by F then $|\hat{f}_{x'}(t)| \leq F$ and $|\hat{f}_{y'}(t)| \leq F$. Define the new control variables $u_{x'}(t)$ and $u_{y'}(t)$ by

$$u_{x'}(t) = \frac{\hat{f}_{x'}(t)}{F} \tag{5.3}$$

$$u_{y'}(t) = \frac{\hat{f}_{x'}(t)}{F} \tag{5.4}$$

thus

$$|u_{x'}(t)| \leq 1, \quad |u_{y'}(t)| \leq 1. \tag{5.5}$$

The control moments are now expressed in terms of $u_{x'}(t)$ and $u_{y'}(t)$:

$$M_{x'}(t) = M\, u_{x'}(t) \tag{5.6}$$

$$M_{y'}(t) = M\, u_{y'}(t) \tag{5.7}$$

where $M = a \cdot F$

Combining (2.28), (5.6), and (5.7) yields the controlled equation

$$\frac{d}{d\tau}\begin{bmatrix} \omega_{x'}(\tau) \\ \omega_{y'}(\tau) \\ L_x(\tau) \\ L_y(\tau) \end{bmatrix} = \begin{bmatrix} 0 & -1 & 0 & 0 \\ 1 & 0 & 0 & 0 \\ 0 & 0 & 0 & 0 \\ 0 & 0 & 0 & 0 \end{bmatrix}\begin{bmatrix} \omega_{x'}(\tau) \\ \omega_{y'}(\tau) \\ L_x(\tau) \\ L_y(\tau) \end{bmatrix} + \begin{bmatrix} 1 & 0 \\ 0 & 1 \\ 1 & 0 \\ 0 & 1 \end{bmatrix}\begin{bmatrix} u_{x'}(\tau) \\ u_{y'}(\tau) \end{bmatrix} \tag{5.8}$$

where

$$\hat{\omega}_{x'}(\tau) = \frac{I_z \omega_s \omega_{x'}(\tau)}{M}, \qquad \hat{\omega}_{y'}(\tau) = \frac{I_z \omega_s \omega_{y'}(\tau)}{M}$$

$$\hat{L}_x(\tau) = \frac{I_z \omega_x L_x(\tau)}{IM}, \qquad \hat{L}_y(\tau) = \frac{I_z \omega_s L_y(\tau)}{IM}$$

Note that the control jets are assumed to be aligned with the x'- y' axis; that is, the torque about either the x' or y' axis depends only on the thrust from a single pair of jets. The boundary conditions considered in conjunction with (5.8) are:

$$\hat{\omega}_{x'}(0) = \hat{\omega}_{x'}^{o}, \qquad \hat{\omega}_{x'}(T_E) = 0$$

$$\hat{\omega}_{y'}(0) = \hat{\omega}_{y'}^{o}, \qquad \hat{\omega}_{y'}^{o}(T_E) = 0$$

$$\hat{L}_x(0) = \hat{\omega}_{x'}^{o} + \frac{I_z^2 \omega_s^2 \theta_o \sin \varphi_o}{IM}, \qquad \hat{L}_x(T_E) = \frac{I_z^2 \omega_s^2 \theta_f \sin \varphi_f}{IM} = \hat{L}_x \tag{5.9}$$

$$\hat{L}_y(0) = \hat{\omega}_{y'}^{o} - \frac{I_z^2 \omega_s^2 \theta_o \cos \varphi_o}{IM}, \qquad \hat{L}_y(T_E) = \frac{I_z^2 \omega_s^2 \theta_f \cos \varphi_f}{IM} = \hat{L}_y$$

Solving (5.8) for $\hat{\omega}_{x'}(T_E)$, $\hat{\omega}_{y'}(T_E)$, $\hat{L}_x(T_E)$, and $\hat{L}_y(T_E)$ subject to (5.9) yields the following set of governing equations which must be satisfied by the steering functions $u_{x'}(\tau)$ and $u_{y'}(\tau)$:

$$\int_0^{T_E} [u_{x'}(\tau) \cos\tau + u_{y'}(\tau) \sin\tau] d\tau + \hat{\omega}_{x'}^{o} = 0 \tag{5.10}$$

$$\int_0^{T_E} [u_{x'}(\tau) \sin\tau - u_{y'}(\tau) \cos\tau] d\tau + \hat{\omega}_{y'}^{o} = 0 \tag{5.11}$$

$$\int_0^{T_E} u_{x'}(\tau)d\tau + \hat{L}_x(0) = \hat{L}_x \tag{5.12}$$

$$\int_0^{T_E} u_{y'}(\tau)d\tau + \hat{L}_y(0) = \hat{L}_y \tag{5.13}$$

Thus, for those initial and final values of the state variables given by (5.9), the two point boundary value problem is completely specified by the physical parameters $\hat{\omega}_{x'}^{o}$, $\hat{\omega}_{y'}^{o}$, $\hat{L}_x$, and $\hat{L}_y$ and $\theta_o = 0$ (or by a similar set when $\theta_f = 0$). The mathematical problem is now one of selecting from among the admissible controls that control which drives the system from a given initial state to the given terminal state in less time than any other admissible control.

Since the aim of this study is to investigate the characteristics of the optimal control in terms of the system description and boundary conditions, the two point boundary value problem must be solved repeatedly as changes are made in the physical parameters. One approach for reducing the resulting computational task is to assume that the initial transverse components of angular velocity are zero. This will be the case in a reacquisition maneuver when the vehicle is not nutating at the time control is applied. By making this assumption we are then able to plot minimum time isochrones in the $(\hat{L}_x - \hat{L}_y)$ plane with a reasonable expenditure of computer time.

5.2 Some Symmetry Properties of the Control

Controls which satisfy the governing equations, (5.10) through (5.13), when $\hat{\omega}_{x'}^{o} = \hat{\omega}_{y'}^{o} = 0$, whether they are admissible or not, have

certain symmetry properties when referenced to the de-spun coordinate system. That is, if a control has been found which satisfies (5.10) through (5.13) for a specific value of the pair $(\hat{L}_x, \hat{L}_y)_i$ then we can exploit certain symmetry properties of the system in order to determine the control corresponding to the pair $(\hat{L}_x, \hat{L}_y)_{i+1}$.

To demonstrate the isomorphic properties of the control we first note that the terminal state of the system can be represented by points in the $(\hat{L}_x - \hat{L}_y)$ plane when $\hat{\omega}^{\circ}_{x'} = \hat{\omega}^{\circ}_{y'} = 0$. For example, in Figure 5.2 the point p_1 corresponds to a specific change in the normalized angular momentum as given by the pair $(\hat{L}_x, \hat{L}_y)_{p_1}$. Also note that the $(\hat{L}_x, \hat{L}_y)$ plane has been divided into a number of regions. First, the natural division by the $\hat{L}_x$ and $\hat{L}_y$ axis results in four quadrents denoted by Q_1 through Q_4. Then Q_1 is divided by the straight line $\hat{C}$ into regions denoted by r_1 and r_2.

A point $\hat{p}_1 \epsilon r_2$ is defined as being "symmetric" to $p_1 \epsilon r_1$ when the following relations are satisfied:

$$\left(\hat{L}_x\right)_{\hat{p}_1} = \left(\hat{L}_y\right)_{p_1}$$

$$\left(\hat{L}_y\right)_{\hat{p}_1} = \left(\hat{L}_x\right)_{p_1} \qquad (5.14)$$

Further, the points $p_2 \epsilon Q_2$, $p_3 \epsilon Q_3$, and $p_4 \epsilon Q_4$ are defined as being "similar" to $p_1 \epsilon Q_1$ when the corresponding pairs $(\hat{L}_x, \hat{L}_y)_{p_i}$ satisfy

$$\left(\hat{L}_x\right)_{p_{i+1}} = -\left(\hat{L}_y\right)_{p_i}$$

$$i = 1, 2, 3 \qquad (5.15)$$

$$\left(\hat{L}_y\right)_{p_{i+1}} = \left(\hat{L}_x\right)_{p_i}$$

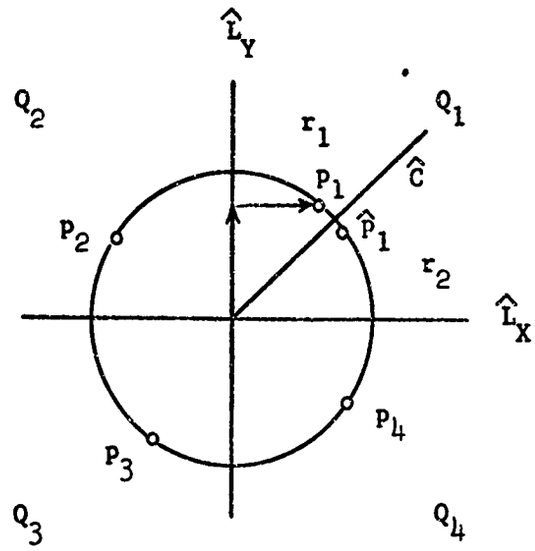

Figure 5.2. An Example of Symmetric and Similiar Terminal State Points

With these definitions we are now able to express certain relations between the controls corresponding to terminal states which lie in quadrents Q_1 through Q_4. First, if the control $(\underline{u}(\tau), T_E)_{p_1}$ satisfies equations (5.10) through (5.13) when the pair $(\hat{L}_x, \hat{L}_y)_{p_1}$ defines a point in r_1 then the control corresponding to a symmetry point in r_2 is defined by the following relations:

$$\left(u_x'(\tau)\right)_{\hat{p}_1} = \left(u_y'(\tau')\right)_{p_1}$$

$$\left(u_y'(\tau)\right)_{\hat{p}_1} = \left(u_x'(\tau')\right)_{p_1} \qquad (5.16)$$

$$(T_E)_{\hat{P}_1} = (T_E)_{P_1}, \quad \tau' = (T_E)_{P_1} - \tau$$

Verification of (5.16) is direct in that equations identical in form to (5.10) through (5.13) are obtained if the mathematical manipulations indicated by (5.14) and (5.16) are carried out. Second, if the control $(\underline{u}(\tau), T_E)_{P_1}$ satisfies Equation (5.10) through (5.13) when the pair $(\hat{L}_x, \hat{L}_y)_{P_1}$ defines a point in Q_1 then the controls corresponding to "similar" terminal state points in Q_2, Q_3 and Q_4 are given by:

$$\begin{aligned} \left(u_{x'}(\tau)\right)_{P_{i+1}} &= -\left(u_{y'}(\tau)\right)_{P_i} \\ \left(u_{y'}(\tau)\right)_{P_{i+1}} &= \left(u_{x'}(\tau)\right)_{P_i} \qquad i = 1, 2, 3 \\ (T_E)_{P_{i+1}} &= (T_E)_{P_i} \end{aligned} \tag{5.17}$$

Verification of (5.17) is also direct; the mathematical procedure follows that for (5.16). The consequence of Equations (5.16) and (5.17) is one of achieving a substantial reduction in the computer time required to plot minimum time isochrones in the $(\hat{L}_x - \hat{L}_y)$ plane. Thus, due to the symmetry of the isochrones only those terminal states which lie in r_1 were considered during the flooding process.

5.3 A Necessary Condition for Time-Optimality

The maximum principle was used to determine necessary conditions for the optimal steering functions. Forming the Hamiltonian

$$H = P_o + P_1(\tau)[\,-\omega_{y'}(\tau) + u_{x'}(\tau)\,] + P_2(\tau)[\,{}_{x'}(\tau) + u_{y'}(\tau)]$$

$$+ P_3(\tau)\,u_{x'}(\tau) + P_4(\tau)\,u_{y'}(\tau). \tag{5.18}$$

Maximization of the Hamiltonian subject to the constraints given by (5.5) occurs when

$$u_{x'}(\tau) = \text{SGN}\left[s_{x'}(\tau)\right] \tag{5.19}$$

$$u_{y'}(\tau) = \text{SGN}\left[s_{y'}(\tau)\right] \tag{5.20}$$

where

$$s_{x'}(\tau) = P_1(\tau) + P_3(\tau) \tag{5.21}$$

$$s_{y'}(\tau) = P_2(\tau) + P_4(\tau). \tag{5.22}$$

The adjoints, $P_1(\tau)$ through $P_4(\tau)$, are solutions to the differential equation

$$\frac{d}{d\tau}\begin{bmatrix} P_1(\tau) \\ P_2(\tau) \\ P_3(\tau) \\ P_4(\tau) \end{bmatrix} = \begin{bmatrix} 0 & -1 & 0 & 0 \\ 1 & 0 & 0 & 0 \\ 0 & 0 & 0 & 0 \\ 0 & 0 & 0 & 0 \end{bmatrix}\begin{bmatrix} P_1(\tau) \\ P_2(\tau) \\ P_3(\tau) \\ P_4(\tau) \end{bmatrix} \tag{5.23}$$

and can be written in vector form as

$$\begin{bmatrix} P_1(\tau) \\ P_2(\tau) \\ P_3(\tau) \\ P_4(\tau) \end{bmatrix} = \begin{bmatrix} \cos\tau & -\sin\tau & 0 & 0 \\ \sin\tau & \cos\tau & 0 & 0 \\ 0 & 0 & 1 & 0 \\ 0 & 0 & 0 & 1 \end{bmatrix} \begin{bmatrix} P_1^o \\ P_2^o \\ P_3^o \\ P_4^o \end{bmatrix} \tag{5.24}$$

In view of (5.24) the switching functions become:

$$s_{x'}(\tau) = \alpha_1 \cos(\tau + \alpha_2) + \alpha_3 \tag{5.25}$$

$$s_{y'}(\tau) = \alpha_1 \sin(\tau + \alpha_2) + \alpha_4 \tag{5.26}$$

The following remarks are a consequence of the necessary condition:

1. Each component of the control vector assumes an extreme value providing α_1 and α_3 (α_2 and α_4) are not simultaneously zero over a finite period of time. In the case when either $s_{x'}(\tau) \equiv 0$ or $s_{y'}(\tau) \equiv 0$ for some interval $\tau_1 \leq \tau \leq \tau_2$ in $(0, T_E)$ then the SGN[ ] function is not defined over $[\tau_1, \tau_2]$. Therefore, the maximum principle provides no information as to the structure of the optimal control.
2. Providing $|\alpha_1| > |\alpha_3|$ ($|\alpha_1| > |\alpha_4|$) then each component of the control vector $\underline{u}(\tau)$ can remain constant over $[\tau_1, \tau_2] < 2\pi$. If $|\alpha_1| < |\alpha_3|$ ($|\alpha_1| < |\alpha_4|$) then one or both components of $\underline{u}(\tau)$ will remain constant over the interval $[0, T_E]$. As will be shown presently, the relative magnitudes of the components of the costate vector $\underline{\alpha}$ have a very profound influence on the behavior of the iterative procedure that was employed to compute minimum time controls.

5.4 Realization of the Optimal Steering Functions

In this chapter, as in previous ones, our goal is to investigate the characteristics of the optimal steering functions through the use of a flooding technique. As described in Chapter 4, flooding involves the computation of optimal controls corresponding to specific sets of boundary conditions - in this case ordered pairs of the dimensionless angular momentum components $\hat{L}_x$ and $\hat{L}_y$ (the initial and final nutation rate is assumed to be zero). In the previous chapter, the basic algorithm described in Appendix A, with modifications as given in Appendix B, proved to be an efficient method for generating solutions to a large number of two point boundary value problems. However, a direct application of the algorithm to the control problem considered in this chapter is not possible since the controlled system is not normal. In a non-normal system the existence of unique optimal controls cannot be guaranteed; in fact, the optimal controls corresponding to certain boundary conditions could very well be singular. For example, if $\alpha_1 = \alpha_3 = 0$ or $\alpha_1 = \alpha_4 = 0$ then either $u_x^*,(\tau)$ or $u_y^*,(\tau)$ is singular; in the sequel it will be shown that the remaining component must: (1) assume an extreme value, and (2) remain constant over the interval $(0, T_E^*)$.

At this point we should note that the optimal control for a non-normal system is not necessarily singular. In fact, in the literature a number of optimal control problems have been considered wherein the state space is divided into regions corresponding to those initial (terminal) state points for which the optimal control is singular. For Control System (E) we find, after examining Equations

(5.10) through (5.13), (5.19) and (5.20), that there exists terminal states which cannot be reached if singular control is applied to the system. In such cases the optimal steering functions are given by (5.19) and (5.20); therefore, the iterative procedure described in Appendix A can be employed providing the basic algorithm is modified to account for the peculiar characteristics of $s_{x'}(\tau)$ and $s_{y'}(\tau)$. Such modifications are made to ensure that the proper number of switching points occur in the interval $(0, T_E)$ at each step in the iterative process. Recalling the control problem considered in Chapter 4, we find that the computational process failed to converge when the third switching point was lost from the interval (0, T). Here, due to the particular form of $s_{x'}(\tau)$ and $s_{y'}(\tau)$ it is possible to lose all the switching points during the $k^{\underline{th}}$ cycle of the iterative process if $|\alpha_1|_k < |\alpha|_k$ and $|\alpha_1|_k < |\alpha_4|_k$. Consequently the basic algorithm was modified to prevent this situation for occuring; the details are discussed in Appendix B. However, prior to any numerical computation the question concerning the existence of singular optimal controls had to be resolved. Therefore, in the following sections a necessary condition for extremal singular control is discussed, the general form of a singular steering law is developed, and an effort is made to determine analytically those sets of therminal states for which the optimal control is singular.

5.4.1 Singular Control

For the control system considered in this chapter it is possible to test in a systematic manner for the existance of singular extremal

controls. To do this we make use of the Hamiltonian which is a necessary condition for time-optimality. If either component of the control vector is singular over an interval $[\tau_1, \tau_2] \subset [0, T_E]$ then the corresponding switching function must be zero over this interval. Suppose that $s_{x'}(\tau) \equiv 0$ for $\tau \in [0, T_E]$. Since the system is autonomous and the final time is free, the Hamiltonian must remain constant over this interval; and in fact

$$H = P_o + P_4^o u_{y'}(\tau) = 0 \tag{5.27}$$

If $P_o = 0$ then either $P_4^o = 0$ or $u_{y'}(\tau) = 0$ for $\tau \in [0, T_E]$. $P_4 \neq 0$ since the vector $\underline{P}(\tau)$ cannot be zero; from the maximum principle we know that the necessary condition for optimality implies the existence of a non-zero adjoint vector. If $u_{y'}(\tau) = 0$ for $\tau \in [0, T_E]$ then almost every point in the $(\hat{L}_x - \hat{L}_y)$ plane is not reachable from the origin (or recoverable with respect to the origin). Therefore, in general, $P_o \neq 0$. Solving (5.27) for $u_{y'}(\tau)$ gives

$$u_{y'}(\tau) = -\frac{P_o}{P_4} \tag{5.28}$$

Thus if the extremal control is singular then $u_{y'}(\tau) = \text{constant}$. This allows us to integrate (5.13) with the following result

$$T_E^* = \left| \frac{\hat{L}_y}{u_{y'}} \right| . \tag{5.29}$$

Hence, T_E will be a minimum when $u_{y'}$ assumes an extreme value (i.e., $u_{y'}^*(\tau) = \pm 1$). Note that the necessary condition is also satisfied since (5.27) is a maximum when $u_{y'}(\tau) = \pm 1$. Therefore, if a point

in the $(\hat{L}_x - \hat{L}_y)$ plane can be reached in finite time when the system is driven by control of the form:

$$\left[\begin{array}{l} u_x(\tau) = \text{piecewise continuous function of } \tau \text{ subject to } u_x(\tau) \leq 1 \\ u_y(\tau) = \pm 1, \end{array}\right]$$

then the minimum terminal time is given by

$$T_E^* = |\hat{L}_y| . \tag{5.30}$$

The result can be readily generalized to include situations when $s_y(\tau) \equiv 0$ for $\tau \in [0, T_E]$. In this case the control becomes:

$$\left[\begin{array}{l} u_x(\tau) = \pm 1 \\ u_y(\tau) = \text{piecewise continuous function of } \tau \text{ subject to } u_y(\tau) \leq 1 \end{array}\right]$$

and the minimum terminal time is given by

$$T_E^* = |\hat{L}_x| . \tag{5.31}$$

Thus, it is apparent that T_E^* depends upon the relative magnitudes of $\hat{L}_x$ and $\hat{L}_y$. That is, if the terminal state point is reachable with singular control then the terminal time is determined by the larger member of the pair $(\hat{L}_x, \hat{L}_y)$.

In the previous discussion one should note that (5.28) is only a necessary condition for singular control. In practice there may be terminal states for which one component of the optimal control vector

is constant and the remaining component is bang-bang and switches according to either $s_{x'}(\tau)$ or $s_{y'}(\tau)$. Such a control is given by the maximum principle if $|\alpha_1| < |\alpha_3|$ ($|\alpha_1| < |\alpha_4|$)and $|\alpha_1| > |\alpha_4|$ ($|\alpha_1| > |\alpha_3|$) respectively. Thus, for certain terminal states true singular control may not be required however, the implication of the necessary condition for singular control, or the non-normality of the system, is the non-uniqueness of that component of the control vector which does not remain constant over the interval $[0, T_E^*]$. This concept will be discussed further in the following section where both the flooding procedure used to determine the minimum time isochrones and the numerical results are summarized.

5.4.2 The Synthesis of Optimal Controls for a Non-Normal System

The iterative procedure described in Appendix A can be employed when the system is non-normal providing we are able to define qualitatively those sets of terminal state points for which the optimal control is non-singular.[1] For the system considered here it is possible to determine whether the optimal control corresponding to certain terminal states is singular or non-singular by simply testing to see if the control in question satisfies Equations (5.10) through (5.13). The specific details of such an analytic investigation are discussed in the following paragraphs.

In section 5.2 we found that the optimal control possesses certain symmetry properties. Therefore in the following discussion

---

[1] Subsequent to the work performed in this report a method was developed for normalizing non-normal, autonomous, linear systems[20].

only those controls corresponding to terminal state points in r_1 are considered. The particular points chosen are shown in Figure 5.3 Our objective is now to derive the optimal control(s) corresponding to points p_1 thru p_8; and, in addition, to determine the mathematical and computational significance of regions r_1^1, r_1^2, and r_1^3.

The time-optimal controls corresponding to $\hat{L}_x = m\pi$, $\hat{L}_y = m\pi$, $m = 2, 4, 6, 8, \ldots$, (e.g., p_1 and p_3) are unique and can be written as follows: $u_x^*(\tau) = 1$, $u_y^*(\tau) = 1$, $T_E^* = m\pi$ for $\tau\ [0, T_E^*]$. Control of this form is given explicitly by Equations (5.25) and (5.26) when $|\alpha_1| < |\alpha_3|$, $|\alpha_1| < |\alpha_4|$, $\alpha_3 > 0$ and $\alpha_4 > 0$. However, the steering function can also be classified as singular since, for example, we can choose $\alpha_1 = \alpha_3 = 0$ and $\alpha_4 > 0$; in this case we are free to select $u_x^*(\tau)$ from the admissible controls, hence, $u_x^*(\tau) = 1$ for $\tau\epsilon[0, T_E^*]$.

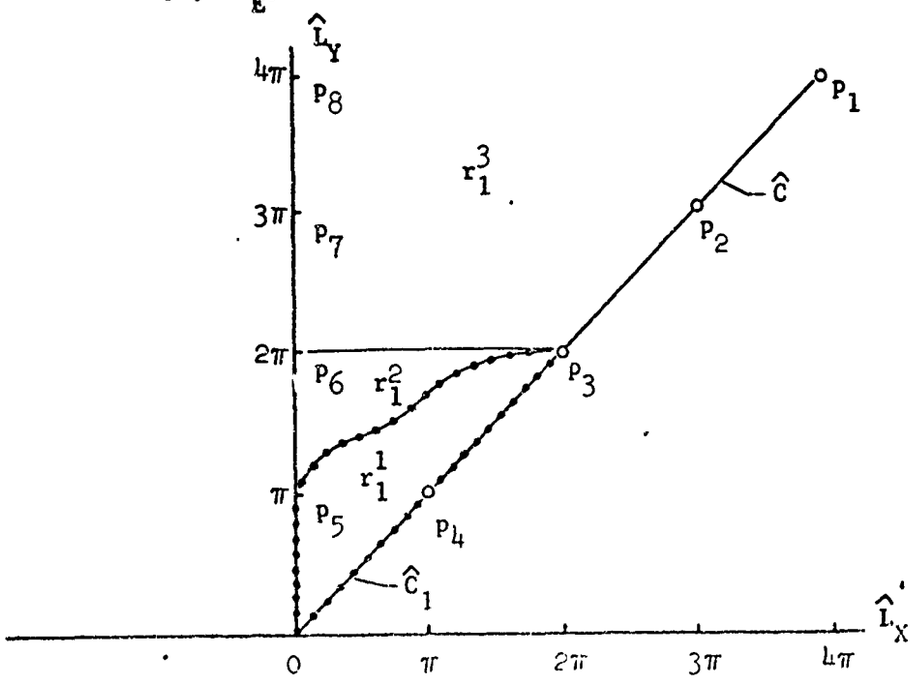

Figure 5.3. Regions of Singular and Non-Singular Optimal Control

The points p_6, p_7, p_8 are representative of those terminal states for which the optimal control is not unique. For example, the following combinations of control laws satisfy equations (5.10) through (5.13) when $\hat{L}_x = 0$, $\hat{L}_y = m\pi$, $m = 2, 4, 6, 8, \ldots$.

1. $u_x^*(\tau) = 0$, $u_y^*(\tau) = 1$, $T_E^* = m\pi$

2. $$u_x^*(\tau) = \left\{ \begin{array}{l} \pm 1 \text{ for } 0 \leq \tau \leq \frac{m}{4} \\ \mp 1 \text{ for } \frac{m}{4} < \tau \leq \frac{3m}{4} \\ \pm 1 \text{ for } \frac{3m}{4} < \tau \leq m\pi \end{array} \right\}, \quad u_y^*(\tau) = 1, \quad T_E^* = m$$

The terminal state represented by p_5 is unique in that it represents the smallest value of $\hat{L}_y$, when $\hat{L}_x = 0$, for which equations (5.10) through (5.13) are satisfied by singular control. In order to verify this claim we proceed as follows: First, if $u_y^*(\tau) = 1$ for all $\tau \in [0, T_E^*]$ and $\hat{L}_y < \pi$ then from (5.13) we find that $T_E^* < \pi$. Also, if the transverse components of angular velocity are to be zero at $\tau = T_E^*$ then:

$$\int_0^{T_E^*} u_x(\tau) \cos\tau \, d\tau = \int_0^{T_E^*} \sin\tau \, d\tau \tag{5.32}$$

$$\int_0^{T_E^*} u_x(\tau) \sin\tau \, d\tau = -\int_0^{T_E^*} \cos\tau \, d\tau \tag{5.33}$$

It is apparent that (5.32) is not satisfied by an admissible $u_x(\tau)$ when $\pi/2 < T_E < \pi$ and that (5.33) is not satisfied when $0 < T_E < \pi/2$. Therefore, the optimal steering functions corresponding to $\hat{L}_x = 0$,

$0 < \hat{L}_y < \pi$, must be defined by (5.25) and (5.26).

Following the procedure outlined in the previous paragraph we can also show that terminal state points defined by the curve $\hat{C}$, when $\hat{L}_y < \pi$, are unreachable from the origin when the control is singular.

In view of the previous discussions the following generalizations concerning the optimal control are conjectured. First, there is at least one set of terminal state points in r_1 which cannot be reached when the control is singular. One possible boundary of such a set is indicated by the closed curve $\hat{C}_1$ in Figure 5.3; the set is denoted by r_1^1. Since singular steering to points in r_1^1 is not possible the optimal control must then be given explicitly by Equations (5.25) and (5.26). A second set, denoted by r_1^2, contains those terminal state points for which the minimum terminal time is given by $T_E^* = |\hat{L}_y|$ and $|\hat{L}_y| \leq 2\pi$. Here, we are assuming of course that $u_{y'}^*(\tau) = 1$ for $\tau \in [0, T_E^*]$. In general, we find that if control of the form $u_{x'}(\tau) = \pm 1$, $u_{y'}(\tau) = 1$, for $\tau \in [0, T_E^*]$ is to satisfy Equations (3.10) through (3.13) when the pair $(\hat{L}_x, \hat{L}_y)$ defines a point in r_1^2 then $u_{x'}^*(\tau)$ must change sign at least three times in the interval $(0, T_E^*)$. Examining the switching functions we note that $u_{y'}(\tau) = 1$ if $|\alpha_1| < |\alpha_4|$ and $\alpha_4 > 0$. However, in view of the functional form of $s_{x'}(\tau)$, it is evident that $u_{x'}(\tau)$ can switch sign at most twice when $0 < \tau \leq 2\pi$. Therefore, the control must be singular; that is, $s_{x'}(\tau) = 0$ for $\tau \in [0, T_E^*]$. This allows us to choose a particular $u_{x'}^*(\tau)$ from among the admissible controls which in conjunction with $u_{y'}^*(\tau) = 1$ satisfies the boundary conditions. Since the system is not normal $u_{x'}^*(\tau)$ may not be unique; however,

in any event, the control will be optimal since $T_E^* = \hat{L}_y$ when the control is singular.

Finally, we conjecture that the characteristics of the optimal control corresponding to terminal state points in r_1^3 are very similar to those for points in r_1^1 and r_1^2. That is, there are sets of points in r_1^3 for which the optimal control is given explicitly by $s_{x'}(\tau)$ and $s_{t'}(\tau)$ (e.g., p_2) and those for which the optimal control is singular (e.g., p_6, p_7, p_8).

5.4.3 A Numerical Procedure for Computing Optimal Controls

In section 5.4.2 we showed that there exists terminal state points which cannot be reached from the origin when singular control is applied to the system. Therefore, the optimal control corresponding to such states must be defined by (5.25) and (5.26). In such cases the change in state of the system and the optimal control can be related by an expression of the form

$$\underline{\chi}(T_E^*) = \underline{F}(\underline{\alpha}, T_E^*). \tag{5.34}$$

If we assume that the terminal state for which the optimal control is required does not lie on a switching surface which contains time-optimal trajectories (i.e., if the total number of switching in $(0, T_E^*)$ is at least three) then the numerical procedure described in Appendix A with those modifications indicated in Appendix B can be employed to iterate for the pair $(\underline{\alpha}, T_E^*)$. The algorithm is then applied repeatedly, as described in the following paragraph, to solve a selected number of two point boundary value problems and in

this manner provide the information necessary to plot minimum time isochrones in the $(\hat{L}_x - \hat{L}_y)$ plane.

By following the guidelines discussed in 5.4.2 it was found that the iterative procedure could by successfully employed to solve the required number of two point boundary value problems. The following outline summarizes the flooding procedure:

1. The terminal state $\hat{L}_x = \hat{L}_y = \pi$ was chosen as the starting point for flooding process; from the previous discussion know that this point cannot be reached from the origin with singular control. A guess was made for the pair $(\underline{\alpha}, T_E^*)_{p_4}$, and the iterative procedure was then used to improve this guess until the boundary conditions were satisfied.
2. Systematic changes were then made in $\hat{L}_x$ by applying the rule: $(\hat{L}_x)_{i+1} = (\hat{L}_x)_i - \Delta\hat{L}_x$ where $\Delta\hat{L}_x$ is a small ($\Delta\hat{L}_x \approx 0.5$) positive perturbation in $\hat{L}_x$. Using $(\underline{\alpha}, T_E^*)_i$ as a nominal control the iterative procedure was then applied successively to compute each pair $(\underline{\alpha}, T_E^*)_{i+1}$. This process was terminated when either $u_y(\tau) = 1$ for τ [0, T^*] or $(\hat{L}_x)_{i+1} = 0$.
3. The procedure described in 2 was then repeated for new starting points on the curve $\hat{C}$. First, perturbations were made in $\hat{L}_x$ and $\hat{L}_y$ according to the rule: $(\hat{L}_x)_{i+1} = (\hat{L}_x)_i - \Delta\hat{L}_x$, $(\hat{L}_y)_{i+1} = (\hat{L}_y)_i - \Delta\hat{L}_y$; starting from $\hat{L}_x = \hat{L}_y = \pi$ and terminating when $\hat{L}_x = \hat{L}_y = 0.1$. Then, similar perturbations were made starting from $\hat{L}_x = \hat{L}_y = \pi$ and terminating when $\hat{L}_x = \hat{L}_y = 8\pi$. The results of this computation are summarized in Figures 5.4 through 5.6 where minimum time isochrones are plotted in the $(\hat{L}_x - \hat{L}_y)$

plane.

The purpose of Figure 5.4 is to show the characteristics of the optimal control for terminal states in the neighborhood of the origin, specifically for those points which lie within the square defined by the $\hat{L}_x - \hat{L}_y$ axis and the isochrone $T_E^* = 2\pi$. The square is further divided into two regions; as predicted in Section 5.4.2 the optimal controls corresponding to those terminal state points enclosed by the dashed line are non-singular and for points exterior the optimal control is singular. The boundary between the two regions was defined during the flooding process by those values of $\hat{L}_x$ and $\hat{L}_y$ for which $u_y^*,(\tau)$ first became a constant, $u_y^*,(\tau) = 1$ for $\tau\epsilon[0,T_E^*]$. Optimal controls for almost every point in the singular region of r_1 can be determined numerically by setting

$$u_x,(\tau) = \begin{bmatrix} \pm 1 \text{ for } 0 < \tau < \tau_1 \\ \mp 1 \text{ for } \tau_1 < \tau < \tau_2 \\ \pm 1 \text{ for } \tau_2 < \tau < \tau_3 \\ \mp 1 \text{ for } \tau_3 < \tau < T_E^* \end{bmatrix}, \quad u_y,(\tau) = T_E^* = \hat{L}_y$$

and then iterating on the normalized switching times τ_1, τ_2 and τ_3 until equations (5.10) through (5.12) are satisfied.

In Figure 5.5 minimum time isochrones are plotted in that region of the $(\hat{L}_x - \hat{L}_y)$ plane defined by the $\hat{L}_x$-$\hat{L}_y$ axis and the isochrone $T_E^* = 4\pi$. Again, the dashed line indicates the boundary between the terminal states for which the optimal control is non-singular and those external points for which the optimal control is singular. Note that the point p_3 which also appears in Figure 5.3

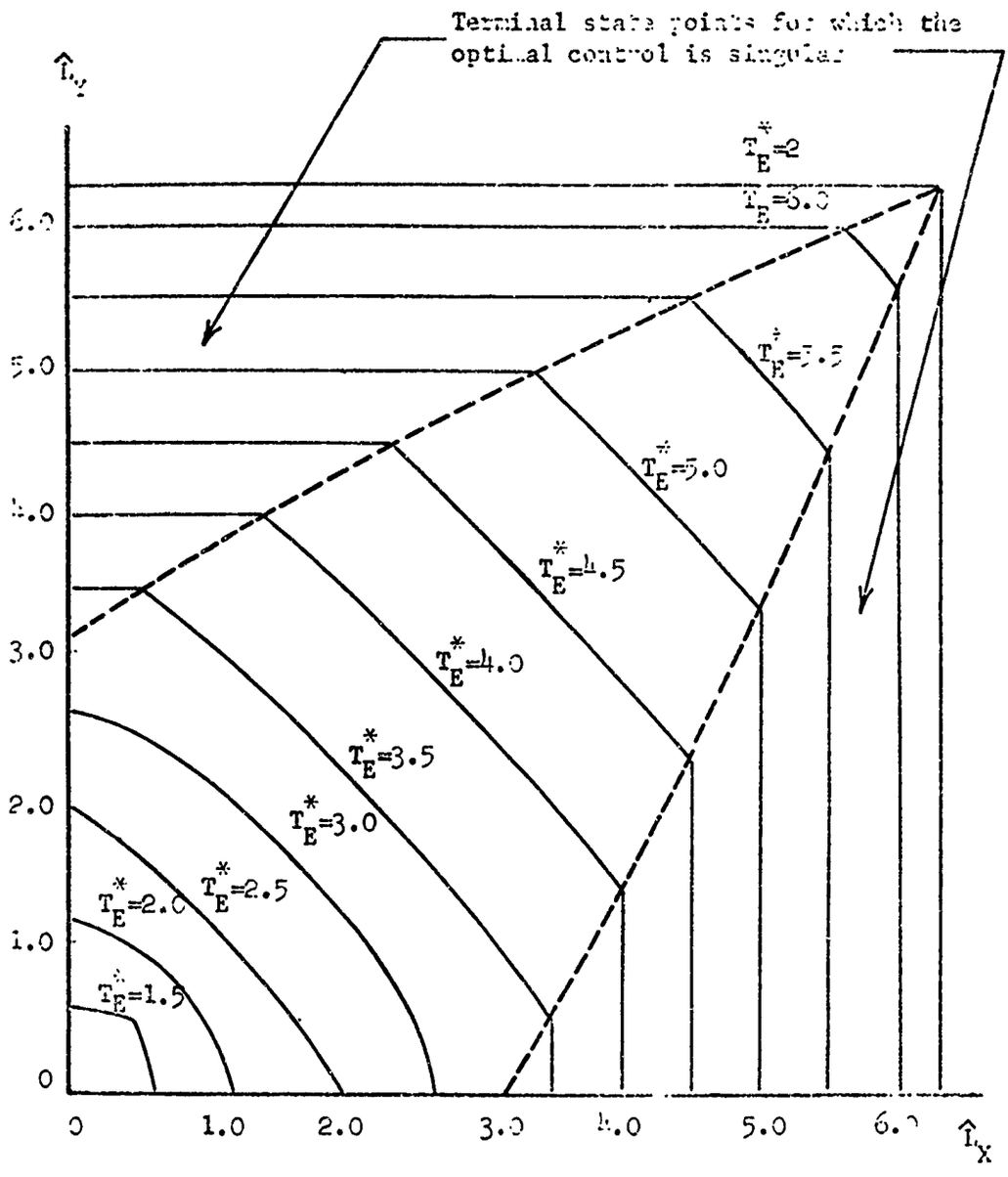

Figure 5.4 Minimum Time Isochrones in Q_1, $\hat{L}_X \leq 2\pi$, $\hat{L}_Y \leq 2\pi$

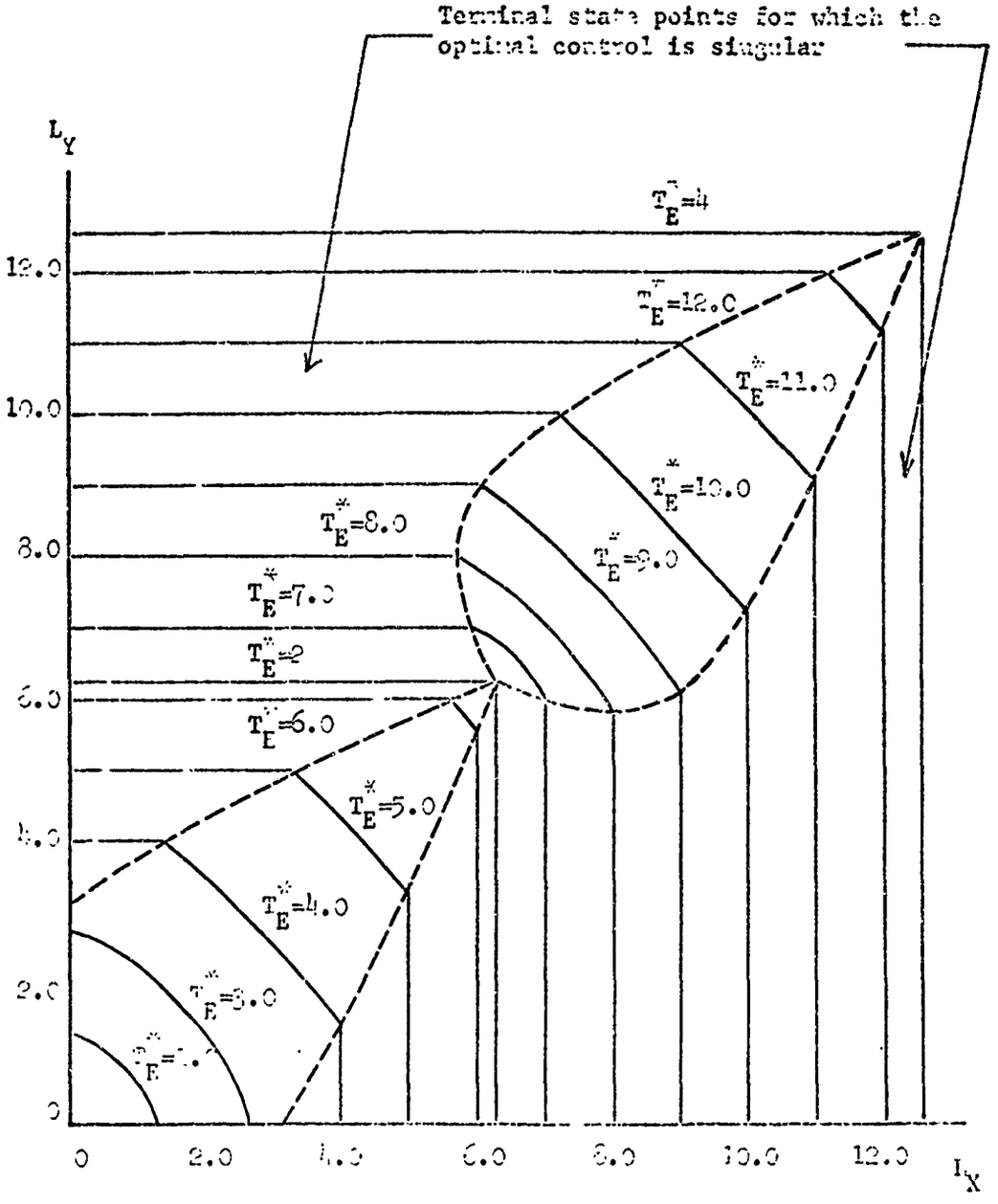

Figure 5.5 Minimum Time Isochrones in Q_-, $L_X \leq 4\pi$, $L_Y \leq 4\pi$

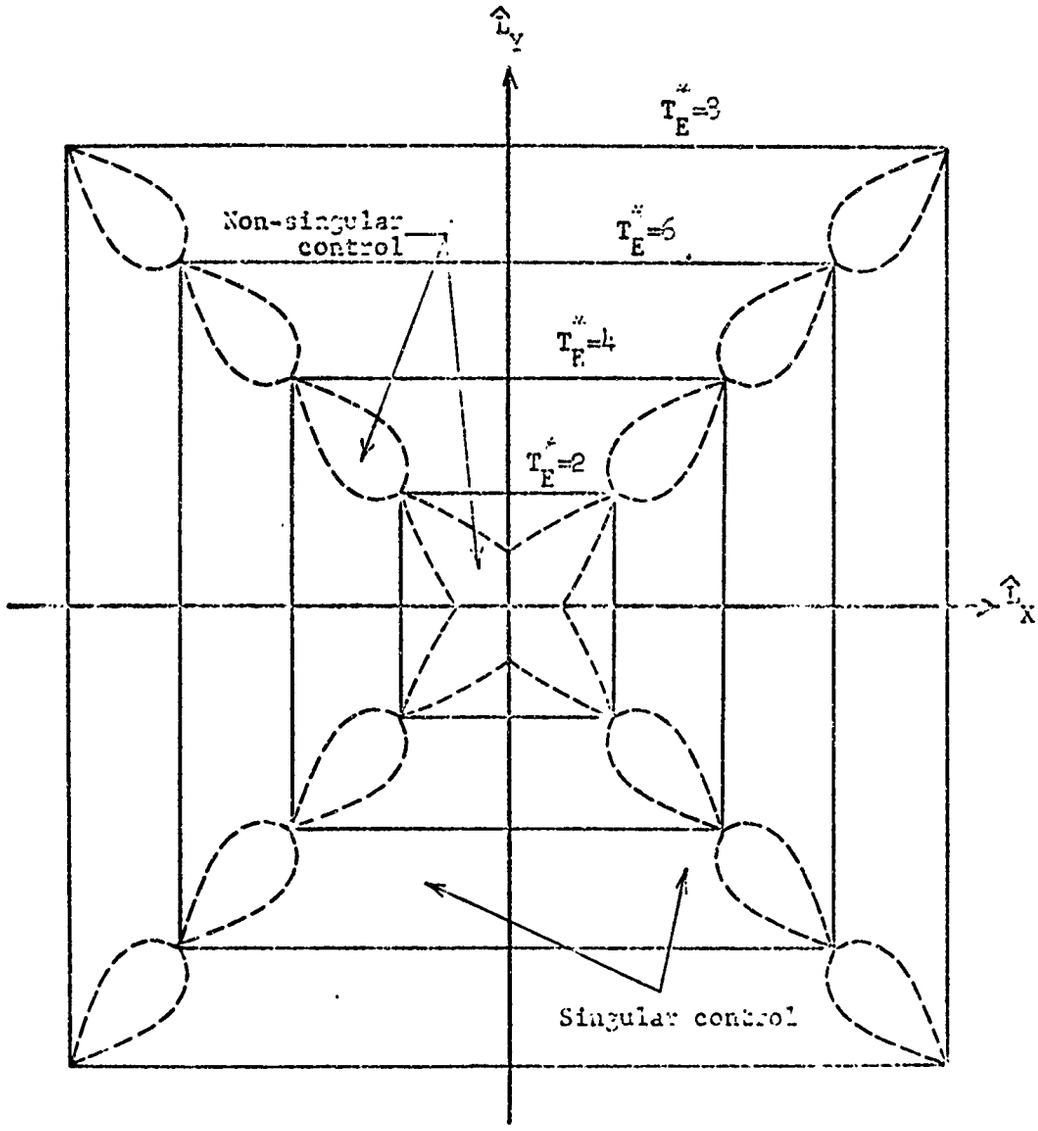

Figure 5.6 Identification of those Terminal State Points for which the Optimal Control is Singular

is unique in that the optimal steering functions ($u_x^*(\tau) = 1$, $u_y^*(\tau) = 1$, for $\tau\epsilon[0, T_E^*]$) corresponding to this terminal state can be expressed in two different forms. First, by singular control when $s_x(\tau) \equiv 0$ and $\alpha_4 > 0$ or $s_y(\tau) \equiv 0$ and $\alpha_3 > 0$ for $\tau\epsilon [0, T_E^*]$. Thus we are free to choose either $u_x^*(\tau)$ or $u_y^*(\tau)$; in this case the obvious choices are $u_x^*(\tau) = 1$ or $u_y^*(\tau) = 1$ for $\tau\epsilon[0, T_E^*]$. Second, explicitly by $s_x(\tau)$ and $s_y(\tau)$ when $|\alpha_1| < |\alpha_3|$, $\alpha_3 > 0$; and $|\alpha_1| < |\alpha_4|$, $\alpha_4 > 0$.

In Figure 5.6 minimum time isochrones are plotted in the $(\hat{L}_x - \hat{L}_y)$ plane for values of $T_E^* \leq 8\pi$. Note that the sets of terminal state points for which the optimal control is non-singular remain fixed in size and shape and occur repeatedly when $|\hat{L}_x|$ and $|\hat{L}_y|$ are monotone increasing and $|\hat{L}_x|$, $|\hat{L}_y| > 2\pi$.

5.5 Some Comments on the Performance of Control System E

Comparing the optimal control for Jet Configuration (E) to those for Configurations (A) through (D) we find several characteristics which are important insofar as performance is concerned. First, let us consider the "short time" case (i.e., $M \gg I_z\omega_s^2\theta_f$) when control is provided by Configurations (B) and (E). Under such conditions the optimal controls for the two systems are nearly identical. Here we find that the time required to reach a given terminal state will be an absolute minimum when the thrusters are initially oriented at 45° with respect to the required change in angular momentum $I_z\omega_s\theta_f$ for Controller (E) (see Figure 5.4) or nearly 45° for Controller (B). However, as illustrated in Figure

5.4, the initial orientation of the non-spinning platform for which the final time is an absolute minimum is no longer 45° for those terminal states which can be reached optimal steering when $T_E^* \gtrsim 1.5$. In such cases, depending upon the magnitudes of $\hat{L}_x$ and $\hat{L}_y$, both coordinate System II and the control jets should be rotated until the terminal state point lies either on the x' or y' axis or on the boundary which divides the $(\hat{L}_x - \hat{L}_y)$ plane into regions of singular and non-singular control. Note that when $|\hat{L}_x| \geq 2\pi$ and $|\hat{L}_y| \geq 2\pi$ the minimum terminal time is relatively insensitive to changes in the initial position of the jets providing the terminal state point lies within the region of non-signular control. Also note that sets of points for which the optimal control is non-singular remain fixed in size and shape as both $\hat{L}_x$ and $\hat{L}_y$ increase. Therefore, in the limit, as $|\hat{L}_x| \to \infty$ and/or $|\hat{L}_y| \to \infty$ the difference between the absolute minimum final time for a given value of $(\hat{L}_x^2 + \hat{L}_y^2)^{1/2}$ and that final time which results when pre-rotation places the jets at an angle of 45° with respect to $\underline{I_z \omega_s \theta_f}$ becomes small when compared to t_f^*. Hence a good approximation to the limiting relation between T_E^* and $(\hat{L}_x, \hat{L}_y)$ can be determined by flooding the straight line defined by $\hat{L}_x = \hat{L}_y$. The results of such numerical computations are summarized in Figures 5.7 and 5.8.

From the analysis to this point it is evident that the optimal steering functions for Controllers (A) and (E) have a common characteristic, apart from those for Configurations (B) through (D), in that they are not directly dependent on the vehicle's roll rate. Thus for

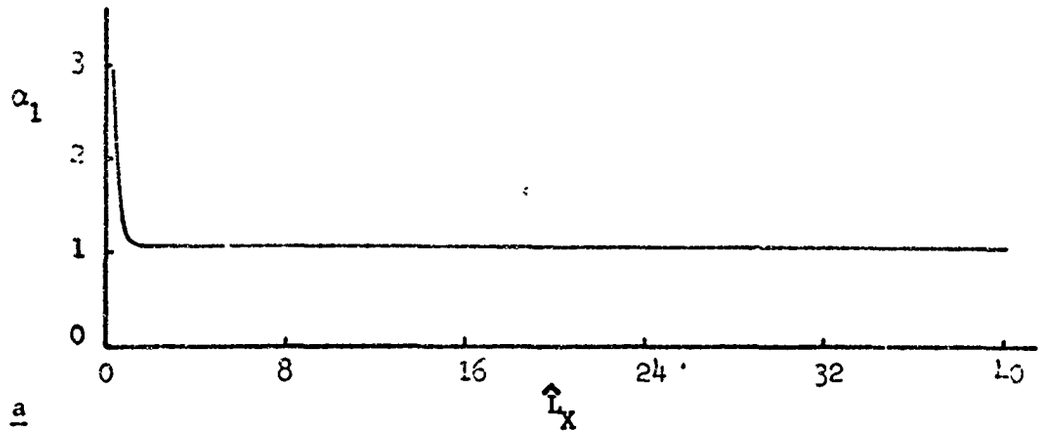

a

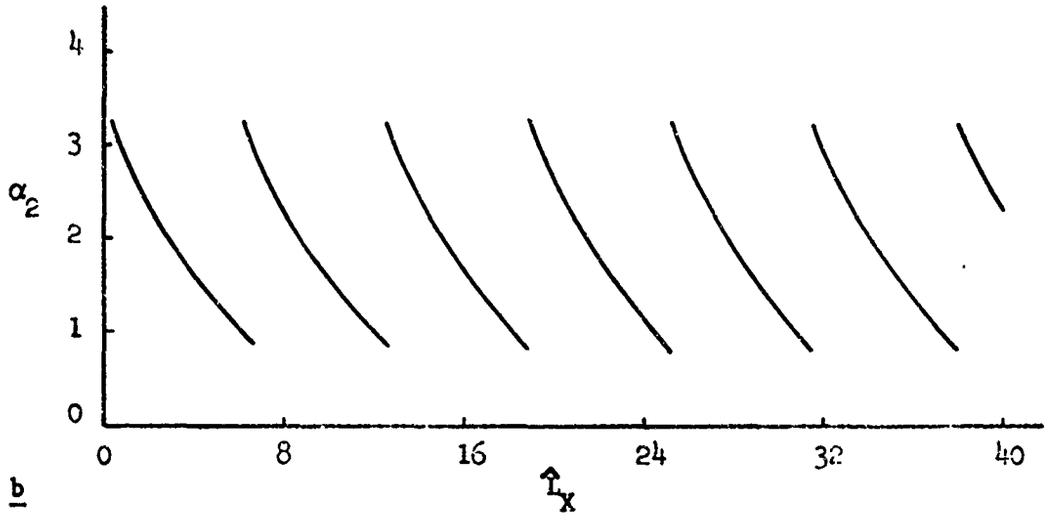

b

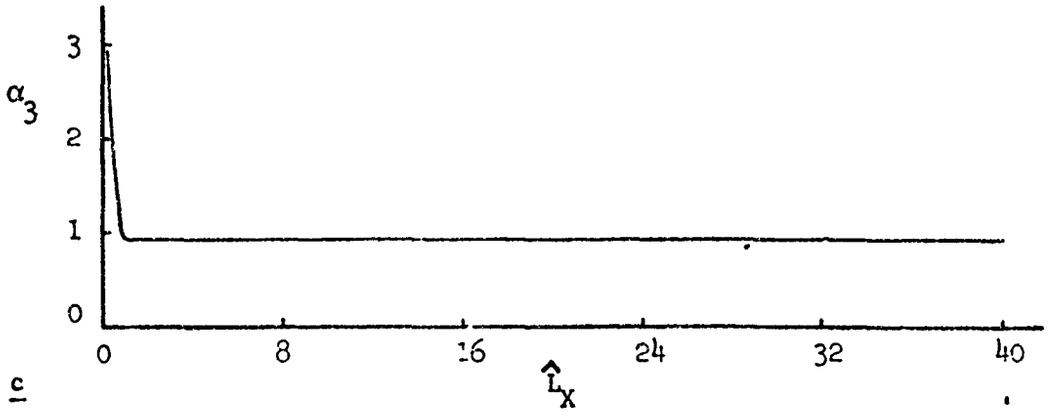

c

Figure 5.7 Solution for α in Terms of $\hat{L}_X$, $\hat{L}_Y = -\hat{L}_X$, $\alpha_{..} = -1$

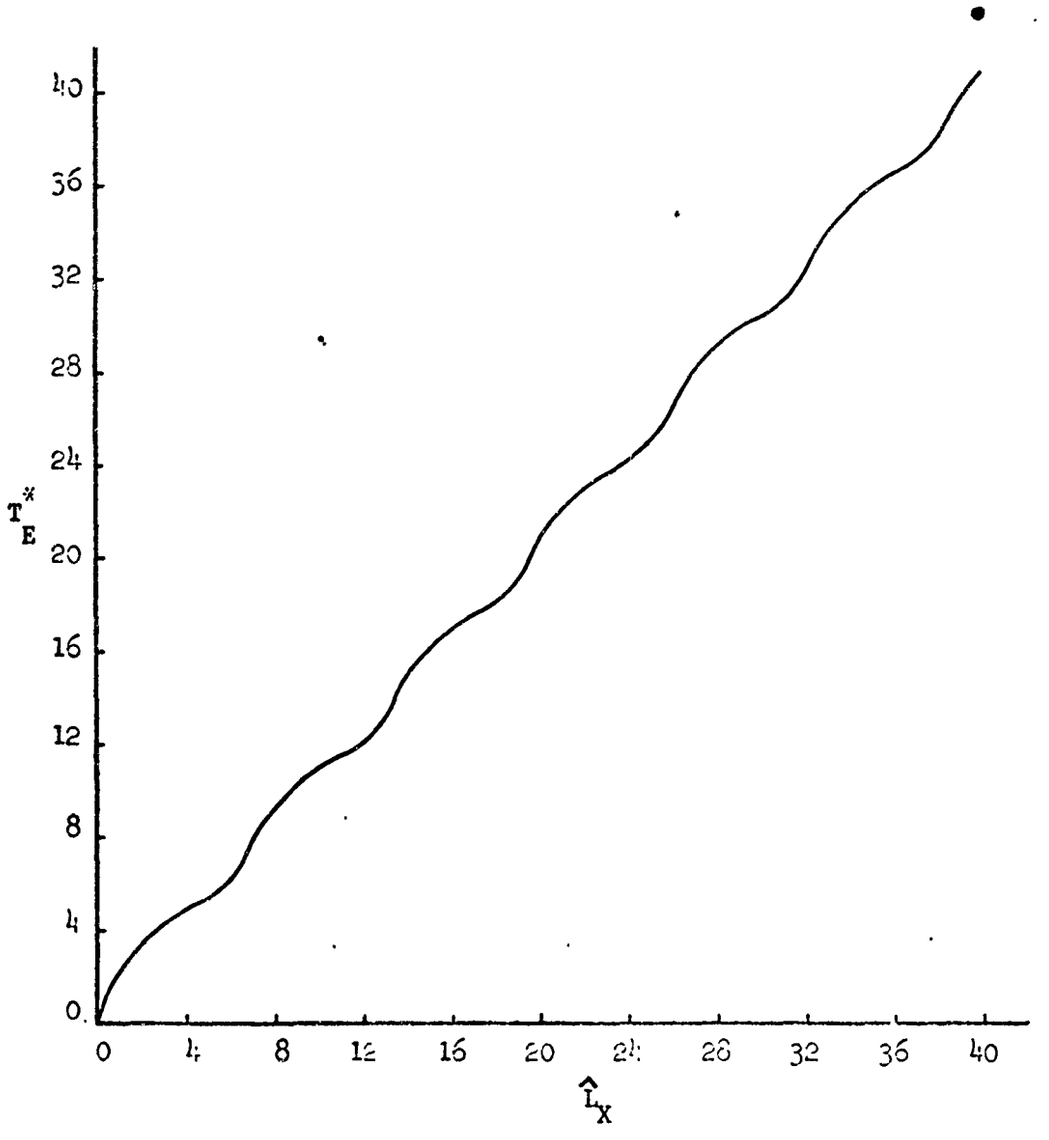

Figure 5.8 Solution for T_E^* in Terms of $\hat{L}_X$, $\hat{L}_Y = -\hat{L}_X$

certain values of the system parameters and boundary conditions the optimal steering functions for Controllers (A) and (E) are constant moments about the x' and/or y' axis. In such cases $T_A^* = T_E^*$ when three of the four jets in Configuration (E) are shut down and the maximum propellant flow $\dot{w}$ supplies the remaining jet.

CHAPTER 6

PERFORMANCE ANALYSIS

This chapter presents a comparison of the performance capabilities of Jet Configurations (A) through (E). Since we are concerned with minimum time solutions the performance of a control system is based on the time required to effect a given change in the system's state. In order to make a fair comparison of the relative performance of the five jet configurations it was assumed that the maximum rate of fuel flow is the same for each system (i.e., $\dot{w}_A = \dot{w}_B = \dot{w}_C = \dot{w}_D = \dot{w}_E$). This assumption also allows us to readily compute the amount of fuel required by each system to effect a given change in the state point in minimum time.

Of the two classes of boundary conditions considered in the previous chapters there is one which is common in all cases - namely, that defined by those initial states where the vehicle is not nutating at $t = t_o$ (i.e., $\underline{\omega}(t_o) = 0$). Hence, in the sequel we will be concerned with the ability of each control system to effect a spin axis reorientation.

6.1. A Performance Comparison When $\omega_s t_f^* \leq 10\pi$

Let us begin by comparing the performance of the five controllers when a reorientation of the spin axis is to be accomplished within five or less revolutions of the vehicle about its axis of symmetry. To provide the required data, results of the flooding process for

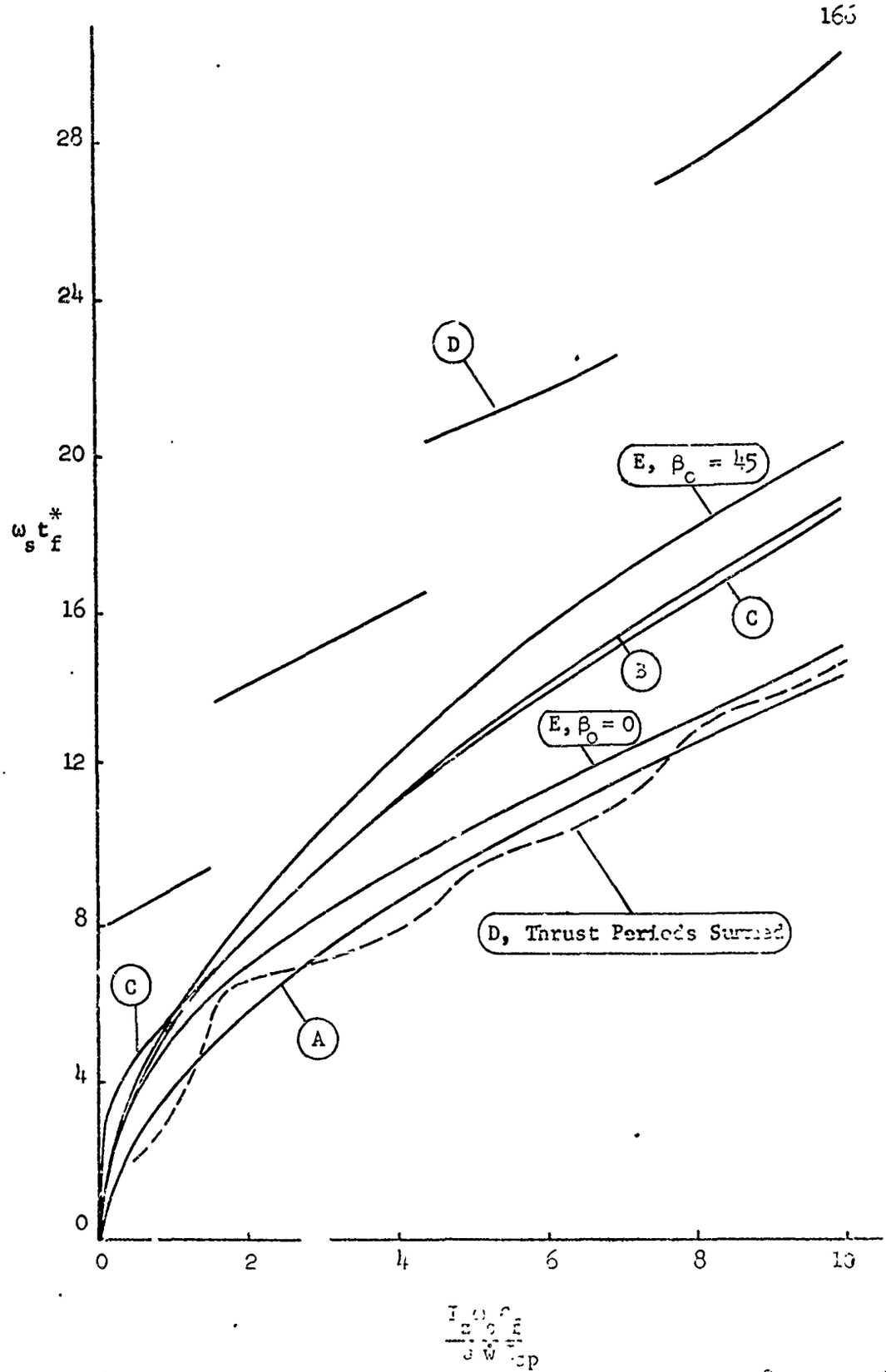

Figure 6.1 Performance Comparison of Systems A - E, $\beta_o = 0$, $\underline{\omega}^2 = 0$, $\gamma = .$

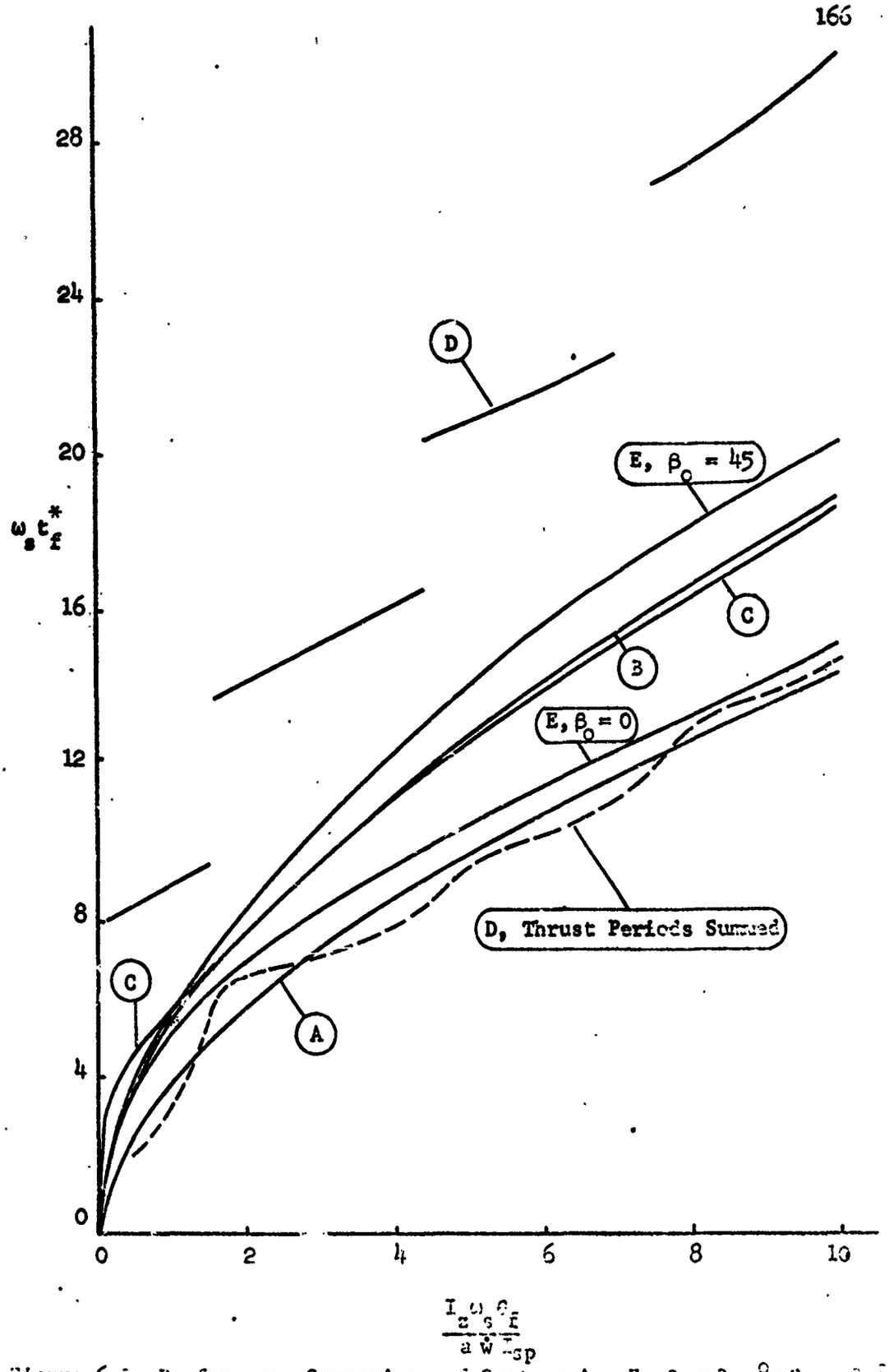

Figure 6.1 Performance Comparison of Systems A - E, $\theta_o = 0$, $\underline{\omega}^o = 0$, $\gamma = 0.2$

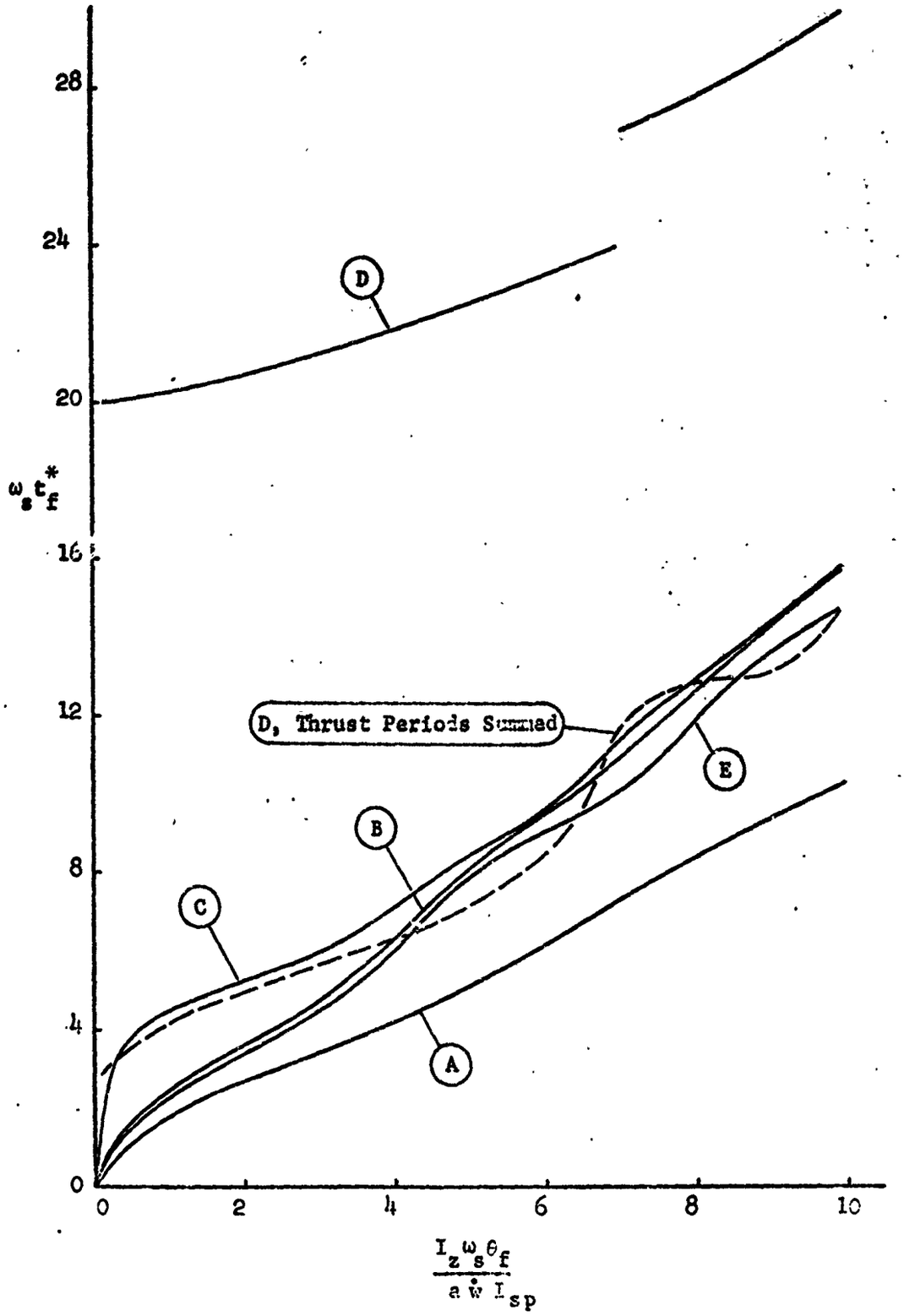

Figure 6.2 Performance Comparison of Systems A - E, $\beta_o = 0$, $\underline{\omega}^o = 0$, $\gamma = -0.2$

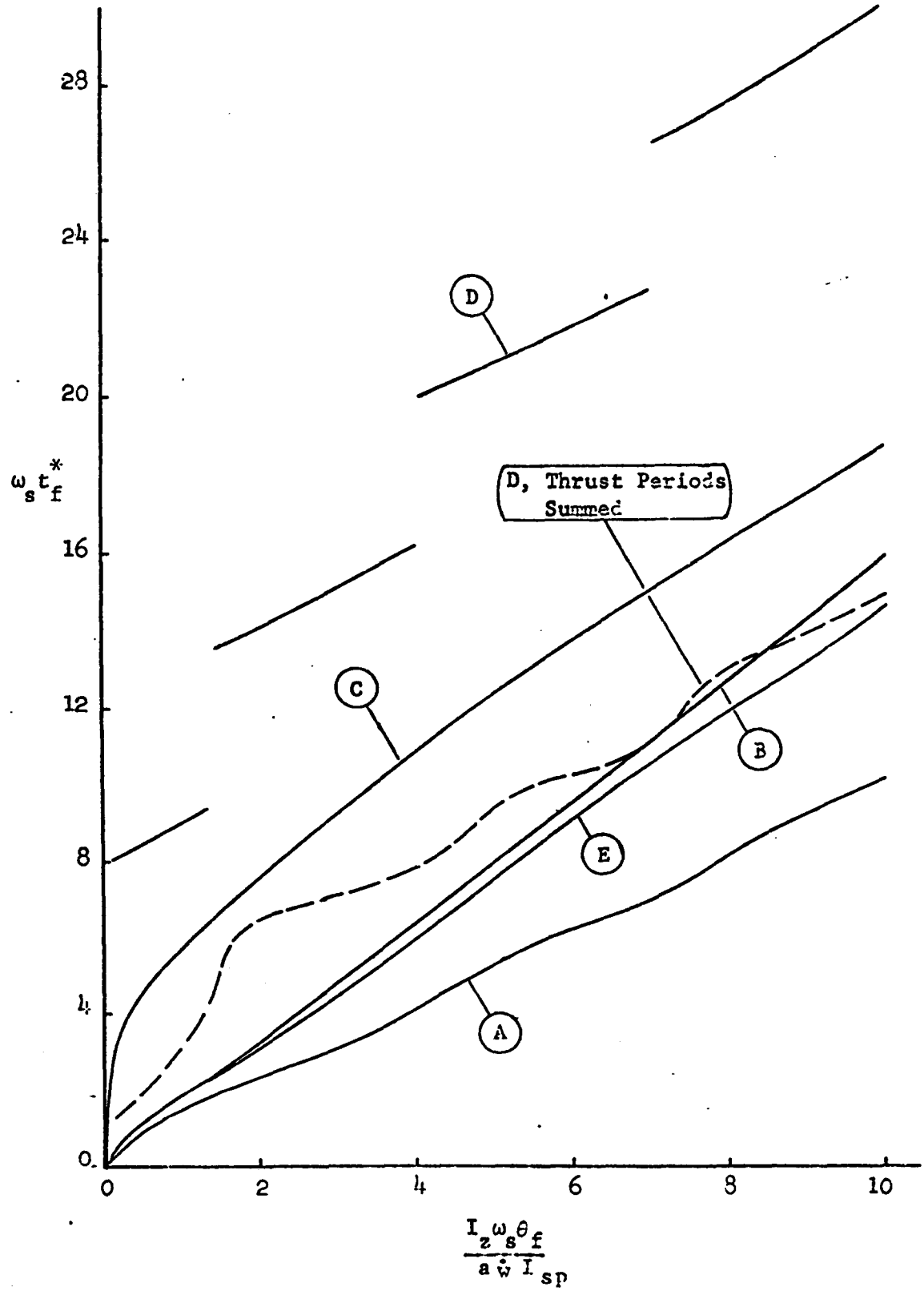

Figure 6.3 Performance Comparison of Systems A - E, $\beta_o = 0$, $\underline{w}^c = 0$, $\gamma = -0.3$

6.2 Control System Performance When $\omega_s t_f^* \gg 1$

In contrast to the features of the control problem discussed in 6.1 are those when control is applied continuously, in the case of Controller (E) a "bang-coast-bang" mode, over a long period of time. Such is the case, for example, when $\dot{w} \ll \frac{I_z \omega_s^2 \theta_f}{aI_{sp}}$. In the limiting case when $\frac{I_z \omega_s^2 \theta_f}{\dot{a}wI_{sp}} \to \infty$ both the analytic and numerical solutions discussed in previous chapters show that the minimum final time is related linearly to the change in angular momentum. Summarizing these results we find:

Configuration A

$$t_f^* = \frac{I_z \omega_s \theta_f}{\dot{a}wI_{sp}} \tag{6.1}$$

Configuration B

$$t_f^* = \frac{\pi I_z \omega_s \theta_f}{2\dot{a}wI_{sp}} \tag{6.2}$$

Configuration C

$$t_f^* = \frac{\pi I_z \omega_s \theta_f}{2\dot{a}wI_{sp}} \tag{6.3}$$

Configuration D

$$t_f^* = \frac{\pi I_z \omega_s \theta_f}{\dot{a}wI_{sp}} \tag{6.4}$$

Configuration E

$$t_f^* = \frac{\sqrt{2}\, I_z \omega_s \theta_f}{\dot{a}wI_{sp}} \tag{6.5}$$

Note that in Configuration (E) the thrusters are initially aligned 45° with respect to the change in angular momentum $I_z \omega_s \theta_f$.

Comparing the control systems in terms of the amount of fuel required to carry out a given change in the state point in minimum time we find:

1. The four, two, and single jet controllers consume 57% more fuel than the gimballed jet.
2. Four thrusters mounted on a non-spinning platform consume approximately 41% more fuel than the gimballed jet.

6.3 An Integrated Design Concept

In situations where minimzation of the time or fuel required to control a spacecraft is of the utmost concern then the integrated design concept becomes important. One way to formulate this notion mathematically is as follows: Given the dynamic system

$$\dot{\underline{\chi}} = \underline{f}(\underline{\chi}(t), \underline{u}(t), \underline{\zeta}, t) \tag{6.6}$$

where the control vector $\underline{u}$ has components $u_1, u_2, \ldots u_m$, $m \leq n$ which are constrained by

$$|u_1| + |u_2| + \ldots\ldots |u_m| \leq K \tag{6.7}$$

and $\underline{\zeta}$ belongs to an admissible parameter set $\tilde{\zeta}$. The optimal control problem is now one of selecting the dimension of the controller (m), as appropriate $\underline{\zeta}$, and $\underline{u}(t)$ so as to maximize (minimize) the cost functional

$$J = \int_{t_o}^{t_1} \mathcal{L}\,(\underline{\chi}(t), \underline{u}(t), \underline{\zeta}, t)\, dt.$$

Admittedly, the problem of choosing $(u^*(t), m^*, \underline{\zeta}^*)$ would be a difficult one; however, in cases where the cost functional is

sensitive to changes in (m) and/or $\underline{\zeta}$ considerable improvement in performance may be obtained.

In previous sections we noted that control jet configuration has considerable influence on both the minimum time and fuel required for spin axis reorientation. Moreover, the simulation results indicate that certain control systems are "better" than others. In view of this observation let us now consider the concept of integrated design as defined in the previous paragraph. For the attitude control problem this notion amounts to selecting both the control system and vehicle geometry so as to minimize the final time. To determine the influence of the vehicle's principal moments of inertia on the performance index we can make use of the numerical results presented in Chapters 3, 4 and 5. Moreover, by systematically changing γ in these solutions we are able to make certain observations as to the "preferred" vehicle shape.

A cursory examination of the simulation results allows us to make the following generalizations when the vehicle is a right circular cylinder; to include operational constraints it is assumed that the vehicles mass remains constant and that the inertial stiffness is specified; i.e., $I_z \omega_s$ = constant:

Controller (B)

A disk shaped vehicle is preferred. Changing γ from +0.8 to -0.8 reduces the minimum final time approximately 25%.

Controller (C)

A pencil shaped vehicle is preferred. Changing γ from -0.8 to +0.8 reduces the minimum final time by approximately 4 %

Controller (D)

A pencil shaped vehicle is preferred. Changing γ from -0.8 to +0.8 reduces the minimum final time by approximately 25%. For this controller there is a considerable loss in performance when γ approaches zero(changing from $\gamma \cong 0$ to $\gamma = -0.8$ reduces the minimum final time by approximately 50%).

Note that the above conclusions are the result of choosing $\bar{L}_y$ such that the solution for T* is not a linear function of the change in total angular momentum - if the final time is close to that given by Equations (6.2), (6.3), or (6.4) then vehicle geometry becomes unimportant.

CHAPTER 7

DISCUSSION AND CONCLUSIONS

In this chapter we first summarize the basic approach taken in the solution of the attitude control problem; results of this work are then discussed in more detail; and finally, extensions and uses of this study are suggested.

Through the use of both analytic and numerical solutions we have determined exact, minimum time, controls corresponding to certain classes of boundary conditions which are of engineering interest. The basic approach was to provide quantitative results in a form which allows one to deduce the qualitative structure of the optimal control for a general class of problems. To provide results which would be useful in the evaluation or selection of spacecraft attitude control systems a number of different control jet configurations were considered. Thus, the overall approach was to synthesize optimal controls for various realizable control systems in a manner which allows the engineer to readily determine such factors as: the relative efficiency of a particular jet configuration, the characteristics of the optimal steering law in terms of the system parameters and boundary conditions, and the minimum time required for correcting spin axis attitude errors in a given spacecraft.

In the text optimal controls are presented for two basic classes of boundary conditions. The first corresponds to those situations where

the total angular momentum vector and the spin axis are aligned at the initiation and termination of control. The second set includes those where the vehicle is nutating at the time control is applied. In the latter case the objective was to reduce the transverse angular rates to zero and at the same time drive the spin axis to a pre-determined position

Exact optimal controls for Thruster Configurations (A) through (E) corresponding to initial and final states of the above form were then computed for a number of vehicle configurations ranging from pencil to thin disk shapes. The results are expressed in terms of from one to four dimensionless parameters. The number of parameters required to completely define the control problem depends on both the jet configuration and the initial and final states. For Controllers (A) and(E) it was possible to combine the system parameters and the spin axis position errors into at most two dimensionless parameters, thus obtaining control laws which are not explicit functions of the vehicle's moments of inertia. Hence, the results are applicable to any vehicle configuration which has one axis of symmetry.

In situations where the minimum time required to maneuver a spacecraft is of importance one would normally employ reaction controllers which produce a sizeable thrust. Hence, the characteristics of the optimal control under such circumstances will be different from cases where the available control forces are very small. In view of the results presented in the text we are able to define qualitatively and to some extent quantitatively three "modes" of operation which characterize optimal steering corresponding to the boundary conditions

described previously. These "modes" are identified in terms of the response characteristics of the system, the control magnitude, and the control jet configurations.

The first is characterized by the "short time" control problem. That is, the time over which control is applied is small compared to either $1/\omega_s$ or $I/I_z\omega_s$. Control in this region is typified by the limiting control for the gimballed jet; for this jet configuration optimal steering becomes "race-brake" when $\tilde{L}_y \to 0$. This mode also characterizes, though to varying degrees, the behavior of optimal steering for Controllers (B), (C), and (E). For these jet configurations, as well as the gimballed jet, $T^* \to 0$ as $\tilde{L}_y \to 0$; therefore, the systems are totally controllable. However, this limiting behavior does not occur in Controller (D). That is, T_D^* is not a continuous function of $\tilde{L}_y$, in addition $(T_D^* - \omega_s t_o) = \text{constant} \neq 0$ as $\tilde{L}_D \to \infty$; therefore, the system is <u>not</u> completely controllable over an arbitrarily small interval of time. This is due to the fact that optimal steering for the single jet contains coast periods.

Response of a spinning vheicle to optimal control when the interval $[t_o, t_f]$ is "small" is illustrated in Figures 3.11, 4.17, 4.35 and 4.46. Here we observe the onset of excessive excursions of the spin axis as the dimension of Ω is reduced and/or as the coupling between the control and state becomes weaker. We also find that in the "short time" case optimal steering for Controller (E) can never be singular.

The second mode of operation is characterized by the transition region between what can be defined as the "short" and "long time"

solutions. In such cases the control moment is sufficiently large to effect a reorientation maneuver within approximately one to ten revolutions of the spacecraft about its spin axis. For a given control magnitude the region is a function of both the vehicle's moments of inertia and the jet configuration. Typical thrust requirements for controlling, within this time period, a cylindrical shaped vehicle which is spinning at a high rate are presented in [9]. Response of the system when operated in this range is illustrated in Figures 3.18, 4.20, 4.23, 4.26, 4.40 and 4.53.

The third mode of operation is characterized by the solution to the "long time" control problem. For most vehicle configurations this situation occurs when the available control moments are very small compared to the required change in the system's total angular momentum. In the limit when $\frac{I_z \omega_s^2 \theta_f}{a w I_{sp}} \to \infty$ we find that the control interval $[t_o, t_f^*]$ is directly proportional to the change in angular momentum; the exact relation depends, of course, on both the initial and final states of the system and the control jet configuration. For operational spacecraft such as Syncom, Early Bird, etc., where the control moments are indeed small compared to the total angular momentum, we find that the actual minimum maneuvering time is very close to that predicted by a linear relation.

The rate at which the actual solution approaches that defined by a linear relation depends upon both the thruster configuration and the vehicle's moments of inertia. For the gimballed jet an empirical approximation to the exact solution is given by Equation 3.26. In the case when control is provided by four jets the oscillatory

behavior of the actual solution damps out very rapidly when $I_z/I > 1$ (see Figures 4.9 and 4.13) and for the two jet controller damping most rapidly when $I_z/I = 1$ (see Figure 4.33). However, when the control is provided by one jet the situation is somewhat different. Here we find that the minimum time curves (i.e., plots of the numerical results relating T_D^* to L_y) are discontinuous and approach a linear relation asymptotically; deviation of the actual solutions from linear depends very strongly on the vehicle's moments of inertia. In fact, the difference becomes infinitely large as $I_z/I \to 1$ (the system is not controllable when $I_z/I = 1$) and is a minimum when $1 - I_z/I \to 1$.

In cases where the vehicle is nutating when control is applied we have demonstrated the characteristics of the optimal steering functions in terms of the required changes in the total angular momentum. For example, it has been shown that the optimal control which satisfied boundary conditions typified by Case 1, Figure 4.5, approaches the minimum time solution found in Reference [1] when the ratio of the initial transverse component of angular momentum to the maximum control moment becomes "large". In addition, the difference between optimal control for the fourth order plant considered in this report and that corresponding to a second order system which includes only ω_x and ω_y depends strongly on I_z/I.

In the design of a physically realized control system one must consider the characteristics of the optimal steering law in addition to performance. From this standpoint Controller (E) is appealing since in most cases one can rotate the non-spinning platform to that position for which the optimal control is singular. This means that

one jet operates "full on" over the interval $[t_o, t_f^*]$ and the remaining pair is driven by either a simple bang-bang or continuous control law; the choice between bang-bang and continuous depends on the position of the non-spinning platform and on the allowable fuel consumption. This control law is appealing since the system does not have to respond to complicated bang-bang or on-off strategies as in Configurations (B), (C), and (D). Also, it was found during the computation of optimal steering for the latter controllers that the error between the desired and actual terminal states is sensitive to errors in the switch times. This was particularly true in cases where the vehicle is disk shaped (i.e., $\lambda_z/I > 1$) and is nutating at the time control is applied.

In terms of contributing to control theory we have shown how the properties of controllability, total controllability, and normality determine the characteristics of the optimal control for a realistic system. In addition, it has been demonstrated to what extent these notions are influenced by the allowable control set. Further, a performance comparison in terms of the time and fuel required to reorient the spin axis through a given angle shows that certain control jet configurations are "better" than others. This difference in performance can be related to the recoverable set concept as discussed by Athan and Falb, [13], in their solution to the angular rate control problem.[1]

---

[1] The influence of controller configuration on performance is also discussed by Dixon [21].

In addition, both the development and the problems associated with the application of an efficient iterative procedure have been discussed in detail. Such documentation of the behavior of a procedure designed to solve two point boundary value problems is necessary, and too often neglected, if we are to compare the utility of various numerical schemes when applied to practical engineering problems. In the present case a Newton type iterative procedure was employed to determine time-optimal controls for a fourth order norm-invariant system.

We have also shown that the method of solution, closed form vs numerical, is dictated to some extent by the allowable control set. For example, in the case of the gimballed jet where Ω_A is a circle of unit radius in R_2, we were able to solve the two point boundary value problem in closed form for a certain class of boundary conditions. Thus, it appears that by "smoothing" the allowable control set (e.g., approximating a hypercube with a super ellipse) one has an increased chance of solving for the optimal control in closed form.

An obvious extension of the present work would be to the problem of properly reorienting and stabilizing an axially symmetric spacecraft when the spin axis attitude error is arbitrarily large. From preliminary analysis we have found that when control is provided by a gimballed jet both the dynamic system and the optimal steering functions can be represented by a set of four linear and three nonlinear, first order, ordinary differential equations. In cases where the total angular momentum vector and the spin axis are aligned at the initiation and termination of control, and either the initial or

final position of the spin axis is colinear with the z_R axis, then the system parameters and boundary conditions are completely specified by two dimensionless parameters. To illuminate the control problem an approach similar to that described in the first paragraphs of this chapter could be employed to determine both the quantitative and qualitative structure of the optimal control. Since rapid convergence is required if one is to solve a number of two point boundary value problems, a technique similar to that proposed by Plant [19] may be required. The change between the linear and non-linear cases could then possibly be effected by modifying the dimensionless parameter used in the linear solution while retaining the dimensionless change in the attitude angle. The first approximation would then be the linear solution.

In terms of the physical parameters the resulting optimal controls would undoubtedly have the same qualitative structure as those for the linear model. In fact, in those cases where the required change in angular momentum is large compared to the maximum control torque the optimal control becomes nearly a steadily applied moment, depending upon the controller configuration, and the response of the system is typified by that of the linear plant. Hence one should be able to make use of the results presented in this report to determine the minimum time required for arbitrarily large reorientations of a vehicle's spin axis.

The ultimate objective of an optimal solution to the attitude control problem is, of course, to develop the control in state feedback form. In the literature one finds many approaches to this

problem. However, due to the sensitivity of the system's response to errors in the optimal control (e.g., errors in the switch times) the only practical solution appears to be that in which the control is given explicitly in terms of the system's current state. Such closed form solutions have been found when the cost functional is described by some combination of the state error and the control effort. It has been shown that large penalties on the control effort tend to "soft" limit the control magnitude. However, in general, the resulting control does not resemble minimum time steering. Thus it would be worthwhile to investigate the problem of selecting a cost functional which penalizes excessive time and at the same time allows a closed form solution (i.e., a quasi-optimal solution to the minimum time problem).

APPENDIX A

AN ITERATIVE PROCEDURE FOR COMPUTING TIME-OPTIMAL CONTROLS

A.1 Introduction

The equations of motion for a spinning body, when motion is limited to small angular excursions, can be described by a vector differential equation of the following form:

$$\dot{\underline{\chi}}(t) = A\underline{\chi}(t) + B(t)\,\underline{u}(t) \qquad (A.1)$$

Time-optimal controls for certain cases of such a linear system are well known, e.g., when $\underline{\chi}$ is a two dimensional vector representing angular velocity. However, for systems of third order or greater the satisfying of both the prescribed initial and final values of the state variables and the necessary condition for optimality usually requires a computational scheme which involves the use of a high speed digital or analog computer.

During the past decade many schemes for computing optimal controls for both linear and non-linear systems have been developed.[1] In this section we present a specific technique for solving two point boundary value problems of the type described in Chapters 4 and 5. Specifically, the iterative procedure proposed by Knudsen [15] with certain modification suggested by Plant [19] is employed to solve for the time optimal controls in Systems (B) through (E).

---

[1] A comprehensive comparison of a number of procedures for computing optimal controls for linear systems is presented in [19].

A.2 Philosophy on the Selection of a Computational Procedure

The iterative procedure discussed in the sequel was developed in view of the requirement for solving a large number of two point boundary value problems with a modest expenditure of computer time. Additional considerations in the synthesis of this algorithm were the dynamics of the plant, and the particular controller configurations and boundary conditions described in Chapters 4 and 5. Since the objective was to compute optimal controls for a particular plant no attempt was made to introduce new theorems pertaining to the convergence of an iterative procedure. In place of formally extending Knudsen's algorithm to include non-autonomous systems with vector controls, the behavior of an iterative procedure developed through a direct extension of his work is discussed extensively in Appendix B.

The choice of a Newton type procedure (Knudsen's and Plant's algorithms rely on the basic Newton recursive relation) was motivated by its simplicity, its straightforward approach to the problem, and by its rapid rate of convergence when the guess $(\underline{\alpha}, t_f)$ is "close enough" to the solution $(\underline{\alpha}, t_f)^*$. In this procedure $\underline{\alpha}$ and t_f are adjusted simultaneously which results in an efficient iterative scheme. Finally, an upper bound on the rate of convergence of this method exists when the derived and optimal controls are "close".

A.3 Statement of the Problem

For systems described by a differential equation of the form

$$\dot{\underline{x}}(t) = A(t)\,\underline{x}(t) + B(t)\,\underline{u}(t) \qquad (A.2)$$

The initial, $\underline{x}_o$, and final, $\underline{x}_f$, states are related by the expression

$$\underline{\chi}_f = \phi(t_f,t_o)\left[\underline{\chi}_o + \int_{t_o}^{t_f} \phi^{-1}(t,t_o)B(t)\underline{u}(t)dt\right] \tag{A.3}$$

where $\phi(t,t_o)$, defined for all (t_o,t), is a fundamental matrix of solutions of the homogenous system satisfying the additional requirement that $\Phi(t_o,t_o) = [I]$ for all t_o.

The systems described by Equation (2.27) are normal when the admissible control sets are defined by Ω_B through Ω_D; therefore, the maximum principle provides both a necessary and sufficient condition for the time-optimal control $\underline{u}^*(t)$ (in the case of Ω_E only a necessary condition). In Chapters 4 and 5 we found that the Hamiltonian is a maximum when

$$\underline{u}^*(t) = \begin{Bmatrix} \text{SGN}[B'(t)\underline{P}(t)]: & \text{Systems B, C, and E} \\ u'[B'(t)\underline{P}(t)] : & \text{System D} \end{Bmatrix}. \tag{A.4}$$

Where $\underline{P}(t)$ is a solution to the systems adjoint differential equations

$$\dot{\underline{P}}(t) = -A'\underline{P}(t), \quad \underline{P}(t_o) = \underline{\alpha}. \tag{A.5}$$

Hence, for non-trivial solutions to this equation the control $\underline{u}^*(t)$, $t\in[t_o,t_f]$, is well defined except at a finite number of switch times.

Substituting (A.4) and the solution to (A.5) into (A.3) gives

$$\underline{\chi}_f = \Phi(t_f,t_o)\left[\underline{\chi}_o + \int_{t_o}^{t_f} \phi^{-1}(t,t_o)B(t)\begin{Bmatrix}\text{SGN}[B'(t)\underline{P}(t)] \\ u'[B'(t)\underline{P}(t)]\end{Bmatrix} dt\right]. \tag{A.6}$$

The only terms on the right side of this equation which are not fixed by a description of the system are $\underline{\alpha}$ and t_f. Thus (A.6) can be re-written as

$$\underline{\chi}_f = \underline{F}_1(t_f) + \underline{F}_2(\underline{\alpha}, t_f) = \underline{F}(\underline{\alpha}, t_f) . \tag{A.7}$$

To define $\underline{F}$ we choose $\underline{\alpha} \neq 0$ in R_4 and a $t_f \in R_1^+$, then the initial value problem defining $\underline{F}$ is given by Equations (A.2) and (A.5). For a given system description the problem of computing an optimal control $([t_o, t_f^*], \underline{u}^*(t))$ which takes the system from a specified initial state $\underline{\chi}_o$ to a given terminal state $\underline{\chi}_f$ is equivalent to that of determining an inverse to (A.7). In general, this inverse cannot be determined analytically; therefore, an iterative technique is proposed.

A.4 An Iterative Solution

In describing the optimal control problem we have taken the maximum principle point of view and have constructed an equivalent two-point boundary value problem. This two-point boundary value problem defines a function $\underline{F}$ which maps the boundary conditions on the differential equations into the state space. Hence, the solution to the optimal control problem becomes equivalent to finding $\underline{F}^{-1}$.

A.4.1 Newton's Method

The iterative procedure is to guess both the unknown boundary conditions on the adjoint system at $t = t_o$ and the final time t_f, then solve the initial value problem and find the error in the conditions at the terminal point. At the same time, the first-order

effects of changing the guessed values are calculated. These first-order effects are then used to find a better guess according to the following recursive formula:

$$\begin{bmatrix} \Delta\underline{\alpha}_k \\ \hline (\Delta t_f)_k \end{bmatrix} = \Gamma_k \begin{bmatrix} \dfrac{\partial \underline{F}(\underline{\alpha},\, t_f)_k}{\partial \underline{\alpha}} & \dfrac{\partial \underline{F}(\underline{\alpha},\, t_f)_k}{\partial t_f} \end{bmatrix}^{-1} \left[\underline{\chi}_f - \underline{\chi}(\underline{\alpha},\, t_f)_k \right] \tag{A.8}$$

$$\Delta \underline{V}_k = \Gamma_k\, G^{-1}(\underline{\alpha}\,,\, t_f)_k\, \Delta \underline{\chi} \tag{A.9}$$

$$\underline{\alpha}_{k+1} = \underline{\alpha}_k + \Delta\underline{\alpha}_k\,, \qquad (t_f)_{k+1} = (t_f)_k + (\Delta t_f)_k \tag{A.10}$$

This relation with $\Gamma_k = 1$ is the basic Newton procedure.

A.4.2 Modifications to the Newton Procedure

The iterative procedures due to Knudsen and Plant differ from the basic Newton method in two respects. First, if $\|\Delta\underline{\chi}\|$ is large the Newton procedure may not converge. Therefore, the algorithms due to Knudsen and Plant incorporate procedures for selecting the iterative scale factor Γ_k. An additional difficulty associated with the Newton approach is one of insuring the existence of G^{-1}. In view of this requirement, Plant approximates the optimal regulator problem with a modified optimal regulator problem (the target is assumed to be a hypersphere centered at the origin) and then establishes conditions under which G is non-singular.

However, due to the fact that the eigenvalues of (2.27) and (2.28) with zero real parts occur with multiplicity, the conditions

under which Plant's iterative procedure can be applied with success are not evident. Hence an iterative technique similar to Knudsen's, which incorporates certain procedures proposed by Plant, was developed specifically for solving the optimal control problem considered in this report. The basic algorithm is summarized as follows:

1. Knudsen's recursive relation, which is similar to (A.9), was modified to include Control Systems (B) through (E). The co-state vector $\underline{P}(t)$ was normalized with respect to one component of $\underline{\alpha}$; hence, G is an 4 x 4 matrix.
2. A procedure was incorporated which prevents the computation from "hanging up" at a switching surface.
3. Plant's method for selecting Γ_k was employed to insure rapid convergence.
4. Starting values for the pair $(\underline{\alpha}, t_f)$ were selected as indicated in Section 4.4.2.

A.4.3 Derivation of the Recursive Relation for Control Systems (B) through (E)

Following Knudsen [15] we find that for the regulator problem a first order relation between $\Delta\underline{\chi}$ and $\Delta\underline{V}$ can be obtained from a Taylor series expansion

$$\Delta\underline{\chi}_f = \underline{F}(\underline{\alpha} + \Delta\underline{\alpha},\ t_f + \Delta t_f) - \underline{F}(\underline{\alpha},\ t_f) \tag{A.11}$$

or

$$\Delta\underline{\chi}_f = \frac{\underline{F}(\underline{\alpha}, t_f)}{\partial\underline{\alpha}}\Delta\underline{\alpha} + \frac{\partial\underline{F}(\underline{\alpha}, t_f)}{\partial t_f}\ \Delta t_f + \hat{R} \tag{A.12}$$

where $\hat{R}$ is the remainder to the linear terms. If we neglect the higher order terms (A.12) can be written as

$$\Delta\underline{\chi}_f = G(\underline{\alpha},\ t_f)\ \Delta\underline{V}\ . \tag{A.13}$$

Reducing $\Delta\underline{\chi}_f$ by an appropriate scale factor and after performing the required inverse we obtain Equation (A.9). In general, G is not square and, therefore, must be modified such that it becomes invertable and yet retains it original mapping properties. Such alterations are discussed in the following section and in References [15] and [19].

The first order relation between the required correction in the terminal state $\Delta\underline{\chi}_f$ and the corresponding change in $(\underline{\alpha},\ t_f)$ is carried out in two parts. First, the effect of varying the switch times and the final time on the state $\underline{\chi}(t_f)$ is expressed in terms of a Taylor series expansion. Then changes in the switch times are expressed in terms of a Taylor series expansion. Then changes in the switch times are expressed in terms of incremental changes in $\underline{\alpha}$.

Equation (A.4) implies that the components $u^*_j(t)$ (for the cases considered in this report $j_{max} = 2$) of the control vector $\underline{u}^*$ are piecewise continuous and assume extreme values over the interval $[t_o,\ t_f^*]$. If $u_j(t)$ changes sign h_j times in the interval $(t_o,\ t_f)$ at the times t_i then Equation (A.6) can be expanded in terms of the switching times as follows:

$$\begin{bmatrix} (\chi_1)_f \\ (\chi_2)_f \\ (\chi_3)_f \\ (\chi_4)_f \end{bmatrix} = \Phi(t_f, t_o) \left[\begin{bmatrix} (\chi_1)_o \\ (\chi_2)_o \\ (\chi_3)_o \\ (\chi_4)_o \end{bmatrix} + \begin{bmatrix} \int_{t_o}^{t_1^1} \hat{\Phi}_{11} dt + \ldots (-1)^{h_1} \int_{t_{h_1}^1}^{t_f} \hat{\Phi}_{11} dt & \int_{t_o}^{t_1^2} \hat{\Phi}_{12} dt + \ldots (-1)^{h_2} \int_{t_{h_2}^2}^{t_f} \hat{\Phi}_{12} dt \\ \vdots & \vdots \\ \int_{t_o}^{t_1^1} \hat{\Phi}_{41} dt + \ldots (-1)^{h_1} \int_{t_{h_1}^1}^{t_f} \hat{\Phi}_{41} dt & \int_{t_o}^{t_1^2} \hat{\Phi}_{42} dt + \ldots (-1)^{h_2} \int_{t_{h_2}^2}^{t_f} \hat{\Phi}_{42} dt \end{bmatrix} \begin{bmatrix} u_1(t_o) \\ u_2(t_o) \end{bmatrix} \right] \tag{A.14}$$

where

$$\hat{\Phi}_{rs} = \sum_{s=1}^{4} \Phi_{rs}^{-1} B_{sj}, \quad r = 1,2,3,4, \quad j = 1,2$$

In general, Equation (A.14) is not satisfied. That is, the terminal state corresponding to "guessed" values for both $\underline{\alpha}$, which specifies the switching times, and t_f is not the required $\underline{\chi}_f$. To determine corrections in the switching times and the final time we form a first order variation of (A.14) in a manner similiar to that of (A.12).

Thus,

$$\Delta\underline{\chi} = G_1(\underline{t})\Delta\underline{t} + \Delta t_f G_2(t_f) + \hat{R} \tag{A.15}$$

where $\hat{R}$ is assumed small compared to the first order terms and

$$\Delta\underline{\chi}_k = \begin{bmatrix} (\chi_1)_f - (\chi_1)_o \\ (\chi_2)_f - (\chi_2)_o \\ (\chi_3)_f - (\chi_3)_o \\ (\chi_4)_f - (\chi_4)_o \end{bmatrix} - \int_{t_o}^{(t_f)_k} (t,t_o)B(t)\,\underline{u}_k(t)\,dt \tag{A.16}$$

$$G_1(\underline{t}) = \left[\begin{array}{c|c} \hat{\Phi}_{11}(t_1^1)+\ldots(-1)^{h_1}\hat{\Phi}_{11}(t_{h_1}^1) & \hat{\Phi}_{12}(t_1^2)+\ldots(-1)^{h_2}\hat{\Phi}_{12}(t_{h_2}^2) \\ \vdots & \vdots \\ \hat{\Phi}_{41}(t_1^1)+\ldots(-1)^{h_1}\hat{\Phi}_{41}(t_{h_1}^1) & \hat{\Phi}_{42}(t_1^2)+\ldots(-1)^{h_2}\hat{\Phi}_{42}(t_{h_2}^2) \end{array}\right] \begin{bmatrix} u_1(t_o) \\ \\ u_2(t_o) \end{bmatrix} \tag{A.17}$$

$$G_2(t_f) = \begin{bmatrix} (-1)^{h_1}\hat{\Phi}_{11}(t_f) & (-1)^{h_2}\hat{\Phi}_{12}(t_f) \\ \\ (-1)^{h_1}\hat{\Phi}_{41}(t_f) & (-1)^{h_2}\hat{\Phi}_{42}(t_f) \end{bmatrix} \begin{bmatrix} u_1(t_o) \\ \\ u_2(t_o) \end{bmatrix} \tag{A.18}$$

$$\underline{t} = \begin{bmatrix} t_1^1 \\ \vdots \\ t_{h_1}^1 \\ t_1^2 \\ \vdots \\ t_{h_2}^2 \end{bmatrix} \tag{A.19}$$

Note that due to the particular form of the boundary conditions considered in this report, $(\chi_1)_f = (\chi_2)_f = 0$, and the fact that $\chi_1(t)$ and $\chi_2(t)$ are uncoupled from $\chi_3(t)$ and $\chi_4(t)$, the transition matrix can be eliminated from (A.14) by operating on both sides of this equation with $\Phi^{-1}(t_f, t_o)$.

If the control $\underline{u}(t)$ is an optimal controller then the following condition was found to be necessary

$$\underline{u}^*(t) = \begin{cases} \text{SGN } [\underline{S}(t)]: & \text{Systems B, C, E} \\ u' [\underline{S}(t)]: & \text{System D} \end{cases} \qquad \text{(A.20)}$$

where

$$\underline{S}(t) = B'(t)\, \underline{P}(t). \qquad \text{(A.21)}$$

The switch times t_i^j occur when

$$S_j(t_i^j) = 0, \quad i = 1,2,\ldots h_j, \quad j = 1,2.$$

Using (A.21) we can now relate small changes in the initial co-state $\Delta\underline{\alpha}$ to variations in the switching times Δt_i^j. Expanding the switching functions S_j in a Taylor series about the known switch times we find

$$S_j(t_i^j + \Delta t_i^j, \underline{\alpha} + \Delta\underline{\alpha}) = S_j(t_i^j, \underline{\alpha}) + \frac{\partial S_j(t_i^j, \underline{\alpha})}{\partial t_i^j} \Delta t_i^j + \qquad \text{(A.22)}$$

$$\sum_{r=1}^{3} \frac{\partial S_j(t_i^j, \underline{\alpha})}{\partial \alpha_r} \Delta\alpha_r + \hat{R}$$

Actually, we have a total of $(h_1 + h_2)$ equations similiar to (A.22).

Setting

$$S_j(t_i^j + \Delta t_i^j, \underline{\alpha} + \Delta\underline{\alpha}) = S_j(t_i^j, \underline{\alpha})$$

since these points must be zeros of S_1 and S_2 and solving the resulting equations for the perturbations in the switching times gives

$$\Delta t_i^j = -\frac{1}{\dfrac{\partial S_j(t_i^j, \underline{\alpha})}{\partial t_i^j}} \sum_{r=1}^{3} \frac{S_j(t_i^j, \underline{\alpha})}{\partial \alpha_r} \Delta\alpha_r. \tag{A.23}$$

Here we have assumed that $\hat{R}$ is small compared to the first order terms and that

$$\frac{\partial S_j(t_i^j, \underline{\alpha})}{\partial t_i^j} \neq 0. \tag{A.24}$$

Conditions for the above inequality are discussed in [15].

Combining (A.15) and (A.23) we can readily form the variational equation relating $\Delta\underline{\alpha}$ and Δt_f to $\Delta\underline{\chi}$.

$$\Delta\underline{\chi} = G_1(\underline{t}, \underline{\alpha})\Delta\underline{\alpha} + \Delta t_f G_2(t_f) \tag{A.25}$$

By scaling $\Delta\underline{\chi}$ with Γ we obtain a recursive relation of the form of (A.9).

A.4.4 Evaluating G^{-1}

In order to solve for the required incremental inverse relation

$$\Delta\underline{V} = G^{-1}\Delta\underline{\chi} \tag{A.26}$$

the (4 x 5) G matrix must be inverted. This is impossible to do directly since G is not square. Knudsen [15] overcomes this difficulty

by augmenting G with an $(n+1)^{st}$ row which is independent of the others. However, for the control problem considered in this report and, in general, for systems to which the algorithm applies, the problem associated with G being non-square can be solved in a number of ways In the following paragraphs we consider the possibility of reducing G to a (4×4) matrix. Such a procedure is desirable since the computer time required for evaluating G^{-1} would be reduced.

In the previously described iterative procedure the maximum principle supplies a necessary condition for time optimality. This necessary condition implies that the projection of $\underline{u}(t)$ on $\underline{P}(t)$ must be a maximum for all $t\epsilon[t_0, t_f]$. Hence, $\underline{u}^*(t)$ is independent of $\|\underline{P}(t)\|$. Therefore the number of independent initial co-states can be reduced to three if $\underline{P}(t)$ is normalized with respect to one component or a combination of several components of $\underline{\alpha}$. This technique is illustrated in Chapters 3, 4, and 5.

It should be noted that the normalizing element must be chosen with caution. First, $\underline{P}(t)$ must not be normalized with an element which would normally be zero. For example, if $\alpha_1 = 1$ in Chapter 4 then $\alpha_4 \to \infty$ for certain values of γ and $\bar{L}_\gamma$. Second, if $\underline{P}(t)$ is normalized improperly certain control sequences may be eliminated. For example, consider the double integrator plant when the cost criterion is time. For this problem the optimal control is given by

$$u^*(t) = \text{SGN}\,[\alpha_1 - \alpha_2 t]$$

If $\alpha_1 = 1$ then $u^*(0) = -1$, and when $\alpha_2 = 1$ we find that $(\alpha_1 - t)$ is a monotonically decreasing function; thus, the control sequence

$$u(t) = \begin{cases} -1 : t \leq t_1 \\ +1 : t > t_1 \end{cases}$$

cannot be obtained by iterating on α_1 alone.

The previous examples illustrate several pitfalls which can arise if $\underline{P}(t)$ is normalized improperly. In order to use this procedure successfully one must examine the characteristics of the switch functions, the dynamic system, and the boundary conditions before choosing a normalizing element.

A.4.5 Selection of the Iterative Scale Factor

From both the theory and applications we find that the iterative behavior of a Newton type algorithm is directly related to the choice for Γ_k.[2] The procedures for selecting Γ_k described in the sequel were motivated by the requirement of achieving a rapid rate of convergence and by the characteristics of both the switching functions for Controllers (B) through (E) and the Newton type iterative procedure.

Ideally we would like to choose Γ_k such that

$$\|\Delta\chi_{k+1}\| = \min_{0 < \Gamma_k \leq 1} \|\Delta\chi(\underline{V}_{k+1}(\Gamma_k), t_{f_{k+1}}(\Gamma_k))\|. \qquad (A.27)$$

However, under certain conditions the problem of ensuring the existence of G^{-1} supersedes that of achieving rapid convergence. Hence, several schemes for selecting Γ_k were employed.

---

[2] For autonomous systems Kundsen [15] discusses the problem of finding a $\Gamma_k \epsilon (0,1]$ such that $\|\Delta \underline{\chi}_{k+1}\| < \|\Delta \underline{\chi}_k\|$

Scheme 1: This procedure was developed by Plant for the iterative method described in Reference [19]. The only justifications for adopting this scheme are: (1) the algorithm employed in this report is similiar to Plant's, (2) it appears to work, and (3) the convergence characteristics of the two methods are similiar when this method is employed.

Step 1: Choose $\Gamma_k = 1$ and solve the initial value problem.

Step 2: If $\|\Delta\underline{\chi}_{k+1}\| < \frac{1}{2}\|\Delta\underline{\chi}_k\|$ then set $\Gamma_{k+1} = 1$ and proceed to the next iteration. However, if $\|\Delta\underline{\chi}_{k+1}\| \geq \frac{1}{2}\|\Delta\underline{\chi}_k\|$ then solve the initial value problem using

$$\Gamma_k = \frac{1}{2}\,\frac{\|\Delta\underline{\chi}_k\|}{\|\Delta\underline{\chi}_{k+1}\|} \tag{A.28}$$

to find $\Delta\tilde{\underline{\chi}}_{k+1}$.

Step 3: If $\|\Delta\tilde{\underline{\chi}}_{k+1}\| < \|\Delta\underline{\chi}_k\|$ then proceed to the next iteration. If $\|\Delta\tilde{\underline{\chi}}_{k+1}\| > \|\Delta\underline{\chi}_k\|$ then solve the initial value problem using

$$\Gamma_k = \frac{\tilde{\Gamma}_k^2\,\|\Delta\underline{\chi}_k\|}{2(\|\Delta\tilde{\underline{\chi}}_{k+1}\| + (\tilde{\Gamma}_k - 1)\|\Delta\underline{\chi}_k\|)} \tag{A.29}$$

This scheme is ideally suited for the flooding process since it continually tests large values for Γ_k. Hence, when the derived and optimal controls are "close", as is usually the case in the flooding process, convergence is very rapid.

Scheme 2: A systematic search wherein the interval [0, 1] was divided into q equal intervals. Each of the values $\Gamma = \frac{1}{q}, \frac{2}{q}, \ldots, 1$ was tested and the one which produced the minimum $\|\Delta\underline{\chi}_{k+1}\|$ was

adopted. The disadvantage of this method is that it requires (q) solutions of the initial value problem per iteration. However, in those cases where the guessed values for $(\underline{\alpha},t_f)$ were not "close" to $(\underline{\alpha}^*,t_f)^*$ this procedure was useful in selecting a starting value for $\Gamma_1(\Gamma_1)$. Also, this method was used to update Γ in Scheme 3.

Scheme 3: The scale factor Γ remained constant over a specified number of iterations. Periodically, a systematic search (Scheme 2) was made around the operating point Γ_k to select an improved value which increases the rate of convergence. This procedure proved to be successful in the following situations:

1. In cases where the iterative process using Scheme 1 to select Γ "hangs-up". This can occur when the number of switching points in (t_o,t_f) is sensitive to changes in $(\underline{\alpha},t_f)$ and, in addition, when the terminal state is sensitive to the number and location of the zeros of S_j. In such cases Γ was held constant at the "best" value computed by Scheme 1 and updated periodically or when $\|\Delta\underline{\chi}_{k+1}\|>\|\Delta\underline{\chi}_k\|$.
2. In cases where the initial guess was "bad" ($\underline{u}_1(t)$ did not have the same form as $\underline{u}^*(t)$). To prevent the computed variations from becoming too large hard limits were placed on $|\Delta t_f|$. Those situations which required this method of solution are discussed in detail in Appendix B.

In certain cases it was not evident which of the above schemes is superior in terms of minimizing the number of iterations required for convergence (i.e., when $\|\Delta\underline{\chi}\|<\epsilon$). For example, Schemes 1 and 2 may require that the initial value problem be solved more than once per

iteration. In contrast when using Scheme 3 the error would normally be reduced for each solution to the initial value problem providing Γ_k was selected properly. However, the improvement per iteration may not be as great as in Schemes 1 and 2.

APPENDIX B

SPECIAL CONSIDERATIONS IN THE COMPUTATION OF OPTIMAL CONTROLS

This section discusses the convergence characteristics of the iterative procedure described in Appendix A as observed during the computation of the results presented in Chapters 4 and 5. In particular, the major pitfalls that were encountered in applying the Knudsen type algorithm to synthesize optimal controls for Systems (B) through (E) are discussed. Also, the techniques employed to mitigate these difficulties are summarized.

B.1 Behavior of the Iterative Procedure

During the computation of the results presented in Chapters 4 and 5 it was found that the iterative behavior of the algorithm is directly dependent upon the following system characteristics and/or computational procedures:

1. The dimension of $\underline{u}(t)$ and the shape of Ω.
2. The quantitative structure of the switching functions.
3. The desired change in the state point $(\underline{x}(t_f) - \underline{x}(t_o))$.
4. The error between the computed (nominal) and the optimal controls.
5. The scheme for selecting Γ_k.

By iterative behavior we mean the effect of $\Delta\underline{V}$, which is computed during each iteration, on the control and hence on both the system's trajectory and the characteristics of G. In those cases where the

above mentioned items interacted unfavorably the real computational problem was one of achieving convergence with the rate of convergence becoming of secondary importance.

Let us now examine in detail how the aforementioned items, either alone or through interaction, influence the iterative behavior of a Knudsen type algorithm.

First, during the flooding process as outlined in Section 4.5.1 it was found that the algorithm described in Appendix A would, at times, fail to converge when $|\gamma| \lesssim 0.2$ and $\bar{L}_Y \lesssim 10$. The reason for this behavior becomes evident if one examines Figures 4.30 and 4.41. Here we find that when $\bar{L}_Y$ is small the two terms in each of Equations (4.26) and (4.27) can become of the same order of magnitude (i.e., $\alpha_1 \cong 1$); therefore, in general, the number of switchings in (t_o, t_f) is reduced when both $|\gamma|$ and $\bar{L}_Y$ become small. Should the total number of switchings be reduced to the point where the third switch point is lost from the interval (t_o, t_f) due to a perturbation $\Delta\underline{V}$ then the computation must terminate since G becomes singular. This situation characterizes the major difficulty in applying a Newton procedure when the rank of G depends upon the number of switching points in (t_o, t_f).

Second, providing the initial (terminal) state point does not lie on a switching hypersurface which contains optimal trajectories (i.e., $h_1 + h_2 \geq 3$) then the previously described difficulties will not occur if $(\underline{\alpha}, t_f)$ is close enough to $(\underline{\alpha}, t_f)^*$. In general, this means that in the region where $|\gamma| \lesssim 0.2$ and $\bar{L}_Y \lesssim 10$ the derived and optimal steering functions must have the same shape [15]. This condition will not be satisfied if the "guess" for the optimal control corresponding to

states which lie within this region is "bad" or if during the flooding process $(\underline{\chi}_f)_{i+1}$ $((\underline{\chi}_o)_{i+1})$ is separated from $(\underline{\chi}_f)_i$ $((\underline{\chi}_o)_i)$ by a switching hypersurface. In the latter case $\underline{u}^*_{i+1}(t_o) \neq \underline{u}^*_i(t_o)$. In many cases when $|\gamma|$ and/or $\bar{L}_Y$ were large enough it was found that the algorithm would recover from a bad guess for $(\underline{\alpha}, t_f)$ or from an encounter with a switching hypersurface if the derived and optimal controls were not too different in shape.

Third, in view of the requirement for at least n-1 switching points in (t_o, t_f) the proper selection of Γ becomes of increasing importance in cases where the total number of switchings approaches three. If Γ_k is too large the $\Delta\underline{V}$ computed during the k^{th} iteration may cause the third switch point to be lost from the interval (t_o, t_f). Hence, G becomes singular. Therefore, in such situations, the selection of Γ was motivated by achieving convergence with rate of convergence becoming of secondary importance. When $|\gamma|$ and/or $\bar{L}_Y$ were "large enough" the usual effect of selecting too large a value for Γ was either the onset of oscillations in $\|\Delta\underline{\chi}\|$ or $\|\Delta\underline{\chi}_{k+1}\| > \|\Delta\underline{\chi}_k\|$.

Fourth, as is commonly the case in iterative solutions, the dimension of $\underline{u}(t)$ as well as the shape of Ω has a profound influence on the convergence characteristics of the computational procedure. In general, it was found that the algorithm became less efficient and/or failed to converge more often during the flooding process as the dimension of $\underline{u}(t)$ decreased and when Ω became unsymmetrical (e.g., $\Omega = \Omega_D$). That is, for the four control systems considered the task of computing optimal controls for Jet Configuration (D) proved to be the most difficult in terms of achieving convergence. This was particularly

true when both $|\gamma|$ and $\bar{L}_\gamma$ were small. In such cases the form (ordering of the thrust and coast periods) of the derived control had to be very close to that of the optimal control in order to guarantee convergence. Hence, the iterative procedure would not, in general, converge, due to the loss of the third switch point when both $|\gamma|$ and L_γ were small if a guess was made for the optimal control. However, this was not a major problem since in the flooding process only small changes were made in $\bar{L}_\gamma$ starting from that value for which the optimal control was known; therefore, the derived control at each step was usually very close to optimal.

From the previous discussion it is evident that the major drawback of the iterative procedure described in Appendix A is that of requiring a minimum of three switching points in the interval (t_o, t_f). Therefore during the computation of the results presented in Chapters 4 and 5 it was necessary to modify the basic iterative procedure. Such modifications were designed to improve the iterative behavior are presented in the following sections.

B.2 Convergence Characteristics

To illustrate typical rates of convergence achieved during the computations discussed in Chapters 4 and 5 two examples of the relation between missed boundary conditions defined by

$$\|\underline{e}_k\| = \|\Delta \underline{\chi}_k\| \tag{B.1}$$

and the iteration number are presented in the sequel.

Example 1

Purpose: To illustrate the nearly quadratic convergence of the

Newton type procedure when the nominal and optimal controls have the same form.

Plant: Equation (4.7), $\gamma = -0.8$, 4-jets, $\beta_o = 0$.

Boundary Conditions: Case 1, Figure 4.5; $\bar{\omega}_y^o = -15$.

Remarks:

1. The initial error $\|\underline{e}_o\|$ shown in Figure B.1 is the result of a "guess" for the pair $(\underline{\alpha}, t_f)$.

2. The computation time was approximately three seconds on a B5500 digital computer.

Example 2

Purpose: To illustrate the iterative behavior when $\|\underline{e}_k\|$ is sensitive to the choice for Γ.

Plant: Equation (4.7), $\gamma = -0.8$, 4-jets, $\beta_o = 0$.

Boundary Conditions: Case 2, Figure 4.5; $\bar{\omega}_y^o = -35$.

Remarks:

1. The initial error $\|\underline{e}_o\|$ shown in Figure B.2 is again the result of a "guess" for the pair $(\underline{\alpha}, t_f)$.

2. $\underline{u}_o(t_o) = \underline{u}_e(t_o)$; however, when $k = 2$, $\Gamma = 1, 0.17$, $(u_x(t_o))_2 = (u_y(t_o))_2 = -1$; $(u_x(t_o))_e = (u_y(t_o))_e = +1$. Thus, $\|\underline{e}_2\| = 27.5$ even though $T_B - T_B^* \cong 0$.

3. The computation time was approximately 13 seconds.

B.3 Allowable Perturbations in the Final Time

As mentioned previously, the major drawback of Knudsen's algorithm is that of requiring at least n-1 switching points in the interval (t_o, t_f). In view of this requirement it was found that the following

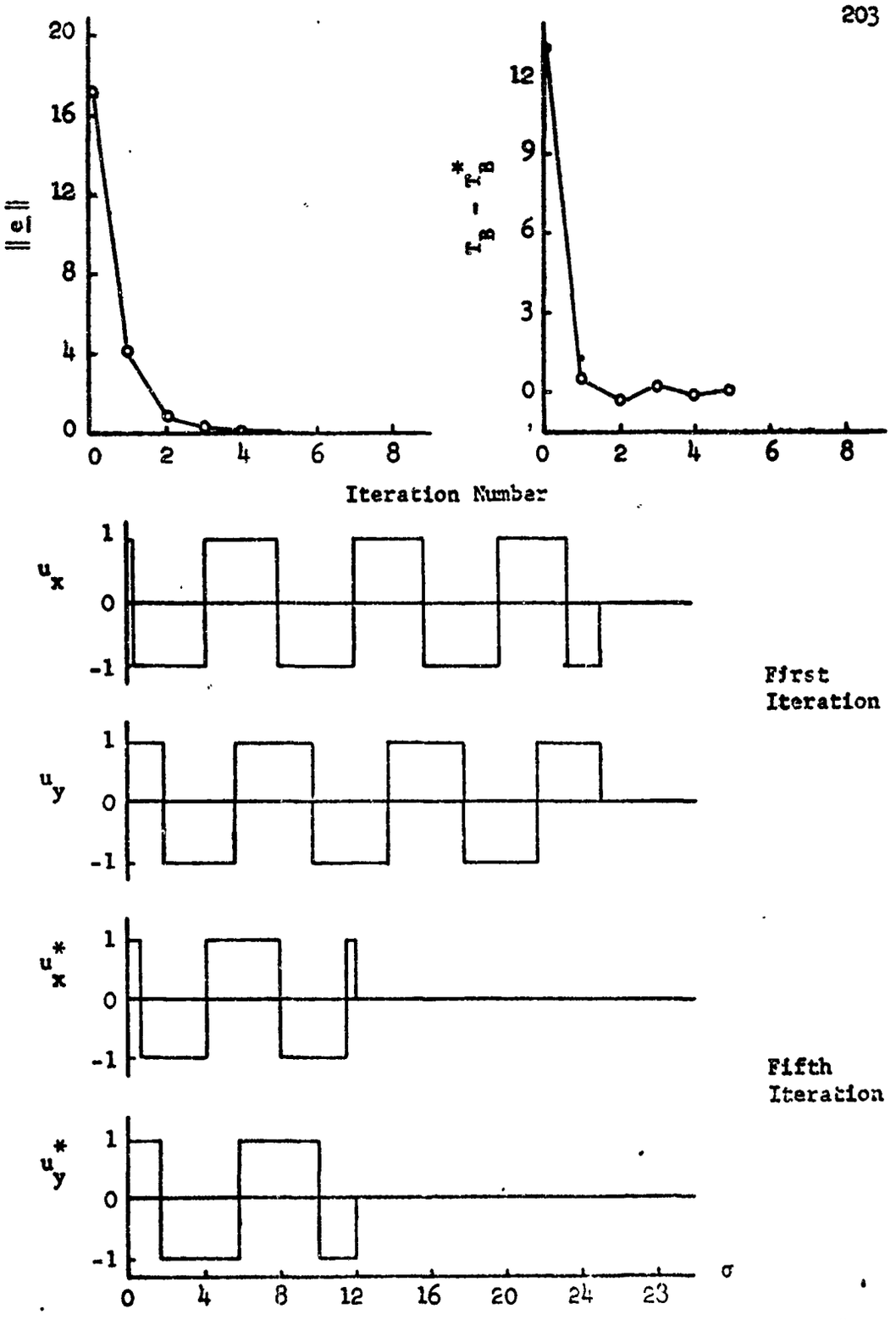

Figure B.1 Example No. 1

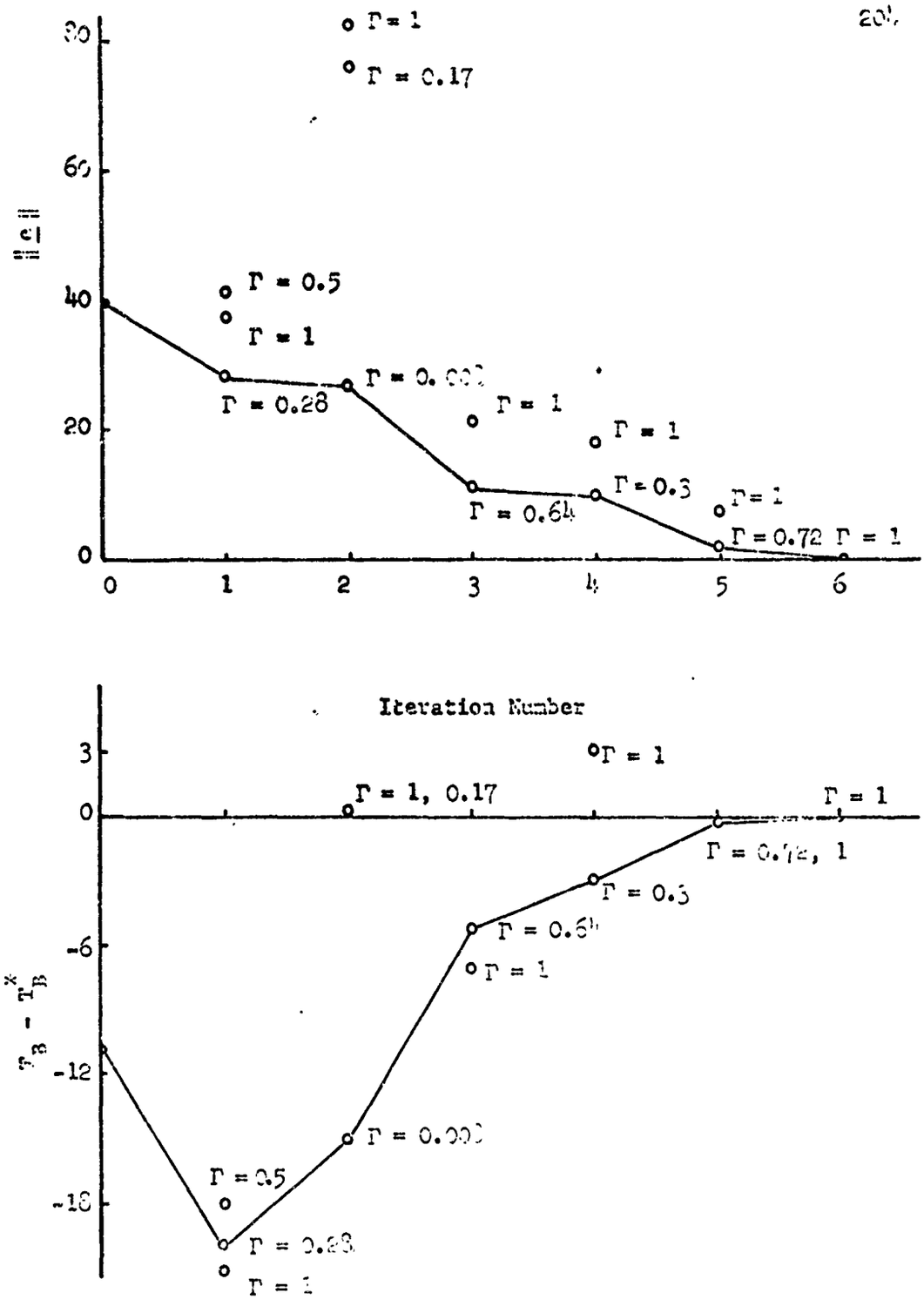

Figure 3.2 Example No. 2

conditions are conducive to G becoming singular:

1. $\underline{u}_o(t_o) \neq \underline{u}^*(t_o)$ and $(t_f)_k - t_o$ "small".
2. The shape of $\underline{u}_k(t)$ being considerably different than that of $\underline{u}^*(t)$.

Such situations occur, for example, when a bad guess is made for $\underline{\alpha}$ or in certain cases during the flooding process when the $(i+1)^{st}$ initial (terminal) state point is separated from the $(i)^{th}$ by a switching hypersurface. In the case when $(t_f)_k - t_o$ is "small enough" even small perturbations in the pair $(\underline{\alpha}_k, (t_f)_k)$ can cause the third switch point to be lost from the interval $(t_o, (t_f)_k)$. To alleviate this problem a systematic procedure was developed for crossing switching hypersurfaces when $t_f - t_o$ is small; the particular technique is discussed in the following section.

In many cases when the iterative procedure failed to converge due to $\underline{u}_k(t)$ being dissimiliar to $\underline{u}^*(t)$, it was noted that large negative perturbations were computed in the dimensionless final time. Hence, within several iterations the interval $(t_f)_k - t_o$ had become small enough to allow $h_1 + h_2 < 3$.[1] To prevent this "failure mode" from occuring a hard limit was placed on the computed perturbation Δt_f according to the following rule:

$$\Delta t_f = \begin{cases} (\Delta t_f)_{max} \text{ if } |\Delta t_f| \geq (\Delta t_f)_{max} \\ \Delta t_f \text{ if } |\Delta t_f| < (\Delta t_f)_{max} \end{cases} \qquad (B.2)$$

where $(\Delta t_f)_{max} \cong 0.05\ t_f$.

---

[1] The reason for this sensitivity to changes in t_f when $\underline{u}_k(t)$ does not have the same form as $\underline{u}^*(t)$ becomes evident if one considers a simple problem such as time-optimal control of the double integrator

The effect of limiting Δt_f in this manner is quite different than decreasing Γ. Reducing the iterative scale factor tends to decrease both $\|\Delta\underline{\alpha}\|$ and $|\Delta t_f|$. However, $|\Delta t_f|$ will still be large compared to $\|\Delta\underline{\alpha}\|$; hence, the overall effect of decreasing Γ is that of increasing the number of iterations until the third switch point is lost from the interval $(t_o, (t_f)_k)$. The beneficial effect of placing a bound on Δt_f is to allow the iterative procedure to cycle a sufficient number of times, thus reducing the error between $\underline{\alpha}_k$ and $\underline{\alpha}^*$. Once $\underline{u}^*(t)$ and $\underline{u}_k(t)$ are of the same form the procedure normally converges with no further difficulty (during the flooding process $(t_f^*)_{i+1} \cong (t_f^*)_i$ if the perturbation $\Delta\underline{X}$ is not too large; note, this is not true for System (D)).

In some cases where t_f^* was not "large" ($\bar{L}_Y \lesssim 10$) it was found that placing a lower limit on $(t_f)_k$ would tend to prevent G from becoming singular. This was accomplished by observing the fact that the required change in the normalized angular momentum dictates the fine time when the thruster "on-off" times are only a function of ω_s and β_o (see Section 4.6.1). At this point it should be noted that only during the application of Scheme 3 (see Appendix A) to select Γ were limits placed on Δt_f. Also note that this procedure was found to be rather ineffective during the computation of those results discussed in Section 4.7, i.e., when $\underline{u}(t) = u_D(t)$.

B.4 The Computation of Optimal Controls when the Initial (Final) State Point is Close to a Switching Hypersurface and the Total Number of Switching Points Equals Three

In this section we present a technique which prevents the iterative procedure from "hanging up" when the $(i+1)^{st}$ initial (terminal) state point in the flooding process is separated from the $(i)^{th}$ by a

switching hypersurface and, in addition, $(h_1 + h_2)^*_{i+1} = (h_1 + h_2)^*_i = 3$. Such a procedure was required during the computation of the results presented in Figures 4.7 through 4.13 and 4.30 through 4.33 when $(\bar{L}_Y)_B \lesssim 1$ and $(\bar{L}_Y)_C \lesssim 4$ (note, the discontinuities in α_B are not large and occur when $(\bar{L}_Y)_B \lesssim 1$ and, therefore, are not shown in Figures 4.6 through 4.8 and 4.10 through 4.12).

As indicated in the previous section the iterative procedure described in Appendix A experiences convergence difficulties when: (1) the interval (t_o, t_f) is "small", and (2) $\underline{u}_k(t)$ does not have the same form as $\underline{u}^*(t)$. Under such conditions the computed perturbations $(\Delta\alpha, \Delta t_f)$ will eventually result in G becoming singular.[2] Such was the situation during the computation of the results discussed in Sections 4.6.1 and 4.7.1; switching hypersurfaces were encountered when $T^*_B \lesssim 3$ and when $T^*_C \lesssim 5$. Therefore, to prevent the flooding procedure from "hanging up" at a switching hypersurface two subroutines were incorporated in the basic program. The first allows the required transition when the control is provided by Jet Configuration (C) and the second when the control is a two dimensional vector $(\underline{u}(t) = \underline{u}_B(t), \underline{u}_E(t))$.

B.4.1 Scalar Control

In this case the state space can be divided into regions defined by $u(t_o) = +1$ or $u(t_o) = -1$. Hence, when $(\underline{\chi}_f)_{i+1}$ is separated from $(\underline{\chi}_f)_i$ by a switching hypersurface we find that $u_{i+1}(t_o) = -u_i(t_o)$. In view of this change in $u(t_o)$ the following procedure is employed

---

[2] Limiting Δt_f does not, in general, provide a solution to this problem when $(f_f - t_o)$ is "small" since small changes in α can also cause $h_1 + h_2 < 3$

to compute the nominal control for $(\underline{\chi}_f)_{i+1}$ when $(u^*(t), t_f^*)_i$ is known:

1. Monitor h_y. If $h_y < 3$ then set $(u_y(t_o))_{i+1} = -(u_y(t_o))_i$.
2. Pick three switching points in $(t_o, (t_f^*)_i)$. Since $\|(\underline{\chi}_f)_{i+1} - (\underline{\chi}_f)_i\|$ is small, $(t_f^*)_{i+1} \cong (t_f^*)_i$.
3. Solve the switching equations $S_y(\alpha_{j+1}, t_j^y) = 0$, $j = 1,2,3$, simultaneously for α_{j+1}. This is possible since $\underline{\alpha}$ is a normalized form of $\underline{P}(t_o)$ (see Appendix C).
4. Use $(u_y(t))_{i+1} = \text{SGN}\,[e^{-At}\alpha_{i+1}]$ as the new estimate for the control and $(t_f^*)_{i+1} = (t_f^*)_i$ for the final time.

The only input required by this procedure are three switching times. In view of the algorithm's "failure mode" the following values for the switching times were found to be satisfactory:

$$(t_1^y)_{i+1} = \tfrac{1}{4}(t_f)_i,\ (t_2^y)_{i+1} = \tfrac{1}{2}(t_f)_i,\ (t_3^y)_{i+1} = \frac{3(t_f)_i}{4}$$

Thus, perturbations in $(\underline{\alpha}, t_f)$ were not as likely to result in $h_y < 3$ as would be the case if $(t_1^y)_{i+1}$ were close to zero or (t_3^y) were close to t_f. It was also found that Schemes 2 and 3 for selecting Γ resulted in a more reliable iterative scheme; $\Gamma > 0.7$ would often result in $h_y < 3$

B.4.2 Two Dimensional Vector Controller

In the sequel we present a technique for crossing a switching hypersurface when the admissible control set is a square in R_2. In this case there are three possible choices for $(\underline{u}(t_o))_{i+1}$. One method for evaluating $(\underline{u}(t_o))_{i+1}$ would be to systematically iterate on all combinations of $u_x(t_o)$ and $u_y(t_o)$ until the correct one is found. However, in view of the conditions (final time, number of switchings per channel, and total number of switchings) which existed when a switching

hypersurface was encountered such a procedure was found to be unnecessary. Instead, a systematic method was developed which takes advantage of the apparent "smoothing" (the reduction in magnitude of the discontinuity of the support hyperplanes at the corners) of the isochrones as the dimension of the control vector increases.

Let us begin by reiterating the behavior of the control as changes were made in $\bar{L}_Y$ (during the flooding process $(\bar{L}_Y)_{i+1} = (\bar{L}_Y)_i - \Delta\bar{L}_Y$). For those results presented in Figures 4.6 through 4.13 the starting value of $(\bar{L}_Y)_B$ was 40 and a switching hypersurface was not encountered until $(\bar{L}_Y)_B \cong 1$. During this flooding neither $u_x(t_o)$ nor $u_y(T_o)$ changed sign due to the introduction of new switch points into the beginning of the interval (t_o,t_f) or due to the loss of existing switching points. However, switching points were lost from the right end of the interval (t_o,t_f) as the terminal time decreased, this situation is illustrated in Figure B.3. Hence, G did not become singular until $h_x = 2$ $(h_x = 1)$, $h_y = 1$ $(h_y = 2)$, and the computed perturbations $(\Delta\underline{\alpha}, \Delta t_f)$ caused the loss of one switch point from the right end of the interval (t_o,t_f). At this point further information as to the form of the new control was found to be essential in order to continue with the flooding process.

From the time-optimal solutions to simple problems (the harmonic oscillator) it appears that the discontinuities in the support hyperplanes at the corners of the minimum time isochrones tend to "smooth out" as the dimension of the control vector increases. Thus, it was conjectured that when $(\underline{\chi}_f)_{i+1}$ was separated from $(\underline{\chi}_f)_i$ by a switching hypersurface, the jump in $\underline{\alpha}$ would not be large when $\underline{u}(t) = \underline{u}_B(t)$, $\underline{u}_E(t)$.

This hypothesis is found to be realistic if one compares the magnitude of the discontinuities in α_C, Figures 4.30 through 4.32, to typical values for α_B, e.g., for $\gamma = 0.2$, $\beta_o = 0$: $(\bar{L}_Y)_B = 0.7$; $\alpha_1 = 1.03$, $\alpha_2 = 0.85$, $\alpha_3 = 3.36$, $\alpha_4 = 1$, $T_B^* = 1.66$; $(\bar{L}_Y)_B = 0.6$; $\alpha_1 = 1.03$, $\alpha_2 = 0.35$, $\alpha_3 = 3.06$, $\alpha_4 = 1$, $T_B^* = 1.51$.

With the previous discussion in mind we can now summarize the procedure for effecting switching hypersurface transitions.

1. Determine the first roots of $S_x(t) = 0$ and $S_y(t) = 0$ which occur outside the interval $(t_o, (t_f)^1_{i+1})$; a typical result is depicted in Figure B.3.[3] Here, the additional switching points t^x_{1-}, t^y_{1-}, t^y_{1+}, and of course the switch point that was lost, t^x_{1+}, are shown. A comparison between t^x_{1-}, t^y_{1-} and t^y_{1+} is then made to determine the switch point closest to $(t_o, (t_f)^1_{i+1})$; this point is denoted by $(t^j_i)^1$. In all cases considered during the computation of the results presented in Chapters 4 and 5 a root of the switching function which did loose a zero from the right end of the interval $(t_o, (t_f)^1_{i+1})$ was found at $t = -\epsilon$, $\epsilon << t_f^*$. This situation is illustrated in Figure B.3 where $u_x(t)$ has lost the switch point t^x_2 and $u_y(t)$ is about to gain the switch point t^y_{1+} at the left end of $(t_o, (t_f)^1_{i+1})$.
2. Based on the premise that the "jump" in $\underline{\alpha}$ is not large, small perturbations are made in $\underline{\alpha}$ so as to achieve the following changes in $\underline{u}(t)$:

   a) $(t^j_i)^1$ moves into the interval $(t_o, (t_f)^1_{i+1})$.

---

[3] $(t_f)^1_{i+1}$ is the result of the first iteration for $(t_f)_{i+1}$.

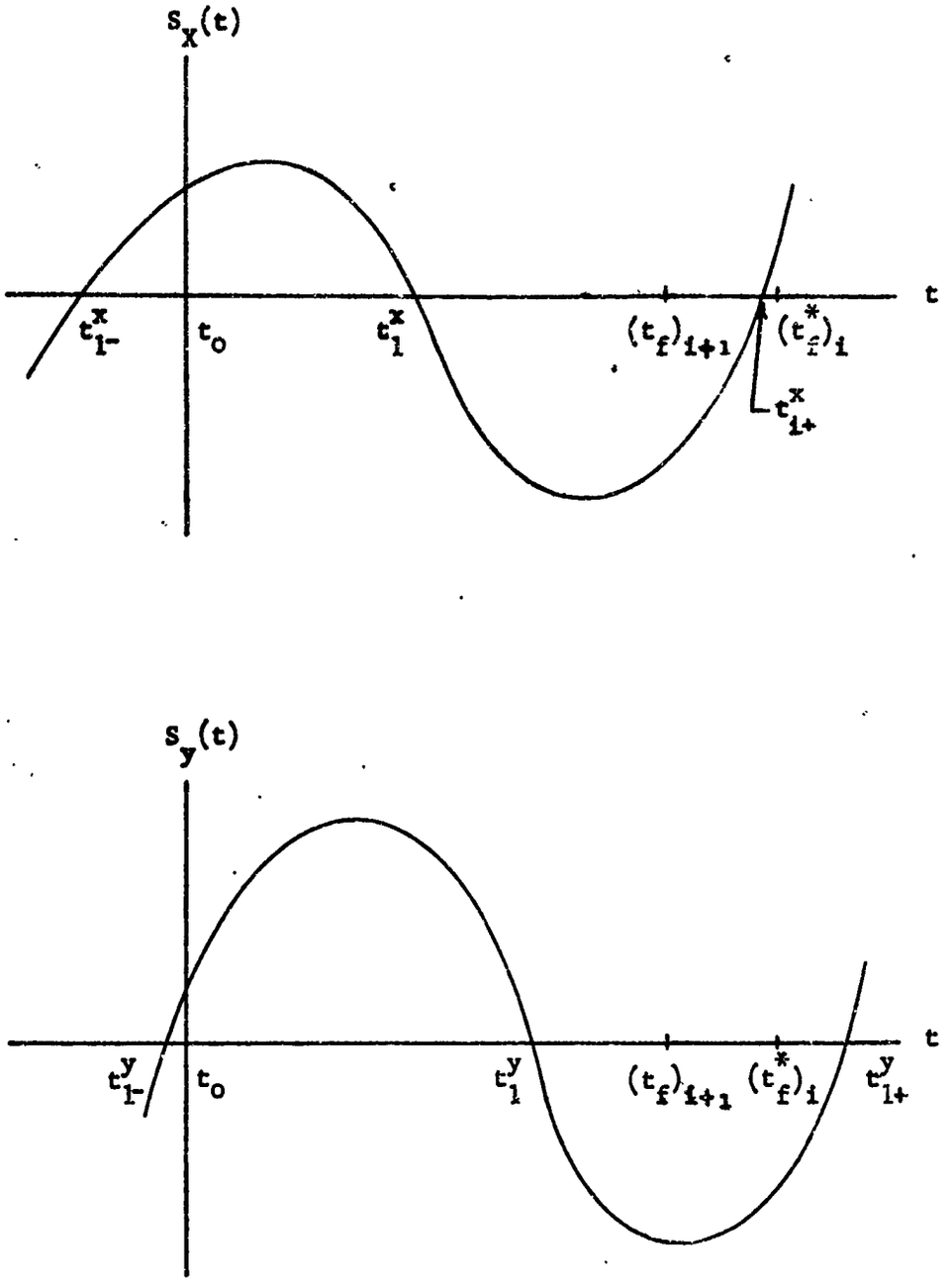

Figure B.3 The Loss of a Switch Point During an Encounter With a Switching Hypersurface

b) The switch points that were not lost remain within the interval $(t_o, (t_f)^1_{i+1}$, e.g., t^x_1 and t^y_1 in Figure B.3.

Thus the following alterations were made in the steering functions:

(1) $h_1(h_2) = 1$, $h_2(h_1) = 2$ changed to $h_1(h_2) = 2$, $h_2(h_1) = 1$, and

(2) as dictated by the location of $(t^j_i)^i$ a sign changed occurred in either $u_1(t_o)$, $u_1(t_f)^1_{i+1}$, $u_2(t_o)$, or $u_2(t_f)^1_{i+r}$. This procedure was accomplished by relating changes in $\underline{\alpha}$ linearly to the desired changes in t^j_i. A recursive relation similar to (A.9) was then employed to compute changes in α such that $(t^j_i)^i$ moved into the interval $(t_o, (t_f)^1_{i+1})$ and at the same time allowing no changes in the two switch points which remained in $(t_o, (t_f)^1_{i+1})$, e.g., t^x_1 and t^y_1.

B.5 Controller Configurations (D) and (E): Additional Computational Requirements

In view of the peculiar characteristics of both $u^*_D(t)$ and $(S_x'(t), S_y'(t))_E$, further modifications designed to improve the iterative behavior were made to the basic algorithm. As in the previous sections the motive for incorporating additional computational rules or procedures was one of ensuring the existence of G^{-1}.

B.5.1 Controller (D)

Of the four systems for which optimal controls were determined by iterating on $(\underline{\alpha}, t_f)$ the computation of $(u_y, t_f)^*_D$ proved to be the most difficult in terms of the effort required to achieve convergence. In preliminary attempts to compute $(\underline{\alpha}, t_f)^*_D$ in terms of $(\bar{L}_Y)_D$ where the nominal and optimal controls did not have similar forms (the ordering of the thrust and coast periods were dissimilar) excessively large perturbations were computed in $\underline{\alpha}$ and/or t_f; hence, at some point

$h_y < 3$ and thus G became singular. In view of this "failure mode" the following procedure was developed to assist in the computation of realistic perturbations.

The primary difficulty in achieving rapid convergence when $u(t) = u_D(t)$ becomes evident when we examine Figures 4.44 and 4.45. Here, we find that T_D^* is not a continuous function of $\bar{L}_Y$, which is in direct contrast to the characteristics of T_A^*, T_B^*, T_C^-, and T_E^*. Hence, this situation is similar to an encounter with a switching hypersurface (see Section B.4) where $\underline{\alpha}$ undergoes a discontinuity. However for Control System (D) the change in control due to the loss of a switch point from the right end of $(t_o, (t_f)^1_{i+1})$ as changes are made in $\bar{L}_Y$ ($(\bar{L}_Y)_{i+1} = (\bar{L}_Y)_i - \bar{L}_Y$) results in $u_y(t_f)^1_{i+1} = 0$. When this situation occurs during the flooding process t_f^* undergoes a discontinuity since the control must terminate with a thrust period. Therefore, to prevent the computation of large perturbations in $\underline{\alpha}$ and/or t_f the nominal control for $(\chi_f)_{i+1}$ was formed by: (1) setting $\underline{\alpha}_{i-1} = \underline{\alpha}^1_{i+1}$, (2) systematically reducing $(t_f)^1_{i+1}$ by a small amount ($(t_f)_{j+1} = (t_f)_j - \Delta t$, j= 1, 2, 3, ... j) until $u_y(t_f)_j = 1$, and (3) setting $(t_f)_{i+1} = (t_f)_j$. This procedure gave good results and allowed rapid solutions for $(\underline{\alpha}, t_f)^*$ in terms of $\bar{L}_Y$ for values of $\bar{L}_Y$ from 40 down to 0.2.

B.5.2 Controller (E)

Due to the form of $(S_x'(t), S_y'(t))_E$ it is possible to loose all the switching points from (t_o, t_f) during the iterative process when $|\alpha_1| \leq |\alpha_3|$ and $|\alpha_2| \leq |\alpha_4|$. To prevent this situation from occuring α_1 and α_2 were defined by

$$\alpha_1 = \alpha_3 \pm \xi_3 , \quad \alpha_2 = \alpha_4 \pm \xi_4$$

whenever the computed perturbation in $\underline{\alpha}$ resulted in $h_x' + h_y' < 3$. The augmenting terms ξ_3 and ξ_4 were chosen such that the control deviation from $u_x(t) = \quad 1$ or $u_y(t) = \quad 1$ for all $t \in (t_o, t_f)$ due to switch points located close together resulted in the iteration cut-off criterion on the normalized angular momentum being satisfied. That is,

$$|\hat{L}_X| - |\hat{L}_X(T_E)| \leq 0.01, \quad |\hat{L}_Y| - |\hat{L}_Y(T_E)| \leq 0.01.$$

Thus, the boundaries shown in Figures 5.4 through 5.6 which separate the singular and non-singular regions were defined when either $\alpha_1 = \alpha_3 \pm \xi_3$ or $\alpha_2 = \alpha_4 \pm \xi_4$.

APPENDIX C

VERIFICATION OF THE SWITCHING SEQUENCES DEFINED IN TABLE 4.1

This appendix consists of two parts. The first section verifies that the switching logic for Controller (B), as defined in Table 4.1, is optimal when $T_B^* < T_B'$, $T_B' = \frac{1}{4}\pi$. The second section demonstrates that $S_x(\sigma)$ $(S_y(\sigma))$ can have three independent zeros in an arbitrary interval (σ_o, σ_f); hence, there exists a solution for $\underline{\alpha}$ in terms of the three roots.

C.1 Optimal Switching Logic for Controller (B) when $T_B^* < T_B'$

In Section 4.4.1 it was assumed that the initial (terminal) state point does not lie on a switching hypersurface which contains optimal trajectories; therefore, $h_x + h_y \geq 3$. Moreover, as shown in C.2 there exists an $\underline{\alpha}$ such that three independent roots of either $S_x(\sigma_i) = 0$ or $S_y(\sigma_j) = 0$ occur in an arbitrary interval (σ_o, σ_f). We shall now demonstrate that the total number of switching points cannot exceed three when $T_B^* < T_B'$.

One way to verify this claim is to show that the function

$$\tilde{T} = T - \tfrac{1}{2} m \pi \tag{C.1}$$

$m = 0, \pm 1, \pm 2, \ldots,$ has at most three zeros for $\sigma \in (0, T_B')$ where

$$T = \tan^{-1}\left[\frac{\alpha_1 \sin(\gamma\sigma + \alpha_2) + \sin(\sigma + \alpha_3)}{\alpha_1 \cos(\gamma\sigma + \alpha_2) + \cos(\sigma + \alpha_3)}\right] \tag{C.2}$$

and (m) is chosen to represent a particular sequence of zeros, e.g.,

$m = 0,1,0$, $m = 0,1,2,3$.

Through a geometric interpretation of the quotient $S_x(\sigma)/S_y(\sigma)$ we find that the magnitude of α_1 has significant influence on the behavior of T. Therefore, the cases when $|\alpha_1| < 1$, $|\alpha_1| > 1$, and $|\alpha_1| = 1$ are considered separately.

Case A: $|\alpha_1| < 1$

Differentiating (C.2) with respect to σ gives

$$\frac{dT}{d\sigma} = \frac{\gamma + 1}{2} + \frac{(\gamma - 1)(\alpha_1^2 - 1)}{2(\alpha_1^2 + 1 + 2\alpha_1 \cos\lambda)} \tag{C.3}$$

where $\lambda = (\gamma - 1)\sigma + \alpha'$. Note that for $-1 < \gamma < 1$ both terms on the right side of (C.3) are always positive. Define λ as the new independent variable. Then (C.3) becomes

$$dT = \tfrac{1}{2}\left[\frac{\gamma + 1}{\gamma - 1} + \frac{\alpha_1^2 - 1}{\alpha_1^2 + 1 + 2\alpha_1 \cos\lambda}\right] d\lambda . \tag{C.4}$$

Integrating the second term from $\lambda = 0$ to $\lambda = 2\pi$ we find that the change in T is

$$\Delta T = \frac{\gamma + 1}{2}\Delta\sigma + \pi . \tag{C.5}$$

Since $dT/d\sigma$ is always positive, roots of the form $m = 0, 1, 2, 3, \ldots$ are of interest. If $\Delta T < 3\pi/2$ then there are at most three roots of this type. For a given interval $\Delta\sigma = \sigma_f - \sigma_o$ the first term on the right side of (C.5) will be a maximum when $\gamma = 1$. Therefore, $\Delta T < 3\pi/2$.

Case B: $|\alpha_1| > 1$

In this case the second term of (C.3) is always negative for $-1 < \gamma < 1$. Furthermore, setting the left side of (C.3) equal to zero

we find that the derivative changes sign when

$$\lambda = \cos^{-1}\left[-\frac{\alpha^2\gamma + 1}{\alpha(\gamma + 1)}\right]. \qquad (C.6)$$

Therefore, unlike the situation encountered in Case A, we must consider the fact that zeros of $\tilde{\Upsilon}$ can occur for values of (m) other than those defined by the sequence m = 0, 1, 2, 3, ..., To show that the total number of zeros of $S_x(\sigma)$ and $S_y(\sigma)$ cannot exceed three it is sufficient to demonstrate that four zeros of the type defined in Table C.1 cannot occur.

Case	m	Case	m
1-a	0, 0, 0, 1	3-b	3, 2, 1, 0
1-b	1, 0, 0, 0	4-a	0, -1, -1, 0
2-a	0, 0, 1, 2	4-b	0, 1, 1, 0
2-b	2, 2, 1, 0	5-a	1, 1, 0, 0
3-a	0, 1, 2, 3	5-b	0, 0, 1, 1

Table C.1

Possible Combinations by Which Four Zeros of $\tilde{\Upsilon}$ Can Occur

To accomplish this task we first consider a geometric interpretation of Equation (C.4) as depicted in Figure C.1. By observing the location of both the zeros of $d\Upsilon/d\sigma$ and the maximum change which occurs in Υ between the zeros it is possible to demonstrate that Cases 1 through 4 cannot occur. Note that Cases 1, 2, and 4 require $|\Delta\Upsilon|$ to be at least $\pi/2$ before and/or after the first or second zero of $d\Upsilon/d\sigma$

and that Case 3 requires: (1) $|\Delta T|$ to be at least $3\pi/2$, and (2) $T(\sigma)$ to be monotone.

From Equation (C.3) it is evident that the maximum positive change in T occurs when $\gamma = +1$ and is

$$\Delta T_{max} < \tfrac{1}{2}\pi$$

when $\Delta\sigma < \pi/2$. Thus, Cases 1-a, 2-a, 3-a, 4-a,b, and 5-b cannot exist.

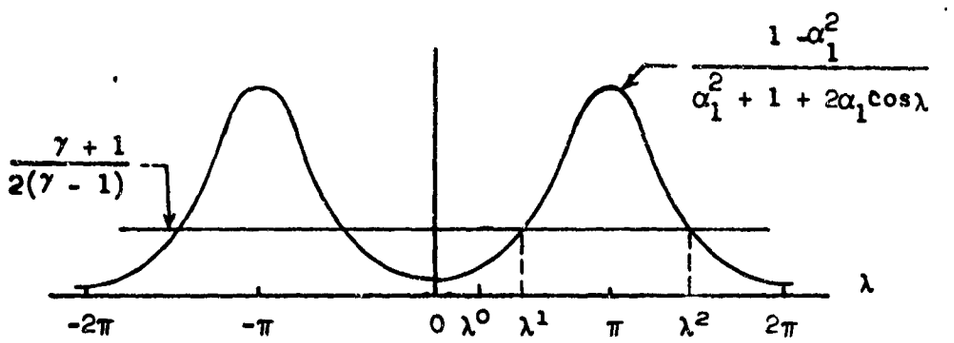

Figure C.1 A Geometric Interpretation of Equation (C.4)

Following the method of integration employed in Case A we find that the maximum negative change in T is $-\pi$ when $\Delta\lambda = -2\pi$. Therefore, Cases 2-b and 3-b cannot occur.

Case 1-b requires that the interval $\Delta\lambda$ contains one of the points defined by $\lambda = 2m\pi$, $m = 0, \pm1, \pm2, \ldots$. Moreover, the negative term of (C.4) is an even function of λ (see Figure C.1). Consequently, the maximum negative change in T when: (1) $|\Delta\lambda| < \pi$, and (2) the interval $\Delta\lambda$ contains the point defined by $\lambda = 2m\pi$, $m = 0, \pm1, \pm2, \ldots$, is greater than $-\pi/2$. Therefore, Case 1-b cannot occur.

To show that Case 5-a cannot occur we must resort to a more sophisticated approach then that used in the previous paragraphs. In fact, it appears that T can change by $-\pi/2$. Therefore, Equations (C.3)

and (C.6) must be examined in detail in order to determine if both the ordering and magnitudes of the positive and negative changes in T required for the existence of four zeros can indeed occur.

To complete the proof and show that Case 5-a cannot exist when $\Delta\sigma < \Delta\sigma'$ (let us assume that $\Delta\sigma' = \pi/2$) the following facts are noted: (1) $|\lambda_f - \lambda_o| < \pi$ when $\Delta\sigma < \pi/2$, and (2) $\lambda^1 \epsilon [\lambda_f, \lambda_o]$ and $\lambda^2 \epsilon [\lambda_f, \lambda_o]$ if two zeros of $dT/d\sigma$ are to occur when $\lambda \epsilon [\lambda_f, \lambda_o]$. Now let $\lambda^2 = \lambda_o$ If $\lambda_f - \lambda_o = \lambda^o - \lambda^2$ where $\lambda^1 \geq \lambda^o$ and, in addition, if $\Delta T = -\pi/2$ for $\Delta\lambda = \lambda^o - \lambda^2$ then it is possible for four zeros of $\tilde{T}$ to occur. Moreover, the aforementioned procedure for locating the interval $[\lambda_f, \lambda_o]$ on the λ axis represents the most efficient means by which $\tilde{T}$ can have four zeros. This is due to the fact that the positive change in T, which occurs between λ^1 and λ^o, is a maximum ($\lambda^1, \lambda^2 \epsilon [\lambda_f, \lambda_o]$). To find the smallest change in λ for which four zeros can occur, the function

$$\Delta\lambda = 2\pi - \lambda^o - \lambda^1 \tag{C.7}$$

must be minimized subject to the constraints

$$g(\alpha_1, \gamma, \lambda^1) = \tfrac{1}{2}\pi - \tan^{-1}\left[\frac{\alpha_1 - 1}{\alpha_1 + 1} \tan \tfrac{1}{2}\lambda^o\right] - \tan^{-1}\left[\frac{\alpha_1 - 1}{\alpha_1 + 1} \tan \tfrac{1}{2}\lambda^1\right] + \frac{\gamma + 1}{2(\gamma - 1)}[2\pi - \lambda^o - \lambda^1] = 0 \tag{C.8}$$

$$|\alpha| > 1, \quad |\gamma| < 1, \quad \lambda^o \leq \lambda^1, \quad \lambda^o > 0 \tag{C.9}$$

$|\Delta\lambda|_{max} = \pi$ and the point $\lambda = \pi$ must be contained in $[\lambda_f, \lambda_o]$. Thus, we must solve a Lagrange multiplier problem where some of the constraints are strict inequalities.

From the theory of constrained maxima or minima (see for example Reference [22]) we find that it is necessary that the point defined by $(\alpha_1, \gamma, \lambda^1)$ at which $\Delta\lambda$ takes on a relative maximum or minimum satisfy the set of equations

$$\frac{\partial \Delta\lambda}{\partial \alpha_1} + \tilde{\lambda} \frac{\partial g}{\partial \alpha_1} = 0 \qquad \text{(C.10)}$$

$$\frac{\partial \Delta\lambda}{\partial \gamma} + \tilde{\lambda} \frac{\partial g}{\partial \gamma} = 0 \qquad \text{(C.11)}$$

$$\frac{\partial \Delta\lambda}{\partial \lambda^1} + \tilde{\lambda} \frac{\partial g}{\partial \lambda^1} = 0 \qquad \text{(C.12)}$$

where $|\gamma| < 1$ and $|\alpha_1| > 1$. For reasons which will become evident presently it is desirable to select values for γ within the allowable range and then solve the lower dimensional multiplier problem. Thus, we are interested in solving (C.8) in addition to

$$\frac{\partial \Delta\lambda}{\partial \alpha_1} + \tilde{\lambda} \frac{\partial g}{\partial \alpha_1} = 1 + \tilde{\lambda}\left[\frac{(\alpha_1^2 - 1)\sec^2 \frac{1}{2}\lambda^1}{(\alpha_1 + 1)^2 + (\alpha_1 - 1)^2 \tan^2 \frac{1}{2}\lambda^1} + \frac{\gamma + 1}{2(\gamma - 1)}\right] = 0 \qquad \text{(C.13)}$$

$$\frac{\partial \Delta\lambda}{\partial \lambda^1} + \lambda \frac{\partial g}{\partial \lambda^1} = \frac{[1 - \alpha_1^2(\gamma + 2)]}{\alpha_1(\gamma + 1)\sqrt{\alpha_1^2\gamma^2(1 - \alpha_1^2) + \alpha_1^2 - 1}} +$$

$$\tilde{\lambda}\left[\frac{\gamma^2\alpha_1(1 - \alpha_1) + (\alpha_1^2 - 1) + 1}{2\alpha_1(1 - \gamma)(\alpha_1 + 1)(1 - \gamma\alpha_1)\sqrt{\dfrac{(\alpha_1 - 1)(1 + \gamma\alpha_1)}{(\alpha_1 + 1)(1 - \gamma\alpha_1)}}} -\right.$$

$$\left.\frac{2\tan \frac{1}{2}\lambda^1}{(\alpha_1 + 1)^2 + (\alpha_1 - 1)^2 \tan^2 \frac{1}{2}\lambda^1} + \right] \qquad \text{(C.14)}$$

$$\left.\frac{\gamma[1 - \alpha_1^2(\gamma + 2)]}{2\alpha_1(\gamma - 1)\sqrt{\alpha_1^2\gamma^2(1 - \alpha_1^2) + \alpha_1^2 - 1}}\right] = 0$$

for $(\alpha_1, \lambda^1, \lambda)$ when $|\alpha_1| > 1$. Due to the non-linearity of these equations a gradient procedure was employed to iterate for the pair (α_1, λ^1). The particular method used [23] required approximately thirty seconds on a B5500 digital computer to converge to a solution of Equations (C.8), (C.13), and (C.14) for each value of γ. The results of this numerical approach are presented in Figure C.2. At this point it should be noted that the graphs shown in Figure C.2 are the result of solving the Lagrange multiplier problem when: (1) only the strict equality, Equation (C.8), is considered, and (2) Equations (C.8), (C.13) and (C.14) are considered (when $0 < \lambda^0 < \lambda^1$).

For values of γ between $\gamma \approx -0.26$ and $\gamma \approx +0.26$ neither λ^0 nor α_1 violated the constraints given by (C.9); hence, simultaneous solutions were obtained for Equations (C.8), (C.13), and (C.14). When γ became approximately + 0.26 it was evident that $\lambda^0 \to \lambda^1$. Therefore, the solution when $\gamma \gtrsim 0.26$, was obtained by setting $\lambda^0 = \lambda^1$ and iterating on α_1 until (C.8) was satisfied.

Due to the fact that $\lambda^0 \to 0$, a simultaneous solution to Equations (C.8), (C.13), and (C.14) could not be found when $\gamma \lesssim -0.26$. When this occurred λ^0 was set equal to zero and the iterative procedure was then employed to solve (C.8) for α_1; as indicated in Figure C.2, no solutions were found.

In the multiplier problem the cost must be evaluated when the constrained variables become saturated at their allowable limits. In

the preceeding discussion it was noted that solutions to (C.8) were obtained in terms of α_1 when $\lambda^o = \lambda^1$ for $\gamma \gtrsim 0.26$. As indicated in Figure C.2 it was also possible to satisfy (C.8) when $\lambda^o = \lambda^1$ for values of γ down to $\gamma \approx -0.38$. Note that the cost is slightly less when $\lambda^o = \lambda^1$ than it is for $0 < \lambda^o < \lambda^1$. Also note that $\Delta\sigma$ appears to approach $\pi/4$ as $\gamma \to +1$. Hence, for those values of γ which are of physical interest, $\tilde{\tilde{T}}$ cannot have four zeros when $\Delta\sigma < \pi/4$.

Case C: $|\alpha_1| = 1$

If $\cos\lambda \neq -1$ then the second term of (C.3) is identically zero; therefore, the conclusions reached in Case A are applicable.

When $\lambda = \pm m\pi$, $m = 1, 3, 5, \ldots$, the second term of (C.3) becomes, in the limit, as $\alpha_1 \to 1$

$$\lim_{\alpha_1 \to 1} \frac{(\gamma-1)(\alpha_1+1)}{(\alpha_1)} .$$

Since this limit is not unique a singular condition exists. This behavior is apparent if one considers a geometric interpretation of the following equations

$$\Theta = \tan^{-1}\left[\frac{\lambda_1 \sin(\sigma+\lambda_2)}{\lambda_1\cos(\sigma+\lambda_2)}\right]$$

where

$$\lambda_1^2 = \alpha_1^2 + 1 + 2\alpha_1\cos(\lambda_3-\alpha_3)$$

$$\lambda_2 = \tan^{-1}\left[\frac{\sin\alpha_3+\alpha_1\sin\lambda_3}{\cos\alpha_3+\alpha_1\cos\lambda_3}\right]$$

$$\lambda_3 = (\gamma-1)\sigma + \alpha_2$$

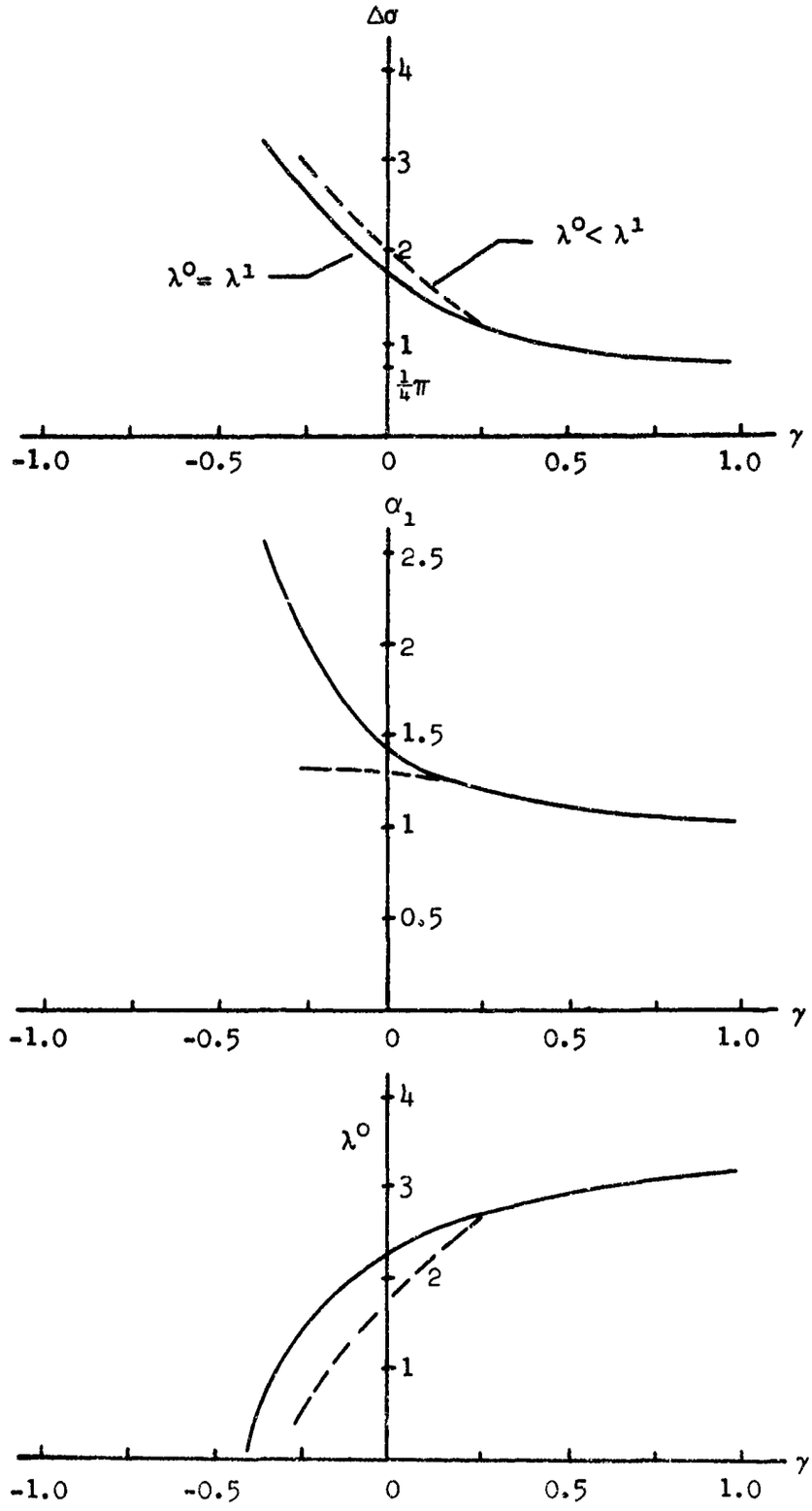

Figure C.2 Solution to the Multiplier Problem

It is readily shown that $|\Delta T| < \pi$ when $\Delta\sigma < \pi$. Therefore, arguments similar to those in Cases A and B can be used to show that T cannot have four zeros when $\Delta\sigma < \pi/4$.

C.2 Independent Zeros of the Switching Functions

The switching function $S_x(\sigma)$, $(S_y(\sigma))$, has three independent zeros $S_x(\sigma_i) = 0$, $(S_y(\sigma_i) = 0)$, $i = 1, 2, 3$. Thus, $S_x(\sigma)$, $(S_y(\sigma))$, can be made to have three zeros in an arbitrary interval (σ_o, σ_f).

Proof:

At the switching times σ_i, $i = 1, 2\ 3$, $S_x(\sigma_i) = 0$. Hence Equation (4.23) becomes:

$$S_x(\sigma_1) = P_{1_o}\cos\gamma\sigma_1 + P_{2_o}\sin\gamma\sigma_1 + P_{3_o}\cos(\sigma_1+\beta_o)+P_{4_o}\sin(\sigma_1+\beta_o) = 0$$

$$S_x(\sigma_2) = P_{1_o}\cos\gamma\sigma_2 + P_{2_o}\sin\gamma\sigma_2 + P_{3_o}\cos(\sigma_2+\beta_o)+P_{4_o}\sin(\sigma_2+\beta_o) = 0$$

$$S_x(\sigma_3) = P_{1_o}\cos\gamma\sigma_3 + P_{2_o}\sin\gamma\sigma_3 + P_{3_o}\cos(\sigma_3+\beta_o)+P_{4_o}\sin(\sigma_3+\beta_o) = 0$$

Finally for some $S_x(\sigma_4) \neq 0$ we have

$$S_x(\sigma_4) = P_{1_o}\cos\gamma\sigma_4 + P_{2_o}\sin\gamma\sigma_4 + P_{3_o}\cos(\sigma_4+\beta_o)+P_{4_o}\sin(\sigma_4+\beta_o).$$

Writing the above equations in matrix form gives:

$$\begin{bmatrix} \cos\gamma\sigma_1 & \sin\gamma\sigma_1 & \cos(\sigma_1+\beta_o) & \sin(\sigma_1+\beta_o) \\ \cos\gamma\sigma_2 & \sin\gamma\sigma_2 & \cos(\sigma_2+\beta_o) & \sin(\sigma_2+\beta_o) \\ \cos\gamma\sigma_3 & \sin\gamma\sigma_3 & \cos(\sigma_3+\beta_o) & \sin(\sigma_3+\beta_o) \\ \cos\gamma\sigma_4 & \sin\gamma\sigma_4 & \cos(\sigma_4+\beta_o) & \sin(\sigma_4+\beta_o) \end{bmatrix} \begin{bmatrix} P_{1_o} \\ P_{2_o} \\ P_{3_o} \\ P_{4_o} \end{bmatrix} = \begin{bmatrix} 0 \\ 0 \\ 0 \\ S_x(\sigma_4) \end{bmatrix} \qquad (C.17)$$

The functions $\cos\gamma\sigma$, $\sin\gamma\sigma$, $\cos(\sigma+\beta_o)$, $\sin(\sigma+\beta_o)$ are linearly indepen-

dent for $-1 < \gamma < 1$. Hence, the coefficient matrix is non-singular and, therefore, its inverse exists. Thus Equation (C.17) can be solved for $\underline{P}_o$ which shows that $S_x(\sigma)$ has three independent zeros (through a similar procedure we can easily show that $S_y(\sigma)$ has three independent zeros).

REFERENCES

1. Athans, M., Falb, P. L., and Lacoss, R. T. "Time-Optimal Velocity Control of a Spinning Space Body," IEEE Transactions of Applications and Industry, No. 67, July 1963, pp. 206-214.

2. Gruber, W. H., Lieberman, S. I., and Margosian, Z. "Attitude Control of Spin-Stabilized Space Stations," Proceedings of the Eleventh Annual East Coast Conference on Aerospace and Navigational Electronics, October 21-23, 1964, pp. (1.1.1-1)-(1.1.1-10).

3. Thau, F. E., Tavantzis, J., and Friedland, B. "Quasi-Optimum Three Axis Control of a Space Vehicle," Proceedings of the Second IFAC Symposium on Automatic Control in Space, 2nd, Vienna, Austria, September 4-6, 1967.

4. Hales, K. A. and Flugge-Lotz, I. "Minimum-Fuel Attitude Control of a Rigid Body in Orbit by an Extended Method of Steepest-Descent," Department of Aeronautics and Astronautics, Stanford University, SUDAAR No. 257, January 1966.

5. Bass, R. W. and Pipino, R. "On an Optimal Nonlinear System for the Attitude Control of an Orbiting Vehicle," Astro-Control Systems Division, Aeronca Manufacturing Corporation, Baltimore, Maryland, Air Force Contract No. 33(616)-8285, October 1962.

6. Studnev, R. V. "Some Problems of Optimal Three-Dimensional Attitude Control of Spacecraft," Proceedings of the First IFAC Symposium on Automatic Control, Stavanger, Norway, September 1965, pp. 268-276.

7. Porcelli, G. and Connolly, A. "Optimal Attitude Control of a Spinning Space-Body: A Graphical Approach," IEEE Transactions on Automatic Control, Vol. AC-12, June 1967, pp. 241-249.

8. Gold[illegible]ein, H. Classical Mechanics, Addison-Wesley, Reading, Mass., 1959.

9. de Does, D. H. "Time-Optimal Attitude Control of a Spinning Vehicle," Office of Aerospace Research, USAF, Proceedings of the OAR Research Applications Conference, March 14, 1967, pp. 226-235.

10. Le May, J. L. "Recoverable and Reachable Zones for Control Systems with Linear Plants and Bounded Controller Inputs," IEEE Transactions on Automatic Control, Vol. AC-9, October 1964, pp. 346-354.

11. La Salle, J. P. "The Time-Optimal Control Problem," Contributions to Differential Equations, V, Princeton University Press, Princeton N. J., 1960, pp. 1-24.

12. Pontryagin, L. S., Boltyanski, V. G., Gamkrelidze, R. V., and Mishchenko, E. F. The Mathematical Theory of Optimal Processes, English translation by Interscience Publishers, New York, N. Y., 1962.

13. Athans, M. and Falb, P. Optimal Control, Mc Graw - Hill, New York, N. Y., 1966.

14. de Does, D. H. "Time-Optimal Position and Velocity Control of a Spinning Vehicle," AAS Spaceflight Mechanics Specialist Conference, Preprint No. 66-116, University of Denver, Denver Colorado, July 6-8, 1966.

15. Knudsen, H. K. "An Iterative Procedure for Computing Time-Optimal Controls," IEEE Transactions on Automatic Control, Vol. AC-9, January 1964, pp. 23-30.

16. Neustadt, L. W. "Synthesizing Time-Optimal Control Systems," J. of Math. Analysis and Applications, Vol. 1, 1960, pp. 454-493.

17. Neustadt, L. W. "Time-Optimal Control Systems with Position and Integral Limits," J. of Math. Analysis and Applications, Vol. 3, 1961, pp. 402-427.

18. Eaton, J. H. "An Iterative Solution to Time-Optimal Control," J. of Math. Analysis and Application, Vol. 5, 1962, pp. 329-344.

19. Plant, J. B. "An Iterative Procedure for the Computation of Optimal Controls," Department of Electrical Engineering, MIT, Ph. D. Dissertation, June 1965.

20. Cook, G. "An Approximation Technique for Singular Control Problems," Proceedings of the Princeton Conference on Information Sciences and Systems, Princeton, N. J., March 25-26, 1968.

21. Dixon, M. V. "Fuel-Time Optimal Spacecraft Reorientation," Instrumentation Laboratory, MIT, T-502, May 1968.

22. Hadley, G. Nonlinear and Dynamic Programming, Addison-Wesley, Reading, Mass., 1964.

23. Bate, R. "COMPRAND - Constrained Minimization of a Function of Several Variables," Library Program, Frank J. Seiler Research Laboratory Computer Center, USAF Academy, Colo.

UNCLASSIFIED

Security Classification

DOCUMENT CONTROL DATA - R & D

(Security classification of title, body of abstract and indexing annotation must be entered when the overall report is classified)

1 ORIGINATING ACTIVITY *(Corporate author)* Frank J. Seiler Research Laboratory USAF Academy, Colorado 80840	2a. REPORT SECURITY CLASSIFICATION UNCLASSIFIED 2b. GROUP

3 REPORT TITLE

Time-Optimal Attitude Control of an Axially Symmetric Spinning Spacecraft

4 DESCRIPTIVE NOTES *(Type of report and inclusive dates)*

Scientific

5 AUTHOR(S) *(First name, middle initial, last name)*

Dirk H. de Does, Captain, USAF

6 REPORT DATE June 1969	7a TOTAL NO OF PAGES 248	7b NO OF REFS 23
8a. CONTRACT OR GRANT NO In-House Research b. PROJECT NO 7904-00-23 c. 61102F d. 681304	9a. ORIGINATOR'S REPORT NUMBER(S) SRL 69-0012 9b. OTHER REPORT NO(S) *(Any other numbers that may be assigned this report)* AD -	

10 DISTRIBUTION STATEMENT

This document has been approved for public release and sale; its distribution is unlimited.

11 SUPPLEMENTARY NOTES	12 SPONSORING MILITARY ACTIVITY Frank J. Seiler Research Laboratory USAF Academy, Colorado 80840

13 ABSTRACT

This report considers the problem of controlling both the attitude and angular velocities of an axially symmetric spacecraft while minimizing the maneuver duration. In particular, various combinations of thrust limited reaction jets are employed to properly orient a spinning space body with respect to specified reference directions starting from known initial conditions of the vehicle's attitude and angular rates. Five control jet configurations are considered: two gimballed systems where torques can be applied about, 1) any axis in a plane normal to the axis of symmetry, 2) two perpendicular non-rotating axis in a plane normal to the axis of symmetry; and three body-fixed configurations where the thrusters are immobile relative to the vehicle and can provide both positive and negative or only positive (negative) control torques about one or both of the vehicle's transverse axis. The control systems are realizable from a hardware standpoint and the corresponding optimal controls can be classified as: 1) a continuous function of time, 2) bang-bang, 3) on-off, and 4) a combination of (1 and 2) or (2 and 3).

The maximum principle is used to provide a necessary (in certain cases also a sufficient)condition for time-optimality. Exact optimal controls in terms of the initial costate and minimum final time are then determined for certain classes of state boundary conditions. In all cases the optimal control is expressed in terms of from one to four dimensionless physical parameters which include: vehicle geometry, spin rate, thrust magnitude, moment arms, and desired final state. In this manner families of solutions are generated with a modest expenditure of computation time.

DD FORM 1 NOV 68 1473

UNCLASSIFIED

Security Classification

14 KEY WORDS	LINK A		LINK B		LINK C	
	ROLE	WT	ROLE	WT	ROLE	WT
Optimal Control						
Minimum-Time Control Problem						
Spacecraft Attitude Control						
Spinning Spacecraft						
Newton's Method						